Loughborough University

This item was submitted to Loughborough's Research Repository by the author.
Items in Figshare are protected by copyright, with all rights reserved, unless otherwise indicated.

Stochastic and related models for the residence time distribution in trickle flow in a packed bed

PLEASE CITE THE PUBLISHED VERSION

PUBLISHER

© M.N. Rathor

PUBLISHER STATEMENT

This work is made available according to the conditions of the Creative Commons Attribution-NonCommercial-NoDerivatives 4.0 International (CC BY-NC-ND 4.0) licence. Full details of this licence are available at: https://creativecommons.org/licenses/by-nc-nd/4.0/

LICENCE

CC BY-NC-ND 4.0

REPOSITORY RECORD

Rathor, Mohammad N.. 2018. “Stochastic and Related Models for the Residence Time Distribution in Trickle Flow in a Packed Bed”. figshare. https://hdl.handle.net/2134/34721.

LOUGHBOROUGH
UNIVERSITY OF TECHNOLOGY
LIBRARY

AUTHOR RATHOR M. N.

COPY NO. Archive Copy. 044882/01

VOL NO. CLASS MARK

FOR REFERENCE ONLY

FOR REFERENCE ONLY

004 4882 01

STOCHASTIC AND RELATED MODELS FOR THE RESIDENCE TIME DISTRIBUTION IN TRICKLE FLOW IN A PACKED BED

by

M. N. RATHOR

STOCHASTIC AND RELATED MODELS FOR THE RESIDENCE TIME DISTRIBUTION IN TRICKLE FLOW IN A PACKED BED

BY

M. N. RATHOR

A thesis submitted for the degree of Doctor of Philosophy of Loughborough University of Technology

Supervisors: Dr. B. A. Buffham

Dr. L. G. Gibilaro

Department of Chemical Engineering

November, 1969

CONTENTS

Contents:

Section			Page
	Acknowledgments		1
1	Abstract		2
2	Introduction		4
	2.1.	Scope of present work	6
3	Literature Survey		
	3.1.	Liquid distribution in packed columns	11
	3.1.1.	Holdup in packed columns	14
	3.1.2.	Mathematical models	19
	3.1.2.1.	Dispersion models	20
	3.1.2.2.	Mixing-cell model	21
	3.1.2.3.	Comparison between the dispersion model and the mixing-cell model	25
	3.1.3.	Random walk models	26
	3.1.4.	Statistical models	28
	3.1.5.	Evaluation of axial dispersion coefficient	29
	3.1.6.	Evaluation of radial dispersion coefficient	36
	3.1.7.	Capacitance-differential models	37
4	Time Delay Models		45
	4.1.	Distributed parameter model	47
	4.2.	Lumped parameter model	48
	4.3.	Probabilistic treatment	49
	4.3.1.	Stopping process	50
	4.4.	Fixed time delays	54
	4.4.1.	Exponentially-distributed time delays	55
	4.4.2.	Gamma-distributed time delays	57
	4.5.	Hopping model	58
	4.5.1.	Hopping process	59
	4.5.2.	The delay process and the residence time distributions	62
	4.6.	Normalisation	64
	4.6.1.	Time delay models	65
	4.6.2.	Hopping model	67
	4.7.	Conclusions	67

Section			Page
5	Analysis of the Proposed Model: moments and related characteristic parameters		70
	5.1.	Transfer fuction derivation	70
	5.2.	Parametric coefficients	73
	5.3.	Conclusions	73
6	Experimental Apparatus and Operating Procedures		76
	6.1.	Packed column	76
	6.2.	Tracers and tracer injection technique	79
	6.3.	Photo-cell detector	81
	6.3.1.	Construction	81
	6.3.1.1.	Calibration of the photo-cell	81
	6.3.2.	Conductivity cell	83
	6.3.2.1.	Calibration of the conductivity cell	83
	6.4.	Stimulus response experiments	83
	6.4.1.	Runs for Water-Air system	85
	6.4.2.	Runs for Glycerine solutions	85
	6.4.3.	Double tracer experiments	86
	6.5.	Stimulus response of the detector	86
	6.6.	Liquid holdup measurements	87
7	Experimental Results		89
	7.1.	Water-Air system	89
	7.1.1.	Glycerine-Water solutions and Air system	89
	7.1.2.	Double tracer experiments: Water system	89
	7.1.3.	Stimulus response of the detector	89
	7.1.4.	Liquid holdup	90
	7.2.	Liquid holdup measurements and correlations	90
	7.3.	Results of the impulse response tests	95
	7.3.1.	Effect of the liquid and the gas flow rates	95
	7.3.2.	Effect of varying packed height	101
	7.3.3.	Effect of liquid viscosity	101
	7.3.4.	Role of molecular diffusion	101
	7.3.5.	Effect of the detector R.T.D. on the overall R.T.D.	109
8	Evaluation of the Model Parameters from the Experimental Response Curves		111
	8.1.	Curve fitting procedure for the exponential time delay model	112

Section			Page
8			
	8.2.	Curve fitting procedure for the gamma delay times and hopping model	115
9	Comparison of the Experimental Results of the Dynamic Tests with the Proposed Models		117
	9.1.	Time delay model with exponentially distributed delay times	117
	9.2.	Time delay model with gamma distributed delay times	129
	9.3.	Hopping model	151
	9.4.	Conclusions	173
10	Discussion		176
	10.1.	Comparison with other models	176
	10.2.	The proposed model	178
	10.3.	Conclusions	189
	10.4.	Suggestions for further work	190
	APPENDICES		
	Appendix A:	Experimental runs	192
	Appendix B:	Normalised experimental responses	196
	Appendix C:	Liquid holdup correlation data	229
	Appendix D:	Evaluated model parameters	233
	Appendix E:	Normalisation programme	241
	Appendix F:	Listing of the programmes	245
	BIBLIOGRAPHY		264

ACKNOWLEDGMENTS

The author wishes to thank the following:
Professor D.C. Freshwater for his interest and encouragement;
his project supervisors, Drs. L.G. Gibilaro and B.A. Buffham,
for their unabated enthusiasm and for many ideas and the guidance
which made the completion of this project possible; Mr. H.W.Kropholler
for his most invaluable comments and suggestions throughout the
research; the departmental technical staff for the help in setting
up and running of the equipment; and the Science Research Council
and Loughborough University for their financial support.

1. ABSTRACT

1. Abstract

Mathematical models have been derived on the basis of the abstraction that material would flow uniformly, in plug flow, through a system were it not that elements have a chance of being delayed at all points of their passage; an element so delayed eventually rejoins the main stream. The models are mutually differentiated by their delay time distributions.

A trickle flow packed bed system was used to test the concepts involved. Liquid side residence time distributions in a $1\frac{1}{2}$ inch diameter column packed with 1/8 x 1/8 inch ceramic Raschig rings were determined by the method of injecting an impulse of a tracer into the liquid stream. For different delay time distributions, the model parameters were obtained by direct comparison of the experimental and model responses. It was possible to obtain a good fit of the experimental responses, the model parameters correlating well with the operating variables.

The effect of varying the packed heights, the liquid and the gas flow rates, the liquid viscosity and the tracer diffusivity on the residence time distributions was investigated. The measured and calculated liquid holdup data fitted several published correlations very well, confirming the reliability of the experimental and processing procedures.

Part of Chapter 4 (development of the mathematical model) and some of the preliminary experimental work contained in this thesis forms the basis of a paper which has been accepted for publication by the Am. Inst. Chem. Eng. Jl., and is due to appear in March 1970.

2. INTRODUCTION

2. Introduction

The importance of the distribution of residence times of material in the design of process equipment depends not only on the extent of the departure from ideality (perfect mixing or pure plug flow) but often more significantly on the nature of the processing and processed materials; this is particularly so in reactor design.

Models for non-ideal flow may be classified according to the extent to which their parameters are determined from theoretical considerations: at one extreme is the model that makes no attempt to explain the mechanism that results in the observed behaviour but contents itself with providing a description in terms of fully empirical parameters; and at the other is the complete mathematical description based on the system geometry and a full knowledge of the fluid mechanics and other processes involved. Models of the second type, while having the advantage that extrapolation out of the region of confirmed validity is safer - although not without danger - are much harder to set up; they also tend to depend critically on such things as geometrical details that from the broader viewpoint of process performance are not particularly important. On the other hand semi-empirical models may often be applied to a wide variety of situations with the aid of correlations of the model parameters with system constants. The division between the two types of model is not very distinct because it is often possible to predict the parameters themselves from the detailed system behaviour. Successful semi-empirical models employ an abstraction that it is felt will lead to the same type of behaviour that is actually observed. Diffusion theory is an example of this approach: the diffusion equation is the semi-empirical model and the diffusion constant a parameter which can be explained by random molecular motion.

For continuous flow systems, whose residence time distributions

do not deviate too far from plug flow, the dispersion model(1) is widely used and commonly employed for the characterisation of fluid mixing in packed beds. In this application the model, which is based on an analogy with diffusion theory, must be regarded as wholly empirical in that it says no more about the mechanism resulting in the observed axial mixing than that it is the result of many repetitions of an underlying random processes. It is applied to both gas and liquid phases regardless of whether the system contains one or two fluid phases in co-current or counter-current flow; it makes no assumptions regarding the nature and arrangement of the packing and ignores the existance of converging and diverging streams (that can be observed in a trickle bed for example), and of the relatively stagnant pockets that inevitably exist in the usual packed bed arrangements.

The fact that the residence time distributions resulting from such diverse mechanisms are so similar, suggests the desirability of a general model such as the dispersion model, rather than the more rigorous treatments based on geometric and fluid mechanic considerations which require to be quite different for each case. This is not to say that such specialised approaches are unnecessary - a large number of models for particular packed bed systems have appeared in the literature and give considerable insight into the process studied - but that as a common mechanism will clearly describe all these systems it should be investigated both for the purpose of facilitating such descriptions and in the hope that it will indicate common physical features which predominantly influence the destribution of residence times.

The dispersion model with only one parameter goes a long way towards describing these distribution curves. A serious inadequacy in this respect, however, is that it almost invariably indicates a more symmetrical distribution than is obtained in practice; small quantities of material tend

to reside in the bed for considerably longer than the dispersion model would suggest, resulting in a slowly decaying tail and the displacement of the peak response to the left of the mean. The experimental results shown in Figure: 2.1 and 2.2 are typical in this respect.

The question then becomes: how much more need be said about the system to account for the observed residence time distributions (R.T.D.) without destroying the generality possessed by the dispersion model? The analysis that follows represents an attempt to answer this question. Material is assumed to pass through the bed in what would be plug flow were it not that fluid elements have a chance of being delayed for a period of time at all points of their passage. The parameters of this model depend on the probability of a delay occurring at any point in the bed, the average time for which material is delayed and the distribution of delay times about this average. The mechanism is analogous to that of surface renewal in the penetration theories of mass transfer, in which fluid elements that find their way to the surface are 'delayed' there before returning to the bulk fluid. In the time-delay model this effect is distributed through the system; bulk material flows at a uniform rate and the delayed elements have negligible velocity in the direction of the main flow.

2.1 Scope of Present Work

The object of the work is to develop models based on the time delay concept and to test their applicability to real physical systems; trickle flow in packed bed has been considered.

The effect of varying packed heights, liquid properties and tracer diffusivities on the liquid side residence time distributions has been investigated.

The gamma distributed delay times and a special case of this

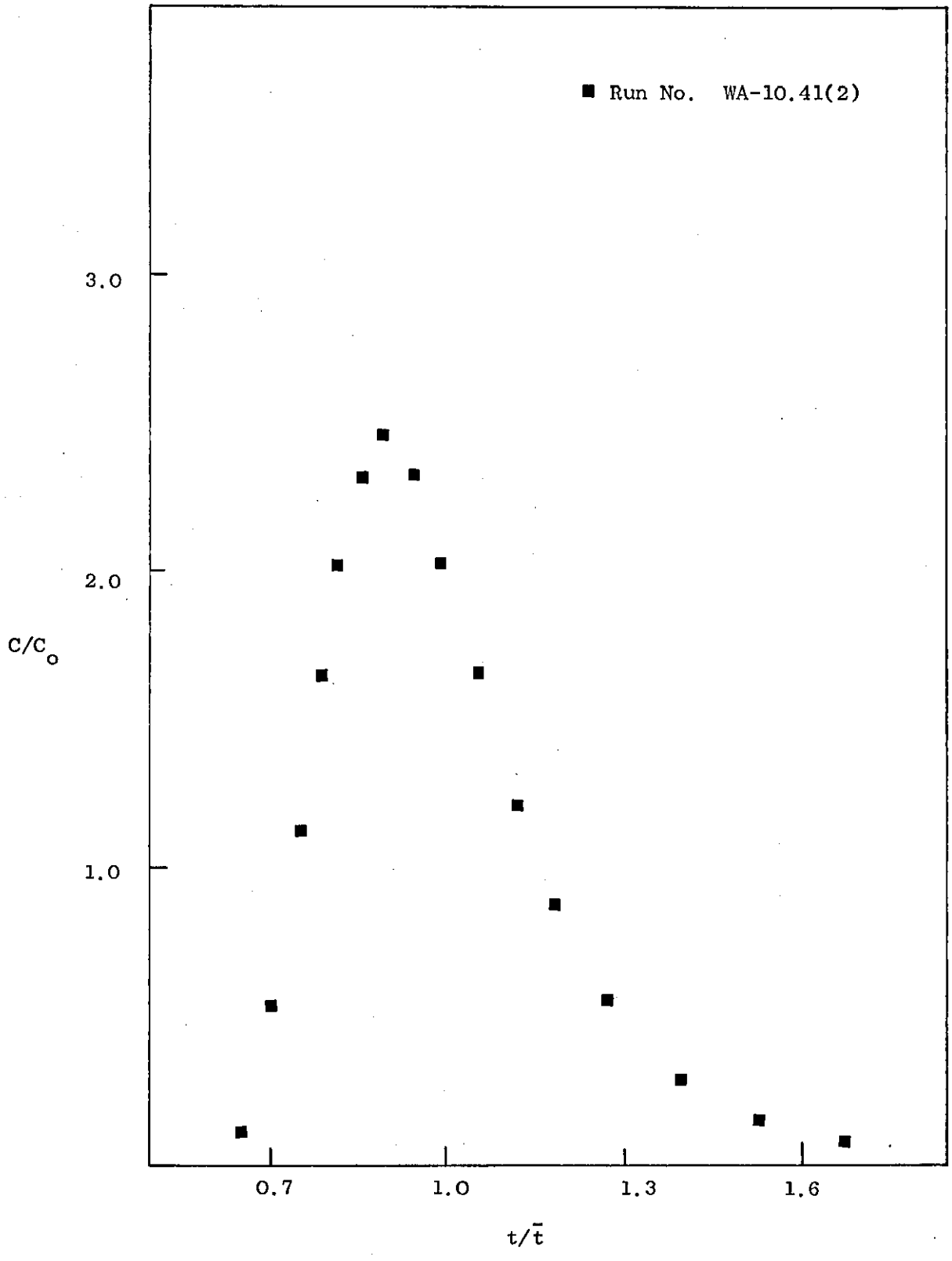

Figure: 2.1. A typical experimental response curve.

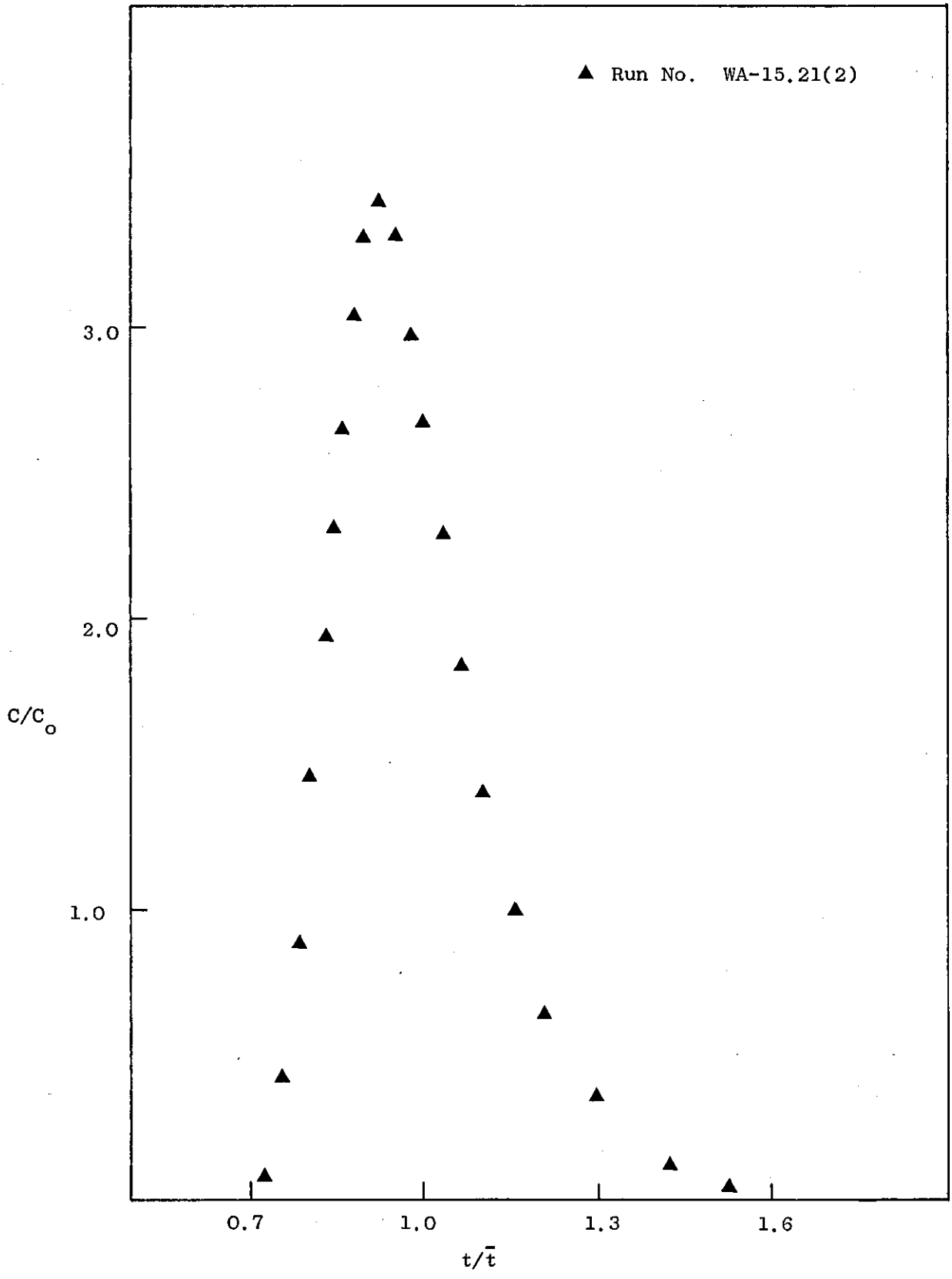

Figure: 2.2. A typical experimental response curve.

distribution, namely the exponential case, have been studied. A modified version of the time delay model - the hopping model - which considers direct axial displacement of delayed material has been postulated.

The transfer function solution of the time delay model is shown to have the same form as the generalised transfer function shown by Paynter (100) to be applicable to a broad class of linear monotone dynamic systems.

The model fitting method of comparing directly the experimental responses with the model solutions has been chosen in preference to the moment-matching method because the latter places considerable stress on the tail end of the distribution and this is the portion of the experimental response curves most subjected to error.

Nomenclature

C	concentration of tracer
C_o	initial concentration of tracer
C/C_o	normalised concentration
t	time
$\bar{t}$	mean residence time of the fluid in the system
$t/\bar{t}$	normalised time

3. LITERATURE SURVEY

3.1 Liquid Distribution in Packed Columns

The way liquid is distributed over and how it wets column packing has a significant effect on the performance of packed columns. Many theoretical relationships for mass transfer are based on the assumption that gas and liquid streams are uniformly distributed over the cross-section of the column and are moving in perfect counter-current or co-current flow. Any deviation from these"ideal" conditions will result in lowering of the column efficiency.

Investigation of liquid distribution over random packing started as far back as the end of the last century. Hunter (2), Tour and Lerman (3) studied the distribution in a column, packed with coke, by feeding water at a single central point, and collecting the water draining from the packing in eight troughs, each 6ins. wide. The results showed an improvement in water distribution with increased packed height, but even with 14ft. of packing, 60% of the liquid was collected by two central troughs. Plotting the percentage of water collected in each trough against the number of trough yielded a curve bearing a marked resemblance to the one representing the Gaussian probability distribution. This observation is in accord with a theory in which it is assumed that as the liquid flows down the packing it undergoes a series of horizontal shifts with an equal chance of moving towards the centre or outwards to the wall, each time.

Tour and Lerman (3) carried out experiments on the radial distribution of water in a 20in. diameter cylindrical column, packed with coke graded to $\frac{1}{4}$ to $\frac{1}{2}$ mesh. They collected the draining water in 16 annular troughs, again similar types of results were obtained.

Kirschbaumm (4) and Weimann (5) studied distribution of water in 110 mm. and 300 mm. columns, packed with 8 mm. and 15 mm.

diameter rings. They found that large packing size and small column diameter size resulted in a high proportion of liquid to flow down the wall. Increasing the column diameter and reducing the packing size improved the distribution. Weimann (5) recommended the ratio to be not less than 25:1.

Scott (6) studied the water distribution in a $4\frac{1}{2}$ in. diameter column with a single central feed pipe, using $\frac{1}{2}$in. rings and $\frac{1}{4}$in. and $\frac{1}{2}$in. coke as packing materials. He used packed heights from 15in. to 15ft.; $\frac{1}{2}$in. rings showed rapid spreading of liquid with the result that a large proportion of liquid flowed down the wall; $\frac{1}{2}$in. coke is less effective in spreading the liquid but the wall flow was pronounced; however with $\frac{1}{4}$ in. coke there was a marked tendency for the liquid to return from the wall to the packing. Similar investigations by Baker et al (7) over various packing size and column diameters indicated the significance of column to packing diameter ratio, with ratio of 8:1 a large proportion of liquid flowed down the wall. Their work also revealed the independence of liquid distribution of air flow up to the loading point where upon it improved; for column diameters of 3in. to 6in., single feed points proved to be adequate, but for larger diameter columns liquid distributors with four or more feed points were required.

Uchida and Fujita (8) found dumped packings to give better distribution than stacked packings. The best distribution was achieved with a column to packing diameter ratio of 10:1. Viscosity and density seemed to have no effect on liquid distribution in the range studied.

Several authors have made visual observations of the paths fluids follow in packed columns. Baker et al (7) noticed that the liquid distribution becomes constant after flowing through a packed height equal to 10 times the column diameter. However, Weimann (5) observed a continuously changing distribution even after the liquid had flowed

through a height equal to 40 column diameters and also maldistribution at column to packing diameter ratios of 15:1 and 20:1. Eckert (9) proposed a minimum ratio for Raschig rings, Intalox, Berl Saddles, and Pall rings of 30:1, 15:1 and 15:1 respectively.

Porter and Jones (10) gave a quantitative mathematical treatment and putforward a model to predict the course of fluid flow down a packed column. The prediction of liquid distribution was stated in terms of two factors:-

(a) a liquid spread factor

and (b) a wall factor.

The authors used techniques similar to that of Cihla and Schmidt (11) to derive a"diffusion type" equation; but used a different set of boundary conditions which were obtained by observing the behaviour of irrigated packed columns. Experimental investigations proved that at small depths of packing the reduction in flow next to the wall was overestimated by their theory which consequently overestimated the flow at the wall. However, results indicated less maldistribution with Pall rings and Berl saddles and suggested the point flow in the packing and the wall flow to be determined by two dimensionless groups.

More recently Jameson (12) also proposed a model for flow of liquid in packed columns. It was shown that for any arbitrary distributor it was possible to calculate the fluid distribution, including the wall flow, as a function of packing height as long as two empirically derived constants were known. In another publication (13) the same author used the proposed model:-

(a) to calculate the proportion of total liquid flow that runs down the walls at steady conditions

(b) to determine the depth at which a steady condition is reached, with different initial modes of distribution

and (c) to investigate the effectiveness of various configuration and wall wipers.

Jameson observed a considerably reduced wall flow with small-size packings and large column diameters, but with ½in. stoneware it was still appreciable. In order to obtain wall flow less than 15% of the total flow, it was recommended to use a column to packing diameter ratio of 20:1, except for ½in. Raschig rings when the ratio should be 65:1.

3.1.1. Holdup in Packed Columns

When gas and liquid flow co-currently or counter-currently in a packed column each phase occupies a certain fraction of the void volume. The total void volume is sum of the volume fractions occupied by liquid phase, E_L, and by the gas phase, E_G :-

$$E_T = E_L + E_G \qquad (3.1)$$

Experimental techniques for evaluating E_L are simple but cannot be applied to the evaluation of E_G, therefore most of the previous work has been concerned with evaluation of liquid holdup, E_L and hence the determination of gas holdup, E_G, with the aid of Equation (3.1). Payne and Dodge (14) determined the holdup values of columns packed with 10mm. Raschig rings. They first determined the amount of liquid required to wet the packing by pouring a known amount of liquid and collecting the drained excess. Then the liquid flow through the column was started at a constant rate. At steady conditions, input to the column was cut off and the draining liquid collected. The drainage plus the amount required to wet the packing was then taken as the holdup of the column. All runs were made at zero gas rate; the authors made no attempt to correlate their data.

Fenske et al (15) reported holdups of packed beds of rivets,

lenghts of chain, and nails. The amount of liquid required to wet the packing was termed, static holdup, Hst, and amount drained after cutting off the constant input, an operating or dynamic holdup, H_{op} ; hence the total holdup, H_T :

$$H_T = H_{st} + H_{op} \tag{3.2}$$

Simons and Osborn (16) went a step further and correlated their holdup data on spheres and broken pieces of coke with zero gas flow rate. These authors found the operating holdup to be proportional to the mass flow rate of the liquid phase :

$$H_{op} = \underline{b}\, L \tag{3.3}$$

The liquids used were water and kerosene. The value of $\underline{b}$ seemed to depend on the type of liquid used, but was independent of packing size. Uchida and Fugita (17) also determined the static and dynamic holdups using the drainage method on columns packed with rings and broken solids, the liquids being water and oil.

Furnas and Bellinger (18) were the first to investigate the effect of gas flow rate on liquid holdup. The effect was found to be negligible for conditions below the flooding point in columns packed with Berl saddles and Raschig rings. Elgin and Weiss (19) carried out similar work, their findings were in agreement with those of Furnas and Bellinger.

Jesser and Elgin (20), working with Berl saddles, glass spheres and carbon rings, found the operating holdup, H_{op} , to be proportional to the liquid mass flow rate, L, raised to some exponent, s:

$$H_{op} = b\, L^{s} \tag{3.4}$$

Otake and Okada's work (21) showed the operating holdup, H_{op} , to depend on the mass flow rate, L, the liquid density, ρ, the liquid viscosity, μ, the packing diameter, d_p, and packing characteristic, $a_k\ d_k$. Dimensionless analysis of these variables yielded the following dimensionless groups for correlating the operating holdup :-

$$a)\quad N_{Rel} = \frac{d_p\ L}{\mu} \tag{3.4a}$$

$$b)\quad N_{Gal} = \frac{d_p^{\,3}\ g\ \rho^2}{\mu^2} \tag{3.4b}$$

The following equation correlated their data and previously published data (21a) within $\pm$ 15% deviation :-

$$H_{op} = 1.29\ .\ \{N_{Rel}\}^{0.676}\ \{N_{Gal}\}^{-0.44}\ \{a_k\ d_k\} \tag{3.5}$$

This correlation is based on data for Raschig rings, Berl saddles and spheres ranging in size from $\frac{1}{4}$in. to lin. using both water and oil.

Shulman et al (22) measured holdups in various packings by weighing the entire column with a suspension system, this gave them quite reproducible data. The total holdup data was correlated by :

$$H_T = \frac{b\ L^s}{d_{ps}^{\,3}} \tag{3.6}$$

where d_{ps} is the diameter of a sphere having the same surface area as the piece of packing. The coefficient, b, and exponent, s, are functions of the type and size of packing. The most interesting correlation in their work is that for static holdup, Hst :

$$H_{st} = a_k\ d_{pe}^{-m} \tag{3.7}$$

a_k and m depend on the type of packing used.

Otake and Kunugita (23) were the first to apply the tracer techniques in the study of holdups. They found total holdup, H_T , to be proportional to the interstitial velocity, U_s , an extrapolation of the plot of the total holdup, H_T , against the interstitial velocity, U_s , to zero velocity, produced a value for the static holdup, H_{st}. For Raschig rings the following correlations were arrived at :

$$H_{st} = \frac{0.038}{d_p} \tag{3.8}$$

and

$$H_{op} = 1.79 \times 10^{-3} \left(\frac{d_p U_s}{\mu}\right) \left(\frac{d_p^3 \, g \, \rho}{\mu^2}\right)^{-1} \tag{3.9}$$

where d_p is in centimeters and the Reynolds number is based on the interstitial velocity, U_s . The term, $a_k \, d_p$, does not appear in the above equation because only one type of packing was used.

Recently two further dimensionless equations for calculating the liquid operating holdup, H_{op} , in packed columns were described. Mohunta and Laddha (24) found the holdup to vary exponentially with liquid rate, and gas counter-flow to have no effect on the holdup up to the loading point. They proposed a generalised correlation for operating holdup, H_{op} , for Raschig rings, Lessing rings, and spherical packings:

$$H_{op} = 16.13 \left(\frac{\mu \, U \, N}{\rho \, g^2}\right)^{1/4} \left(N \, d_{ps}^{\,3}\right)^{-1/2} \tag{3.10}$$

where U is the superficial velocity (based on the empty column), N is the packing number density and d_{ps} is as defined in Equation (3.6). Buchanan (25) subdivided the liquid holdup into two limiting dynamic regimes: the gravity viscosity regime at low Reynolds number

for which:

$$H_{op} = 8.1 \left(N_{Frl}\right)^{0.44} \left(N_{Rel}\right)^{-0.37} \qquad (3.11)$$

for $0.01 < N_{Rel} < 10$

and gravity-inertia regime at high values, for which:

$$H_{op} = 6.3 \left(N_{Frl}\right)^{0.44} \left(N_{Rel}\right)^{-0.20} \qquad (3.12)$$

N_{Fr} = Froude number,

The experimental data used in developing these correlations were for experiments with ceramic Raschig rings only. Gelbe (26) made further extensive studies of liquid holdups because the scatter of the measurements still exceeded $\pm$ 20%, especially at low Reynolds numbers. He arrived at a more accurate correlation by suggesting that the influence of the flowing film on the static holdup had not been taken into account previously. The author proposed the following equation for determining the operating holdup :

$$H_{op} = 1.59 \left(\frac{d_i'}{d_p}\right)^{-5/9} \left(\frac{N_{We}}{N_{Fr}}\right)^{-1/7} \left(N_{Gal}\right)^{-0.33} \left(N_{Rel}\right)^{n} \qquad (3.13)$$

where d_i' = hydraulic diameter of the smallest inner area of a ring.

The exponent n has a value of 1/3 for N_{Re} less than one, and 5/11 for N_{Re} greater than one.

The static holdup, H_{st}, which represents the difference between the measured total holdup and the calculated operating holdup, was expressed dimensionless as a function of a reduced number, $X_r = X/X_k$, and the geometric number, $a_k\, d_k$, in the range, $10^{-3} < X_r < 1$. The equation applicable to all

the packing tested is:

$$H_{st} = 1.67 \times 10^{-4} \; (a_k \, d_k)^2 \log X_r \qquad (3.14)$$

Where X is a variable that gives physically correct description of the static holdup behaviour in two different regions, namely $N_{We}/N_{Fr} < 10$ and $N_{We}/N_{Fr} > 10$.

For $N_{We}/N_{Fr} < 10$,

$$X = \frac{N_{We} \; N_{Fr}}{N_{Re}^2 \, (a_k \, d_k)^6} \qquad (3.15)$$

and for

$N_{We}/N_{Fr} > 10$,

$$X = \frac{N_{We}^3/1000}{N_{Re}^2 \, N_{Fr} \, (a_k \, d_k)^6}$$

where X_k is a common critical value corresponding to a critical Reynolds number which determines the onset of static holdup. For all ring packings $X_k = 1.4 \times 10^{-13}$.

3.1.2 Mathematical Models

The complexity of fluid patterns (18 , 19 , 20) in packed columns makes it difficult to describe the turbulent fluid flow mathematically. However, consideration of several general observations about the passage of fluid elements through a column, such as : the wetting of the packing and the walls ; filling of void spaces and often the accumulation of fluid in hollow spots, in conjunction with a possible fluid spread theory can lead to the postulation of models that approximate to reality. The suitability of such models is tested by comparing the model and the system response.

Many types of model have been suggested to represent non-ideal flow in process equipment . Some, called dispersion models, draw analogy between mixing and diffusional processes. Others consider flow regions connected in series or parallel; when perfect- mixing occurs in these

regions - these models are called tanks-in-series or mixing-cell models. Some of these models account for the deviation of the real system from plug-flow, while others describe the deviation of the stirred tanks from the ideal of perfect-mix flow.

3.1.2.1. Dispersion Models

In packed columns, mixing is the result of "splitting" of the fluid streams as they flow around particles and the variation in velocity across the column.

A phenomenological description of turbulent mixing (27) gives good results for many situations: an apparent diffusivity is defined so that a diffusion-type equation may be formulated, and the value of the parameter is then experimentally determined. An extensive survey of the evaluation of the parameter for different boundary conditions is given further on in section 3.15.

Bischoff and Levenspiel (28) have included the following table of dispersion models for various situations.

Table: 3.1: Dispersion Models

Name of model	Simplifying assumptions or restrictions in addition to those for model	Parameters of model	Defining differential equation
General dispersion: includes chemical reaction and source terms	Constant density	D, U	$\frac{\partial C}{\partial T} + U.\nabla C = \nabla.(D.\nabla C) + S + r_c$ (I)
General dispersion in cylindrical co-ordinates	Bulk flow in axial direction only. Radial symmetry	$D_R(R), D_L(R), U(R)$	$\frac{\partial C}{\partial T} + U(R)\frac{\partial C}{\partial x} = \frac{\partial}{\partial x} D_L(R)\frac{\partial C}{\partial x} + \frac{1}{R}\frac{\partial}{\partial R} R D_R(R)\frac{\partial C}{\partial R} + S + r_c$ (II)

Name of model	Simplifying assumptions or restrictions in addition to those for model	Parameters of model	Defining differential equation
Uniform dispersion	Dispersion coefficients independent of position hence constant	$D'_{Rm}, D'_{Lm}, U(R)$	$\frac{\partial c}{\partial T} + U(R)\frac{\partial c}{\partial x} = D'_{Lm}\frac{\partial^2 c}{\partial x^2} + \frac{D'_{Rm}}{R}\frac{\partial}{\partial R}R\frac{\partial c}{\partial R} + S + r_c$ (III)
Dispersed plug flow	Fluid flowing at mean velocity, hence plug flow	D_R, D_L, U	$\frac{\partial c}{\partial T} + U\frac{\partial c}{\partial x} = D_L\frac{\partial^2 c}{\partial x^2} + \frac{D_R}{R}\frac{\partial}{\partial R}R\frac{\partial c}{\partial R} + S + r_c$ (IV)
Axial dispersed plug flow	No variation in properties in the radial direction	D'_L, U	$\frac{\partial c}{\partial T} + U\frac{\partial c}{\partial x} = D'_L\frac{\partial^2 c}{\partial x^2} + S + r_c$ (V)

As it can be observed that dispersion can be described approximately by the solutions of diffusion equation with properly chosen boundary conditions.

Klinkenberg and Sjenitzer (29) have discussed the necessary conditions for equivalence between dispersion and diffusion as far as the residence time distributions are concerned. They proposed the idea of additive variances for the different mechanisms provided these occur successively and independently. However, these conditions are not satisfied exactly in many real systems. Several other authors (29a) have also pointed out the equivalence between diffusion model and a series of perfectly mixed cells in limiting cases.

3.1.2.2. Mixing-Cell Model

The series mixing-cell model was first proposed by Ham and Coe (30). This model assumes that the packing can be characterised by several completely mixed cells in series. See Figure 3.1.

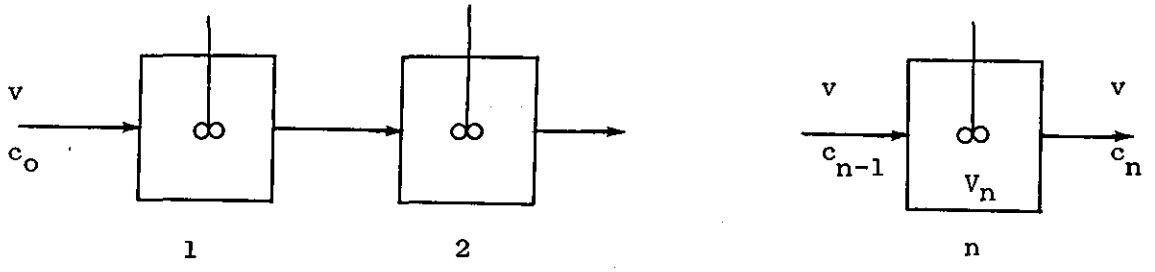

Figure: 3.1. Mixing-cell Model

A mass balance on a single cell results in :-

$$V_n \frac{dc_n}{dt} = v\, c_{n-1} - v\, c_n \qquad (3.16)$$

where V_n = volume of the nth cell

v = volumetric flow rate.

If V is the total void volume of the column, and all the cells have equal volumes

then $$n\, V_n = V \qquad (3.17)$$

and $$\frac{V_n}{v} = \frac{EV}{nv} = \frac{L}{n\, U_s} \qquad (3.18)$$

L = length of the bed

U_s = interstitial velocity

which indicates that mixing is characterised by only one parameter, n, the number of cells in the column.

The pulse response can be found for the set of Equations (3.16) for n = 1,2,..... with the conditions that the input to the first tank, n = 1, is a delta function of tracer, i.e. $c_{n\neq 0}(0) = 0$ and $c_{n=0}(0) = \frac{c_o V}{v}\, \delta(t)$

The real time solution of Equation (3.16) for these boundary conditions is:

$$c_n = \frac{c_o}{(n-1)!} \frac{V}{V_n} (t\ v/V_n)^{n-1}\ e^{-tv/V_n} \qquad (3.19)$$

Using Equation (3.17):

$$V = n\ V_n$$

Mean time :

$$\bar{t} = V/v = n\ V_n/v$$

Therefore Equation (3.19) in dimensionless form becomes :

$$c'_n = \frac{n^n}{(n-1)!}\ \theta^{n-1}\ e^{-n\theta} \qquad (3.20)$$

To find the parameter, n, the mean and the variance can be found from Equation (3.20) and then compared with the mean and the variance of experimental response curve. From Equation (3.20)

The mean, $\mu_1 = 1$ (3.21)

and the variance, $\sigma^2 = \frac{1}{n}$ (3.22)

The preceeding scheme for parameter evaluation is only possible for a perfect delta function input which in practice is difficult to achieve. Aris (**31**), Bischoff (**32**), and Bischoff and Levenspiel (**28**) proposed a technique utilising two measurement points for the evaluation of the parameter, n :

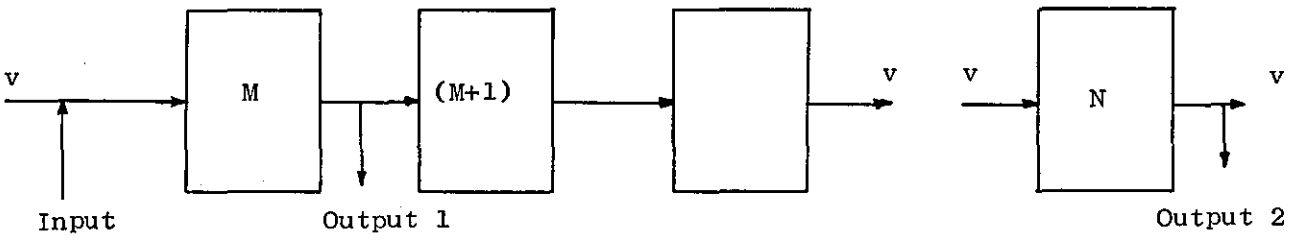

Figure: 3.2.

Considering the above set up, Figure 3.2., the following relationships relate the means and variances of the outputs to the parameters for any pulse input :

$$\mu 1 = \mu 1N - \mu 1M = 1 \tag{3.23}$$

and

$$\sigma^2 = \sigma_N^2 - \sigma_M^2 = \frac{1}{(N - M)} = \frac{1}{n} \tag{3.24}$$

The tanks-in-series model has been used by many workers in the investigation of packed columns. As mentioned previously if the fluid in each void space of the column can be represented by a perfectly mixed cell, the mixing can be represented by a series of stirred tanks each with a size and magnitude of the particle. This has been discussed in detail by Amundson (33); Carberry (34) proposed that the fluid in the void is not perfectly mixed, therefore an "efficiency" of mixing in void space has to be introduced.

Deans and Lapidus (35) described a three dimensional array of stirred tanks, called a finite stage model, that takes radial as well as longitudinal mixing into account. By a geometrical argument authors arrived at the following equation for (i,j)th tank :

$$\frac{dC_{i,j}}{dt} + C_{i,j} = Q_{i-1,j} \tag{3.25}$$

$$Q_{i-1} = \frac{(j-\frac{3}{4})C_{i-1,j-\frac{1}{2}} + (j-\frac{1}{4})C_{i-1,j+\frac{1}{2}}}{(2j - 1)} \tag{3.26}$$

with boundary conditions :

$$C_{i,j} = C_o$$

$$C_{o,j} = C'$$

which describe the initial condition and the inlet to bed respectively.

3.1.2.3. Comparison between Dispersion Model and Mixing-Cell Model

Several methods of comparing mixing-cell and dispersion model have been suggested. Kramers and Alberda (36) used the variance for the doubly infinite dispersion model :

$$\sigma^2 \approx 2(D/UL) \tag{3.27}$$

Comparing this with mixing-cell model variance Equation (3.22) :

$$\frac{1}{n} = 2(D/UL) \tag{3.28}$$

However this does not apply for small number of mixers, because $n \neq 1$ as $D \rightarrow \infty$.

Kramers and Alberda suggested using

$$\frac{1}{(n-1)} = 2(D/UL) \tag{3.29}$$

which does extrapolate correctly to $n = 1$ as $D \rightarrow 0$, and is approximately the same as for Equation (3.28) for large values of n.

Levenspiel (37) later showed that the reason for incorrect extrapolation was that the doubly infinite vessel was not the proper one to use for the comparison, instead closed vessel (in which plug flow exists in the entering and leaving streams) must be used:

$$\frac{1}{n} = 2(D/UL) - 2(D/UL)\left\{1 - e^{-UL/D}\right\} \tag{3.30}$$

It is seen that $n \rightarrow \infty$ as $D \rightarrow 0$, which is the basis for the statement that an infinite number of tanks in series is equivalent to plug flow, but it must be remembered that the total volume is held constant in the limiting case.

Trambouze (38) suggested two alternative methods of comparison. One by matching the C curve at maxima for these two models i.e.

$$D/UL = \frac{(2n - 1)^2}{2n(n - 1)(4n - 1)} \tag{3.31}$$

this equation does not extrapolate for $D \rightarrow 0$ and gives $n = 1$ for $D \rightarrow \infty$, and further reduces to Equation (3.28) for large values of n. Second method is by matching the curves at $\theta = 1$

hence

$$\left[(UL/D)^2 + 2(UL/D) - \tfrac{3}{4}\right] = \frac{2n}{(1 + \frac{1}{12n})} \tag{3.32}$$

Thus it is concluded that there is no unique way of matching the two models.

3.1.3 Random Walk Models

Random walk approach was made by Baron (50), Ranz (39), Beran (40), Scheidegger (41), Latiman (51), and de Josselin de Jong (42) and Saffman (43)(44,45). The latter two did not exactly use random walk, since a completely random process was not considered.

Other methods based on statistical mechanics have been proposed by Evans et al (46), Prager (47) and Scheidegger (48).

The random walk analysis postulates that the mixing is caused by "splitting" or "side-stepping" of the fluid around the particles

Thus one might imagine the mass flux to be proportional to the particle diameter and the velocity:

$$D_R \propto U d_p \tag{3.33}$$

Baron considered radial dispersion and assumed that when each time a fluid element approached a particle it is deflected by an amount $\pm \beta d_p$, where β is of the order one-half, for n, deflections through a passage of length, L, $n = \frac{\alpha L}{dp}$, where α is of the order of one. Thus the mean square deviation of the deflections is :

$$\Delta x^2 = n \hat{\beta}^2 d_p^2 \tag{3.34}$$

Using Einstein's equation for diffusion (52), and substituting approximate values of α and β, he arrived at :

$$D_R/Ud_p = \frac{\alpha \hat{\beta}^2}{2} \simeq 0.1 \tag{3.35}$$

Radial dispersion data for a packed column showed good agreement with Equation (3.35) and confirmed the independence of $\frac{D}{Ud_p}$ with flow rate, which is true for larger Reynolds numbers.

Prausnitz (49) using an approximate mixing length model estimated the axial dispersion coefficient :

or $$D_L \simeq (7/4\ d_p)\ U/d_p\ (d_p/4) = 7/16\ U\ d_p$$

$$D_L/Ud_p \simeq 7/16 \tag{3.36}$$

which is of right order of magnitude.

The experimental results of Scott (6) and Tour and Lerman (3) indicated that the liquid spreading process over packing might be a random walk type. Cihla and Schmidt (11) and Porter and Jones (10) suggested using diffusion theory for large number of steps in the random walk. Le Goff and Lespinesse (53) contradicted this and proposed a theory of "preferred paths".

Porter (54) proposed a rivulet model demonstrating that there is no contradiction between diffusion and Le Goff theory of "preferred paths" provided that the preferred paths - called rivulets - change direction in random manner while flowing down the column. Also it considers column wall as a mixing and generating zone of incoming and outgoing rivulets.

3.1.4. Statistical Models

These models assume that mixing process consists of "motion phases" and "rest phases". The first model was proposed by Einstein (55) for the motion of pebbles in streams. This idea was promoted by Jacques and Vermeulen (56), Cairns (57) and Cairns and Prausnitz (58), it is assumed that the duration of a motion phase is much smaller than that of a rest phase. For packed columns, motion phase might be taken as the period when the fluid element is passing through the restriction between particles, and the rest phase as the period when the fluid element is in the void space. This is, as a matter of fact, a time delay model with no dead time.

The probability density for any "jump" of the element will be given :

$$p(x, t)dxdt = e^{-x-t}d_x dt \qquad (3.37)$$

Equation (3.37) is applied to n motion phases and n phases after which the element is found at a relative position x and at relative time t. Probability of finding all elements at that position is:

$$P_{tot} = e^{-x'-t'} I_o (2\sqrt{x' t'}) \qquad (3.38)$$

the relationship between x' and x depends on the length of each step, similarly there is a relationship between t and t'.

Comparing the above Equation (3.38) with the solution of axial dispersed plug-flow model at any large x and t yields :

$$x' = x U/D_L \qquad (3.39)$$

and

$$t' = U^2 t/D_L \qquad (3.40)$$

Cairns and Prausnitz used Equations (3.39) and (3,40) to find the dispersion coefficients.

Giddings and Eyring (59), Giddings (60), and Klinkenberg (61) have also proposed models based on similar concepts.

3.1.5 Evaluation of Axial Dispersion Coefficient

To evaluate the dispersion coefficient, D_L , tracer techniques have been used. This involves the injection of an identifiable tracer into the inlet stream at a rate that varies with time. At some point downstream concentration is recorded with respect to time; the dispersion coefficient is determined by analysis of the response curves.

For a fixed distance between the injection and measurement points, the amount of spreading depends on the intensity of dispersion

in the system; Levenspiel and Smith (62) first showed that the variance, or second moment of tracer curve relates this spread to the dispersion coefficient.

Therefore the real problem involves the derivation of functional relationship between the variance of the tracer curve and the dispersion coefficient. This is achieved by solving the differential equation for concentration with dispersion coefficient as a parameter, and finding the variance of this theoretical expression for the boundary conditions appropriate to the system being studied; the dispersion coefficient for the system is then calculated from the expression and the experimentally found variance.

Equation (II) of Table 3.1. is put into a form required for mathematical treatment by setting the radial terms to zero, making the velocity constant and substituting D_L' for D_L (R) thus :

$$\frac{\partial c}{\partial t} + U\frac{\partial c}{\partial x} = D_L' \frac{\partial^2 c}{\partial x^2} + 1/\pi \quad \delta(x - x_o)\ (1/R_o^2) \qquad (3.41)$$

$f(R) = \frac{1}{R_o^2}$, since injection is uniform over the entire plane.

Again reducing Equation (3.41) to dimensionless form by substituting :

$$\theta = Ut/L$$

$$z = x/L$$

$$P_e = UL/D_L'$$

L = length of test section

$c' = c/c_o$

c_o is the concentration of injected tracer throughout the system.

$$\frac{\partial c'}{\partial \theta} + \frac{\partial c'}{\partial z} = 1/P_e \frac{\partial c^2}{\partial z^2} + \delta(z-z_o) \quad \delta(\theta) \tag{3.42}$$

Most of the investigation from this point on has been to solve Equation (3.42) for different boundary conditions.

Levenspiel and Smith (62) took the simplest case, shown in Figure: 3.3.

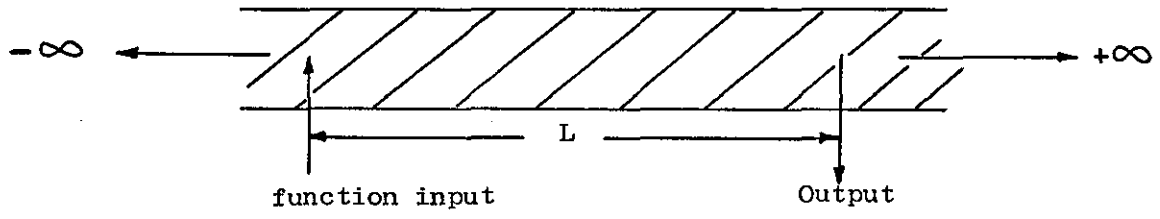

Figure: 3.3.

This is to be an open vessel (i.e. one where neither the entering nor leaving fluid streams satisfy the plug flow requirements) and a perfect delta-injection input. The first and second moments for this case are:

$$\mu_1 = 1 + 2/P_e \tag{3.43}$$

$$\sigma^2 = 2/P_e + 8/P_e^2 \tag{3.44}$$

Van der Laan (63) took the boundary conditions which were originally introduced by Wehner and Wilhelm (64), this included dispersion both in the entrance and exit section; see Figure: 3.4.

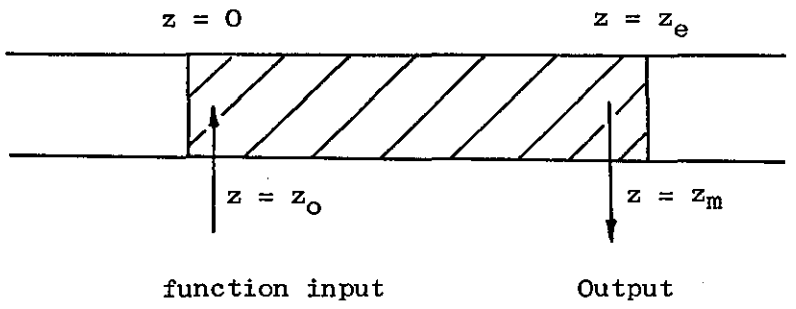

Figure: 3.4.

System was divided into three sections: an entrance section from Z =$-\infty$ to Z = 0 (designated by subscript, a), the test section from Z = 0 to Z = Z_e (no subscript), and the exit section from Z = Z_e to Z = $+\infty$ (subscripted b). The expressions for the first moment, μ_1 , and second moment, σ^2 , work out to be quite complicated:

$$\mu_1 = 1 + 1/P_e \left\{2 - (1-a)\, e^{-P_e z_o} - (1-b)\, e^{-P_e(z_1 - z_m)}\right\} \tag{3.45}$$

$$\begin{aligned}\sigma^2 = {} & 2/P_e + 1/P_e^2 \left\{8 + 2(1-a)(1-b)\, e^{-P_e z_1} - (1-a)\, e^{-P_e z_o}\right. \\ & \left[4\, z_o\, P_e + 4(1+a) + (1-a)\, e^{-P_e z_o}\right] \\ & \left. - (1-b)\, e^{-P_e(z_1 - z_m)} \left[4(z_1 - z_m)P_e + (1+b) + (1-b)\, e^{-P_e(z_1 - z_m)}\right]\right\}\end{aligned} \tag{3.46}$$

where

$$a = \frac{P_e}{P_{ea}}$$

and

$$b = \frac{P_e}{P_{eb}}$$

Equations (3.45) and (3.46) reduce to the solution of Levenspiel and Smith for a = b = 1, for the open system.

In practice it is impossible to inject a perfect delta function input. Aris (31) proposed a technique which is also described in "mixing-cell models" section 3.1.2.2. Figure : 3.2 that eliminated the need to know the shape of the input function; any inputs can be used as long as the initial and the final concentrations are zero. The method is based on measuring the response at two points downstream . Injection point should be upstream before the first measurement point either in the entrance section or into the column itself: see Figure; 3.5.

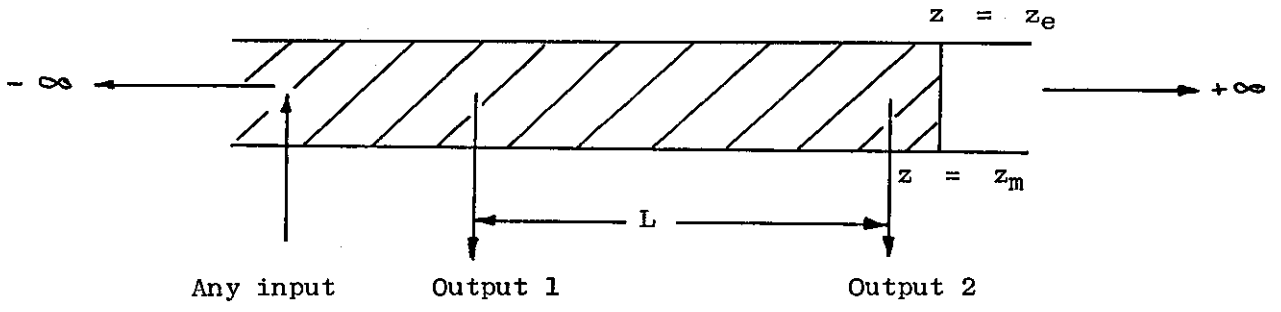

Figure: 3.5.

First moment:

$$\mu_1 = \mu_{1m} - \mu_{1o} = \emptyset_1(P_e, P_{ea}, P_{eb}, z_o, z_m, z_e) \qquad (3.47)$$

Variance:

$$\sigma^2 = \sigma_m^2 - \sigma_o^2 = \emptyset_2(P_e, P_{ea}, P_{eb}, z_o, z_m, z_e) \qquad (3.48)$$

$\emptyset_1$ and $\emptyset_2$ are complicated functions given by Bischoff and Levenspiel (28). A simplification of these expressions occurs when both are measured within the test section as shown in Figure:3.5. see Aris (31) and Bischoff (32).

These expressions reduce even further for the case of an infinite tube or where b = 1 in which case the mean and variance are:

$$\mu_{1o} = 1$$

and $$\sigma^2 = 2/P_e$$

Bischoff and Levenspiel (28) have also calculated mean and variance for the following cases:

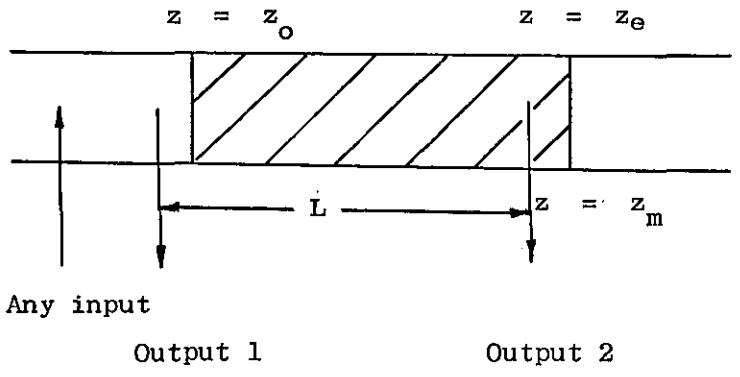

Figure: 3.6.

and

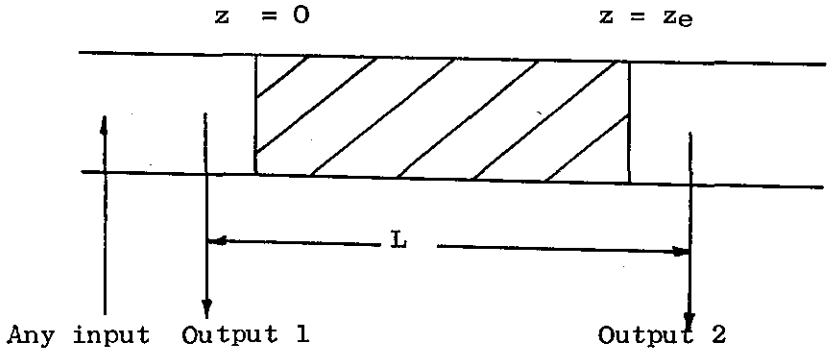

Figure: 3.7.

Data on liquid systems have been obtained by using pulse inputs with a single measurement point by Carberry and Bretton (65)

and Ebach and White (66), only Sater (67) used the method of two measurement points. Step inputs have been used by Ampilogov et al (68), Cairns and Prausnitz (58), Danckwerts(69), Jacques and Vermeulen (56), Klinkenberg and Sjenitzer (29) and von Rosenberg (70). Frequency response methods have been used by Ebach and White (66), Liles and Geankoplis (71), Kramers and Alberda (36) and Straug and Geankoplis (72).

3.1.6. Evaluation of Radial Dispersion Coefficient

In this section methods for measuring radial dispersion will be given briefly. The technique is similar to that outlined for the axial dispersion coefficients, i.e. the injection of a tracer at a point upstream and measuring its concentration at a point downstream, however in this case tracer is injected at the centre of the column.

The dimensionless equation of the type (3.42) was formed, see Bischoff and Levenspiel (28). The method of solution is similar to that for the axially dispersed plug-flow model, however the method was modified to keep both the axial and the radial dispersion terms in the equation.

Various simplifying assumptions and boundary conditions lead to the following results:

a) For the case :

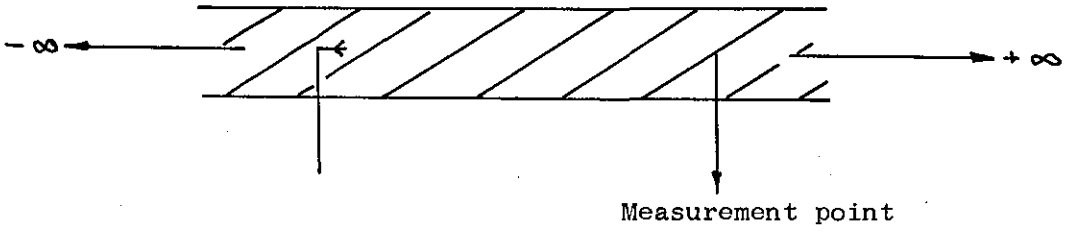

Towle and Sherwood (73) arrived at the following solution:

$$C = \frac{P_{eR}}{4} \quad \frac{\exp\left[-P_{eR}\left(\sqrt{z^2 - r^2} - z\right)\right]}{\sqrt{\left(z^2 + r^2\right)}} \qquad (3.49)$$

Bernard and Wilhelm (74), Klinkenberg et al (75), Fahien and Smith (76), Bischoff and Levenspiel (28), Jacques and Vermeulen (56), Latinen (51) and Prausnitz (77), and Blackwell (78) considered various boundary conditions, derived and measured radial dispersion coefficients mainly for liquid systems.

Data on gas systems, again using a point source, was obtained by Bernard and Wilhelm (74), Dorweiler and Fahien (79), Fahien and Smith (76), and Plautz and Johnstone (80). The last authors measured the dispersion coefficients for both isothermal and non-isothermal cases and found the two to be different at low Reynolds numbers.

The data was plotted using the effective diameter as a characteristic length; for fully turbulent flow, liquid and gas data merged, although two types of systems remained different at low Reynolds number.

There was not as much scatter in data on radial dispersion coefficients as there was with axial dispersion coefficients.

3.1.7. Capacitance Differential Model

The measurement of dispersion coefficients in liquid flow system made by Geankoplis et al (71) and other workers produced values which were in sharp disagreement with the perfectly mixing-cell model. Carberry and Bretton (65) inferred this to be due to some kind of capacitance effect that seemed to exist. Deans and Lapidus (35) suggested that the stagnant fluid regions produced the capacitive effect. Now the experimental response curves of a packed column

usually show some degree of asymmetry and "tailing", which cannot be accounted for by dispersion models or mixing-cell model . So in an attempt to reproduce these effects mathematical models based on the proposed capacitive concept, incorporating different possible mass transfer mechanisms, have been put-forward.

Turner (66) proposed two models for packed columns which closely approximated to the true physical situation. The first model considers channels of equal diameters and lengths but with stagnant pockets of different lengths connected to the channels through which mass transfer takes place but only by molecular diffusion. It was assumed that the dispersion in each channel is represented by an axial-dispersed plug flow model, and the axial dispersion coefficient to be equal to that for flow in empty tubes, however Aris (81) showed that it is influenced by the pockets.

The second model considers channels of varying length and diameters and by a procedure similar to one adopted for the first model, he obtained a set of equations.

Deans (82) modified the mixing-cell model to include diffusion or mass transfer into the stagnant fluid pockets, the mass balance equations for the nth cell becomes

$$C_{n-1} - C_n = (1 - f') \frac{dC_n}{d\bar{T}} + f' \frac{dC_n^*}{d\bar{T}} \qquad (3.50)$$

$$f' \frac{dC_n^*}{d\bar{T}} = \bar{\alpha} (C_n - C_n^*) \qquad (3.52)$$

$$n = 1,2,.....\bar{N}$$

where f'is a fraction of cell volume which is non-flowing, C_n^* is tracer concentration in the fraction, $\bar{\alpha}$ is a dimensionless mass transfer parameter.

The author discussed the limiting behaviour of this model: with large values of $\bar{\alpha}$ or f'approaching zero, Equations (3.50) and (3.51) reduce to the mixing-cell model. The limit of large $\bar{N}$ for fixed path length corresponds to a small value of length of the mixing-cell and three-parameter reduce to a one-parameter in this case.

Levich et al (83) showed that Deans model could represent the effects of "stagnant" regions and axial dispersion independently provided finite values of N were used and thus developed approximate solution for large values of N. Buffham and Gibilaro (84) presented the analytical solution of Deans-Levich model, extending the usefulness of the model by enabling any value of N to be used.

Gottschlich (85) presented a "film" model which treated bed capacitance by supposing the stagnant volume to occur as thin film over the packing surface and mixing took place incompletely by molecular diffusion:

the continuity equation was given as :

$$D_L \frac{\partial^2 c}{\partial x^2} - U/\varepsilon_f \frac{\partial c}{\partial x} - \frac{\partial c}{\partial t} - \frac{E - E_f}{E_f} \frac{\partial q}{\partial t} = 0 \qquad (3.53)$$

The equation to describe the mass transfer in the stagnant fluid was written as :

$$D_m \frac{\partial^2 w}{\partial z^2} - \frac{\partial w}{\partial t} = 0 \qquad (3.54)$$

where "q" is average concentration in the stagnant film

D_L = axial dispersion in the stagnant film.

D_m = molecular diffusivity of tracer in solution.

w = local tracer concentration in the stagnant film.

Z = distance measured from the pore wall.

Three parameters involved are D_L , the amount of liquid in the film, and a parameter involving film thickness and diffusion coefficient.

Other workers who have discussed differential capacitance models are Van Deemter et al (86), they employed frequency response methods, and Lapidus and Amundson (87) presented a double- integral form of the solution for this model.

Most of the above workers considered dispersion to be an integral effect of a number of mechanisms that contribute to the axial dispersion. Generally, there are two dispersion mechanisms considered:

1. The fluid phase diffusion is characterised by a dispersion coefficient containing the effect of eddy mixing of the fluid as it flows through the void spaces and the effect of molecular diffusion within the fluid.

2. The finite time lag required for transfer between fluid and particle which consists of two distinct steps, transport across a stagnant film surrounding the particles, and transport within the particles which requires time to even out the concentration gradients within the voids.

Van Deemter et al (86), modified the mass transfer work of Lapidus and Amundson (87), approximated their general solution

by a Gaussian solution in which the variances due to mechanism 1 and first step of mechanism 2 were found to be additive. Klinkenberg and Sjenitzer (29) also proposed this idea of additive variances for different mechanisms. Rosen (88) studied the combined effect of mechanism 2 for a concentration step input; Kasten et al (89) made a study of the same mechanism. Deisler and Wilhelm (90) studied all the above mechanisms by using steady state frequency response and presented expressions that showed the individual contributions of the various mechanisms to be additive. McHenry and Wilhelm (91) work on gases indicated the dispersion to be due to the machanism 1 only, and that transfer between particle and fluid does not occur; they also showed that at high velocity, dispersion is essentially due to eddy mixing of fluid. Gottschlich (85) subdivided eddy mixing into interstitial velocity effects and capacitance effect of a stagnant fluid film. Glaser (92,93) and co-workers also suggested subdividing the eddy mixing in the same manner and discussed the relative contribution of each effect. Babcock et al (94) described a means of determining the exit profile of a packed column in which axial dispersion of the step input was considered as a result of all the above listed mechanisms.

Nomenclature

a	P_e/P_{ea}
a_k	surface area of packing per unit volume of bed, sq. ft. / cu. ft.
$a_k d_k$	packing characteristic
b	constant in Equation (3.4), section 3.1.1.
b	P_e/P_{eb}, section 3.1.5.
$\underline{b}$	constant in Equation (3.3.), section 3.1.1.
c	concentration
c'	normalised concentration
c_o	initial concentration
C	concentration
$d_k d_p$	nominal packing diameter
d_{ps}	diameter of the sphere having the same surface area as the piece of packing, Equation (3.6.)
d_i'	hydraulic diameter of the smallest inner area of a ring.
D_m	molecular diffusivity
D	dispersion coefficient
D_L, D_L'	axial dispersion coefficient, dispersed plug flow model
D'_{Lm}	axial dispersion coefficient, uniform dispersion model
$D_L(R)$	axial dispersion coefficient, general dispersion model in cylindrical coordinates
D_R	radial dispersion coefficient, dispersed plug flow model
$D_R(R)$	radial dispersion coefficient, cylindrical coordinates
E_G	volume fraction occupied by the gas phase
E_L or E_f	volume fraction occupied by the liquid phase
E_T	total void volume
f'	fraction of cell volume which is non-flowing Equation (3.50)

g	acceleration due to gravity
H_{op}	operating holdup
H_{st}	static holdup
H_T	total holdup
i	number of ideal stirred tanks in series
I_o	Bessel function
j	number of ideal stirred tanks in series
L	liquid mass flow rate, lb/hr-sq.ft.,section 3.1.1.
L	distance between measurement points
m	exponent in Equation (3.7)
n	exponent in Equation (3.13)
n	number of cells, section 3.1.2.2.
N	packing number density
N_{Fr}	Froud number
N_{Ga}	Galileo number
N_{Re}	Reynolds number
N_{We}	Weber number
P_e	(UL/D), dimensionless parameter
r	dimensionless radial position
r_c	rate of chemical reaction
s	exponent in Equations (3.4) and (3.6)
s	source term
t,T	time
U	velocity vector in Equations (I) to (V)
U	superficial velocity , Equation (3.10)
U_s	interstitial velocity
v	volumetric flow rate
V	total void volume of the packing
V_n	volume of the nth cell

w	local tracer concentration in the stagnant film
x,X	axial position measured from the start of the test section
X	variable in Equation (3.14)
X_k	a common critical value as defined in Equation (3.14)
X_r	a reduced dimensionless function , $X_r = X/X_k$
z,Z	dimensionless axial variable
$\bar{\alpha}$	dimensionless mass-transfer parameter Equation(3.52)
μ	viscosity
$\mu 1$	mean of the tracer curve at measurement point
	density
σ^2	variance of the tracer curve at measurement point
$\emptyset$	tortuosity factor
a	refers to entrance or upstream
b	refers to exit or downstream
e	refers to the end of test section
m	refers to single measurement point or to the second of two measurement points
o	refers to the injection point or the first of two measurement points
	refers to doubly infinite tube, the open vessel

4. TIME DELAY MODELS

4. Time Delay Models

The method of formulating models, based on a simplified physical representation of a process has been proved to be capable of solving problems that become too complicated when tackled by classical methods. However, the usefulness of a model depends on how accurately it describes the performance of a system over a reasonably wide range of operating conditions. The approach can be either entirely empirical, such as is the case of tanks-in-series model, or it can be of a more fundamental nature, actually describing the intrinsic mechanisms of the process, for example a mathematical equation representing flow and diffusion effects. In general it is desirable to have flexible models applicable to a variety of situations - not necessarily exactly defining a particular system - than a more complex one accurately describing the behaviour of one such system.

The time delay model represents a simple and a physically plausible picture of flow in many engineering processes, the trickle flow in packed beds is one such process.

Consider a packed bed down which liquid flows in the form of a highly distorted film partly covering the packing; there are stagnant regions at points of contact in the packing, between the packing and the walls, and on horizontal surfaces. Downward flow takes place mainly in the film; the effect of the slow flow in the almost stagnant regions is to remove some of the liquid from the film flow and return it some time later.

In the absence of turbulence the velocity at any point in the liquid is constant. In principle one can imagine calculating the time it would take for a particular fluid element to pass through the bed from fluid mechanic considerations. Although this calculation could

not recognise the existance of random molecular motion it is worth persisting with the fluid mechanic picture for the insight it provides into the mechanism. From this point of view, as passage through the bed is a deterministic process, it is only necessary to say where a fluid element enters the bed to be able to say where and when it will leave. If tracer is released at the bed entrance, it will travel in the film for a short distance but soon some will enter near-stagnant regions and be delayed until later it returns to the main stream. Different tracer elements will be delayed more or fewer times depending on the path they take; some will pass through faster than all the others, there being an absolute minimum transit time through the bed. With respect to this minimum, delay occurs because not all of the main stream moves at the same speed, not all the paths are of the same length and so on.

The hydrodynamic time-delay model is based on this qualitative description. The hypothesis is that it is a reasonable idealisation to consider the flow to be made up of axial and lateral components as indicated in Figure:4.1. Delay is due to fluid elements passing into lateral passages and returning later at the same axial position. Stream splitting causes lateral mixing so that if entry into a lateral pore is relatively rare "after effects" will be relatively unimportant. This is idealised by assuming perfect lateral mixing of the main stream: at any axial position the behaviour of particles that have been delayed is indistinguishable from those that have not. It is assumed that all hydrodynamic mechanisms can be accounted for in this way by suitably choosing the distribution of delay times.

In the analysis below it is shown how the hydrodynamic flow model can be treated in a deterministic way by writing a differential material balance. However, there is an immediate probabilistic interpretation that suggests that the model applies more generally. With the assumption of perfect lateral mixing, assigning the ratio of the

lateral flow to the forward flow in a differential element of bed length amounts to assigning the probability of a given fluid element being delayed at that point. The return process is independent of the stopping process. Clearly the process of diffusion into pores can be described in a similar way by introducing extra micro-scale lateral flows superimposed on the hydrodynamic lateral flows. The role of lateral diffusion in the main stream is to put the assumption of perfect lateral mixing on a sounder basis while it is assumed that the effects of axial diffusion can be lumped into the general delay process.

4.1. Distributed Parameter Model

The basic postulate of the time-delay treatment is that the flow can be considered as a forward flow and a lateral flow, the former alone serving to transfer material in the axial direction. Referring to Figure:4.1, the main forward flow rate is F and the lateral flow rate is f per unit length. If the transit time through the lateral passages is a constant, t_D, a material balance over a differential length of the main flow passage yields:

$$A \frac{\partial c(x,t)}{\partial t} = -F \frac{\partial c(x,t)}{\partial x} + f\, c(x,t-t_D) - f\, c(x,t) \qquad (4.1)$$

It can be seen that if the input to the bed is an impulse of tracer material the output will be a sequences of impulses; the first occuring at the minimum residence time t_o and the rest being seperated by intervals of t_D, the only delaying mechanism being the fixed delay t_D in the lateral 'pores'. In order to relax the condition that t_D is constant it is necessary to split f into components with differential t_D values,

either in a continuous or discrete way.

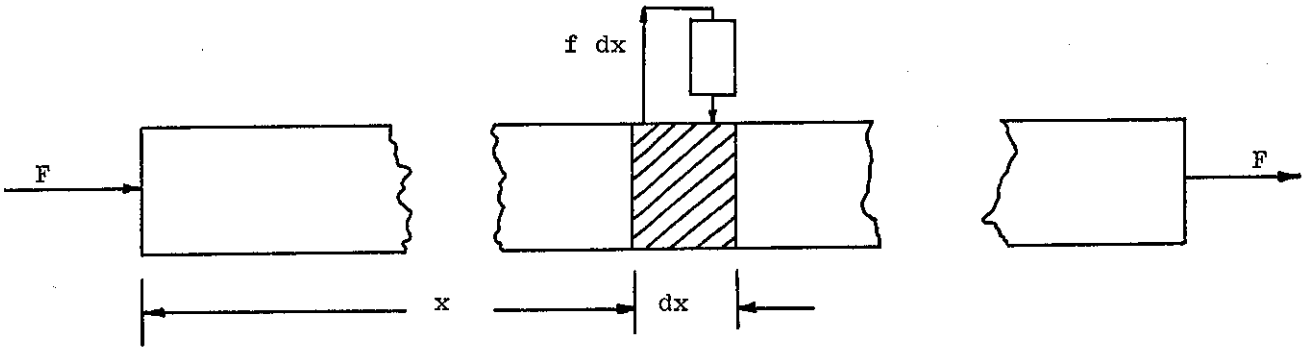

Figure: 4.1.

4.2. Lumped Parameter or Cell Model

The notion of expressing diffusion equations in terms of mixing cells has been quite fruitful, especially when the object has been to calculate dispersion constants from first principles (95) or to determine liquid distribution (12). Basically the diffusion equation is expressed in finite difference form and the mesh size is identified in some way with the packing size. The same procedure can be adopted in the present case. Figure:4.2 shows the cell model equivalent to the fixed time-delay flow-model. The convention is adopted that an elongated rectangle indicates a plug flow region and a square a perfectly mixed 'cell'. The result of an impulse tracer input will be an output consisting of a sequence of identically shaped pulses each delayed in time by some integer multiple of t_D. It is easy to see how the cell model can be modified to take account of a distribution of lateral pore transit times. For example if the pore transit times are exponentially distributed the appropriate modification would be to replace the lateral pore plug-flow region with a stirred tank, Figure:4.3. This particular case with a finite sequences of N identical units has been suggested as a model for flow through beds of porous material (83). Increasing the number of units

in the cell model to infinity, while keeping the total system volume constant, reduces it to the equivalent continuously distributed flow model with the same distribution of delay times.

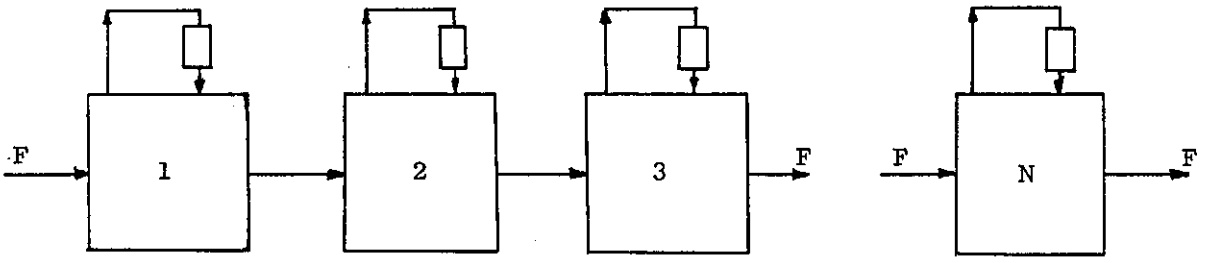

Figure: 4.2.

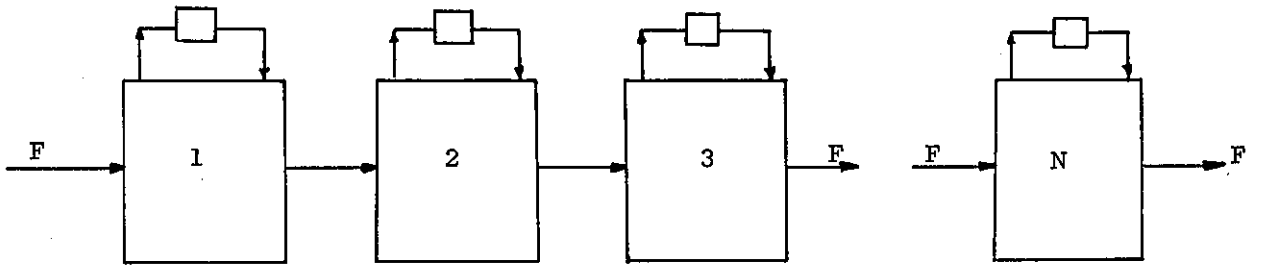

Figure: 4.3.

4.3. Probabilistic Treatment

In the flow-model and the cell-model it is considered that at splitting nodes, which are continuously distributed in the former case and at discrete points in the latter case, the concentrations of the streams into which flow divides are equal. Conversely at merging nodes the mixing is instantaneous and perfect. In terms of concentrations the analysis is deterministic provided that the flows are constant. If the input is a unit impulse the output is identical with the residence time distribution, a concept which is meaningful without any probabilistic interpretation. However, one can imagine a tracer experiment being carried out with a single tracer molecule, in which case the result of the experiment would be random. A tracer experiment can be regarded as the simultaneous performance of an extremely large number of single-molecule

experiments, so that the measured impulse response may be regarded as a frequency diagram for many individual molecule experiments. The usual abstraction of probability theory is to say that a frequency diagram constructed for a sufficiently large number of independent trials is identical with the probability density diagram. Conversely for a given mathematical model the residence time distribution can be calculated by determining the probability that a molecule will pass through the system in a given time.

The probabilistic treatment of the time-delay model falls into two independent parts: establishing the distribution of the number of times a particle stops, and then assessing the effect of the random nature of the stopping process itself. Generally there will be several ways in which a tracer particle can pass through the bed in a given time; the probabilities of these ways must finally be combined.

4.3.1. Stopping Process

Stopping is a stochastic process and the number of stops, n, can only take non-negative integral values. Discrete random processes of this type are the basis of many branches of applied probability theory, for example queueing theory. The random events considered are usually sequential in time rather than in space, but this makes no difference to the mathematical analysis.

Two independent probabilistic approaches have been adopted to establish the distribution of particle stopages.

Continuous approach

Referring to Figure:4.1, the proportion of tracer particles arriving at x that enters lateral pores in the bed zone $(x,x+dx)$ is $(f/F)dx$. This may be restated in terms of probability by saying that the probability of a particle, which has arrived at x, entering a lateral pore in $(x,x+dx)$ is $(f/F)dx$. As there is no need to take the original

model too literally suppose merely that the stopping probability is αdx, where α is a constant to be identified empirically, or perhaps related to other concepts in a separate theoretical excercise.

Now let the probability of a particle being delayed n times while travelling a distance x be, $p_n(x)$, then the probability that a particle is delayed n times while travelling a distance (x+dx) is $p_n(x+dx)$. There is no reason to suppose that whether a particle is delayed depends on whether or not it has been delayed previously; that is to say the events are independent.

n retardations in distance (x+dx) can occur as follows:

n in (0,x), 0 in (x,x+dx)

(n-1) in (0,x), 1 in (x, x+dx)

(n-2) in (0,x), 2 in (x, x+dx)

and so on.

The corresponding probabilities are obtained by multiplying the probabilities of the constituent events, as these are independent. Hence:

$$p_n(x+dx) = p_n(x)\,(1-\alpha dx) + p_{n-1}(x)\alpha dx + 0\left\{(dx)^2\right\} \tag{4.2}$$

or

$$\frac{p_n(x+dx) - p_n(x)}{dx} = \alpha\, p_{n-1}(x) - \alpha\, p_n(x) + 0dx \tag{4.3}$$

In the limit as $dx \longrightarrow 0$

$$\frac{dp_n}{dx} = \alpha\,(p_{n-1} - p_n) \tag{4.4}$$

Now, it is certain that a particle is not delayed in travelling no distance and it is impossible for a particle to be delayed in travelling no distance.

Therefore the initial conditions are:

$$p_o(0) = 1 \tag{4.5}$$

$$p_1(0) = p_2(0) = p_3(0) = \ldots = 0 \tag{4.6}$$

This set of equations is satisfied by:

$$p_n(x) = \frac{(\alpha x)^n}{n!} e^{-\alpha x} \tag{4.7}$$

a result established by substituting $n = 0,1,3,..$ successively and solving the resulting differential equations. Equation (4.7) indicates n to be distributed in a Poisson distribution with parameter αx.

Discrete approach

This approach considers the physical analogue of n stirred tanks. Consider the packed length to consist of n small sections of each length δx, as shown in Figure:4.1.

The probability $p_o(x)$ of an element moving right through the whole packed length without being delayed is:

$$p_o(x) = \left(\frac{F}{F+f\,\delta x}\right)^{x/\delta x}_{n} = \left(\frac{1}{1+\alpha x/n}\right) \tag{4.8}$$

In the limit as $n \longrightarrow \infty$

$$p_o(x) = \lim_{n \to \infty} \left(\frac{1}{1+\alpha x/n}\right)^n$$

$$= e^{-\alpha x} \tag{4.9}$$

The probability of being delayed once in a particular increment

δx is:

$$p_1(\delta x) = \left(\frac{1}{1 + \alpha x/n-1}\right)^{n-1} \frac{f\ \delta x}{F + f\ \delta x} \tag{4.10}$$

In the limit as $\delta x \longrightarrow 0$ and $n \longrightarrow \infty$

$$p_1(\delta x) = \lim_{\substack{\delta x \to 0 \\ n \to \infty}} \frac{f\ \delta x}{F}\ e^{-\alpha x}$$

$$= \frac{f}{F}\frac{x}{n}\ e^{-\alpha x} \tag{4.11}$$

that is : $$p_1(x) = \alpha x\ e^{-\alpha x} \tag{4.12}$$

The probability $p_2(2\ \delta x)$ of two delays in two specific increments (both could also be in the same increment) is:

$$p_2(2\ \delta x) = \left(\frac{1}{1 + \alpha x/n-2}\right)^{n-2} \frac{(\alpha x)^2}{n^2} \tag{4.13}$$

In the limit as $\delta x \longrightarrow 0$ and $n \longrightarrow \infty$

$$p_2(2\ \delta x) = \lim_{\substack{\delta x \to \\ n \to \infty}} \left(\frac{1}{1 + \alpha x/n-2}\right)^{n-2} \frac{(\alpha x)^2}{n^2}$$

$$= \frac{(\alpha x)^2}{n^2}\ e^{-\alpha x} \tag{4.14}$$

The two delays can occur in $\frac{n^2}{2!}$ ways so that:

$$p_2(x)_{\delta x} = \frac{(\alpha x)^2}{2!}\ e^{-\alpha x} \tag{4.15}$$

Following the above procedure, a general expression $p_n(x)$

for n delays can be derived:

$$p_n(x) = \frac{(\alpha x)^n}{n!} e^{-\alpha x} \qquad (4.16)$$

4.3.2. The Delay Process and Residence Time Distribution

So far nothing has been assumed about the delay process itself. In statistical treatment of processes in which a prototype process is repeated many times, the final result is not very sensitive to the detailed description of the prototype. In order to predict the residence time distribution as simply as possible, the pore residence time distribution should be simple and easily combined. In view of the analogy between the time delay model and the surface renewal models of steady state mass transfer and the success of those models, suitable choices for the pore residence time distribution include the impulse distribution - Higbie's (96) model - and the exponential distribution proposed by Danckwerts (69). Physically these distributions correspond to the pores or pockets being regions of either plug-flow or perfect mixing. This is not to say that these conditions exist physically, but merely that the observed behaviour can be described in this way. For instance a situation in which perfect mixing is obtained in the pores is indistinguishable from plug-flow in pores where the residence times are exponentially distributed due to the difference in lateral flow rates and pore sizes.

4.4 Fixed Time Delays

For those tracer elements which make n stops in their journey through the bed, the total delay time is the sum of n independent observations from the pore residence time distrbution. For the case of plug-flow in pores the sum of n independent observations is nt_D and

those tracer elements that are delayed n times emerge from the bed after a residence time (t_o+nt_D); so that the probability of an element emerging after t is given by:

$$p(t) = \frac{(\alpha x)^n}{n!} e^{-\alpha x} \tag{4.17}$$

where $n = \dfrac{(t - t_o)}{t_D}$

It follows that the residence time distribution, $\emptyset(t)$, may be written as:

$$\emptyset(t) = e^{-\alpha x} \sum_{n=o}^{\infty} \frac{(\alpha x)^n}{n!} \delta(t - t_o - nt_D) \tag{4.18}$$

where $\delta(\quad)$ is the Dirac delta function.

4.4.1. Exponentially-Distributed Time Delays

The exponential distribution is the case of perfect mixing in the pores, it is given by:

$$f(\theta) = \frac{1}{t_D} e^{-\theta/t_D} \tag{4.19}$$

This distribution goes under a variety of names in the literature: in queueing theory it is known as the Erling distribution and n is restricted to integral values; as the Gamma distribution when this restriction does not apply - this particular case has been presented further on in section 4.4.2; it is also closely related to Chi-square distribution.

The sum of n independent observations, θ, from an exponential distribution with mean, t_D, has the probability desity function:

$$g_n(\theta) = \frac{t_D^{-n}\ \theta^{n-1}}{(n-1)!}\ e^{-\theta/t_D} \qquad (4.20)$$

as may be established by an n-fold convolution of an exponential, or by considering the physical analogue of n stirred tanks.

The total delay time distribution is obtained by weighting the $g_n(\theta)$ by the $p_n(x)$ and summing over all values of n. The justification for this procedure is that the probability of both being delayed n times and being delayed for total time in the interval $(\theta, \theta + d\theta)$ is $p_n(x)\ g_n(\theta)\ d\theta$ by the multiplication rule for conditional probabilities; and as the ways of being delayed for this time in different numbers of stops are mutually exclusive the probability regardless of n is obtained by summing over all possible values of n. The residence time distribution is obtained by displacing the total delay time by t_o with the result:

$$\phi(t) = 0 \quad , \qquad t < t_o$$

$$= \frac{e^{-(\alpha x + t^*/t_D)}}{t^*} \sum_{n=0}^{\infty} \frac{(\alpha x\ t^*/t_D)^n}{n!\ (n-1)!} \ , \qquad (4.21)$$

$$t \geq t_o$$

where $t^* = (t - t_o)$. The first term in the series in an impulse which is usually negligible in practice, so that Equation(4.21) could be expressed in terms of a Bessel function:

$$\phi(t) = 0, \qquad t < t_o$$

$$= e^{-(\alpha x + t^*/t_D)} \sqrt{\frac{(\alpha x)}{t_D\ t^*}}\ I_1\left(2\sqrt{\frac{(\alpha x\ t^*}{t_D}}\right) \qquad (4.22)$$

4.4.2. Gamma-Distributed Time Delays

Corrigan et al (97) suggested the addition of a recycle stream to the tanks-in-series model to increase the dispersion. It enabled the responses of the tanks-in-series model to be fitted for the values of n that lie between n and $(n-1)$. This renders the model more flexible especially at low values of n. It also introduced other less desirable features, such as oscillating responses at low recycle rates; van de Vusse(98) has shown this to be true for values of $n > 2$.

An alternative modification of the tanks-in-series model that does not suffer from this disadvantage is to allow n to take non-integral positive values. The inversion of a transfer function for a tanks-in-series model is given by:

$$f_1(t) = \frac{t^{n-1}\, e^{-t/t_D}}{t_D^n\ (n-1)!} \qquad (4.23)$$

For non-integral values of n the inversion becomes:

$$f_2(t) = \frac{t^{n-1}\, e^{-t/t_D}}{t_D^n\ \Gamma(n)} \qquad (4.24)$$

where $\Gamma(n)$ is a gamma function of n defined by the integral:

$$\Gamma(n) = \int_0^{\infty} e^{-x}\, x^{n-1}\, dx \qquad (4.25)$$

and converges for all positive values of n.

If the distribution transfer function is taken as:

$$f(s) = \frac{1}{(t_D s/m + 1)^m} \qquad (4.26)$$

where m is not necessarily an integral, then the gamma distribution

is:

$$f_m(t) = \frac{\left(\frac{t_D}{m}\right)^{-m} t^{m-1}}{\Gamma(m)} \; e^{-m\, t/t_D} \qquad (4.26a)$$

the mean being t_D regardless of the value of m.

By following the reasoning given in section 4.4, for the exponentially distributed time delays, the residence time distribution for the present case can be obtained by displacing the total delay time by t_o with the result:

$$\begin{aligned} \phi(t) &= 0, \qquad t < t_o \\ &= e^{-(\alpha x + mt^*/t_D)} \sum_{n=0}^{\infty} \left(\frac{m}{t_D}\right)^{mn} \frac{t^{*mn-1}}{(m)} \; \frac{(\alpha x)^n}{n!}, \qquad (4.27) \\ & \qquad\qquad t \geq t_o \end{aligned}$$

where $t^* = t - t_o$. The first term in the series is again an impulse which in practice, is usually negligibly small.

4.5. Hopping Model

The hopping model is a modified time-delay model in which delayed material returns to the main stream at some axial distance from the point where the delay took place. The flow mechanism suggested here is again quite a feasible one and bears a resemblance to the steady state model proposed by Porter (99) describing random splitting and merging of fluid streams. The cumulative effect of the individual time delays and hopping times is to distribute the total residence time in some way.

The probabilistic treatment of the model again falls into two separate sections: the establishment of the distribution of the number of complete hops a particle makes and the estimationof the random

nature of the delay process during the hop. There are a number of ways that particles can pass through the column whose probabilities must be combined together.

4.5.1. Hopping Process

Consider a particle moving along a line; the probability of the particle leaving in an elemental length dx is αdx, which has been shown in section 4.3, i.e. the probability of a particle starting a hop in the element dx is αdx. If a particle hops at x, it moves to $(x + h)$, where h is the hopping distance.

Let the probability of not hopping in a distance x be $p_o(x)$, then the probability of not hopping in distance $(x + dx)$ is:

$$p_o(x + dx) = p_o(x) \left[1 - \alpha dx\right]$$

and the solution as before is:

$$p_o(x) = e^{-\alpha x} \tag{4.28}$$

To find the probability of n complete hops first consider a specific sequence of hops occuring at $x_1, x_2, \ldots\ldots, x_n$; see Figure:4.4

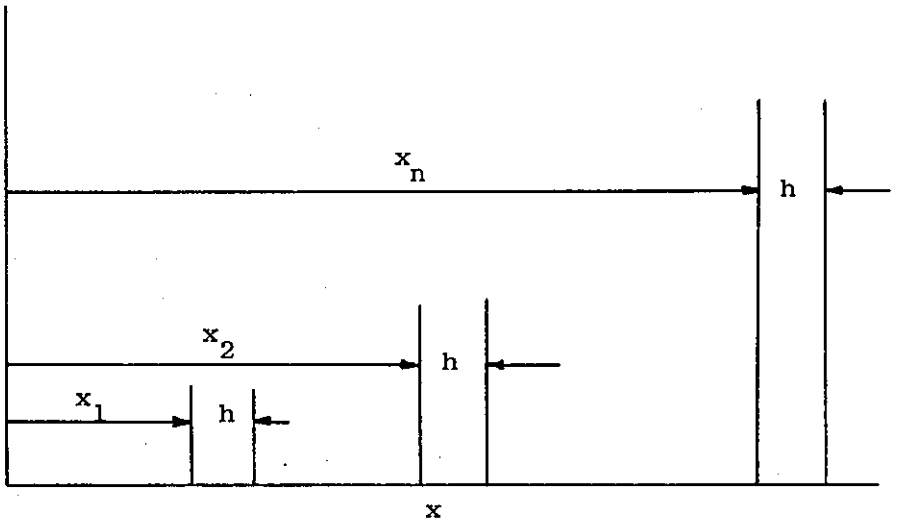

Figure: 4.4.

The probability, $p'_n(x)$, of this sequence occuring is:

$$p'_n(x) = e^{-\alpha x_1}\,\alpha dx_1 e^{-\alpha\,[x_2-(x_1+h)]}\alpha dx_2 \ldots\ldots e^{-\alpha\,[x_n-(x_{n-1}+h)]}\alpha dx_n \times e^{-\alpha\,[x-(x_n+h)]} \tag{4.29}$$

$$= e^{-\alpha(x - nh)}\,\alpha^n\, dx_1 dx_2 \ldots dx_n \tag{4.30}$$

Hence the probability, $p_n(x)$, of exactly n complete hops occuring is:

$$p_n(x) = \int_{(n-1)h}^{x_n-h} \int_{h}^{x_2-h}\int_{0}^{x_2-h} dx_1 dx_2 \ldots\ldots dx_n \alpha^n\, e^{-\alpha(x - nh)} \tag{4.31}$$

which is obtained by integrating over all possible values of $x_1, x_2, \ldots x_n$. For example if the second hop occurs at x_2, the first hop must have occured in $(0, x_2 - h)$; if the third hop occurs at x_3, the second must have occured at $(h, x_3 - h)$ and so on until finally the nth hop must have occured at $((n-1)h, x - h)$.

The multiple integral, Equation(4.31), is evaluated by successive substitution:

$$\int_{0}^{x_2-h} dx_1 = x_2 - h \tag{4.32}$$

$$\int_{h}^{x_3-h} (x_2 - h)\, dx_2 = \int_{0}^{x_3-2h} y\, dy = \frac{(x_3 - 2h)^2}{2!} \tag{4.33}$$

$$\int_{2h}^{x_4-h} \frac{(x_3 - 2h)^2}{2!} dx_3 = \int_{0}^{x_4-3h} \frac{y^2}{2!}\, dy = \frac{(x_4 - 3h)^3}{3!} \tag{4.34}$$

and so on, in general for $i < n$

$$\int_{(i-1)h}^{x_{i+1}-h} \int_{h}^{x_3-h} \int_{0}^{x_2-h} dx_i \ldots dx_2 dx_1 = \frac{(x^{i+1} - ih)^i}{i!} \qquad (4.35)$$

and finally:

$$\int_{(n-1)h}^{x-h} \frac{\{x_n - (n-1)h\}^{n-1}}{(n-1)!} dx_n = \int_{0}^{x-nh} \frac{y^{n-1}}{(n-1)!} dy$$

$$= \frac{(x - nh)^n}{n!} \qquad (4.36)$$

thus substituting in Equation(4.31) gives:

$$p_n(x) = \frac{\{\alpha(x - nh)\}^n}{n!} e^{-\alpha(x - nh)} \quad \text{for } n \leq x/h \qquad (4.37)$$

If $h = 0$, Equation (4.37) reduces to the stopping (time delay) model:

i.e. $$p_n(x) = \frac{(\alpha x)^n}{n!} e^{-\alpha x} \qquad (4.7)$$

and in particular if $h = x$,

$$p_0(x) = 1$$

$$p_1(x) = 0$$

that it is impossible to execute a complete random hop of distance h, while travelling a total distance h.

4.5.2. The Delay Process and Residence Time Distribution

The case of complete mixing in pores is considered here; during each complete hop a patricle can be assumed to pass through a perfectly mixed tank of mean time, t_D, otherwise following the axial plug-flow. For n such tanks the residence time distribution for an impulse input and pure dead time, t_o, is:

$$f'(t) = \frac{(t - t_o)^{n-1}}{t_D^n\,(n-1)!}\, e^{-(t - t_o)/t_D} \tag{4.38}$$

The distribution of the number of times a particle hops would range between 1 and n complete hops; the probability of this distribution is given by Equation(4.37). Therefore the response of the hopping model consists of:

$$\text{Material that did not hop} = e^{-\alpha x}\,\delta(t - t_o) \tag{4.39}$$

$$\text{Material that hopped once} = \frac{\alpha(x - h)}{1!}\, e^{-\alpha(x - h)}\, \frac{e^{-(t - t_o)/t_D}}{t_D^2} \tag{4.40}$$

$$\text{Material that hopped twice} = \frac{[\alpha(x - 2h)]^2}{2!}\, e^{-\alpha(x - 2h)}\, \frac{(t - t_o)}{t_D^2}\, e^{\frac{-(t-t_o)}{t_D}} \tag{4.41}$$

$$\text{Material that hopped n times} = \frac{[\alpha(x - nh)]^n}{n!}\, e^{-\alpha(x - nh)}\, \frac{(t - t_o)}{t_D^n\,(n-1)!}\, e^{\frac{-(t-t_o)}{t_D}} \tag{4.42}$$

The sum of these individual contributions is the final response:

$$\phi'(t) = \sum_{n=0}^{N_{max.}} p'_n(x)\, \frac{(t - t_o)}{t_D^n\,(n-1)!}\, e^{-\frac{(t - t_o)}{t_D}} \tag{4.43}$$

Now the maximum value of the number of hops, $N_{max.}$, is determined by the integer x/h; in practice both, the length, x, and the hopping distance,

h, have finite values. After n complete hops a particle would rejoin the main flow stream, that is in plug-flow, an axial distance, nh, down stream, thus emerging earlier than the material that does not hop. This would effect the overall residence time distribution by varying the dead times of individual elements. Thus modifying Equation(4.43) as follows:

$$\phi''(t) = \sum_{n=0}^{N_{max.}} p'_n(x) \quad \frac{t-t_o(1-nh/x)}{t_D^n\,(n-1)!} \quad e^{-\frac{t-t_o(1-nh/x)}{t_D}} \tag{4.44}$$

If the hopping process is visualised as shown in Figure:4.5, it becomes clear that the hopping probabilities cannot sum to unity. It is due to the finite bed length; at the exit of the bed, hopping of particle would occur outside the bed.

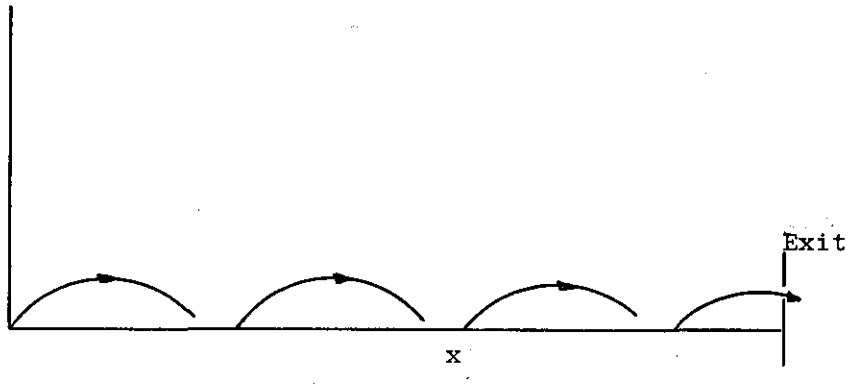

Figure: 4.5.

To eliminate this complication, provision has been made by dividing each hopping probability with the overall hopping probability based on the finite bed length and summing it over all possible values of n. Mathematically this is achieved as follows:

$$\text{say} \qquad N_{max.} = \text{integer}(x/h) \tag{4.45}$$

$$\text{Overall hopping probability} \quad P = \sum_{n=0}^{N_{max.}} p'_n(x) \tag{4.46}$$

The new probability is now defined as:

$$p_n(x) = \frac{p'_n(x)}{P} \tag{4.47}$$

which sums to unity over $n = N_{max.}$

$$\text{i.e.} \quad \sum_{n=0}^{N_{max.}} p'_n(x) = \sum_{n=0}^{N_{max.}} \frac{p'_n(x)}{P} = 1 \tag{4.48}$$

The value of average number of hops:

$$N_{av.} = \sum_{n=1}^{N_{max.}} p'_n(x).\ n \tag{4.49}$$

and the final residence time distribution expression for the hopping model is thus:

$$\phi(t) = \sum_{n=0}^{N_{max}} p_n(x) \quad \frac{t-t_o(1-nh/x)}{t_D^n\ (n-1)!} \quad e^{-\frac{t-t_o(1-nh/x)}{t_D}} \tag{4.50}$$

This final modification ignores the material that hops out of the bed, Figure:4.5, whilst maintaining the unit area property of the distribution. It makes little difference to the nature of the model response except for cases where the average number of hops is small.

4.6. Normalisation

It is often convenient, especially when dealing with the experimental data, to express residence time distributions in normalised form by converting the time scale to units of the mean time. To preserve the unit area property of the residence time distrinbution, the frequency density is multiplied by the mean time.

4.6.1. Time Delay Models

The mean or expectation is defined by:

$$\bar{t} = E(t) = \int_0^\infty t\, \phi(t)\, dt \tag{4.51}$$

The expectation of a sum is the sum of the expectation of the components of sum so that:

$$E(t) = t_o + E(t^*) \tag{4.52}$$

and further, because the distribution of t^* is made up of infinitely many distributions with weighting factors $\frac{(\alpha x)^n}{n!} e^{-\alpha x}$ and expectation nt_D:

$$E(t^*) = \sum_{n=0}^{\infty} \frac{(\alpha x)^n}{n!} e^{-\alpha x}\, nt_D \tag{4.53}$$

a result that is independent of the delay time distribution.

Hence:

$$\bar{t} = t_o + \alpha x\, t_D \tag{4.54}$$

Often the mean time may be measured independently of the residence time distribution; it is equal to the ratio of the total volume through which flow takes place to the volumetric flow rate. If this condition is to be met the number of adjustable parameters are reduced by one.

Therefore in normalised units, the model response for fixed time delays consists of a series of impulses of strength $p(t/\bar{t})$

separated by $(t_D/\bar{t})$, as indicated in Figure:4.6.

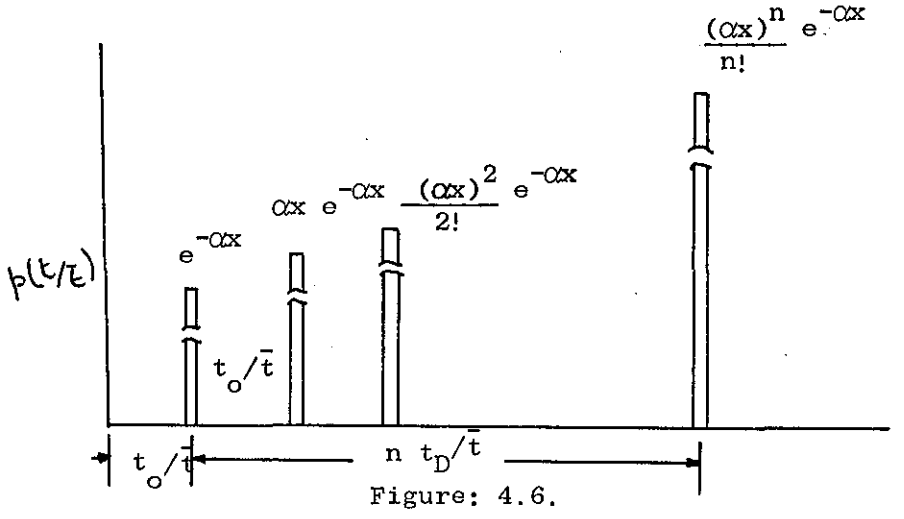

Figure: 4.6.

The real time response of the exponentially distributed delay times is given by Equation(4.21); the mean time, $\bar{t}$, is given by:

$$\bar{t} = t_o + \alpha x\ t_D \tag{4.55}$$

therefore

$$\frac{t_D}{\bar{t}} = \frac{1 - t_o/\bar{t}}{\alpha x} \tag{4.56}$$

Substituting Equation(4.56) in Equation(4.21) expresses the residence time distribution in normalised form:

$$\phi(t/\bar{t}) = e^{-\left[\alpha x + \frac{\alpha x}{(1-t_o/\bar{t})}\ t^*/\bar{t}\right]} \sum_{n=1}^{\infty} \frac{(\alpha x)^2/(1-t_o/\bar{t})\quad t^*/\bar{t}}{n!\ (n-1)!} \tag{4.57}$$

Similarly for gamma distributed time delays Equation(4.27) becomes:

$$\phi(t/\bar{t}) = e^{-\left[\alpha x + \frac{m\ \alpha x}{(1-t/t_o)}\right]\frac{t^*}{\bar{t}}} \sum_{n=1}^{\infty} \frac{m\ \alpha x}{(1-t_o/\bar{t})}\ \frac{(t^*/\bar{t})}{(mn)}\ \frac{(\alpha x)^n}{n!} \tag{4.58}$$

4.6.2. Hopping Model

The mean time, $\bar{t}$, of the hopping model is given by:

$$\bar{t} = \sum_{n=0}^{N_{max.}} p_n(x) \quad t_o(1 - \langle n \rangle h/x) + \langle n \rangle t_D \tag{4.59}$$

where the average number of hops is, $\langle n \rangle$:

$$\langle n \rangle = N_{av.} = \sum_{n=0}^{N_{max.}} p'_n(x) . n \tag{4.60}$$

Therefore $$\bar{t} = t_o \left(1 - \frac{h}{x} N_{av.}\right) - t_D N_{av.} \tag{4.61}$$

and $$\frac{t_D}{\bar{t}} = \frac{1 - t_o/\bar{t}(1 - \frac{h}{x} N_{av.})}{N_{av.}} \tag{4.62}$$

Substitution of Equation(4.62) in the real time expression for the hopping model transforms it to the normalised version:

$$\phi(t) = \sum_{n=0}^{N_{max}} p_n(x) \frac{\left\{t/\bar{t} - t_o/\bar{t}(1 - nh/x)\right\}^{n-1} N_{av.}}{\left\{1 - t_o/\bar{t}(1 - nh/x\ N_{av.})\right\}^{n} (n-1)!}$$

$$X \quad e^{-\left\{t/\bar{t} - t_o/\bar{t}(1-nh/x)\right\} N_{av.} \Big/ \left\{1 - t_o/\bar{t}(1 - h/x\ N_{av.})\right\}} \tag{4.63}$$

4.7. Conclusions

In summary, time delay and related models describe the flow in packed beds in terms of:

a) Main stream axial flow that is either plug-flow (distributed parameter case) or characterised by the tanks-in-series model(cell model).

b) Random delays: the distribution of delays times being conveniently described by the gamma distribution.

c) Return of delayed elements to the main stream at the same axial position at which they were delayed(Time delay models), or at some distance down stream(Hopping model).

Nomenclature

A	cross sectional area through which forward liquid flow takes place
c	tracer concentration
c/c_o	normalised concentration
f	lateral liquid flow rate per unit bed length
F	forward liquid flow rate
h	hopping distance
$g_n(\theta)$	probability density function for θ
m	gamma distribution parameter
n	number of stops
N	number of stages in series
N_{ave}	average number of stops
N_{max}	maximum number of hops
$p_n(x)$	probability of stopping n times while travelling a distance x
$p(t/\bar{t})$	probability of leaving the system at time $t/\bar{t}$
t	residence time in a section of bed of length x
t_D	average delay time
t_o	minimum residence time in a section of bed of length x
$t/\bar{t}$	normalised time
s	Laplace transform parameter
t^*	$t - t_o$
$\bar{t}$	mean residence time
αdx	probability of stopping while travelling a distance dx
θ	the sum of n independent observations from an exponential distribution with mean t_D
$f(t), \phi(t)$	residence time distribution density function
$\Gamma(\ )$	gamma function

5. ANALYSIS OF THE PROPOSED MODELS

5. Analysis of the Proposed Model:

Moments and related characteristic parameters.

In Chapter 4, a probabilistic description of the flow in packed beds has been outlined. The basic concepts considered and the overall description of the model are so general that it can fit many physically occuring processes. There are also mathematical reasons that emphasise the generality of the model, these are best illustrated by first outlining a general transfer function of the model and then analysing the transfer function to study the properties of the model.

5.1. Transfer Function Derivation: distributed parameter case

Consider the discrete cell form of the time delay model by visualising N well-mixed stages in series for the main flow, as shown in Figure:5.1, with the lateral flow of f per unit length of bed, therefore for a bed length x, side flow for each cell is $f\frac{x}{N}$.

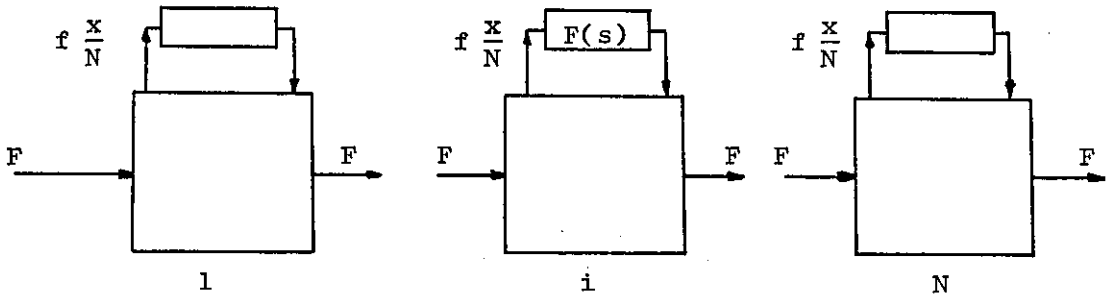

Figure: 5.1.

Let a transfer function F(s) characterise the delay times in the lateral zones; the throughput flow is F and the total holdup of the main flow region V, so that the holdup of one cell is $\frac{V}{N}$.

A mass balance on the ith cell yields:

$$FC_{i-1} + C_i\, f\frac{x}{N} F(s) - C_i\, f\frac{x}{N} - F\, C_i = \frac{V}{N}\,\frac{dC_i}{dt} \qquad (5.1)$$

The Laplace transformation of Equation(5.1) and rearrangement gives:

$$\bar{C}_i(s)\left[1 + \frac{1}{N}\left(\frac{f}{F}x - \frac{f}{F}x\,F(s) + \frac{V}{F}s\right)\right] = \bar{C}_{i-1}(s) \qquad (5.2)$$

letting $\alpha = \frac{f}{F}$

and $t_o = \frac{V}{F}$

Equation(5.2) becomes:

$$\frac{\bar{C}_i(s)}{\bar{C}_{i-1}(s)} = \left\{1 + \frac{1}{N}\left[t_o s + \alpha x - \alpha x\,F(s)\right]\right\}^{-1} \qquad (5.3)$$

Therefore the transfer function, G(s), of the whole system is:

$$G(s) = \left\{1 + \left[\frac{1}{N}\,t_o s + \alpha x - \alpha x\,F(s)\right]\right\}^{-N} \qquad (5.4)$$

The distributed form of the model is obtained by allowing N in Equation(5.4) to approach infinity:

$$G(s) = \exp\left\{-t_o\,s - \alpha x + \alpha x\,F(s)\right\} \qquad (5.5)$$

For reasons discussed in Chapter 4 a suitable choice for F(s) is the transform of the gamma distribution:

$$F(s) = \left(\frac{1}{\frac{t_D}{m} + 1}\right)^m, \quad m > 0 \qquad (5.5a)$$

Expanding the expression for F(s) in Equation(5.5a) and substituting

in Equation(5.5) yields:

$$G(s) = \exp\left\{-(t_o+\alpha x\ t_D) + \frac{(m+1)\ \alpha x\ (t_D s)^2}{2!\ m} - \frac{(m+1)(m+2)\ \alpha x\ (t_D s)^3}{3!\ m^2} + \ldots\right\} \quad (5.6)$$

Equation(5.6) is identical in form to the generalised transfer function of Paynter(100) who showed that a linear dynamic system whose step response is monotonic and nondecreasing with time could be characterised by:

$$G(s) = \exp\left\{-c_1 s + \frac{c_2 s^2}{2!} - \frac{c_3 s^3}{3!} + \ldots\ldots\right\} \quad (5.7)$$

where c_i is the ith cumulant of the impulse response. Cumulants are closely related to moments(101), in fact c_1 is the mean or the first moment about the origin, c_2 is the variance or the second moment about the mean and c_3 is the skewness or the third moment about the mean; fourth and higher cumulants are not as simply related to the moments

Comparing Equation(5.6) and (5.7) the cumulants of the time delay model may be written as:

$$c_1 = t_o + \alpha x\ t_D \quad (5.8)$$

$$c_2 = \frac{(m+1)\ \alpha x\ t_D^2}{m} \quad (5.9)$$

and

$$c_3 = \frac{(m+1)(m+2)\ \alpha x\ t_D^3}{m^2} \quad (5.10)$$

where m may assume any value between zero and infinity. When m is equal to unity exponentially distributed time delay form of the model is obtained whereas zero value of m reduces it to that of fixed delay times.

5.2. Parametric Coefficients

Moments and cumulants are both dimensional quantities; it is somewhat convenient to define another two parameters which are dimensionless, namely coefficient of variance, γ_1, and the coefficient of skew, γ_2. Mathematically these are equivalent to:

$$\gamma_1 = \frac{(c_2)^{\frac{1}{2}}}{c_1} = \frac{\text{Standard deviation}}{\text{Mean}} \tag{5.11}$$

$$\gamma_2 = \frac{c_3}{(c_2)^{3/2}} \tag{5.12}$$

Therefore for the case under study the corresponding values are:

$$\gamma_1 = \left[\frac{1}{\alpha x}\left\{1 + \frac{1}{m}\right\}\right]^{1/2} (1 - t_o) \tag{5.13}$$

and

$$\gamma_2 = \frac{(m + 2)}{\left[\alpha x\, m\, (m + 1)\right]^{1/2}} \tag{5.14}$$

Equation(5.14) is of interesting form, it shows the significance of skewness relative to the variance, which increases as m decreases; the skewness increases more rapidly than the variance. For large values of m and αx, skewness approaches zero.

5.3. Conclusions

A transfer function of the time delay model has been derived for the general case of any delay time distribution and a particular case, but flexible one, of gamma delay times has been considered.

The final form of the transfer function is such that the cumulants of the impulse response are readily available.

It is shown that the characteristics of model response are extremely sensitive to the gamma distribution parameter, m, particularly for small values of m.

Nomenclature

C	liquid concentration
C_i	liquid concentration of ith cell
$\bar{C}_i$	Laplace transform of the concentration of material leaving ith cell
$F(s)$	Laplace transform of delay time distribution
$G(s)$	system transfer function
i	cell number, counting index
m	gamma distribution parameter
N	number of cells
f	lateral flow rate per unit length of bed
F	throughput flow rate
s	Laplace transform parameter
t	time
t_o	dead time
t_D	average delay time
c_i	ith cumulant
V	volume of main flow region
x	length of bed
α	f/F
$\Gamma(\ )$	gamma function
	ith parametric coefficient

6. EXPERIMENTAL APPARATUS AND OPERATING PROCEDURES

6. Experimental Apparatus and Operating Procedure

Stimulus-response methods were employed to study the liquid side R.T.D. in trickle-flow packed beds. All the experimental work was carried out on counter-current liquid-air continuous flow system.

The effect on the impulse response of varying packed lengths, liquid and air flow rates, and liquid viscosities, was studied. Additional experiments were carried out to measure the contribution of tracer detector R.T.D. on the overall R.T.D. of the liquid. Tracers with different diffusivities were employed to provide some measure of the effect of molecular diffusivity on the axial mixing process.

6.1 Packed Column

A schematic diagram of the packed column and accessory piping is shown in figure 6.1. The column itself consisted of sections of $1\frac{1}{2}$" Q.V.F. glass pipe, each section being 5 feet long. To the lower end of the bed a $1\frac{1}{2}$" copper tube, 6" long, was connected. This section contained an air distributor. The distributor was constructed of $\frac{1}{4}$inch copper tube; one end of this tube was sealed off and coiled into a shape shown in Figure 6.2. Some sixty equally spaced 1/16 inch holes were drilled all round the coil; the assembly was lowered in position and soldered to the wall of the larger tube. A circular gauze was placed on top of the distributor to act as a packing support. A pipe reducer on the $1\frac{1}{2}$inch tube was connected to the $1\frac{1}{2}$inch glass tube that directed the outflowing liquid into the vertical line which carried the tracer detector.

The column was randomly packed with 1/8 x 1/8 inch ceramic Raschig ring packings. The manufacturer's data on the packing is given in Table 6.1. The packing was gently poured into the column after filling with water in order to avoid the danger of breakage. Broken packing causes an increase in pressure drop and mal-distribution of the liquid (102).

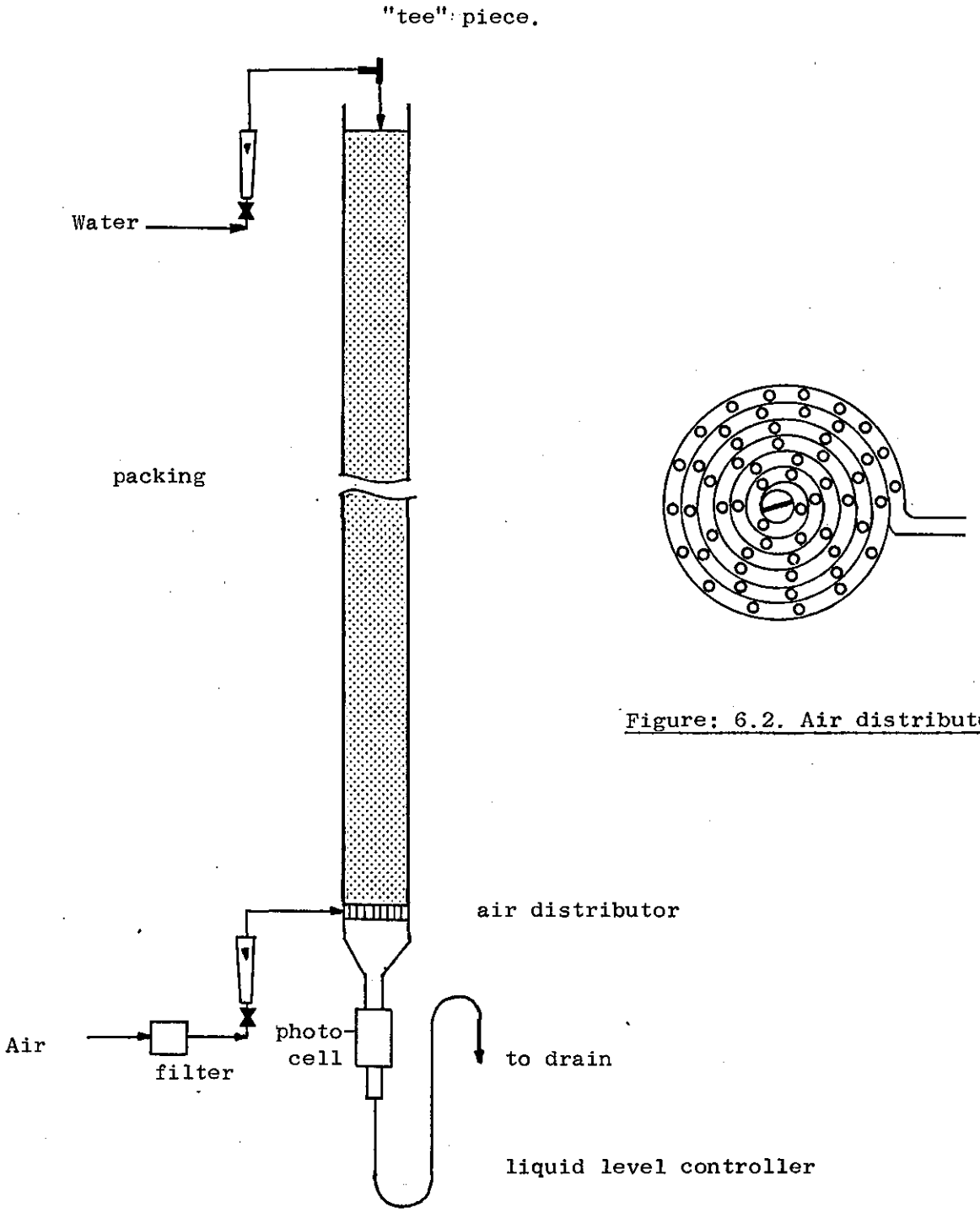

Figure: 6.2. Air distributor

Figure: 6.1. Schematic flow digram

Once the column was packed to the required height, the water was drained off.

Table 6.1 Manufacturer's Packing Data

Packing	Number of units per cubic foot	Surface area of packing:sq.ft/cu.ft	Percent free space
1/8 x 1/8 inch Raschig rings	550,000	360	69

A proper liquid level in the bottom of the column was maintained by attaching a piece of flexible polythene tube that enabled the head, at the down stream end of the return bend to be controlled. The effluent was passed to the drain.

Feed water was taken off a mains header tank on the roof of the building. It passed through a globe valve and a 1-30 ccs/sec. Rotameter, mounted on the column support structure. The globe valve outlet was connected to the Rotameter via $\frac{1}{2}$ inch polythene tubing; a further section of the polythene tubing joined the Rotameter to the "tee" section at the top of the column.

Air was obtained from the compressed air supply available in the laboratory. The mains pressure of 80 psig. was reduced to a working pressure of about 10 psig. by means of a "Taylor" reducing valve. To eliminate any minor fluctuations in the air pressure, a stainless steel buffer vessel was placed between the reducing and the air Rotameter which was connected to the air distributor. (High pressure tubing was used throughout)

Prior to the running of the column, water and air were fed to the packing for a few hours. This ensured the final shrinkage and settling of the packing which would otherwise result in the non-reproducability of response data.

Glycerine-deionised water solutions were prepared to study the effect of varying viscosities. Glycerol of 99% purity was acquired from Wiffins Ltd.. A 200 gallon deionisation plant provided the necessary deionised water. Using the weight/weight % - composition (%) chart, Figure: 6.3, approximate solutions of 4cp and 7cp viscosity were prepared. The exact magnitude of the solution viscosity was later determined with an Ostwald viscometer. Both solutions were stored in standard Q.V.F. spherical vessels of 200 litres capacity, 30 feet above ground level. The outlet of these vessels was connected to the inlet of the rotameter in place of the water line. Before commencing a glycerine-solution run, the solution was allowed to flow through the packed column to replace the water.

6.2. Tracers and Tracer Injection Technique

Two types of detector devices were employed. The photocell was used during water-air impulse response experiments with the "Nigrosine" dye solution as a tracer in the liquid phase. However, the limited supply of the glycerine-water solution and the limited working range of the photocell at all but very low concentrations rendered re-use of the dye-contaminated glycerine-solution impractical; for this purpose the conductivity cell detector was found to be more suitable.

The tracer solutions were injected into the flow system through the "tee" piece at the top of the packed column, by means of a graduated 5ccs. hyperdermic syringe. It was found to be sufficient to introduce only ½cc. of the tracer solution; it required about ½ second for the injection. Because the time taken to introduce the tracer is so small compared with the system mean residence time of 100-300 secs., for the R.T.D. experiments, the tracer was assumed to be injected as a true impulse.

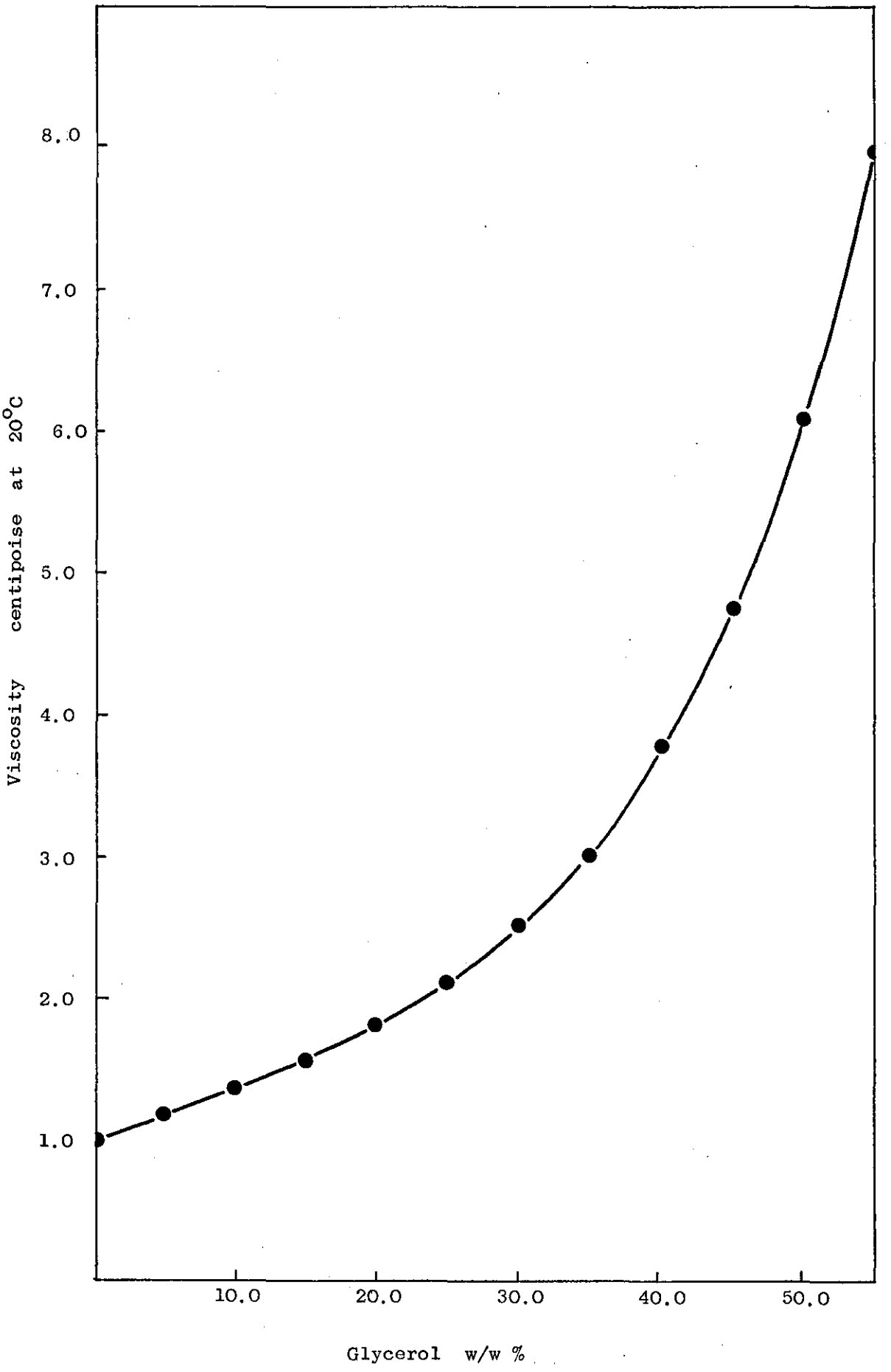
8.0
7.0
6.0
5.0
4.0
3.0
2.0
1.0
Viscosity centipoise at 20°C
10.0
20.0
30.0
40.0
50.0
Glycerol w/w %

Figure : 6.3.

6.3 The Photo-cell Detector

6.3.1. Construction

The detector device used to measure the dye concentration in the outflowing fluid was built around a ½ inch diameter, 12 inches long, Q.V.F. glass tube.

The detector consisted of a Mullard 90AV photo-emissive cell and a 8.6 M ohm resistor, arranged to form the circuit shown in Figure:6.5. On the other side of the outlet tube,was located a 6 watt filament bulb, and the entire assembly was then fixed in a Lektrokit box. The glass tube was clamped firmly to the detector housing to ensure a permanently characterised detector.

Power was supplied from two transistorised power packs which provided stabilised voltages to the bulb and the cell. A ten-turn potentiometer was attached to the voltage adjusting knob of the bulb so that minute alterations could be made to the base-voltage of the detector.

Further modifications considerably improved the stability of the instrument e.g. a vent was fixed above the bulb to prevent overheating of the filament and also the circuit was thermally insulated.

6.3.1.1. Calibration of the Photo-cell

The calibration of the photo-cell was carried out by detaching it from the column and clamping to a suitable support. A standard solution containing exactly 1 gm/litre of Nigrosine dye was prepared and quantities of this solution were diluted to the desired concentrations in a number of graduated flasks. The lower end of the detector tube was sealed off with a rubber bung and the diluted solutions introduced. The output of the cell corresponding to the solution was displayed on a digital vdtmeter and recorded.

Figure:6.4 is the plot of the solution concentration versus the real voltage on a semi-logarithmic scale; it shows a straight line

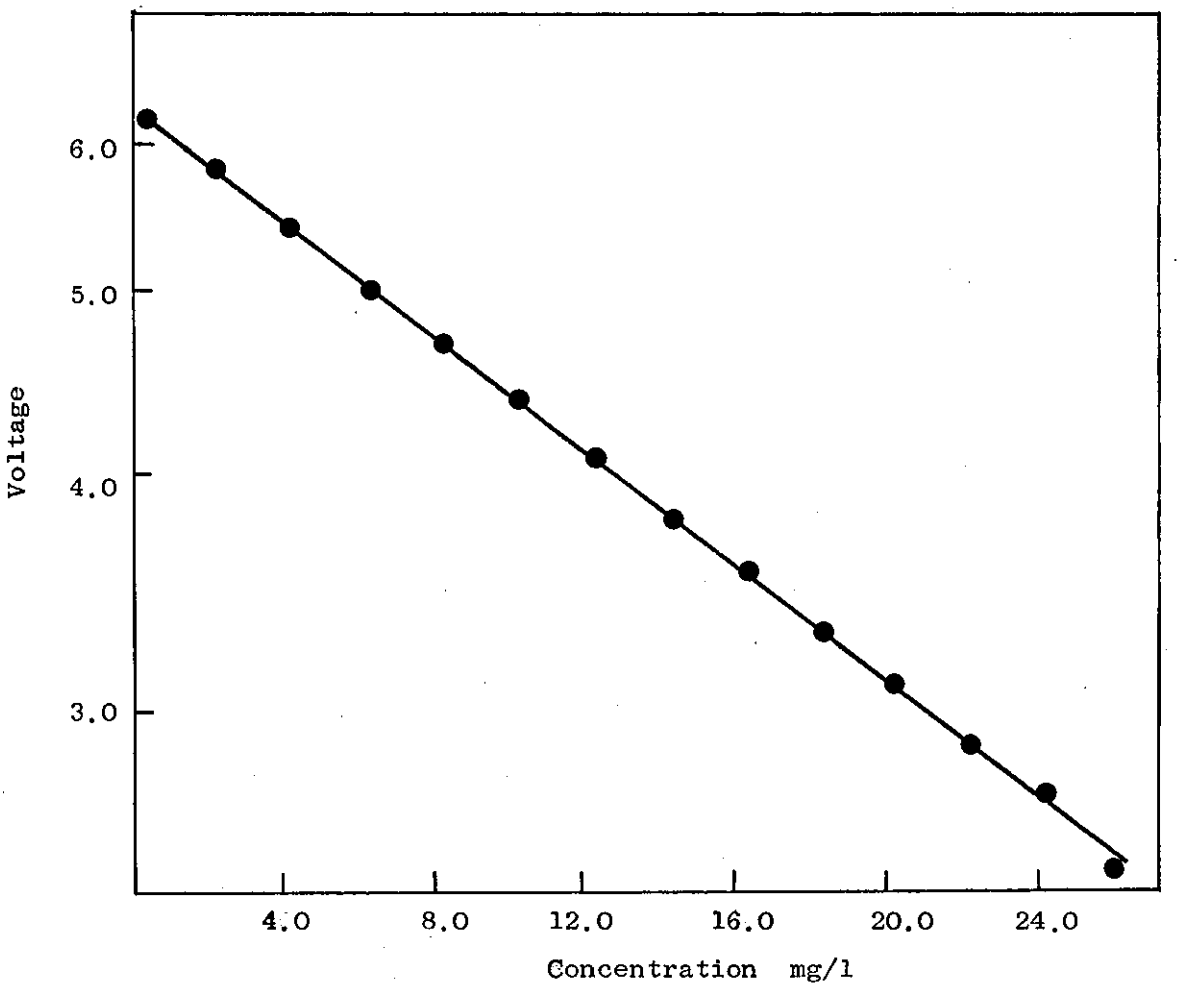

Figure : 6.4. Photo-cell calibration curve

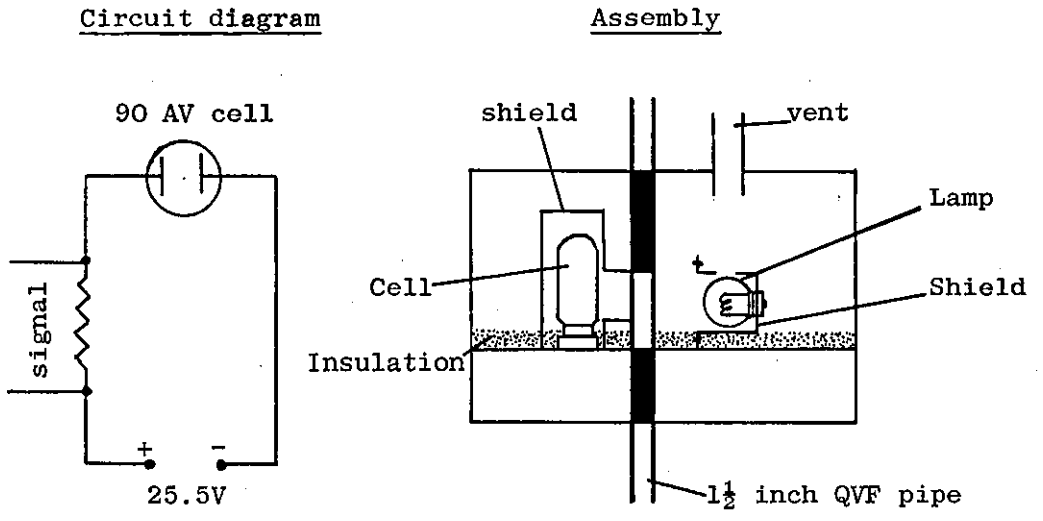

Figure: 6.5. Photo-cell detector

relationship over a reasonable concentration range. However, the impulse response experiments were carried out in such a manner that most of the output voltages were contained within the initial part of the calibration curve, this part being most reliable and reproducible.

6.3.2. Conductivity Cell

The conductivity cell was commercially manufactured by Electronic Switch Gear Ltd., it contained three annular ring electrodes equally spaced within ½inch diameter bore in an epoxy resin moulding, see Figure:6.6. The tubular bore was threaded at each end to enable the cell to be mounted vertically as an integral part of the outlet pipe. Conduction through the solution took place from within the cell between the central electrodes and the two outer rings which were connected to the earth terminal of the measuring instrument.

Variation of conductivity was recorded with the aid of an A.C. Autobalance bridge.. Output of the Autobalance bridge was amplified by a factor of 30 using a precision amplifier, Model 361 Instrument Amplifier, manufactured by Redcor; the general arrangement is shown in Figure:6.7.

During the course of each run the cell was tapped lightly every few minutes to dislodge any bubbles which might have adhered to the cell surface.

6.3.2.1. Calibration of the Conductivity Cell

The calibration procedure was exactly similar to the one adopted for the photo-cell. The relationship between the output conductivity and potassium chloride solution concentration is linear over most of the working range as shown in Figure:6.8.

6.4. Stimulus Response Experiments

An almost identical procedure was followed for all the stimulus response investigations, the only difference being due to the type of detector used.

The first part of the operating procedure involved the

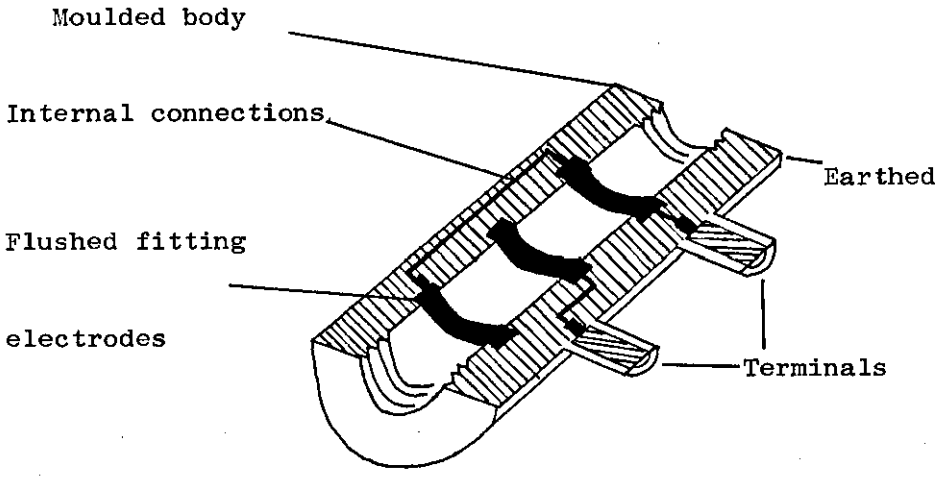

Figure: 6.6. Conductivity cell detector

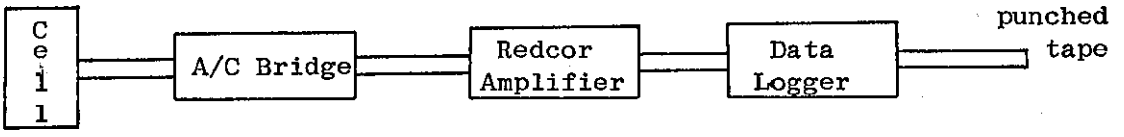

Figure: 6.7. Layout of the Detecting and Recording Equipment

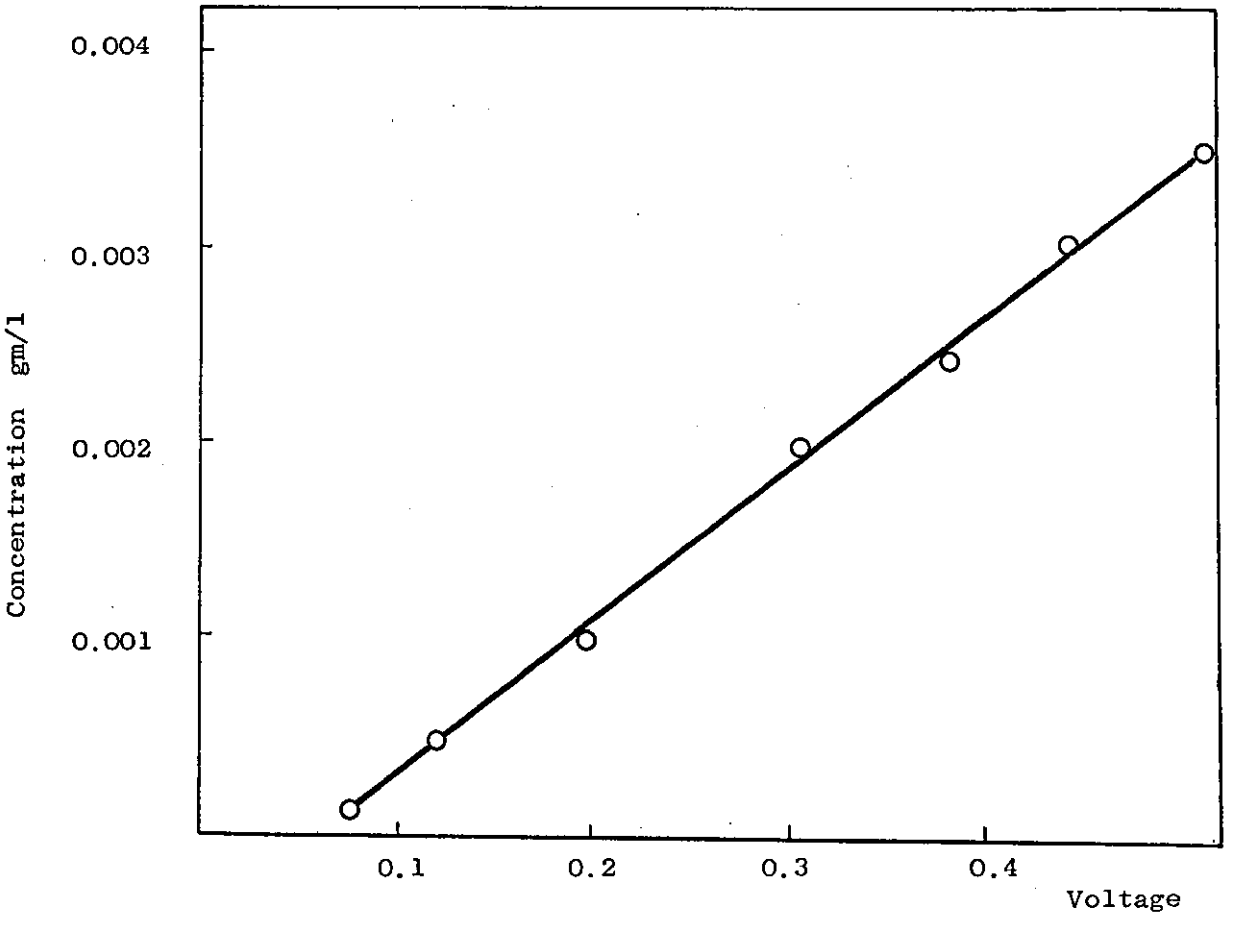

Figure: 6.8. Conductivity cell calibration curve

calibration of the water and air flow rotameters. The water flow rotameter was calibrated by collecting liquid for a fixed time over a range of float positions; for the air flow rotameter the exit air was passed through a gas flow meter for fixed periods of time.

6.4.1. Runs for Water-Air Systems

To attain stabilised conditions, the photo-cell was switched on over night; it was calibrated as described in section 6.3.1.1. and attached to the exit line, at the bottom of the column.

The water flow rate was set to the desired value by means of ½inch needle valve and the liquid level in the detector adjusted to minimise its holdup by manipulating the height of the flexible discharge tubing. The system was then allowed to steady out under the desired conditions. In the meanwhile the output socket of the photo-cell was connected to the logging equipment. This consisted of scanner drive unit, and a multi-channel recorder that was coupled to a five holed paper tape punching machine. The equipment was set to scan one channel only, at a suitable time interval.

About ½cc of concentrated Nigrosine dye solution was then injected into the liquid stream with a hyperdermic syringe through the "tee" piece at the top of the column. At this instance the logger was started by pressing an external trip switch, located close to the injection point. After the initial base line, the displayed output was seen to pass through a peak before returning to the base-line, when logging was terminated.

New operating conditions were then set up and the above described procedure repeated.

6.4.2. Runs for Glycerine-Solutions

The water line to the rotameter was replaced with a line from the glycerine-solution storage vessel. All the traces of water were then removed by flushing the column with the solution and the

rotameter recalibrated for each solution. The conductivity cell was then substituted for the photo-cell and the liquid, air flow rates were adjusted to the desired values.

Before connecting the "Autobalance Bridge" to the cell, it was calibrated in a manner described in the Manual and the output signal was suitably amplified prior to coupling it to the data logging equipment.

Runs were performed using different viscosity solutions and various packed lengths; the resultant tapes were processed to obtain the normalised response, the mean residence time and the liquid holdup of the system.

6.4.3. Double Tracer Experiments

To investigate the effect of tracer diffusivity on the R.T.D. of the flowing liquid in the bed, both detectors were utilised simultaneously: one to record the dye response and the other the electrolyte response.

The liquid leaving the column was split up into two streams and each passed through the appropriate detector.

The tracer solution used in this case was prepared by dissolving potassium chloride in Nigrosine dye solution. The injection and the logging procedure followed were again identical to the previously described ones, however the logger was arranged to record two channels, each output being logged alternately. Two bed lengths were studied.

6.5 Stimulus Response of the Detector

The contribution of the R.T.D. of the liquid in a detector to the overall R.T.D. in the system should be kept to a minimum. The procedure normally recommended (103) is to employ a detector having a mean residence time of ten per cent or less of the system mean residence time. To ensure this, random checks were made during the course of the present investigation.

At the end of each run, while holding steady conditions, tracer liquid was injected into the liquid stream entering the detector cell; limiting the response within the detecting range of the cell. The output was logged and the tapes processed as described in section : 1 of Appendix : F.

6.6 Liquid Holdup Experiments

A study of the column liquid holdup was also conducted. The operating holdup was determined at the end of each run by turning off the liquid and air control valves and collecting the draining liquid. The total liquid holdup was determined from the R.T.D. results.

7. EXPERIMENTAL RESULTS

Note on the numbering of experimental runs

Every run number has been formed in terms of the experimental conditions the run was carried out. The first letters indicate the system itself e.g. WA means water-air system or GWA represents glycerine-water-air system. The digits before the decimal point indicate an approximate length of the packed section; first digit after the decimal place gives the liquid flow rate in ccs per second; the second digit after the decimal point , the run number; the last digit shows the glycerine solution viscosity, namely zero for viscosity, μ = 4.5cp and 1 for viscosity, μ =7.5cp. The figure in brackets shows the inclusion of second experimental runs carried out under indentical conditions.

As an illustration take run number: GWA-10.310(2). This represents glycerine-water-air systems of packed height 10.5ft. , solution viscosity of 4.5cp, liquid flow rate of 3ccs per second and experimental response consisting of run 1 and 2 under these conditions.

7. Experimental Results

The following runs were performed as described in the preceding section.

7.1. Water-Air System

Three packed column length viz. 5.5ft., 10.5ft., and 15.5ft., were used. A total of ten runs were carried out on each column length. These runs comprised of two runs for each flow rate, one with water only and the other with water-air: see Table: 1. of Appendix: A.

7.1.1. Glycerine-Water Solutions and Air System

In this section six runs were carried out on 5.5ft. length and eight runs on 10.5ft. length column using 4.5cp viscosity solutions and counter-current air flow; a further eight on the 5.5ft. length column and six runs on 10.5ft. length column were carried out with 7.5cp viscosity solutions: see Table: 2. of Appendix: A.

7.1.2. Double-Tracer Experiments: Water System

As outlined in section: 6.4.3., three runs were carried out on the 10.5ft. packed section : see Table: 3. of Appendix: A.

7.1.3. Stimulus-response of the Detector

For each packed length, and liquid air system investigated three runs were carried out on the detector, the procedure is outlined in section:6.5. The liquid flow rates were selected at random : see Table: 7.1.

7.1.4. Liquid Holdup

Operating liquid holdup was determined at the end of each run as described in section:6.6. Total liquid holdup was calculated from the system response data; all the results are tabulated in Table: 1, of Appendix: c.

7.2 Liquid Holdup Measurements and Correlations

The normalisation procedure described in section: E requires an accurate estimate of the system mean residence time, and hence that of the total holdup.

Holdup measurements, made by suddenly closing the liquid inlet valve and draining the packing, were always smaller than found from the mean residence time. This indicated that part of the total holdup had been retained in the bed, Figure:7.1.1. shows the plots of the total holdup, H_T , against the liquid flow rates, F, for various operating conditions. To confirm the reliability of the response experiments, calculated total holdup values have been compared with the published correlations.

A review of literature, section:3.1.1., reveals a number of dimensionless correlations of total, operating and static holdup. Three such correlations, whose accuracy ranges between $\pm$ 20 to $\pm$ 6 per cent, have been selected to fit the present data.

i) The Otake and Okada (21) correlations :

Equation (3.5) is reported by these authors:

$$H_{op} = 1.295 \ (N_{Rel})^{0.676} \ (N_{Gal})^{-0.44} \ (a_k \ d_k)$$

Let $$R = (N_{Rel})^{0.676} \ (N_{Gal})^{-0.44} \ (a_k \ d_k)$$

Figure: 7.2.1. shows three plots of total, H_T , versus R, each line corresponds to a different viscosity liquid. It demonstrates

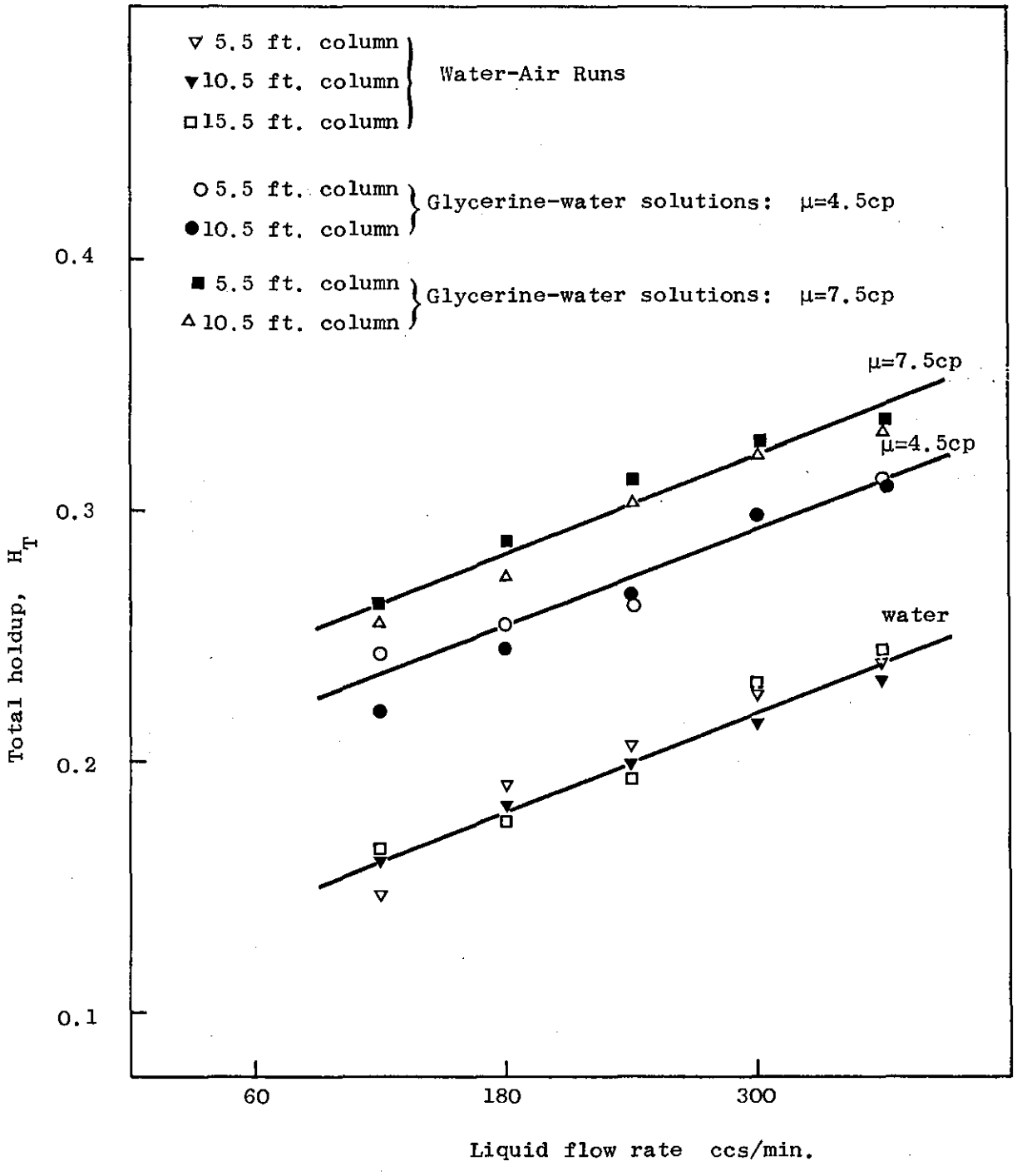

Figure: 7.1.1. Plot of total holdup versus liquid flow rate

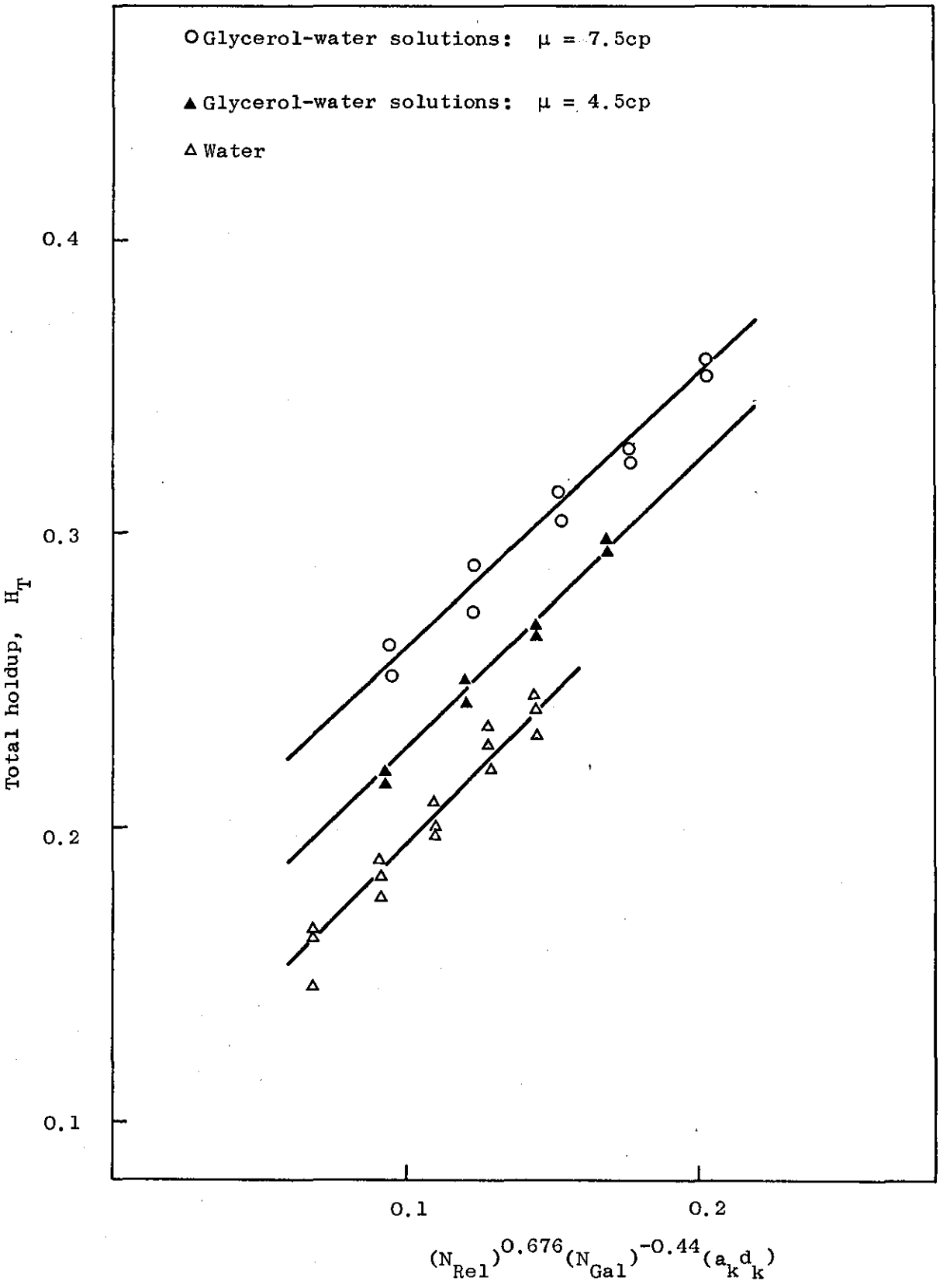

Figure: 7.2.1. Comparison of total holdup values with the correlation of Otake and Ökadá(21)

that the data points follow a straight line, the slope of each line being approximately 1.2. An extrapolation to zero flow rate provides values for static holdup:

For water	μ = 1.0cp	H_{st}	= 0.080
Glycerine/water	μ = 4.5cp	H_{st}	= 0.116
Glycerine/water	μ = 7.5cp	H_{st}	= 0.166

ii) Mohunta and Laddha (24):

These workers proposed the following correlation, Equation (3.10) for operating holdup only:

$$H_{op} = 16.13 \left(\frac{\mu N U^3}{g^2} \right)^{1/4} \left(N d_k^3 \right)^{-1/2}$$

Figure:7.3.1 represents the present data correlated by the above equation.

iii) Gelbe (26) very recently correlated his data and data obtained by several other authors by the following relationships:

$$H_{op} = 1.59 \left(\frac{d_i'}{d_p} \right)^{-5/9} \left(\frac{N_{We}}{N_{Fr}} \right)^{-1/7} \left(N_{Ga} \right)^{-0.3} \left[N_{Re} \right]^{n}$$

for $N_{Re} < 1$ $\quad n = 1/3$

and $N_{Re} > 1$ $\quad n = 5/11$

$$H_{st} = 1.67 \times 10^{-4} \left(a_k d_k \right)^2 \log X_r$$

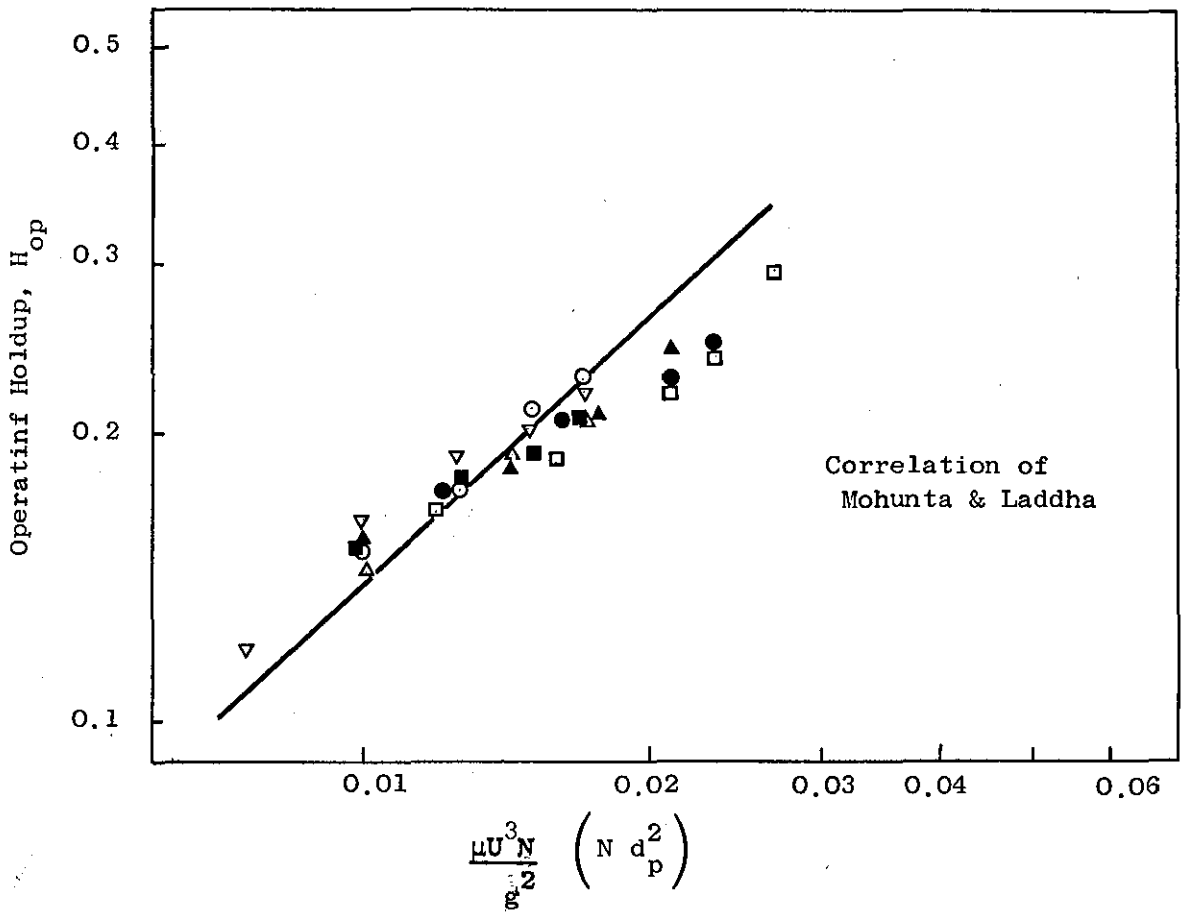

Figure: 7.3.1. Comparison of operating holdup with the correlation of Mohunta and Laddha

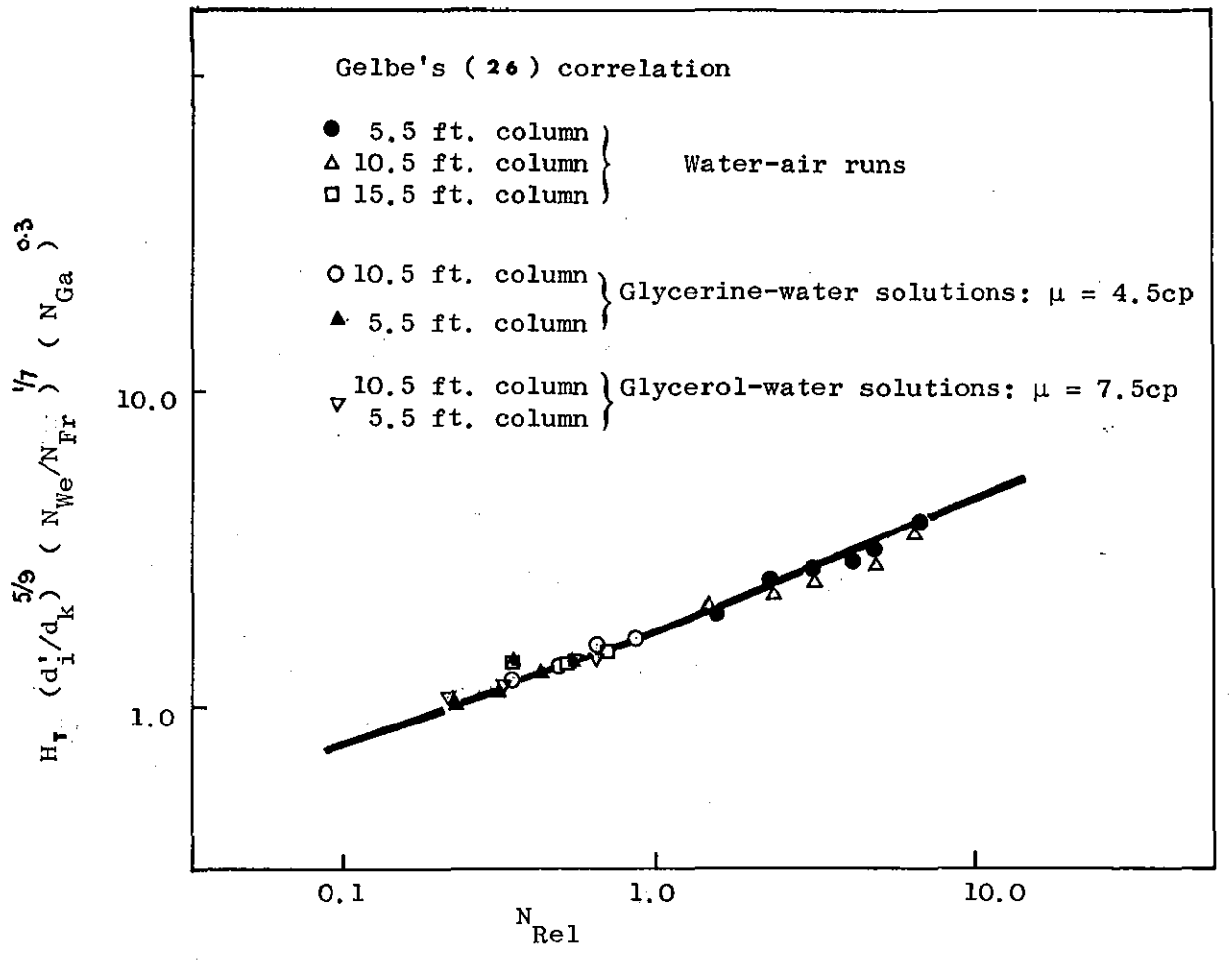

Figure:7.4.1. Comparison of the operating holdup with correlation of Gelbe (26)

Operating and static holdup were calculated according to Equations (3.13)(3.14) respectively. Plots of H_T ( )( )( ) versus N_{Rel} are shown in Figure:7.4.1.

An inspection of Figures: 7.2, 7.3, and 7.4 shows the data to fit all three correlations within the prescribed range and deviation: thus confirming the reliability of the data and the processing techniques.

7.3. Results of Impulse Response Tests

All experimental data has been converted to normalised response form and presented in Appendix: B , the normalisation procedure is outlined in Appendix: E .

In this section experimental responses have been plotted and the effect of varying packed lengths, changing liquid viscosity, the effect of liquid and gas flow rates and the influence of tracer diffusity on the liquid side R.T.D. have been investigated.

7.3.1. Effect of Liquid and Gas Flow Rates

Figures:7.1. to 7.5. are the experimental response curves for the water-air system; these illustrate liquid side R.T.D. as functions of the air flow rates. Each set of two runs corresponds to the three packed lengths studied. It can be seen that for all cases the gas flow rates have negligible effect on the liquid side R.T.D.

Figures:7.1 to 7.4. also show the influence of varying liquid throughput on the liquid side R.T.D. For low liquid flow rates the response appears to be strongly asymmetrical, however as the flow rate increases the skewness becomes less pronounced. At high liquid flow rates the curves are almost symmetrical and of Gaussian appearance.

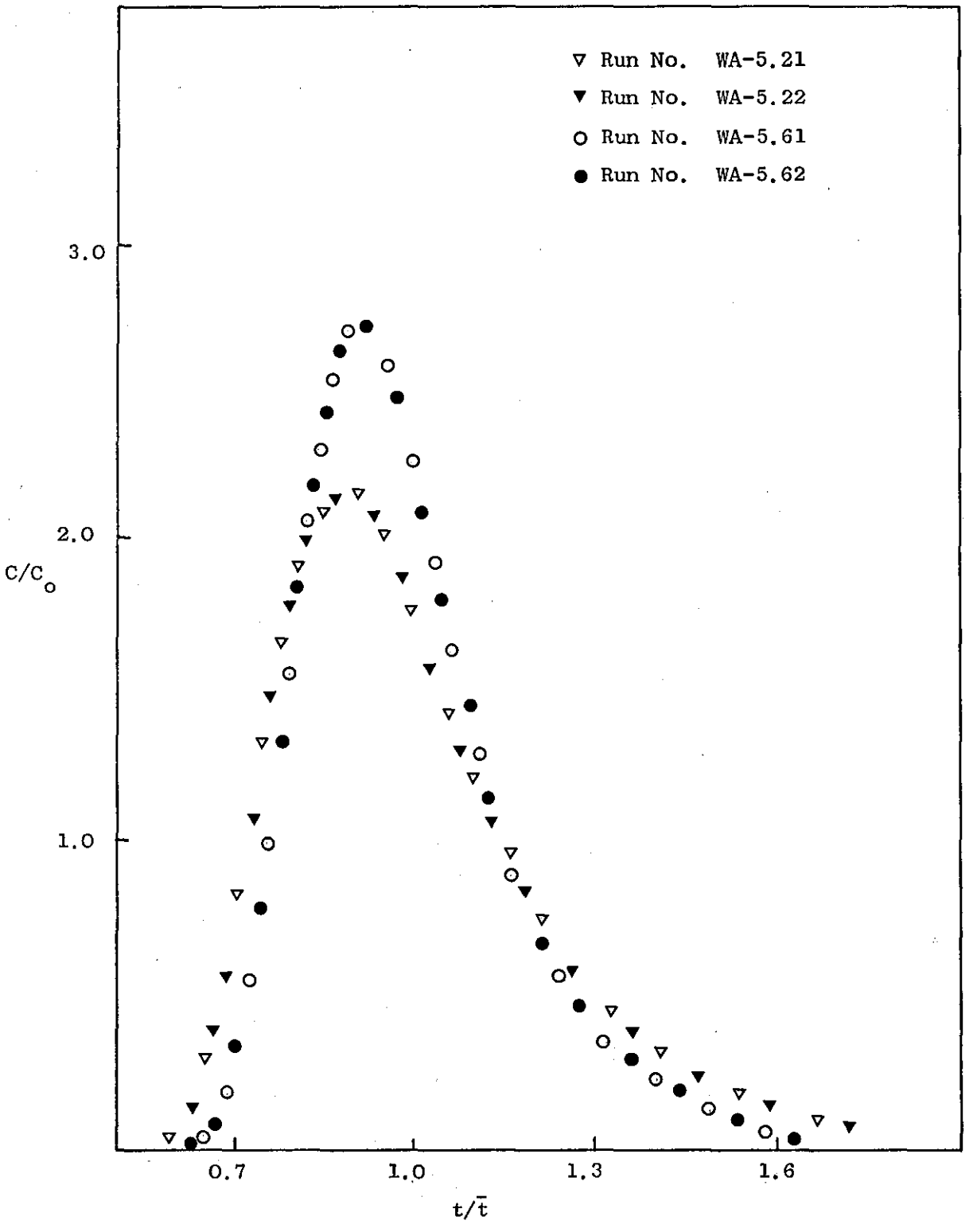

Figure: 7.1. Effect of liquid and gas flow rate on the liquid side R.T.D. in 5.5 ft. column.

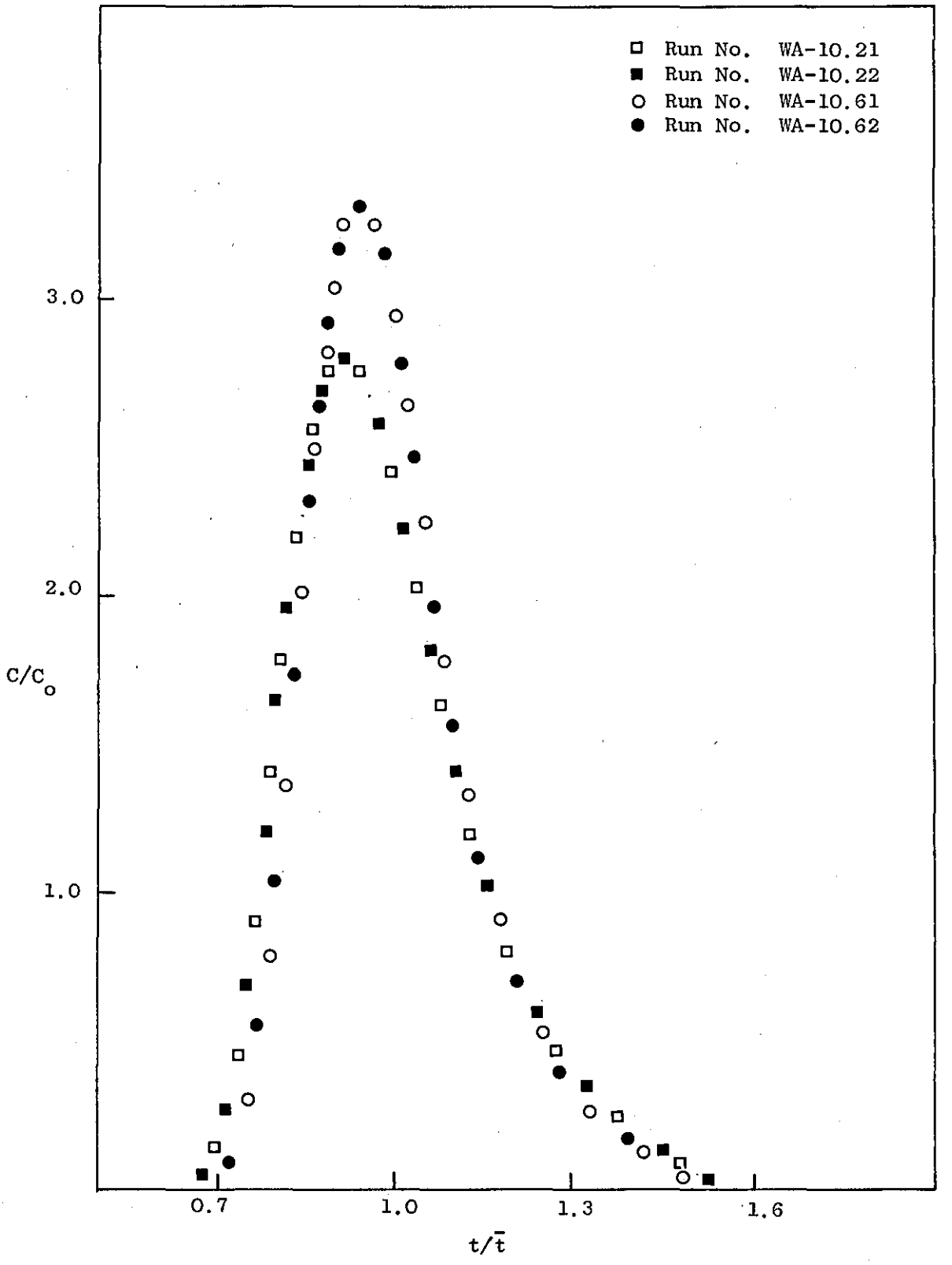

Figure: 7.2. Effect of liquid and gas flow rate on the liquid side R.T.D. in 10.5 ft. column.

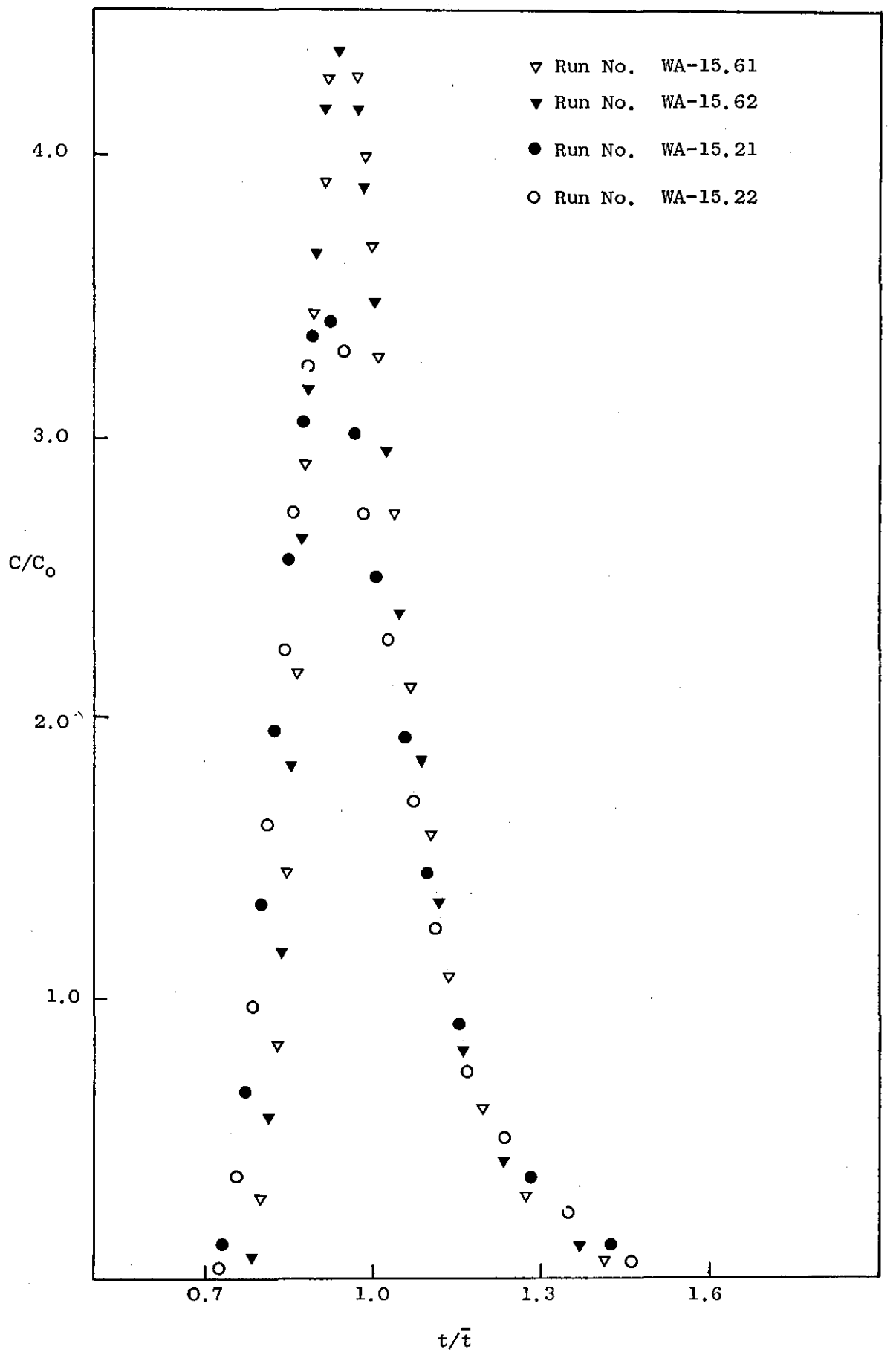

Figure: 7.3. Effect of liquid and gas flow rate on the liquid side R.T.D. in 15.5 ft. column.

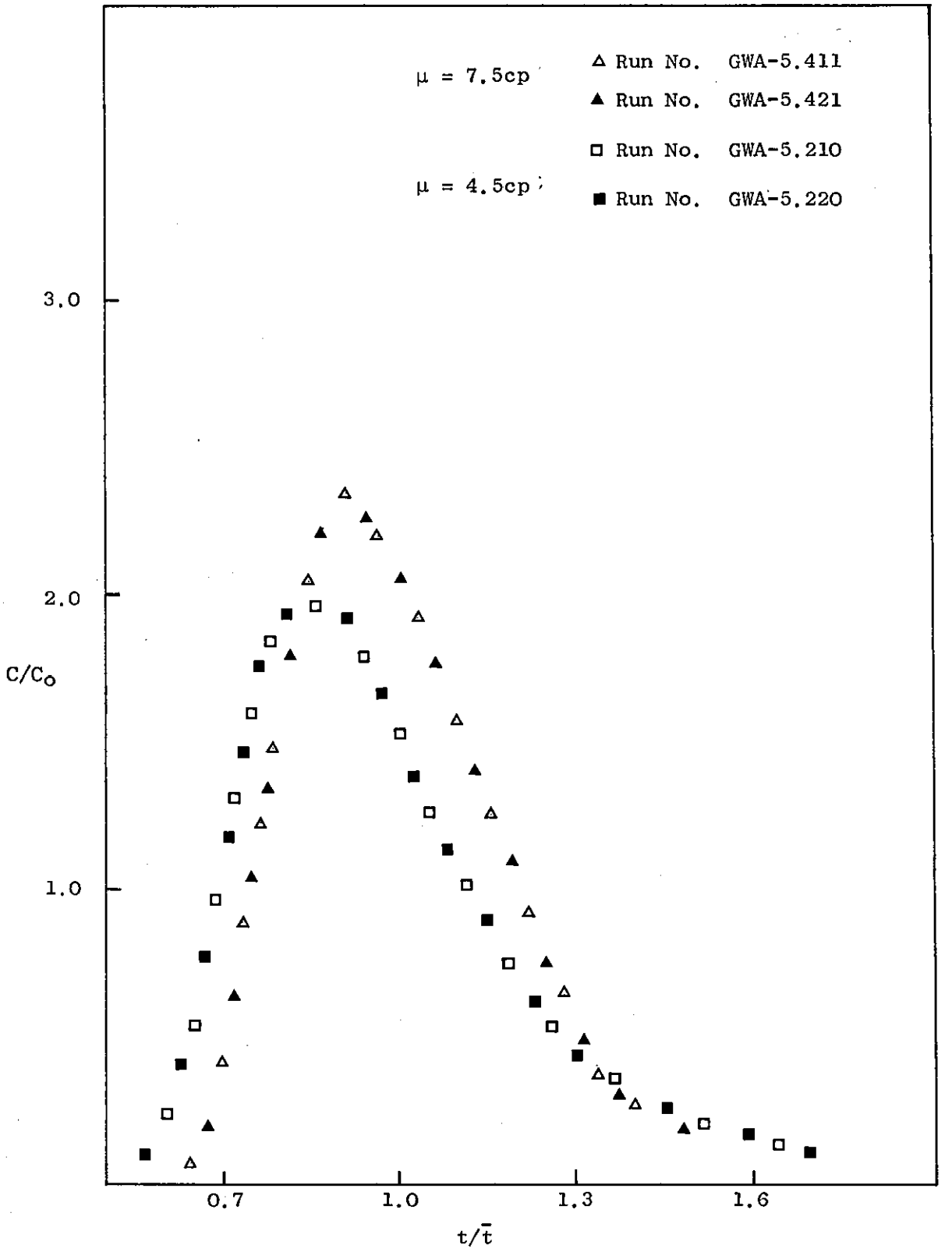

Figure: 7.4. Effect of liquid and gas flow rate on the liquid side R.T.D. in 5.5 ft. column.

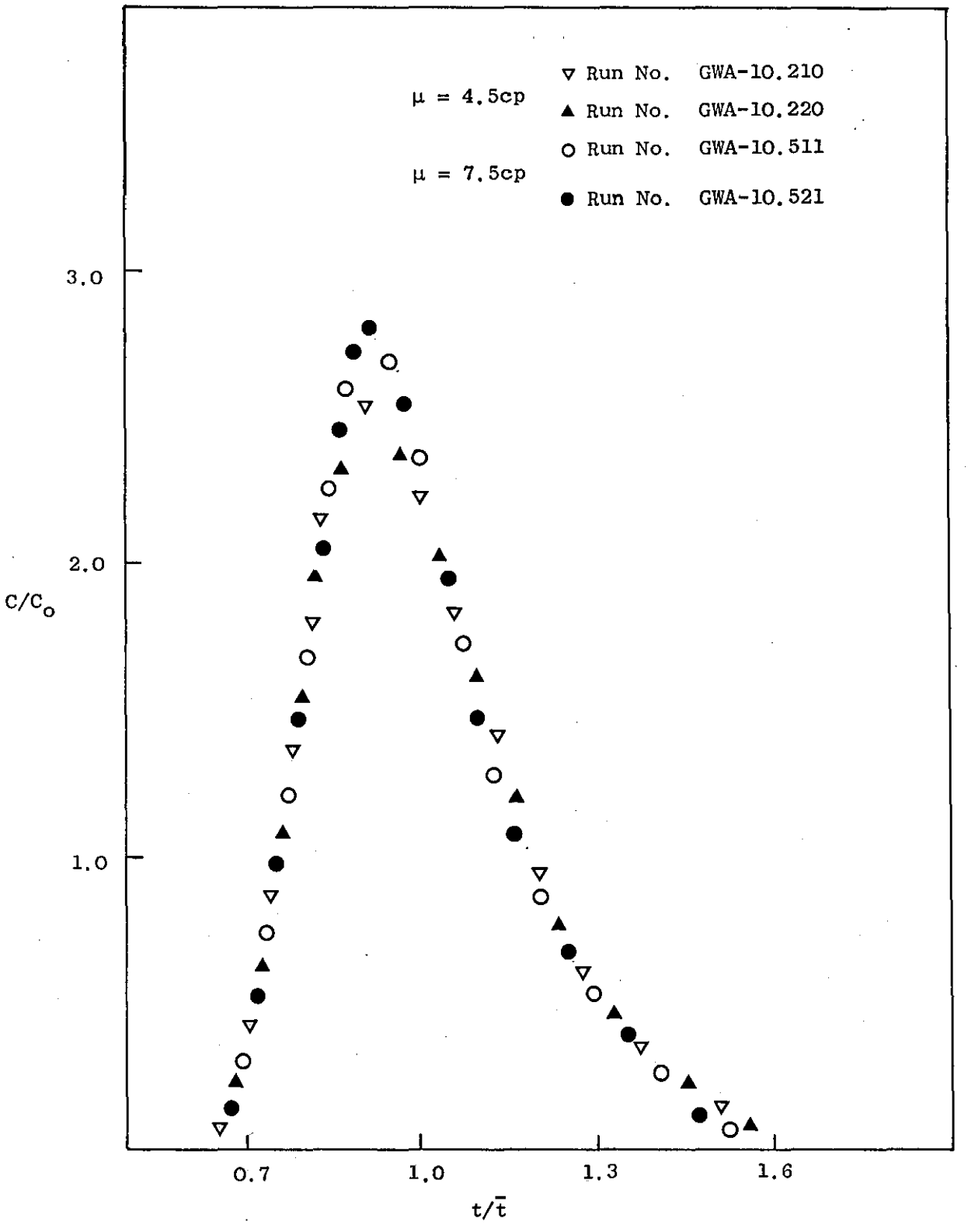

Figure: 7.5. Effect of liquid and gas flow rate on the liquid side R.T.D. in 10.5 ft. column.

7.3.2. Effect of Varying Packed Height

Figures : 7.6, 7.7 and 7.8 show experimental response curves of the liquid side R.T.D. as a function packed height under otherwise identical conditions. An increase in packed height results in reduced dispersion of material (on a normalised basis) thus more symmetric curves.

7.3.3. Effect of Liquid Viscosity

Glycerine-water solutions were used to study the effect of varying liquid viscosities on the liquid side R.T.D. Figures: 7.9 and 7.10 are two sets of typical response curves. Plots show the R.T.D. of water and solutions of viscosity 4.5cp and 7.5cp under similar operating conditions; two sets of graphs are given for two different packed heights. In both cases the more viscous solutions produce higher dispersion of material, enhancing the asymmetric "tailing" effects; an increase of packed height damps down this effect giving more symmetric curves.

7.3.4. Role of Molecular Diffusion

The contribution made by the molecular diffusion of the tracer material in the determination of liquid side R.T.D. was investigated by a double tracer technique as has been outlined in section : 6.4.3. Figures 7.11 and 7.12 are representative of such studies. Although the tracers employed had widely different coefficients - potassium chloride has diffusion coefficient of 2×10^{-5} cm^2/sec (104), while Nigrosine dye has 2×10^{-6} cm^2/sec (105) - the normalised response curves do not show any dissimilarities; thus indicating a negligible effect on the overall dispersion coefficient.

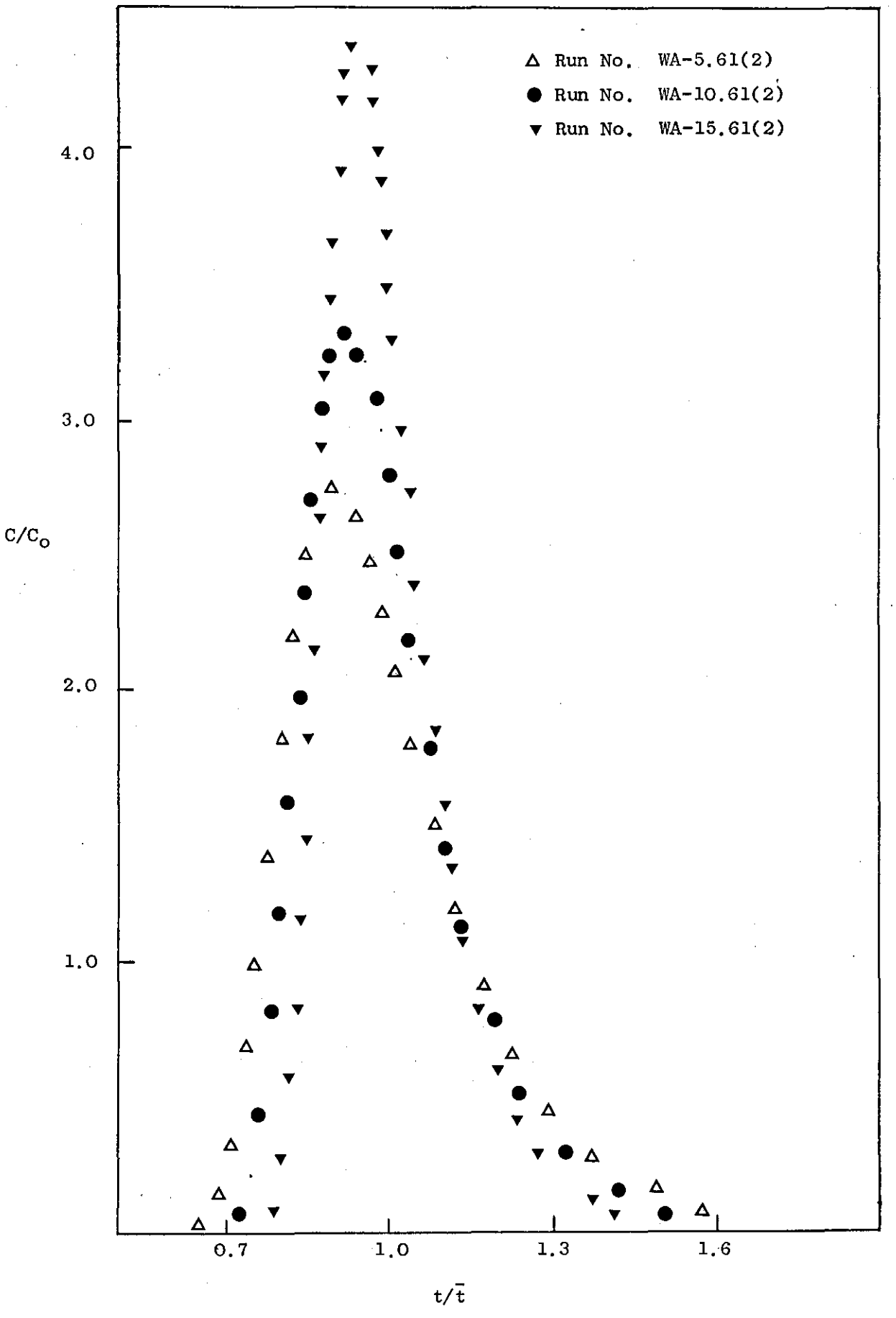

Figure: 7.6. Effect of varying packed height on the liquid side R. T. D., water runs only.

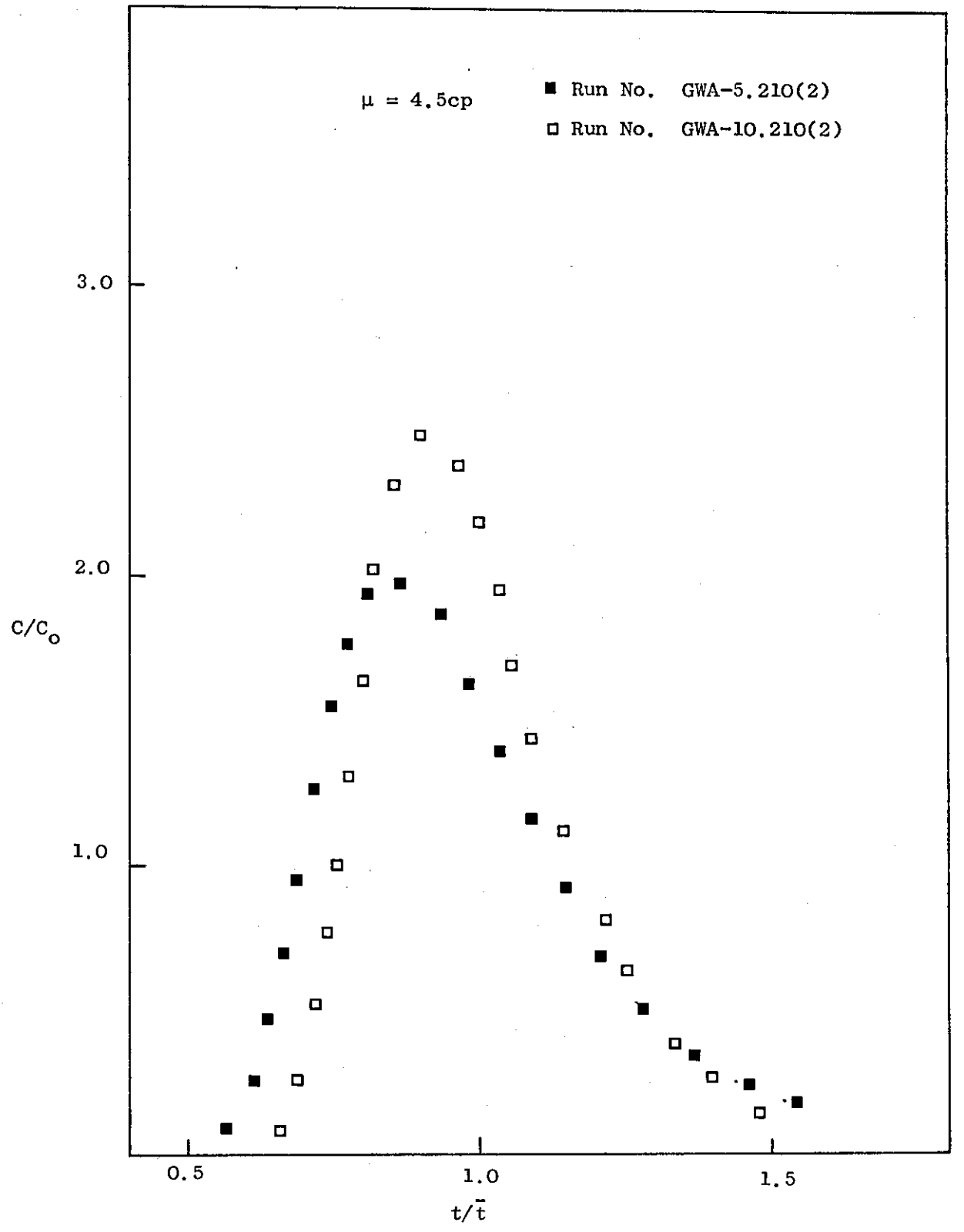

Figure: 7.7. Effect of varying packed height on the liquid side R. T. D., glycerine-water solutions.

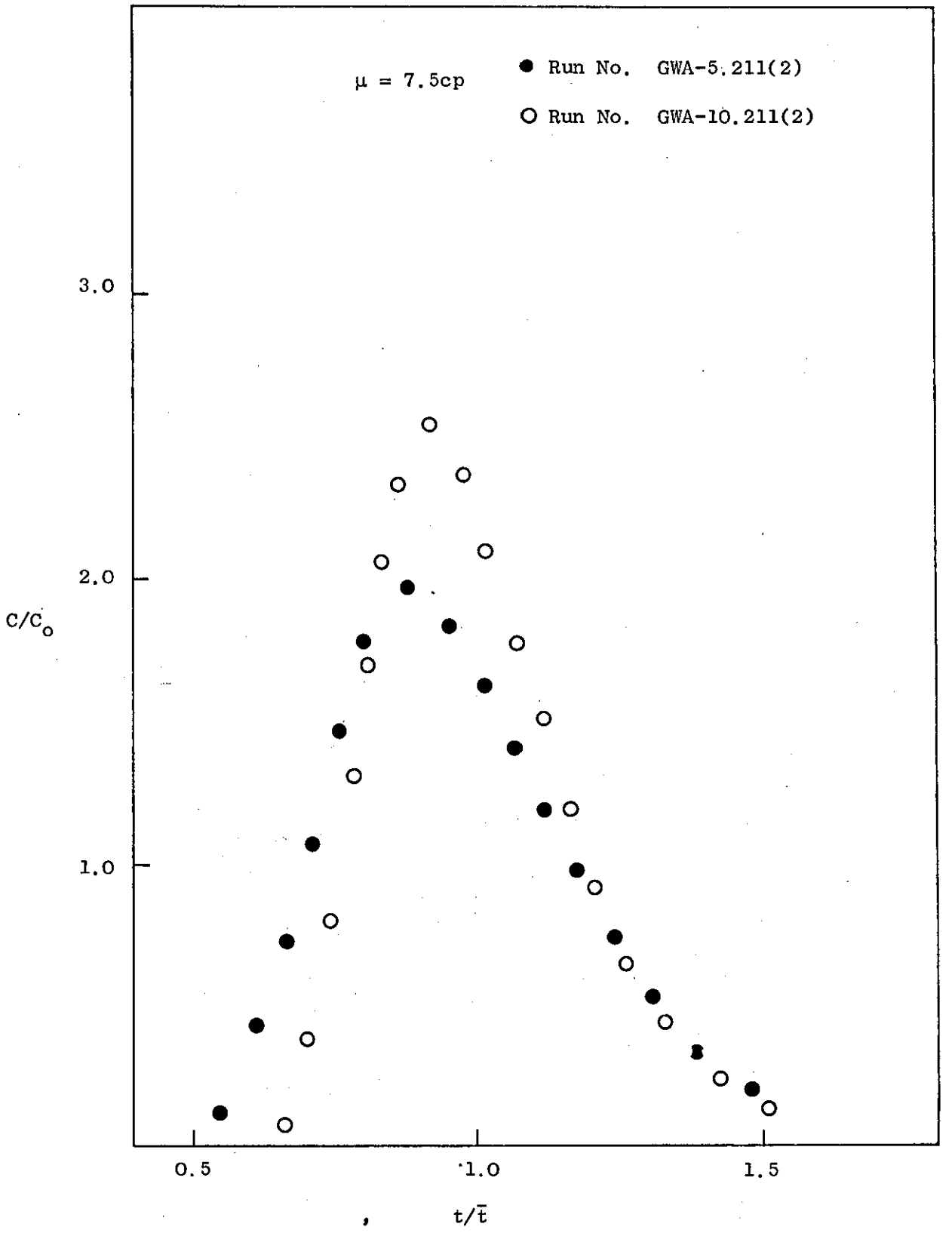

Figure: 7.8. Effect of varying packed height on the liquid side R.T.D. glycerine-water solutions.

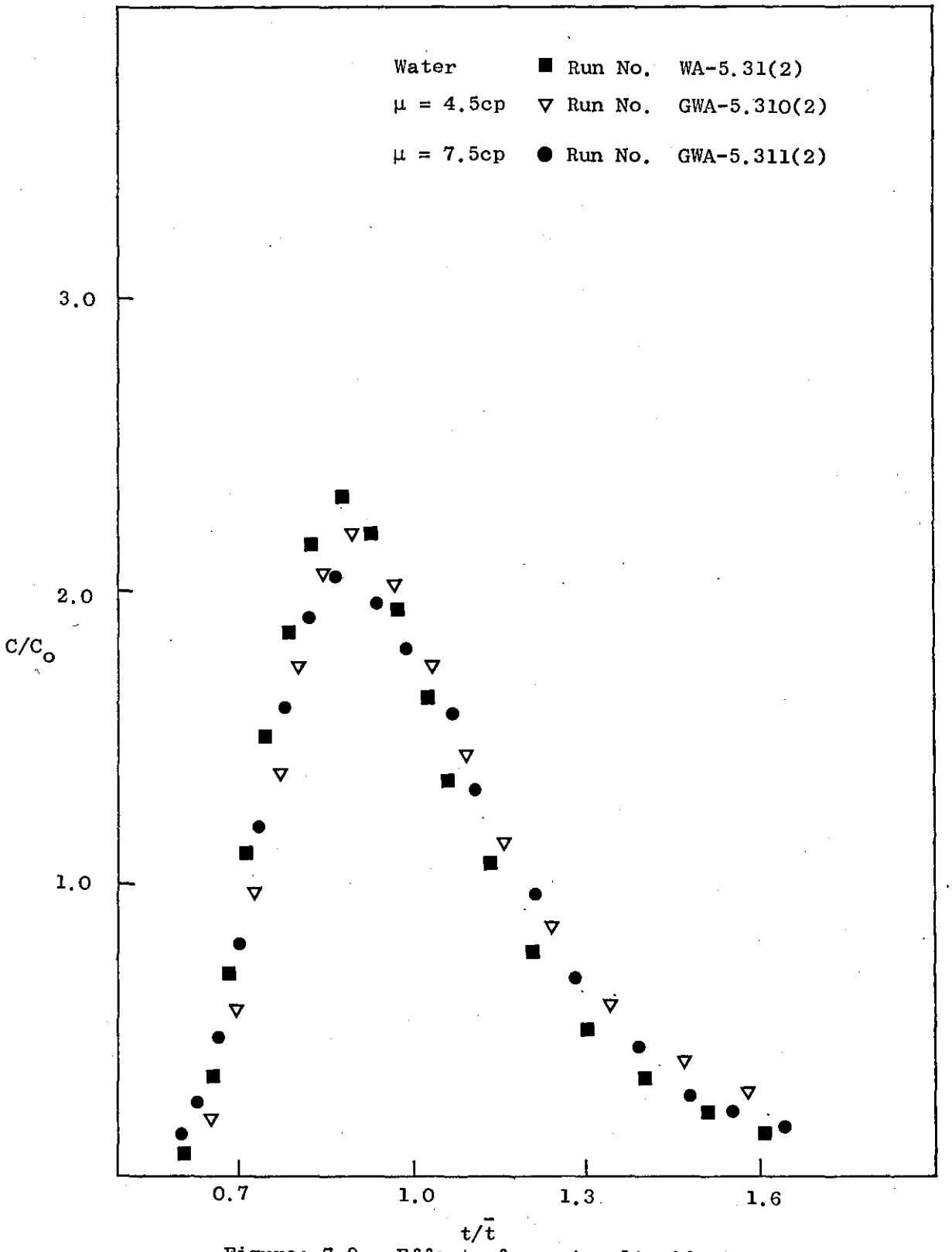

Figure: 7.9. Effect of varying liquid viscosity on the liquid side R.T.D., 5.5 ft. column.

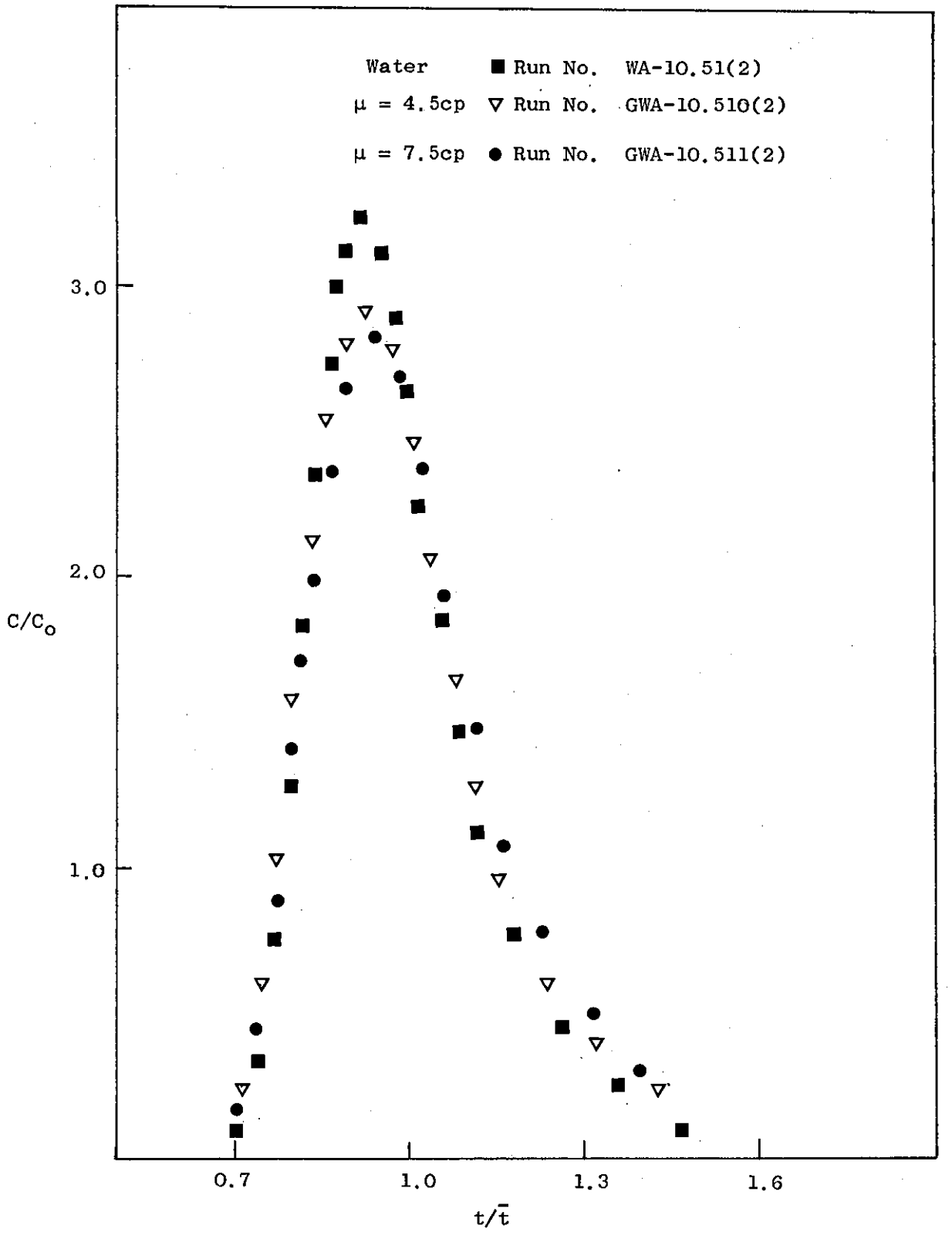

Figure: 7.10. Effect of varying liquid viscosity on the liquid side R.T.D., 10.5 ft. column.

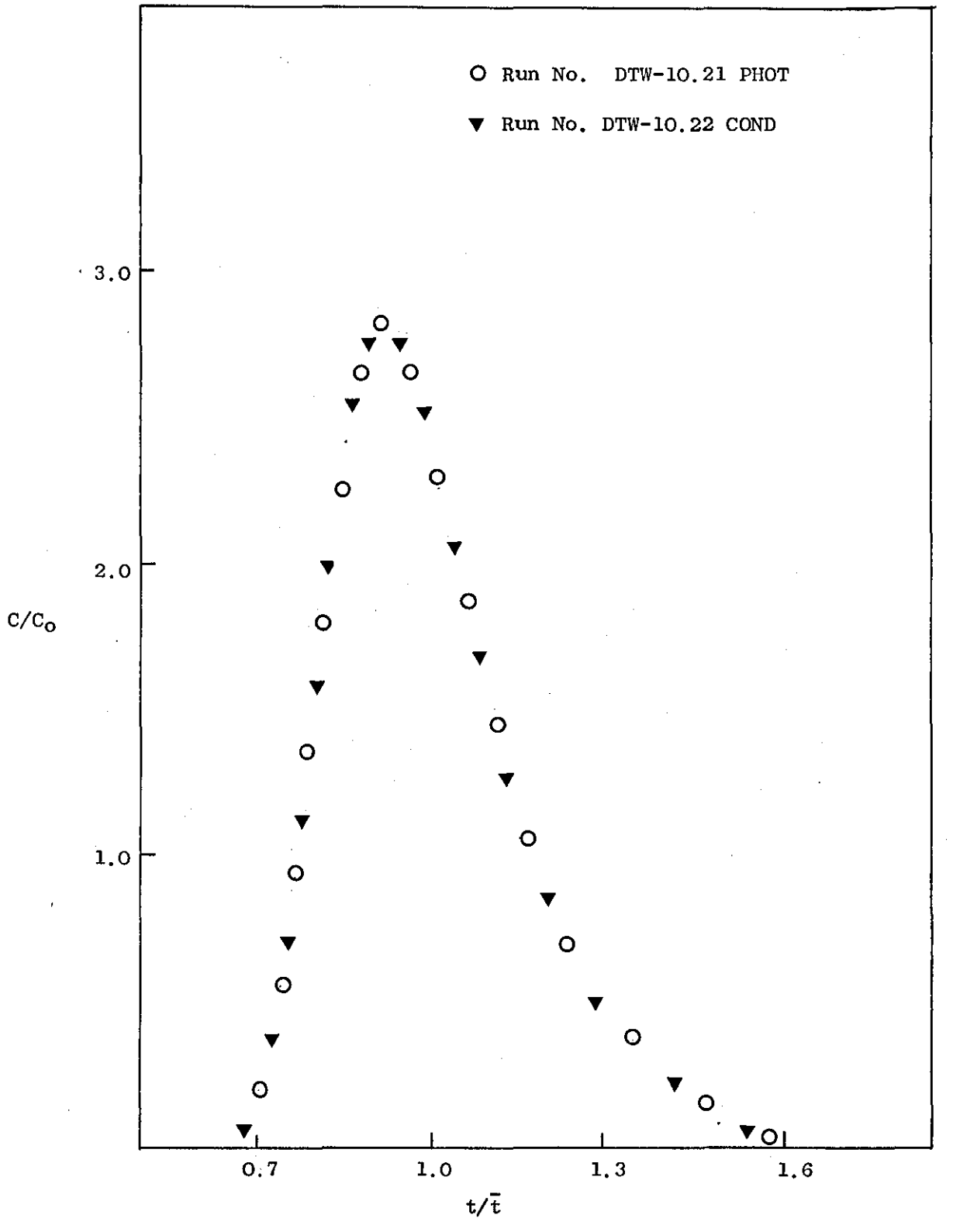

Figure: 7.11. Effect of the molecular diffusion of the tracer on the liquid side RTD., 10.5 ft. column.

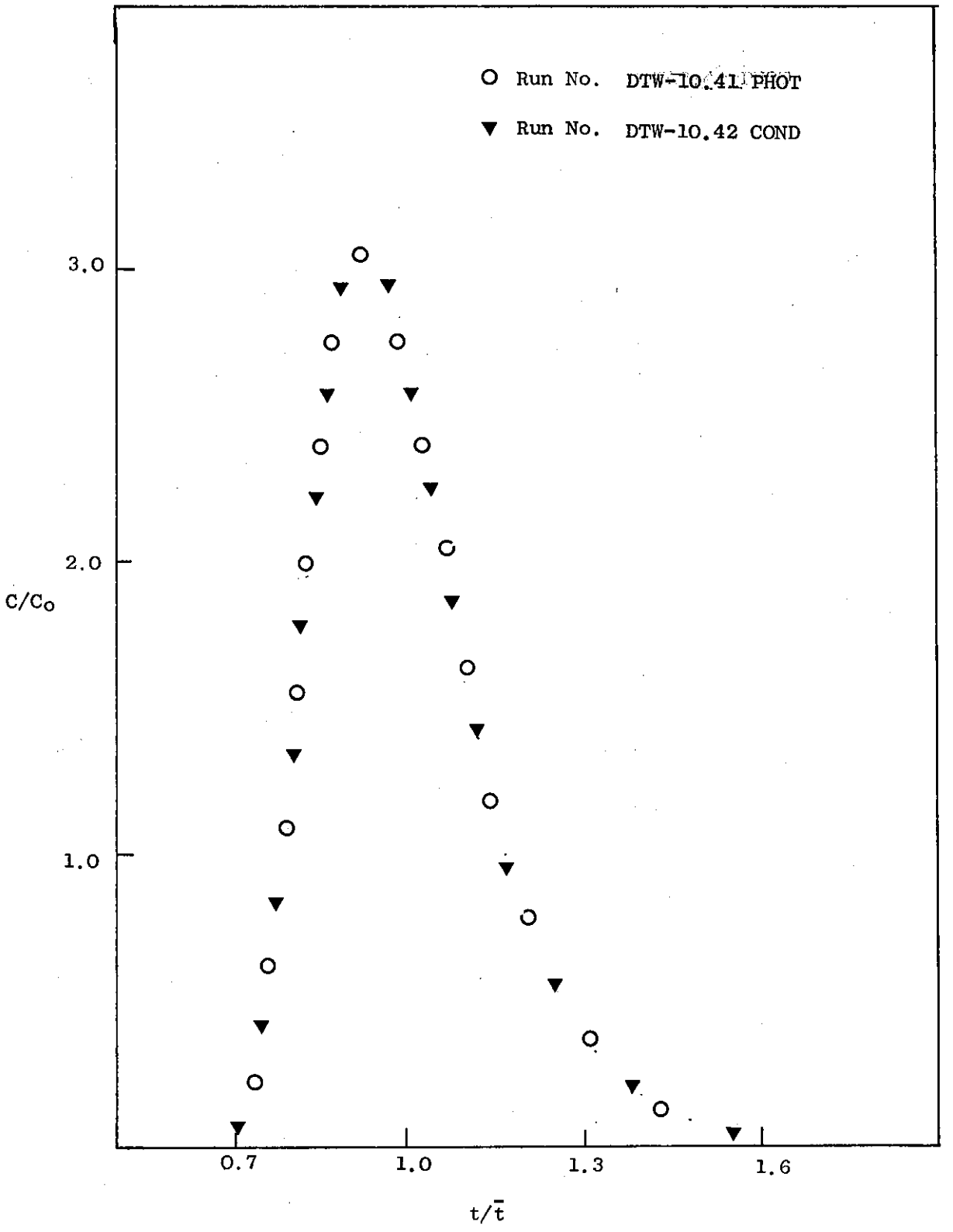

Figure: 7.12. Effect of molecular diffusion of the tracer on the liquid side R.T.D., 10.5 ft. column.

7.3.5. Effect of Detector R.T.D. on the Overall R.T.D.

All the R.T.D.s have been measured outside the column. The liquid R.T.D. of the detector was determined as described in section: 6.5, and the results are given in Table: 7.1 below.

Table: 7.1. Mean Residence Time of the Photocell Detector, 10.5 feet Column.

Liquid Flow Rate. ccs/min.	Mean Residence Time of the Detector. secs.	Mean Residence Time based on the Overall Meantime.
2	2.6	.0086
3	1.8	.0086
4	1.1	.0062
5	0.9	.0052
6	0.5	.0034

The mean residence time of the detector was found to be negligibly small, between 0.34 to 0.86 % of the total mean residence time of the column.

Nomenclature

$a_k d_k$	packing characteristics
d_i'	hydraulic diameter of smallest inner area of a ring
C/C_o	normalised concentration
d_k, d_p	nominal packing diameter
g	acceleration due to gravity
H_{op}	operating holdup
H_{st}	static holdup
H_T	total holdup
n	exponent
N	packing number density
U	superficial velocity
N_{Fr}	Froud number
N_{Ga}	Galileo number
N_{Re}	Reynolds number
N_{We}	Weber number
t/t	normalised time

8. EVALUATION OF MODEL PARAMETERS FROM THE EXPERIMENTAL RESPONSE CURVES

8. Evaluation of Model Parameters from Experimental Response Curves

To establish how accurately a model represents a system, it is necessary to compare the model and the system impulse response for a suitably chosen parameter values. Several methods have been used over the years; frquency response techniques and the method of matching moments are two such methods.

The method of matching moments has been probably the most widely used one. The moments provide a way of characterising a probability distribution without making any assumptions to its nature; since the impulse response of a system has been shown to be such a distribution (110), it can be easily characterised by moments. However, due to the practical difficulty of measuring the higher order moments it is only suitable to match the low frequency regions of the response curve.

The direct comparision of the experimental and model response is basically a very tedious and time consuming procedure- the frequency response technique falls in this class - but the availability of efficient computational facilities expel these problems; and it is becoming more common in use.

In the case of simple one-or two-parameter models it has been found possible to estimate the parameters by making use of simple and easily measured curve characteristics such as the peak height, span at the half or one-third of the height, and the "dead time" as indicated by the normalised time at which the normalised concentration attains a definite and detectable value.

The method described last has been used to fit the exponential delay time model and for the remaining models direct method of comparison has been found to be more appropriate to use.

8.1. Curve Fitting Procedure for Exponential Delay Time Model

To evaluate the response of the model, precise values of the normalised dead time, $t_o/\bar{t}$, and the parameter, αx, are required. While in principle the dead time and peak height can be used to determine these values, in practice the true dead time is unobservable due to the insensitivity of the detector at very low tracer concentrations.

To overcome this difficulty, an apparent dead time, $t_o'/\bar{t}$, has been defined. It is taken to be the time at which the normalised concentration reaches 0.05; to relate this to the true dead time, two sets of curves have been prepared. Figure:8.1 relates the peak height to the apparent dead time and Figure:8.2, the true dead time to the apparent dead time; both for different values of αx.

To obtain the model parameters $t_o/\bar{t}$ and αx, the apparent dead time, $t_o'/\bar{t}$, and the peak height are obtained from the normalised response curve. Figure:8.1 is then used to obtain a value for αx.

This value of αx is then used to determine the true dead time, $t_o/\bar{t}$, from Figure:8.2.

For example, consider run numbers W-10.41 and WA-10.42, the apparent dead time is obtained by plotting more accurately the initial portion of the response curve, its value at which the normalised concentration reaches 0.05 is 0.700. The peak height for this particular run is 3.10; Figure:8.1 gives a value of αx equal to 13.2, which is then used, together with the apparent dead time of 0.700 to read off the value of true dead time from Figure:8.2, it is equal to 0.660.

The model parameter values are listed in Table: 1 to 3 of Appendix: D , for all the runs carried out during the present investigation.

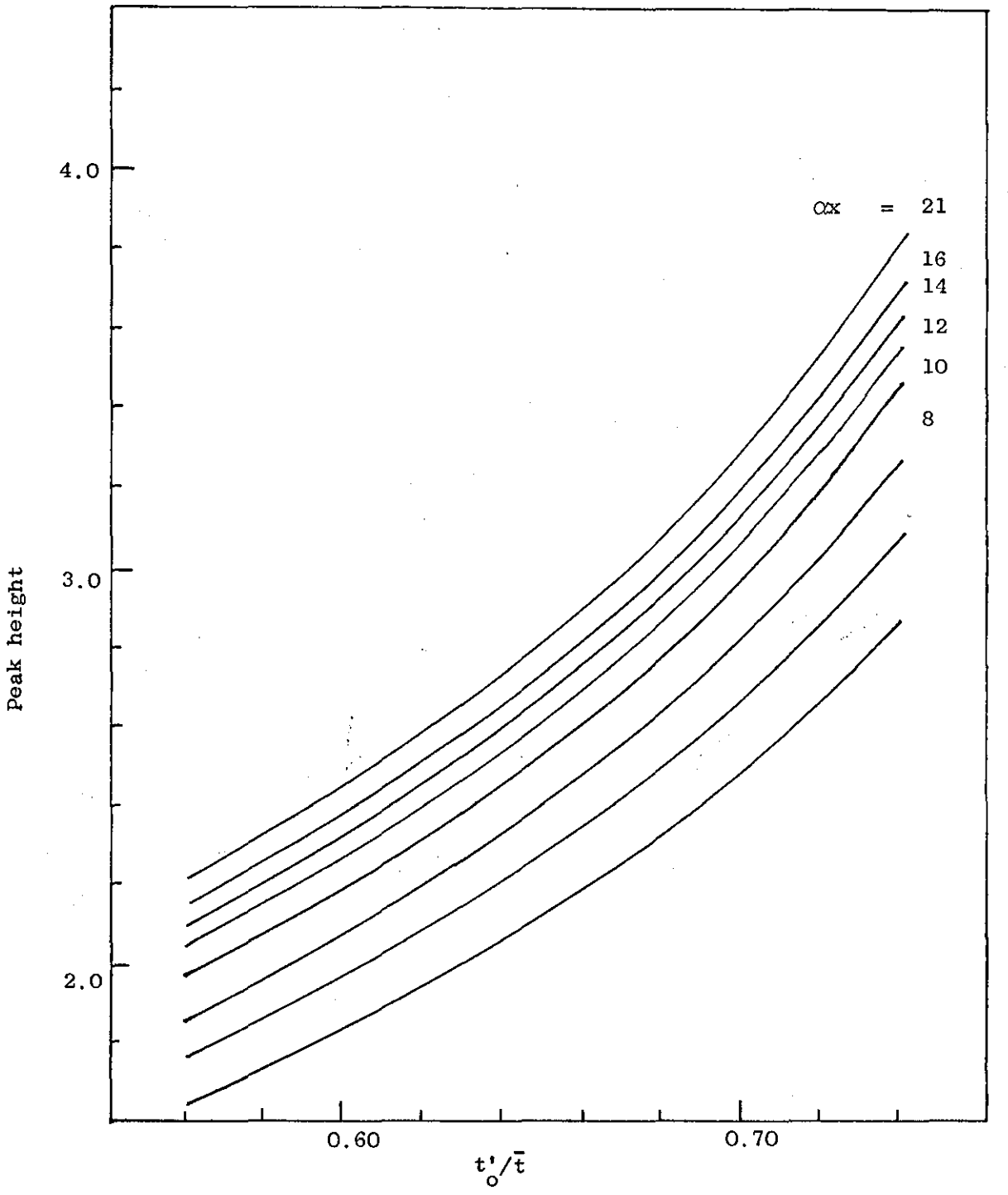

Figure: 8.1. The exponentially distributed time delay model: estimation of model parameters from the peak height and the apparent dead time, $t_o'/\bar{t}$.

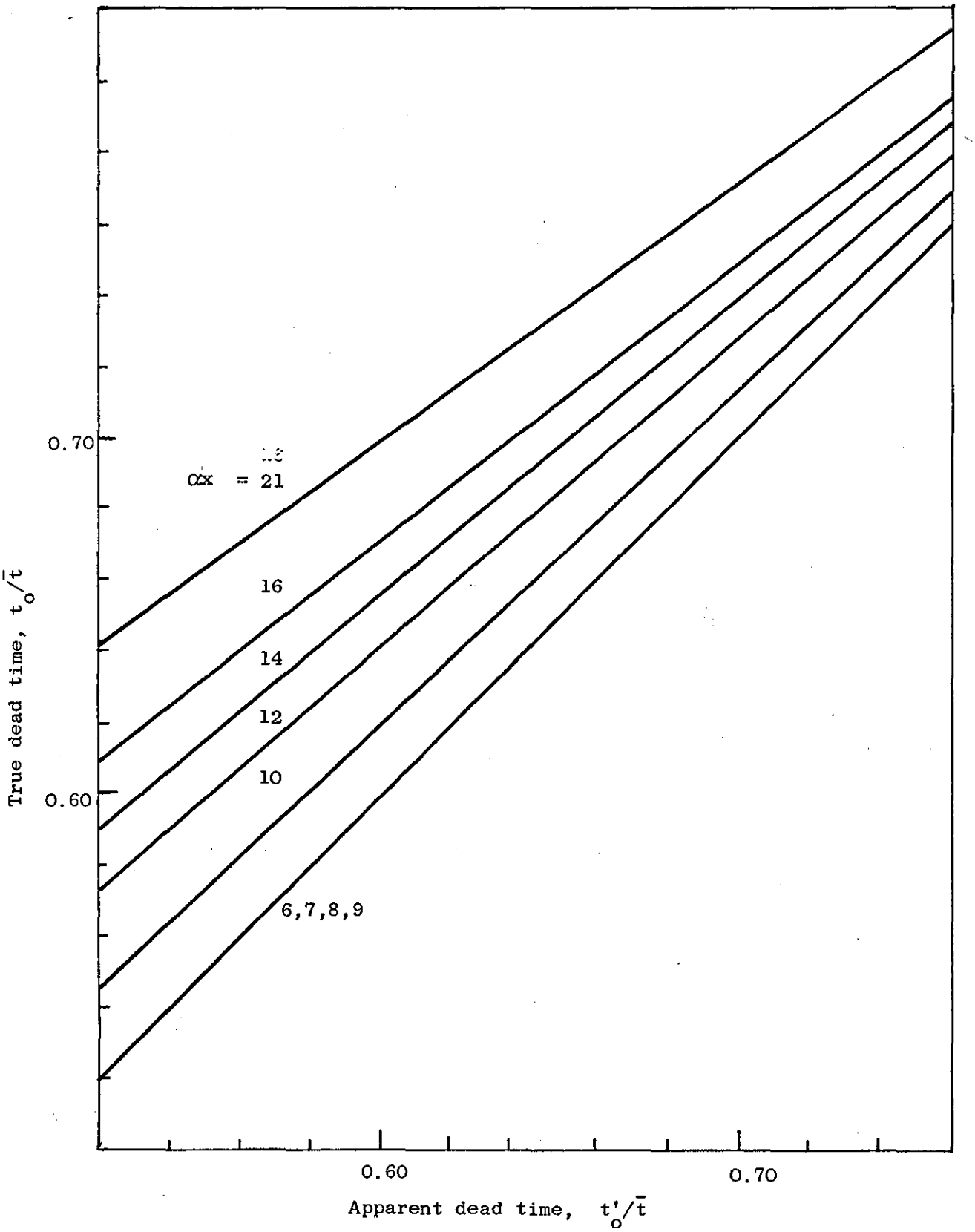

Figure: 8.2. The exponentially distributed delay time model: estimation of the model parameters from the apparent dead time, $t'_o/\bar{t}$ and αx.

8.2 Curve Fitting Procedure for Gamma Delay Times and Hopping Model

The method of direct comparison of the model and system response curves can be carried out provided an explicit real time solution of the model is possible. When such a solution is available, then a curve fitting criterion such as the least squares would give the desired parameter values.

In section 8, it was pointed out that the mathematical evaluation of the time-domain solution of the model may be a time consuming process especially when summation of series or the evaluation of some special function which might present computational problems is required. Moreover, during the performance of curve fits, many model solution evaluations for the intermediate values for each iterative function minimisation might be necessary before it actually converges to the best final values. An optimisatic technique, in which least square criterion is incorporated, is usually employed for function minimisation. Many optimisation procedures are available. Rosenbrock's[111] method was chosen, firstly as it minimises the function of several variables when variables are restricted to a region and secondly a library subroutine of the method was readily accessible.

The overall curve fit procedure is summarised below:

From the initial estimates of the parameters, first N values are calculated and compared with the corresponding data points. The least square criterion was then used and the parameter values adjusted by the optimisation subroutine to minimise the function.

Calculated parameter values for all the curve-fits are presented in Tables: 4, 5, and 6 for the gamma-distributed delays and in Tables: 7, 8 and 9 for the hopping model. All tables are given in Appendix: D.

Nomenclature

x	distance
t	time
t_o	true dead time
t'_o	apparent dead time
$\bar{t}$	mean residence time
$t/\bar{t}$	normalised time
$t_o/\bar{t}$	normalised true dead time
$t'_o/\bar{t}$	normalised apparent dead time
α	number of stops per unit length

9. COMPARISON OF THE EXPERIMENTAL RESULTS OF DYNAMIC TESTS WITH THE PROPOSED MODELS

9. Comparison of Experimental Results of Dynamic Tests with the Proposed Models

In this section experimental responses have been compared with those of the proposed models for different operating conditions, liquid properties and packed lengths.

The normalised response curves are presented in Appendix: B.

9.1. Time Delay Model with Exponentially Distributed Delay Times

The curve fitting procedure described in section 8.1 is used for this case and the model solutions obtained by the computer program which is given in Appendix : F.

Figures: 9.1 through 9.10 are the experimental responses under varying situations with the solid line representing the model solution. The results are typical of each set of runs: the sharp initial rise is well fitted and the slowly decaying long time response of the model comes close to that obtained in practice. However, the position of the peak and the subsequent decay of the model response represents a more symmetrical distribution than that obtained experimentally. These characteristics are common in all the curve fits for this two parameter model.

Tables: 1 to 3 of Appendix : D , summarise the results of the complete set of experimental runs carried out during this investigation. It is interesting to note that the parameter, α, which measures the ratio of the lateral flow rate per unit length to the axial flow rate remains remarkably constant, independent of packed height for one type of fluid: the average value of α and its variation with the liquid viscosity is given in Table:9.1 below:

Table: 9.1. Variation of α with the liquid viscosity

Type of fluid	Viscosity of fluid μ cp	α	Standard deviation
Water	1.00	1.30	0.04

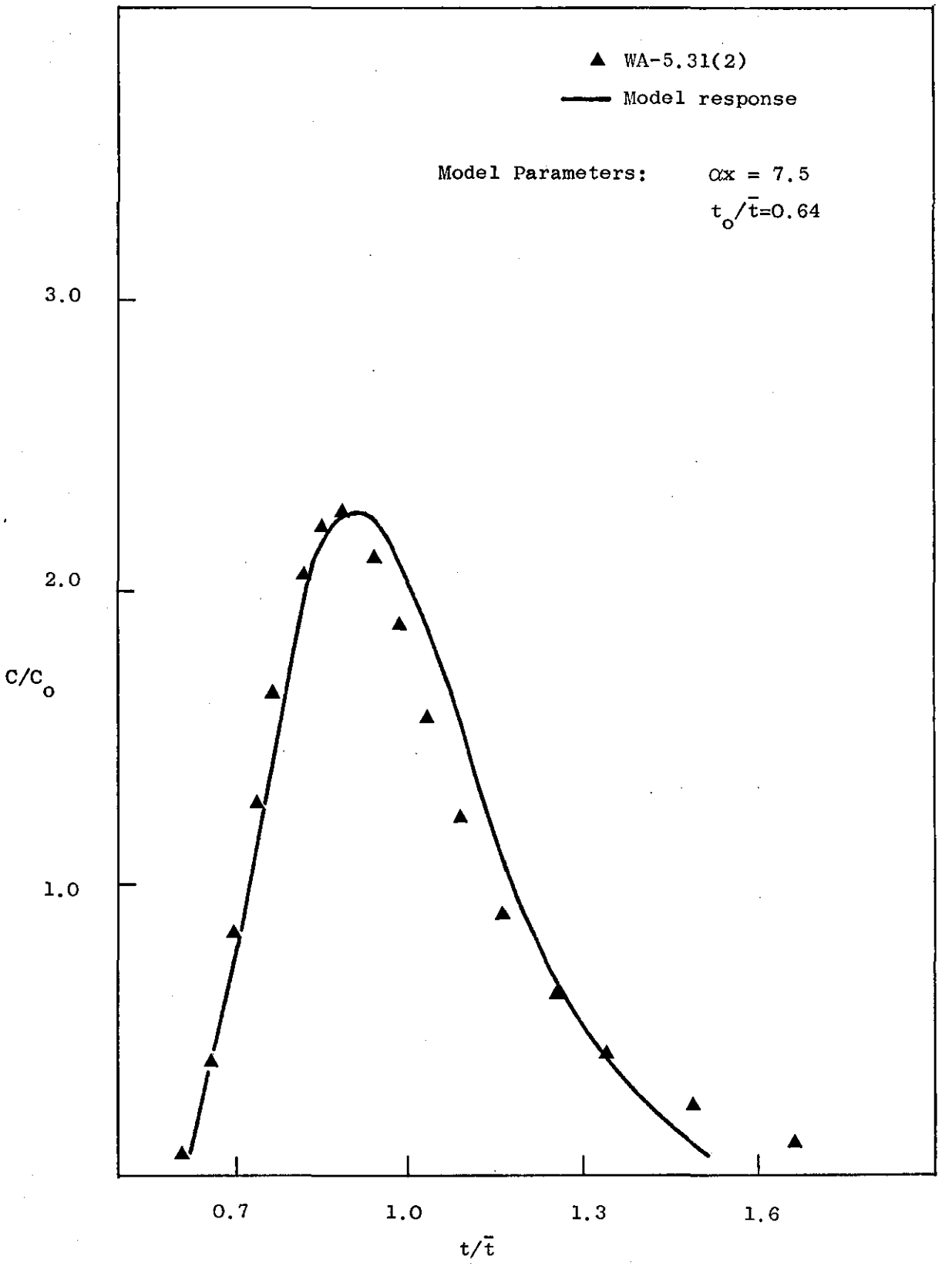

Figure: 9.1. Comparison of the experimental response and the exponential time delay model solution.

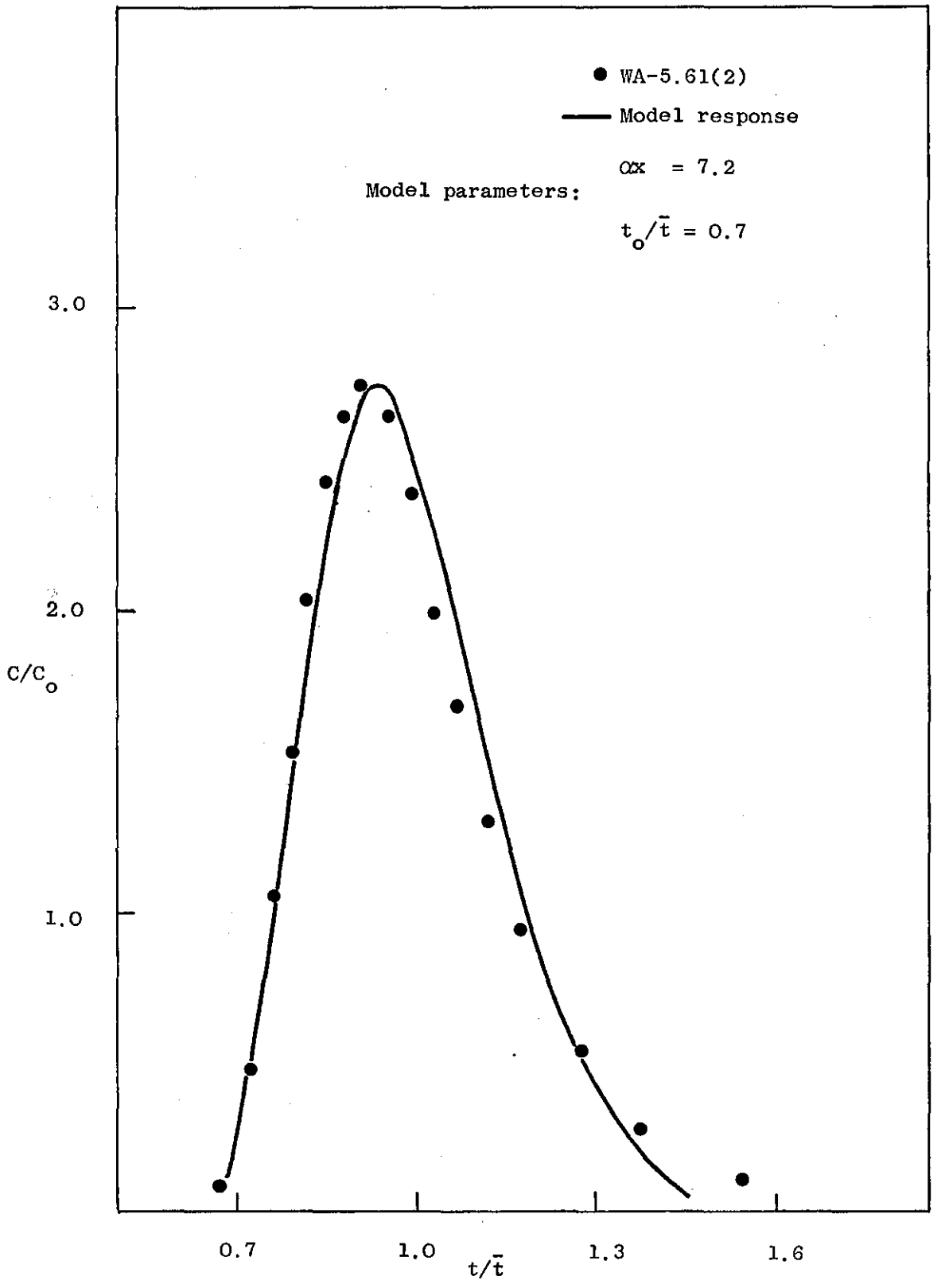

Figure: 9.2. Comparison of the experimental response and the exponential time delay model solution.

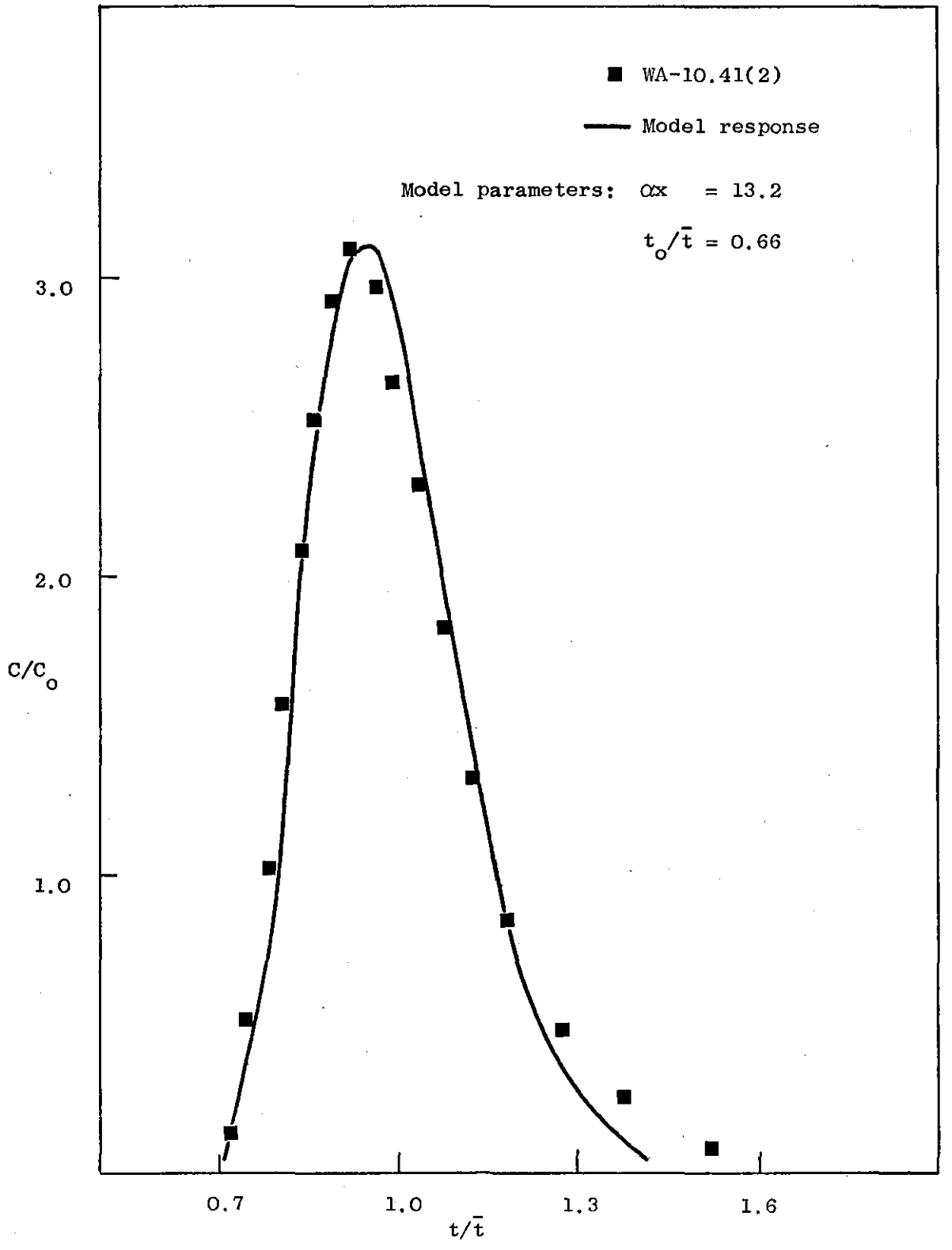

Figure: 9.3. Comparison of the experimental response and the exponential time delay model solution.

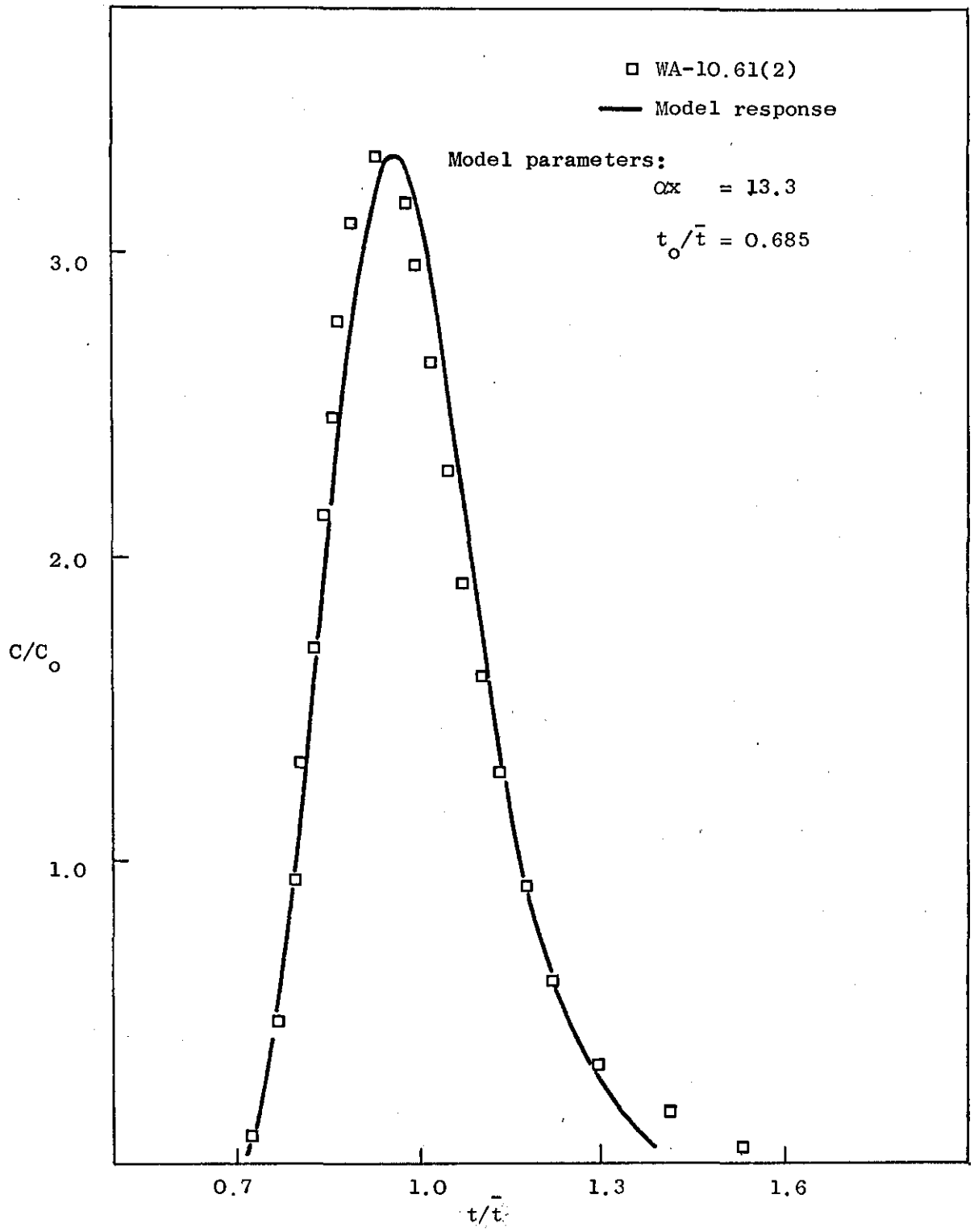

Figure: 9.4. Comparison of the experimental response and and the exponential time delay model solution.

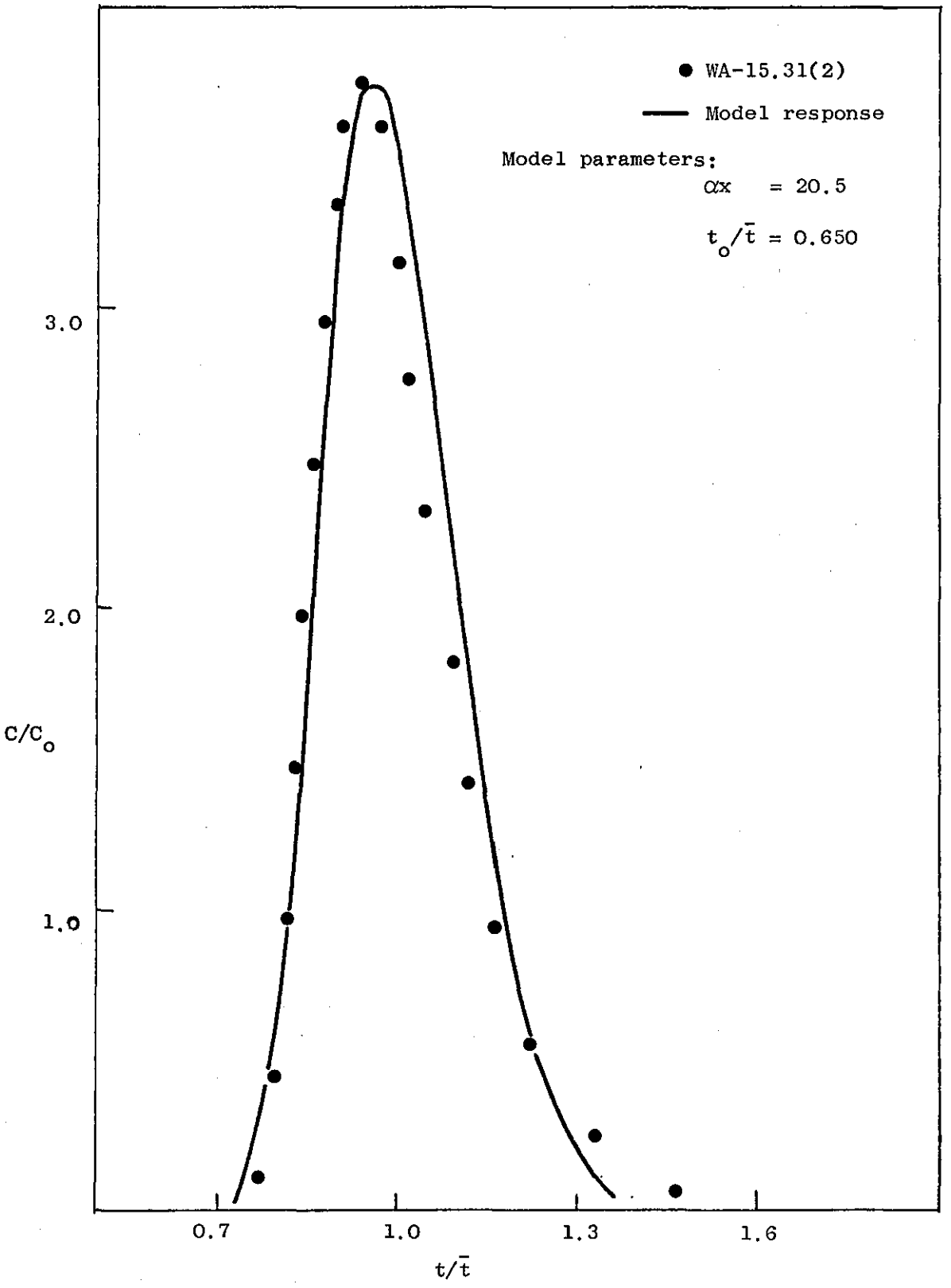

Figure: 9.5. Comparison of the experimental response and the exponential time delay model solution.

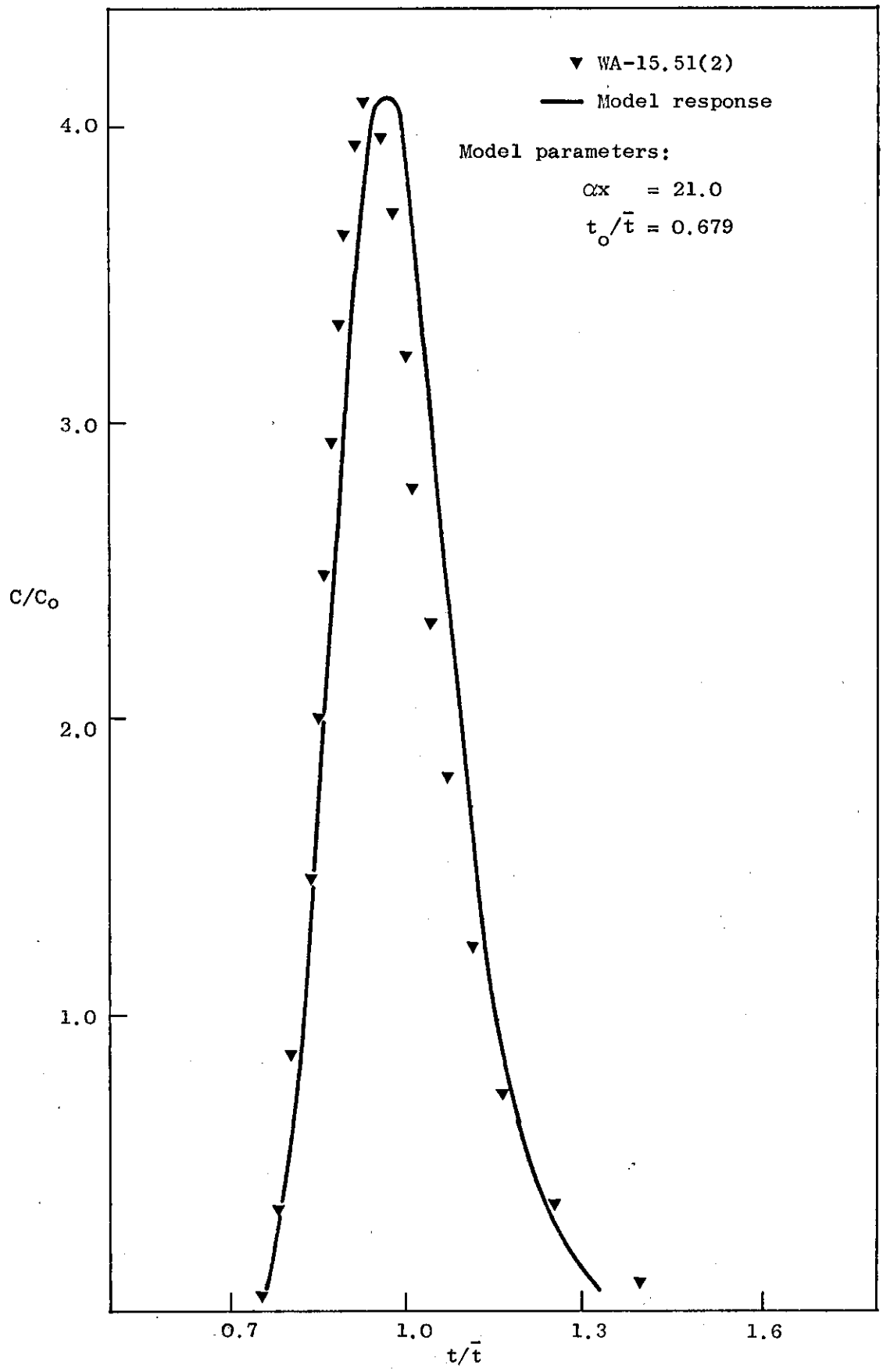

Figure: 9.6. Comparison of the experimental response and the exponential time delay model solution.

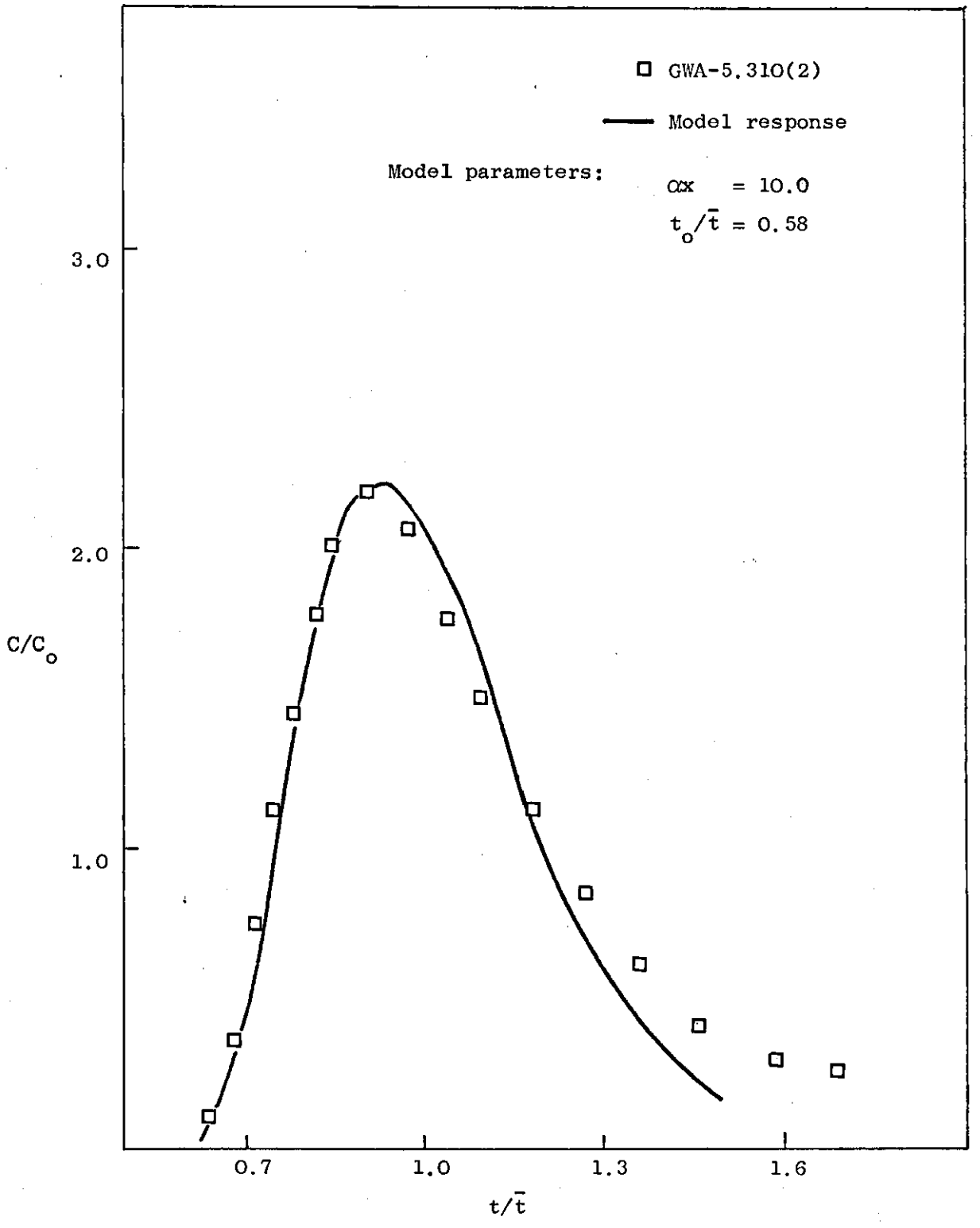

Figure: 9.7. Comparison of the experimental response and the exponential time delay model solution.

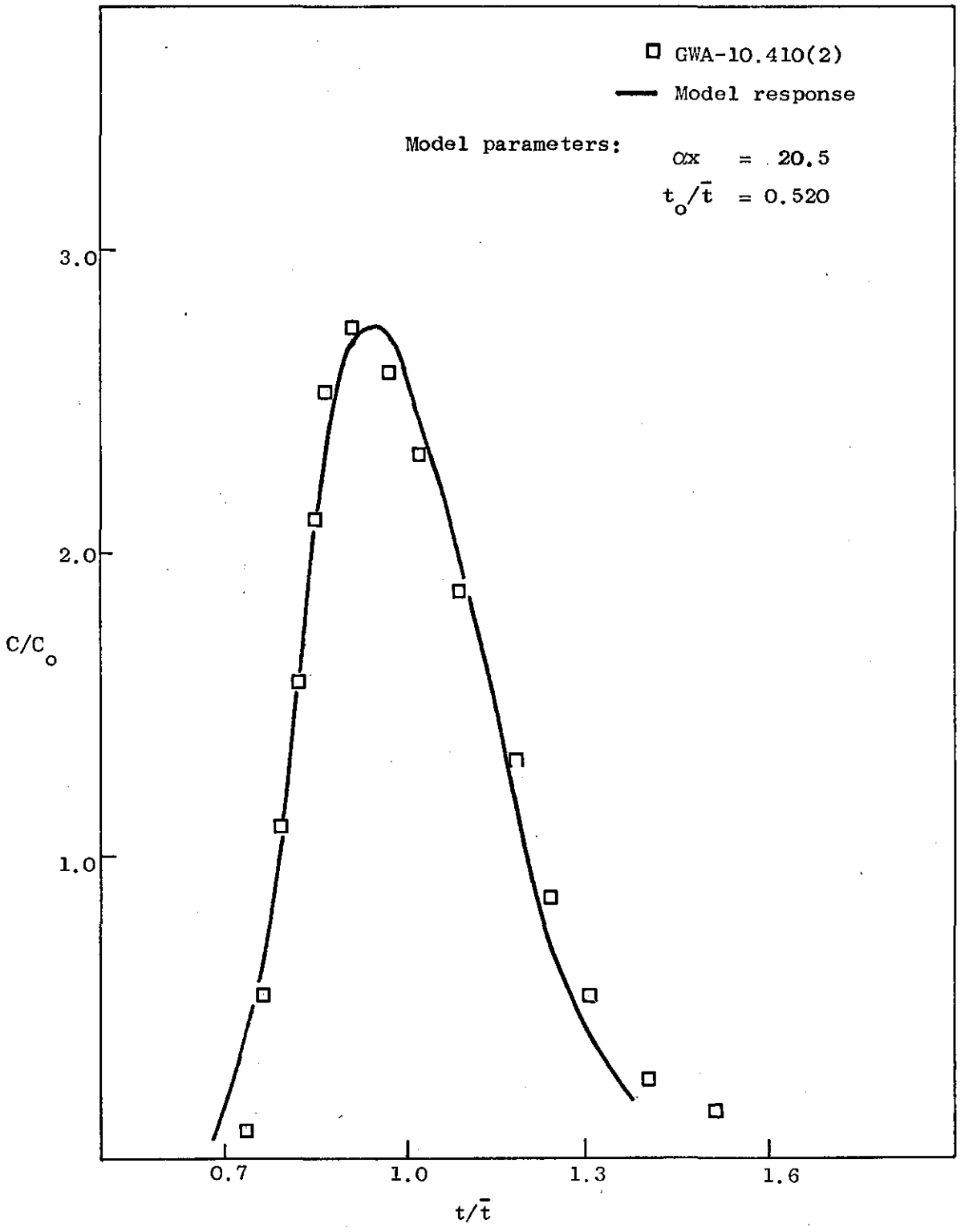

Figure: 9.8. Comparison of the experimental response and the exponential model solution.

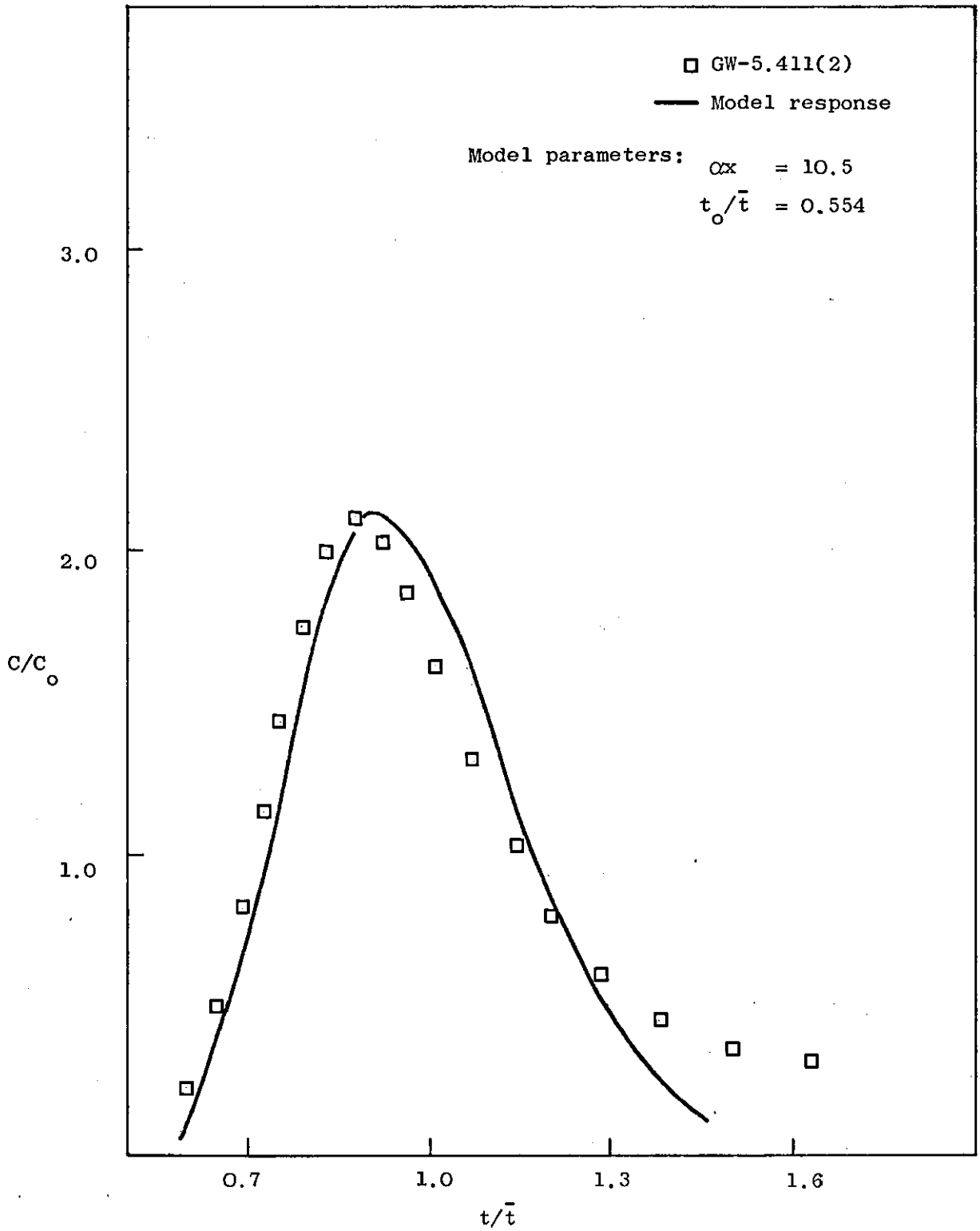

Figure: 9.9. Comparison of the experimental response and the exponential time delay model solution.

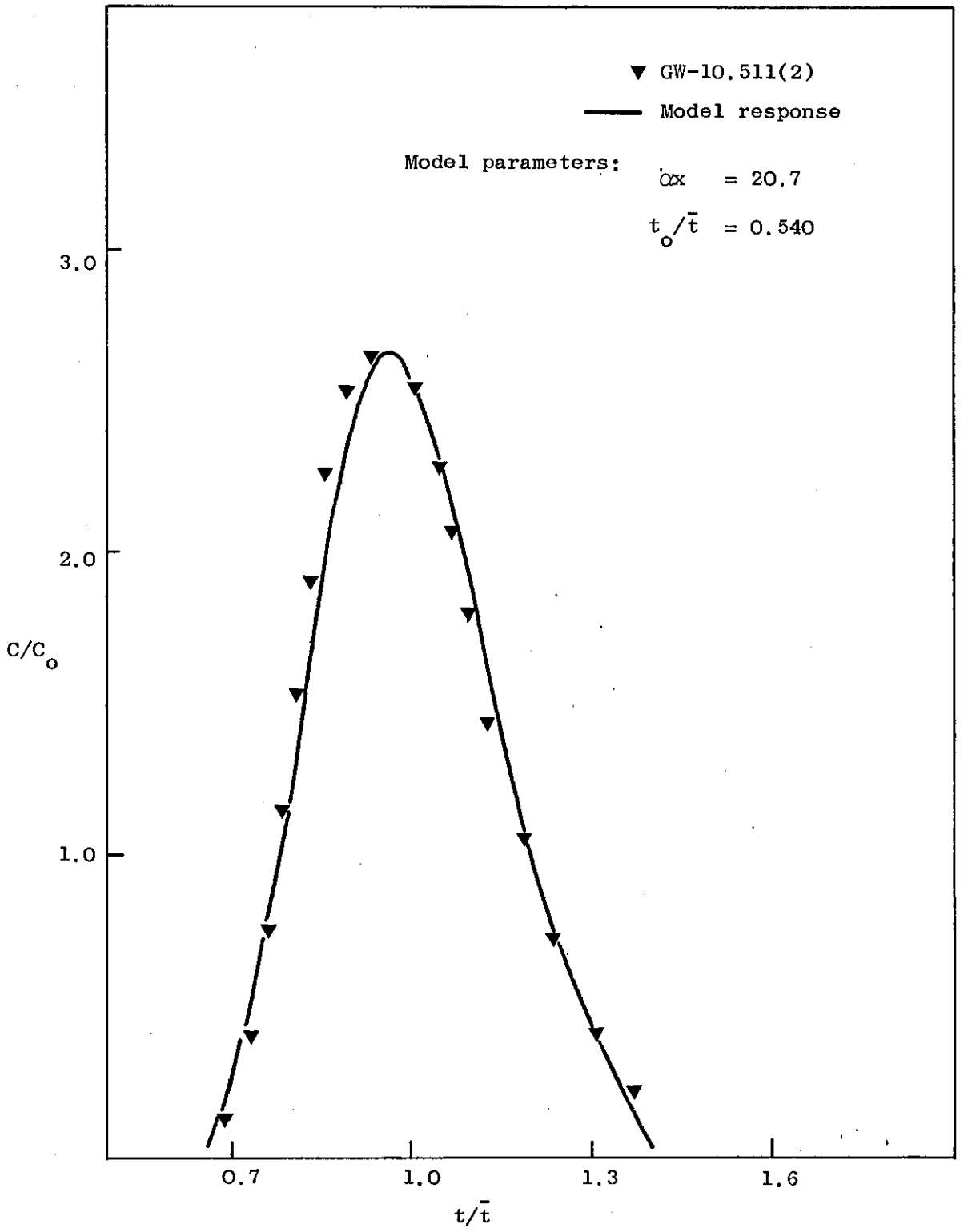

Figure: 9.10. Comparison of the experimental response and the exponential time delay model solution.

T ype of fluid	Viscosity of fluid μ cp	α	Standard deviation
Glycerine-solution	4.50	1.89	0.07
Glycerine-solution	7.50		

Tables: 1D to 3D also provide the corresponding term in the dispersion model, D, which show considerable scatter and no clear trend being discernable.

The value of parameter $t_o/\bar{t}$ increases with the increasing liquid flow rates. The time delay model postulates that the main flow region is in plug-flow and the holdup correlations of section 7.2 indicate the static holdup to be constant. If the plug-flow assumtion is reasonable then the true dead time $t_o/\bar{t}$, determined from the model fitting procedures, correlate in some manner with the operating holdup H_{op}, of the column. Figure 9.11 shows the plots of dead time, $t_o/\bar{t}$, versus the operating holdup, H_{op}, for both water and glycerine-solutions. Both results can be correlated by a straight line relationship, each line corresponding to one type of fluid.

The correlations are strictly applicable to the present column and packing geometry: thus for exponentially distributed case:

For water-air system:

$$t_o/\bar{t} = 0.465 + 1.2\ H_{op} \qquad (9.1)$$

For glycerine-solutions:

$$t_o/\bar{t} = 0.290 + 1.2\ H_{op} \qquad (9.2)$$

Thus for the system studied, it is only a matter of determining the operating holdup, under the operational conditions, to calculate all the corresponding model parameter values, the parameter α being constant for each fluid type.

To test the applicability of the above proposed correlation, values of the dead time $t_o/\bar{t}$, were obtained for a number of runs and the response curves plotted and compared with corresponding parameter values already determined. Figures:9.12,9.13 and9.14,9.15 are two sets of such compared runs. It can be seen that both curves fit the experimental curve quite well.

9.2. Time Delay Model with the Gamma Distributed Delay Times

The curve fitting procedure for the three-parameter model described in section 8.2, required the minimisation of a function. A considerable amount of time and work is saved if the boundary limits are set in the search method before embarking on the actual procedure.

These boundary limits consist of a set of upper and lower likely values of the optimisation parameters, in the present case namely αx, m and $t_o/\bar{t}$, which can be set by examining the shape of the experimental responses and the time-domain solution of the model.

It can be seen from the experimental response curves, and has been in fact pointed out in Chapter 8, that the precise values of the true dead time , $t_o/\bar{t}$, cannot be read off the curves, however it can be predicted to lie within a certain possible range. For example by examining the normalised response curves of the $5\frac{1}{2}$feet packed column for water-air system; all the curves start between dead time values of 0.55 and 0.65, clearly dead time must lie at the outset between a value of 0.50 and 0.70. These values are taken as the lower and upper limits of the parameter, $t_o/\bar{t}$, with the initial starting values chosen arbitrarily as 0.60.

In section 5.3, it was pointed out that the skewness of the response curve of the gamma distributed delay time model increases as m approaches the limit of zero, and the model reduces to the exponentially distributed time delay form for m equal to unity. Since the aim of the

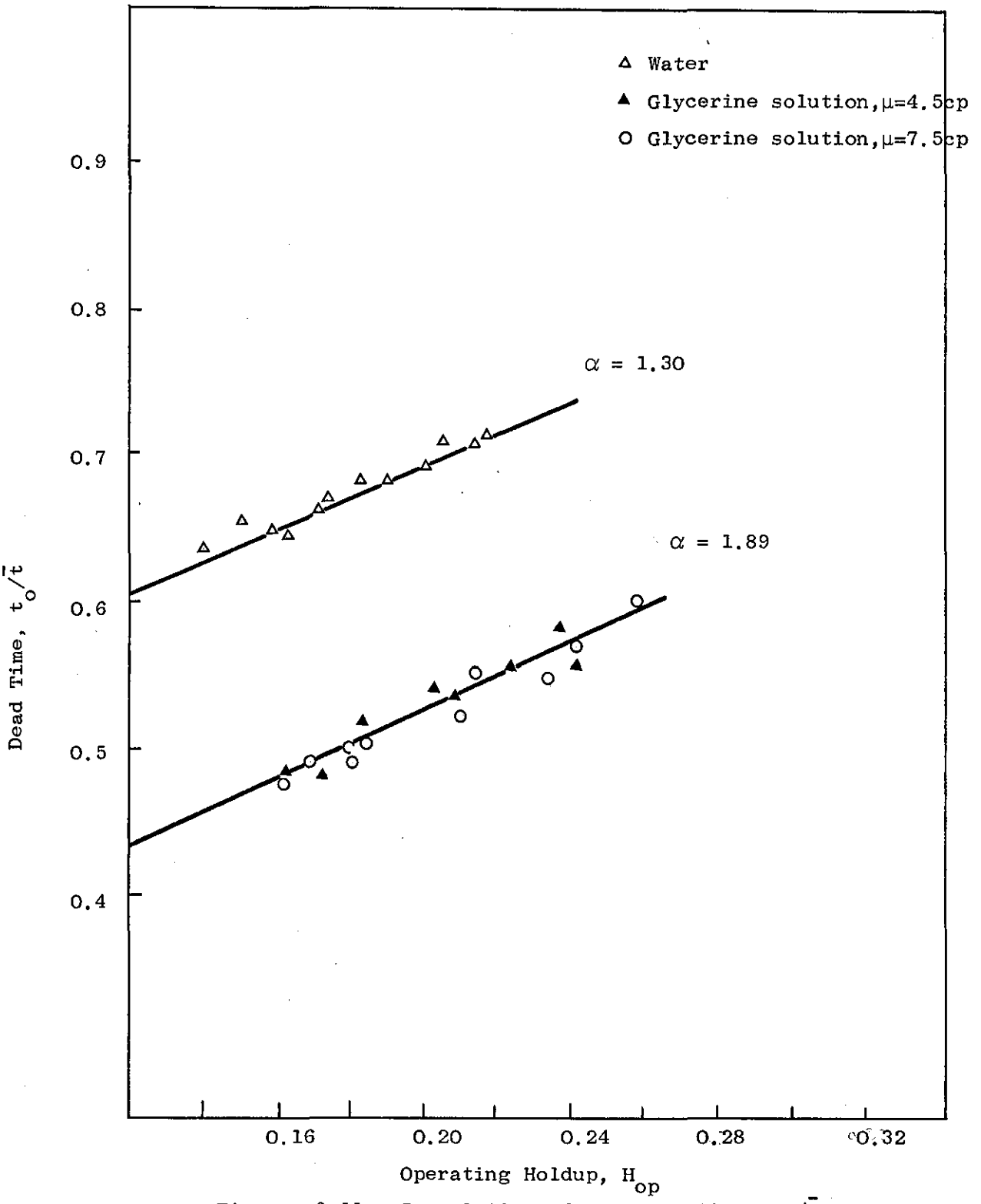

Figure: 9.11. Correlation of the dead time, $t_o/\bar{t}$, and the operating holdup, H_{op}

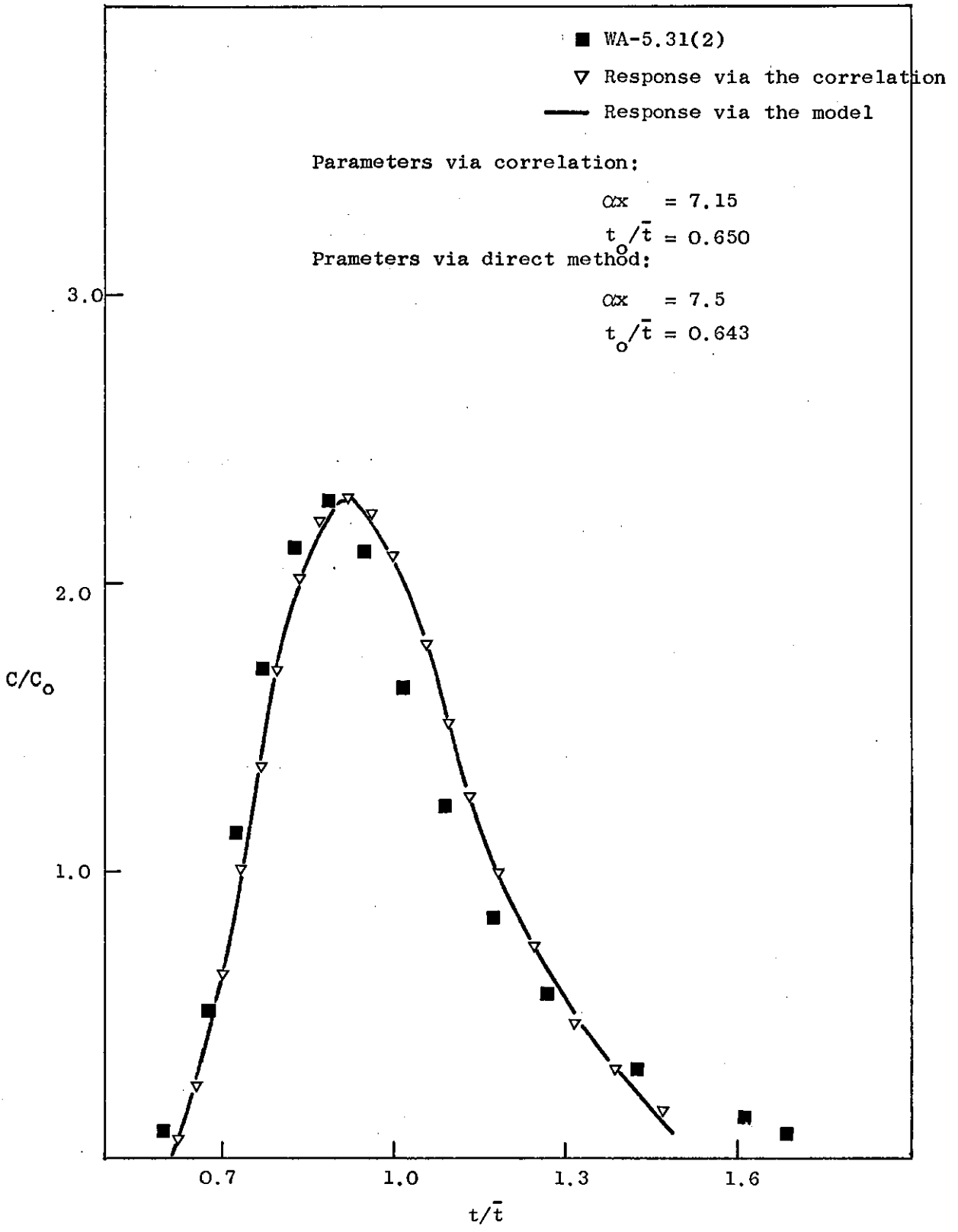

Figure: 9.12. Comparison of the experimental, the correlation and the exponential time delay responses.

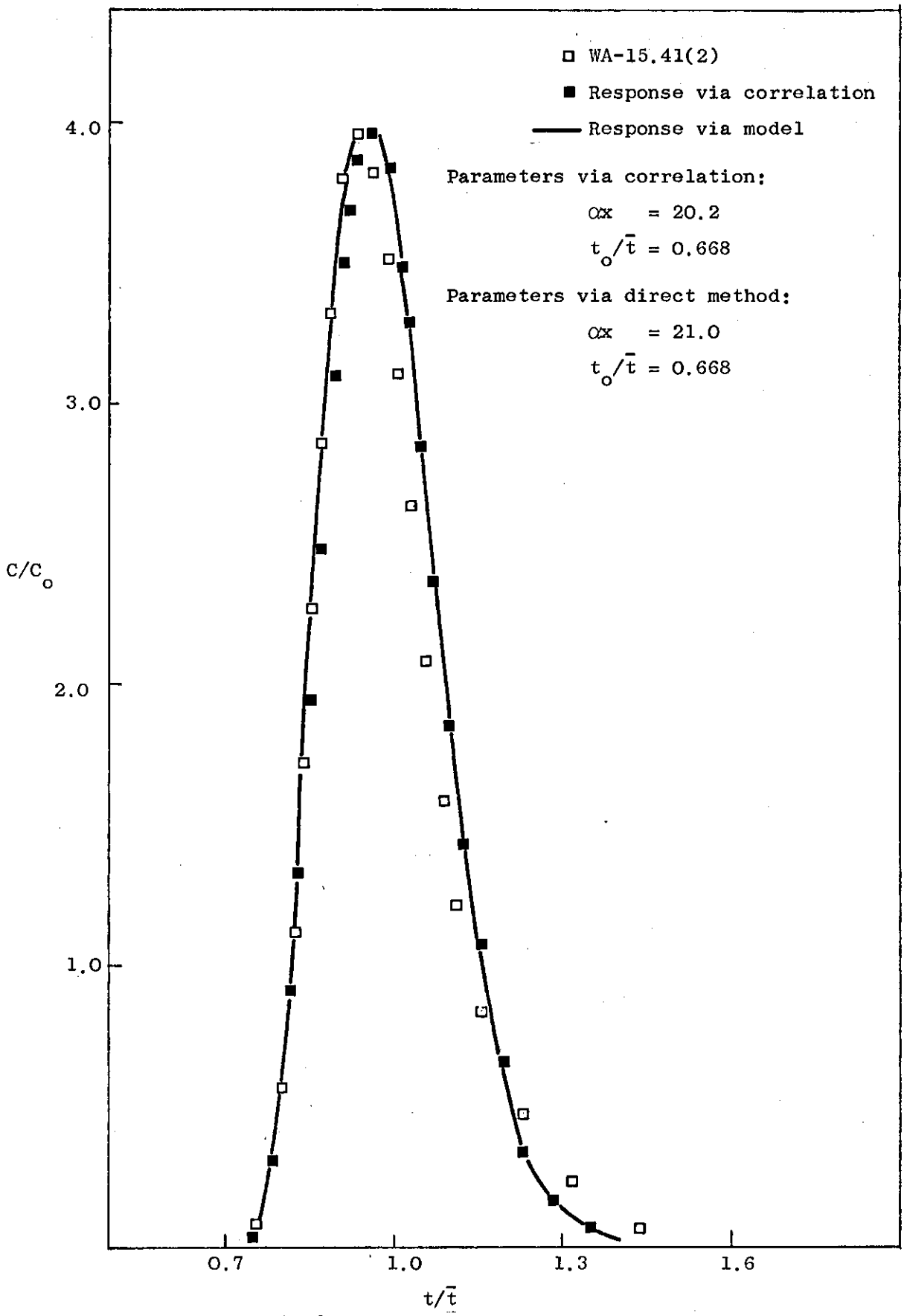

Figure: 9.13. Comparison of the experimental, the correlated and the exponential time delay model responses.

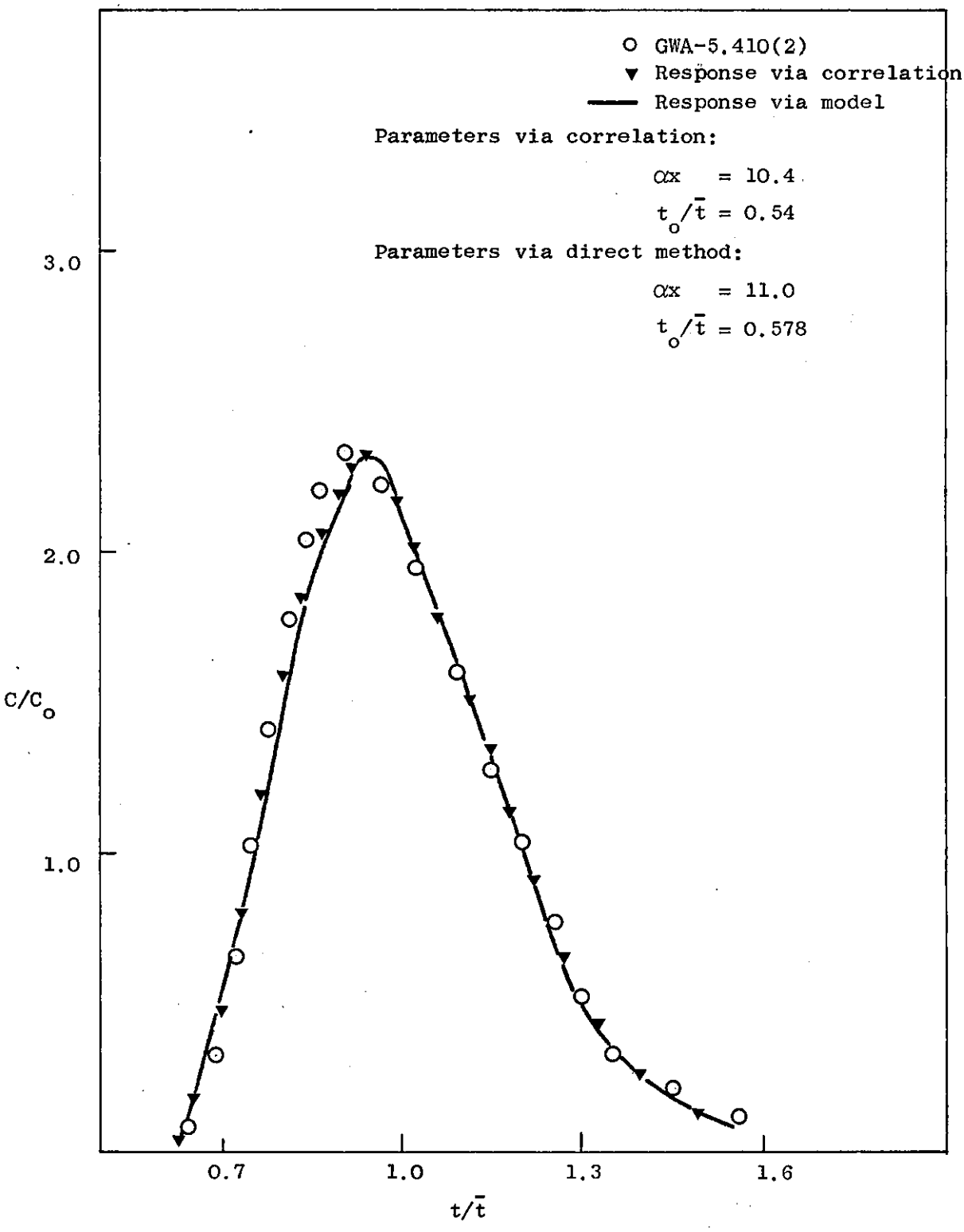

Figure: 9.14. Comparison of the experimental, the correlated and the exponential time delay model responses.

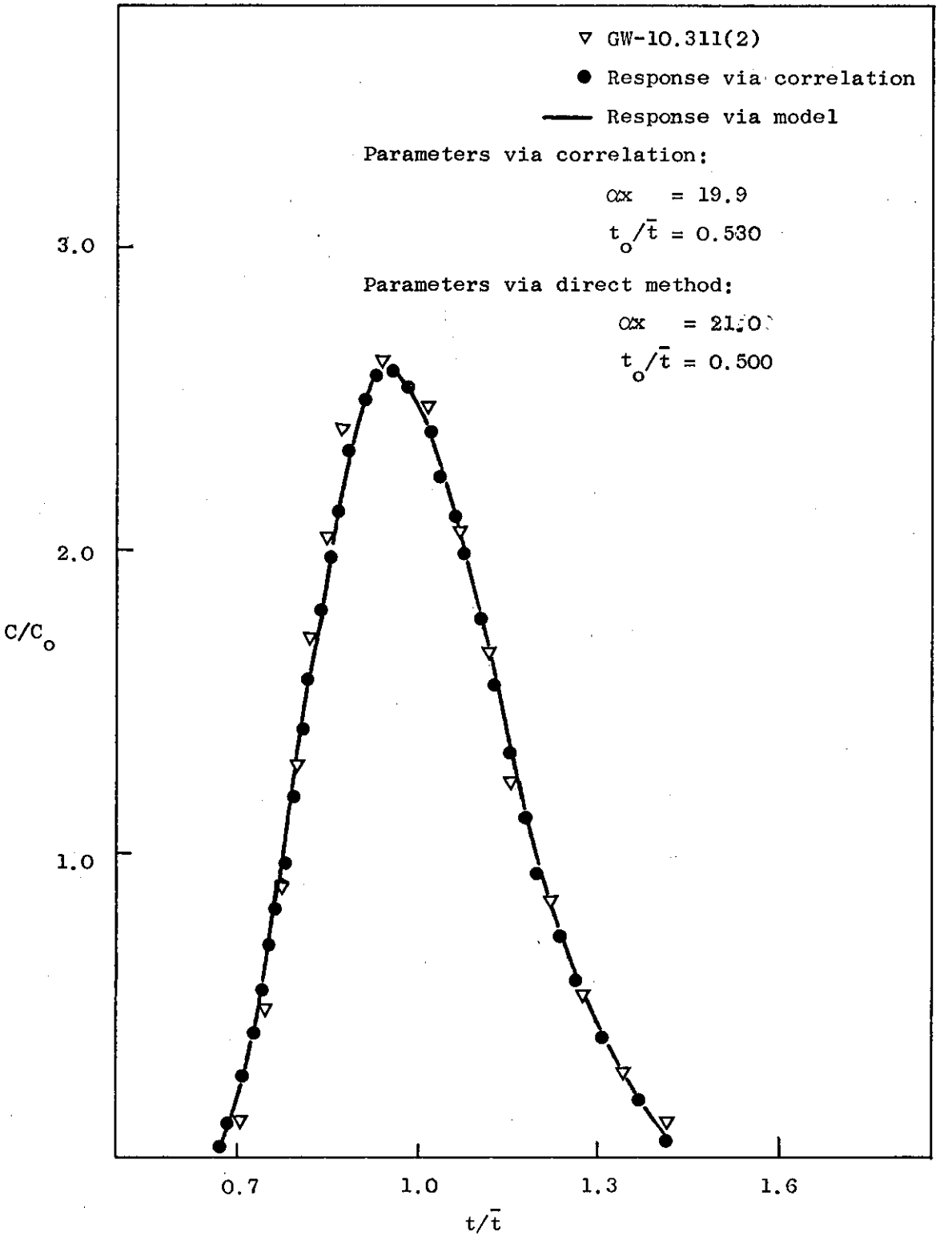

Figure: 9.15. Comparison of the experimental, the correlated and the exponential time delay model responses.

third parameter is to increase the skewness, it is only necessary to limit the possible values of m between 0 and 1.

Theoretically the upper and lower limit of the parameter αx are ∞ and 0; if the range is fixed as such the search programme would be unduely prolonged. It would be worthwhile to narrow this range; an estimate can be based on the previously determined values of this parameter for the exponential case, thus for shorter length of columns these were taken as 20 and 1; for the longer packed sections as 50 and 1. However, if during the course of the parameters search either of the limits exceeded, these were appropriately readjusted to a new set of values.

It is usually assumed that all experimental work inherits a certain amount of error from the experimental techniques employed, sometimes it is incorporated during data processing. The calculation of the mean residence time suffers from such unavoidable faults. In the holdup section 7.2, the possibility of introducing ± 4 % error in the determination of the mean time was indicated. It is therefore quite reasonable to include this parameter as one of the variables in the optimisation procedure. The upper and lower limits of the mean time were based on the $\pm$ 4% experimental error; values of 1.04 and 0.96 respectively were chosen as the mean is equal to unity.

Following the above scheme, all the curve fitting was carried out and the parameters evaluated. Figures:9.16 through9.25 show how the response of this model compares with the response obtained for different runs under varying operating conditions. It can be observed that most parts of the curves are well fitted except for the initial rise. During the course of curve fitting, minimisation function failed to converge especially when a number of data points were selected at the very beginning of the curve. The fault was revealed when the model solution was analysed.

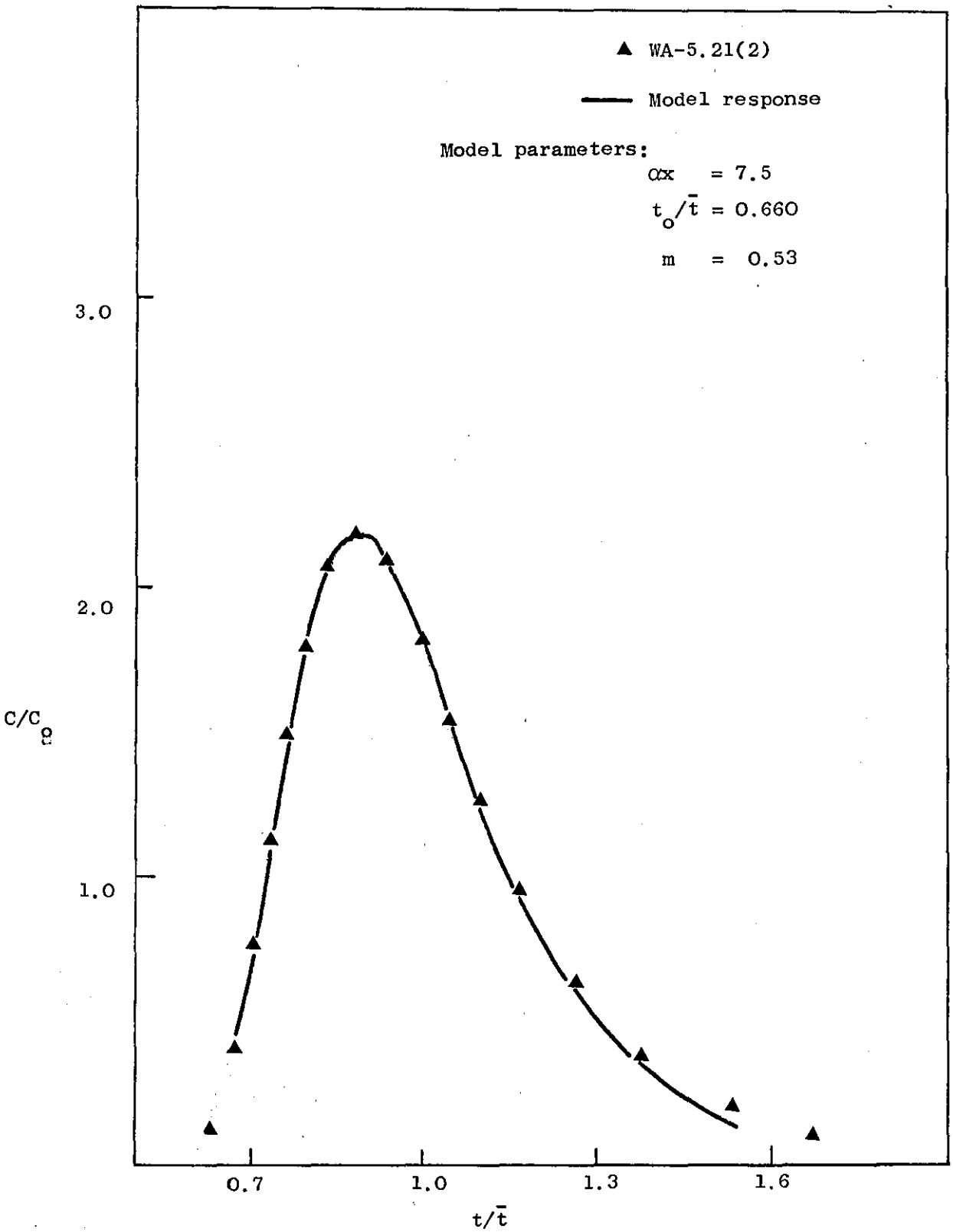

Figure: 9.16. Comparison of the experimental response and the gamma distributed time delay model solution.

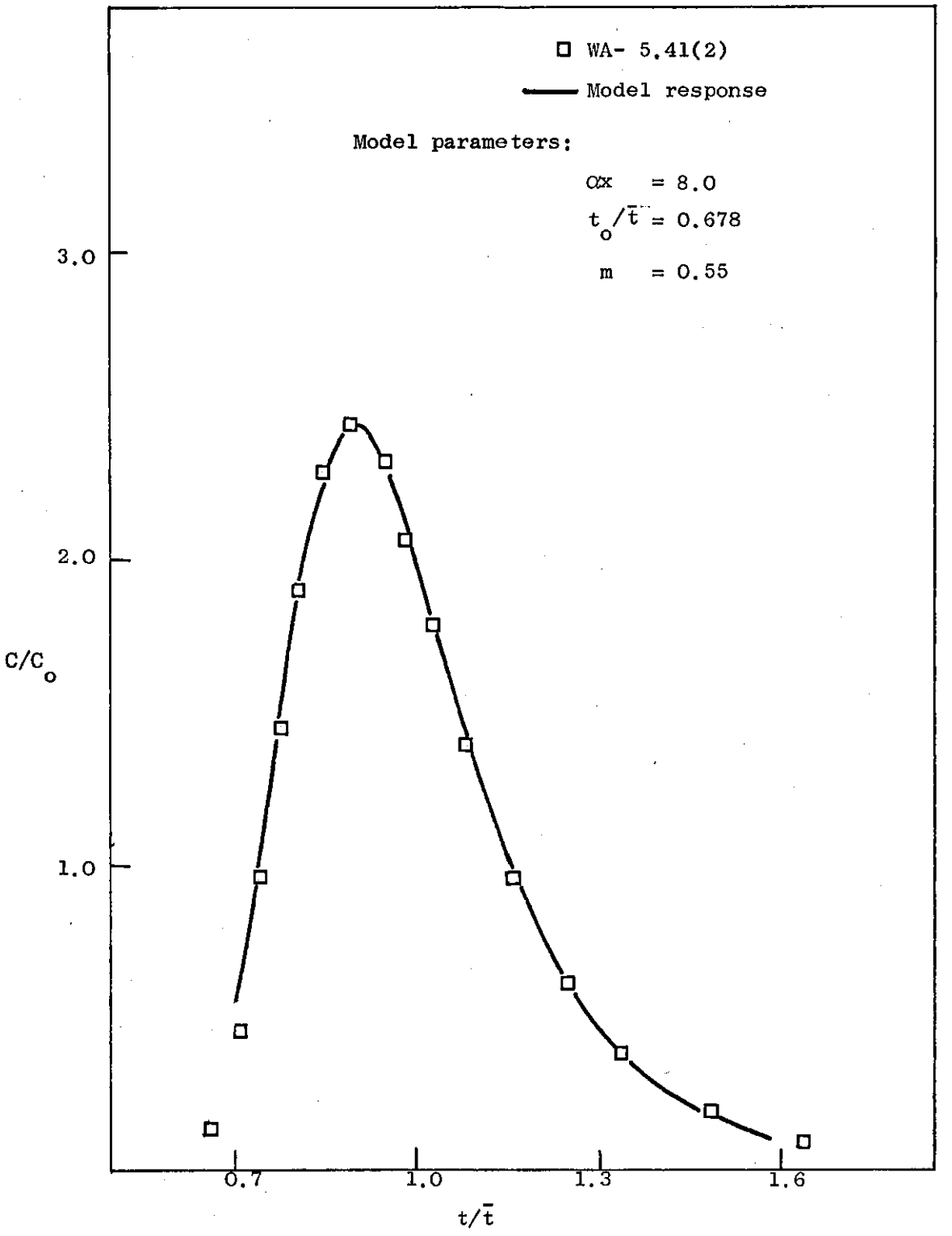

Figure: 9.17.Comparison of the experimental response and the gamma distributed time delay model solution.

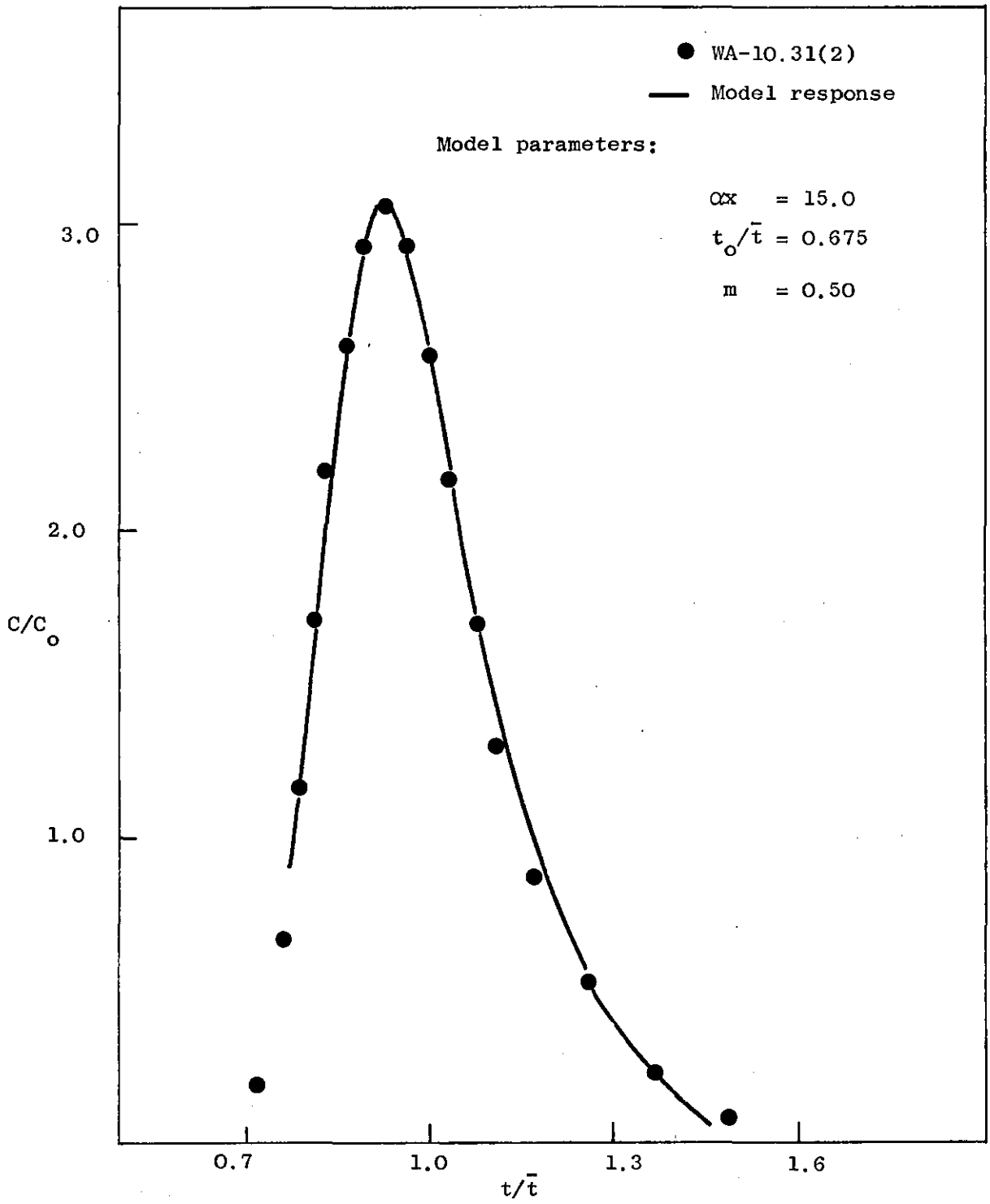

Figure: 9.18. Comparison of the experimental response and the gamma distributed delay time model solution.

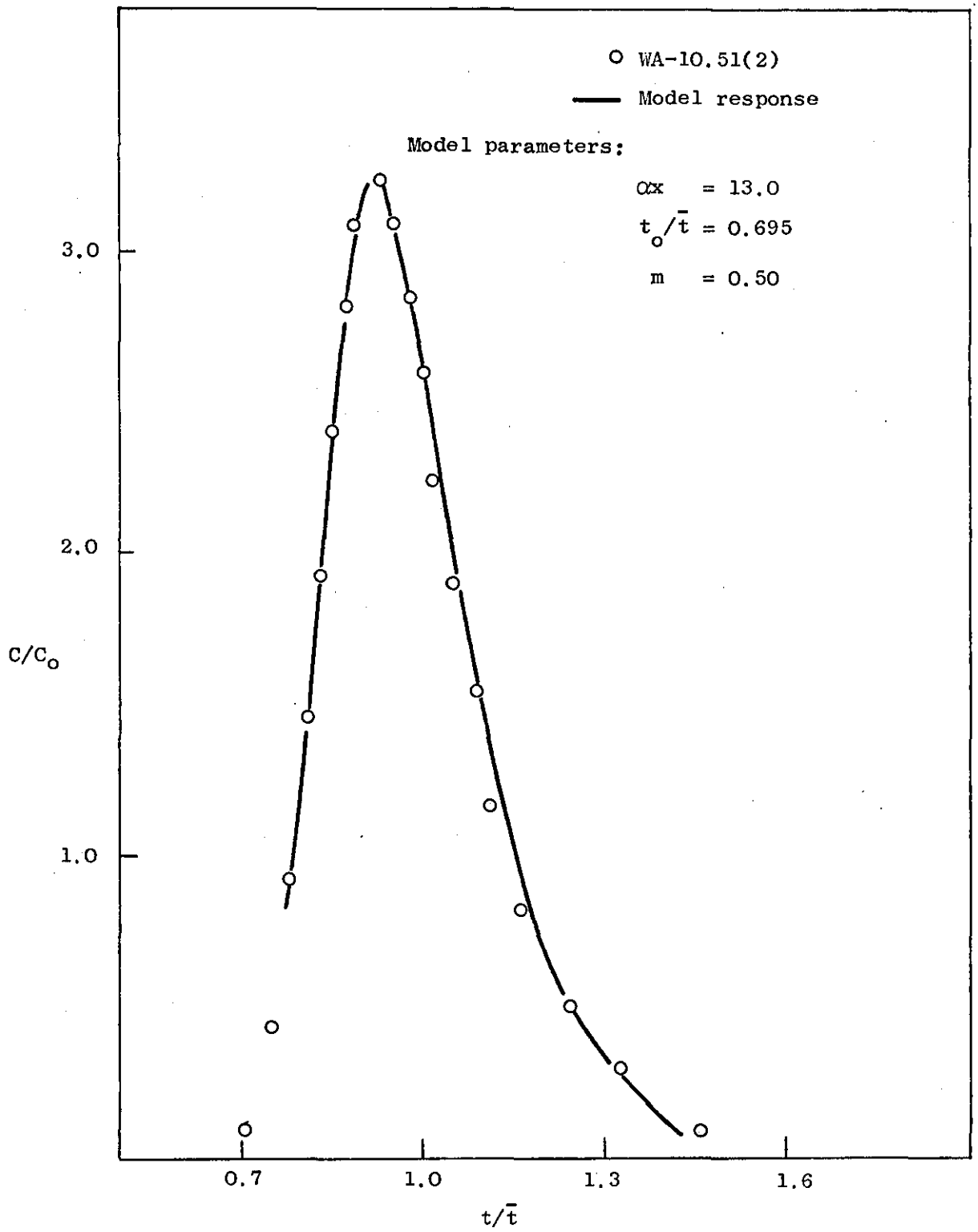

Figure: 9.19. Comparison of the experimental response and the gamma distributed time delay model solution.

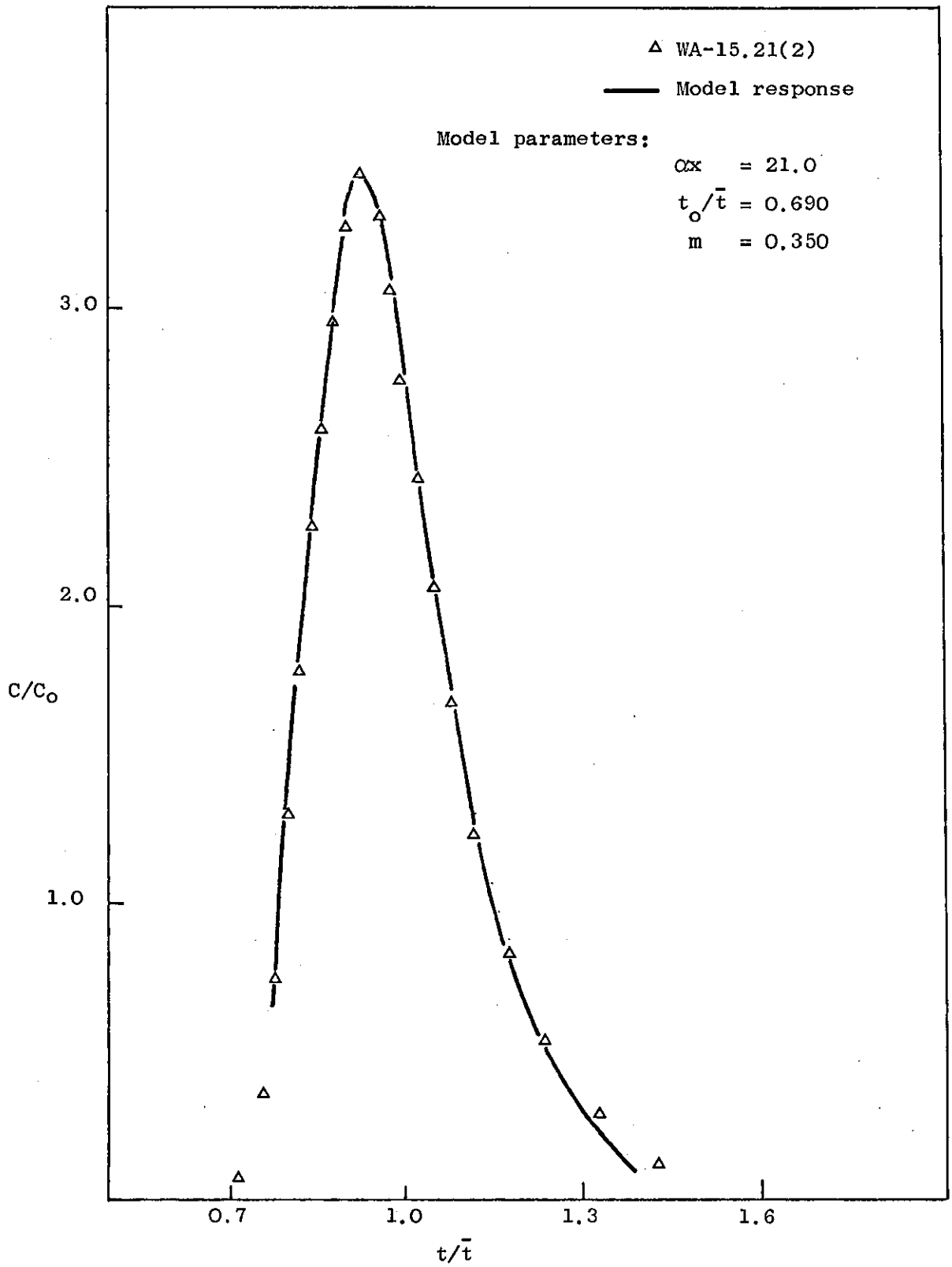

Figure: 9.20. Comparison of the experimental response and the gamma distributed time delay model solution.

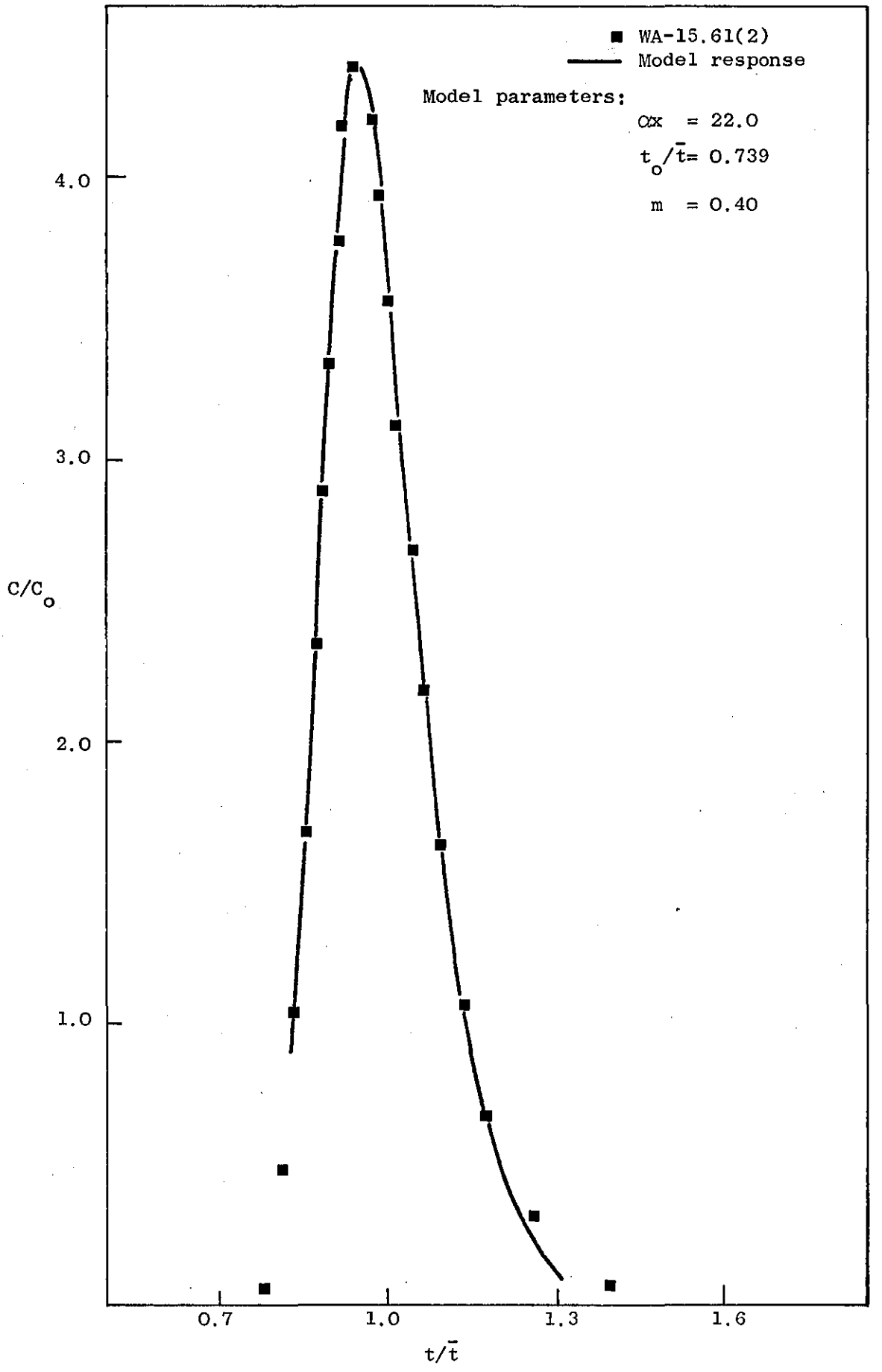

Figure: 9.21. Comparison of the experimental response and tha gamma distributed time delay model solution.

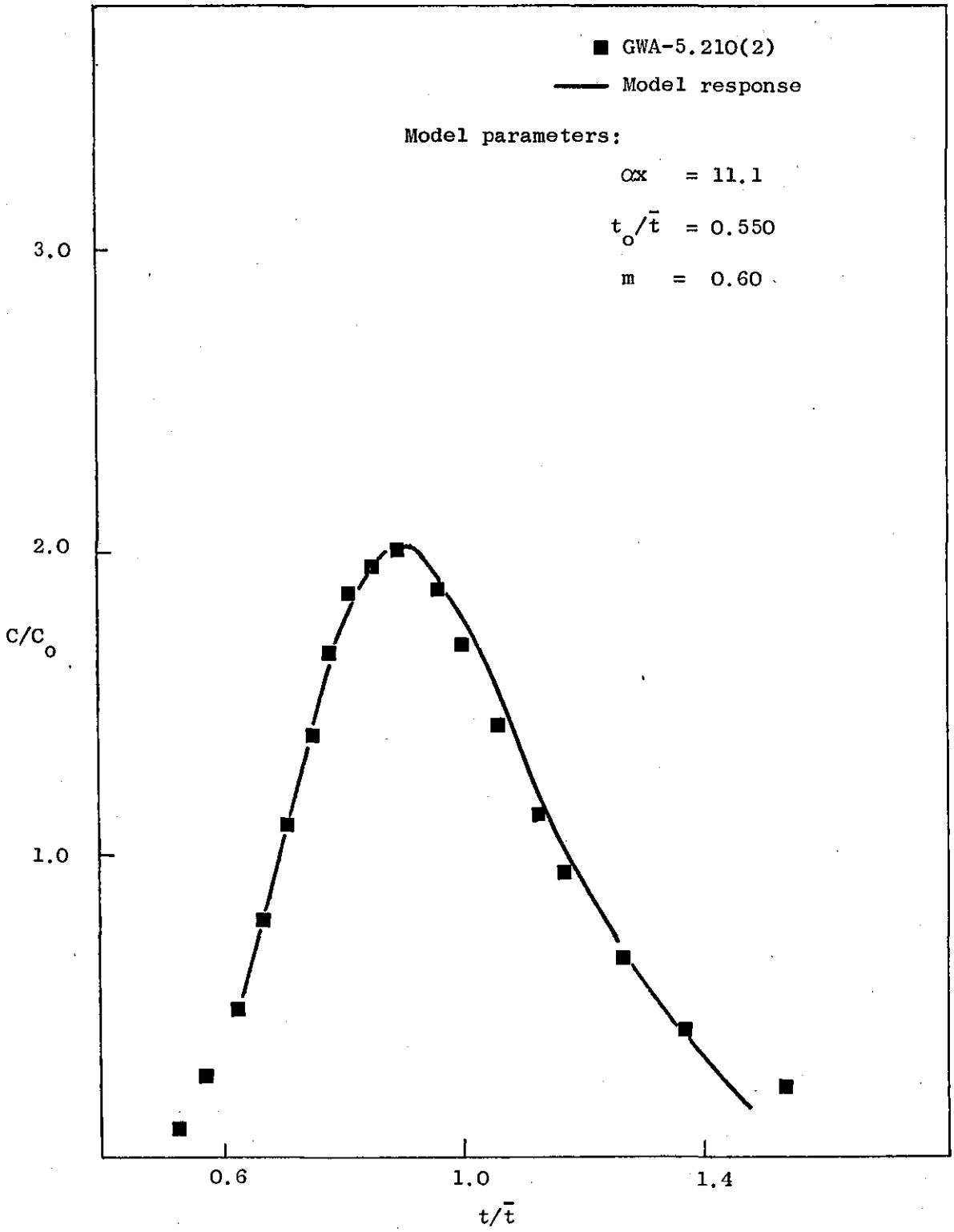

Figure: 9.22. Comparison of the experimental response and the gamma distributed time delay model solution.

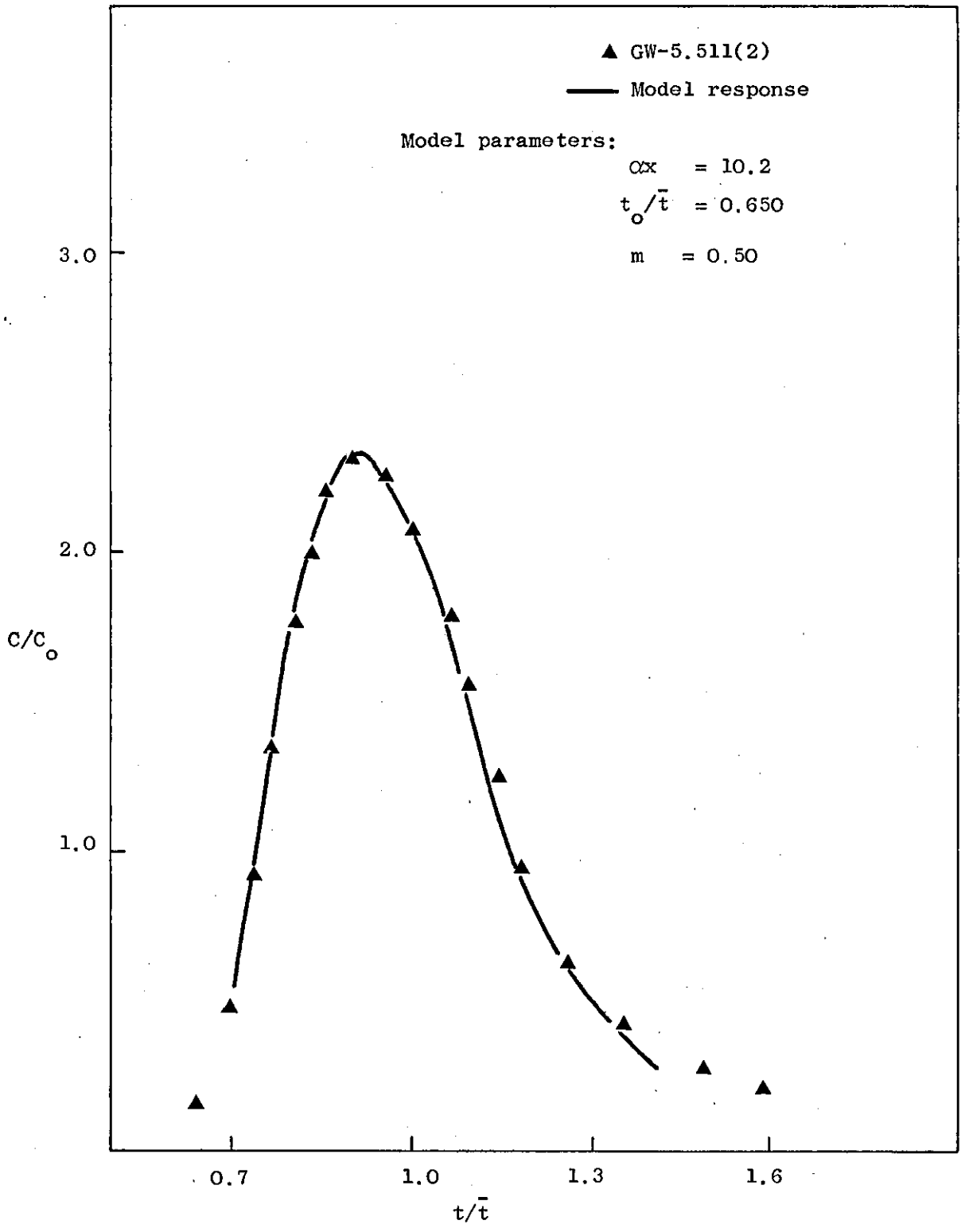

Figure: 9.23. Comparison of the experimental response and the gamma distributed time delay model solution.

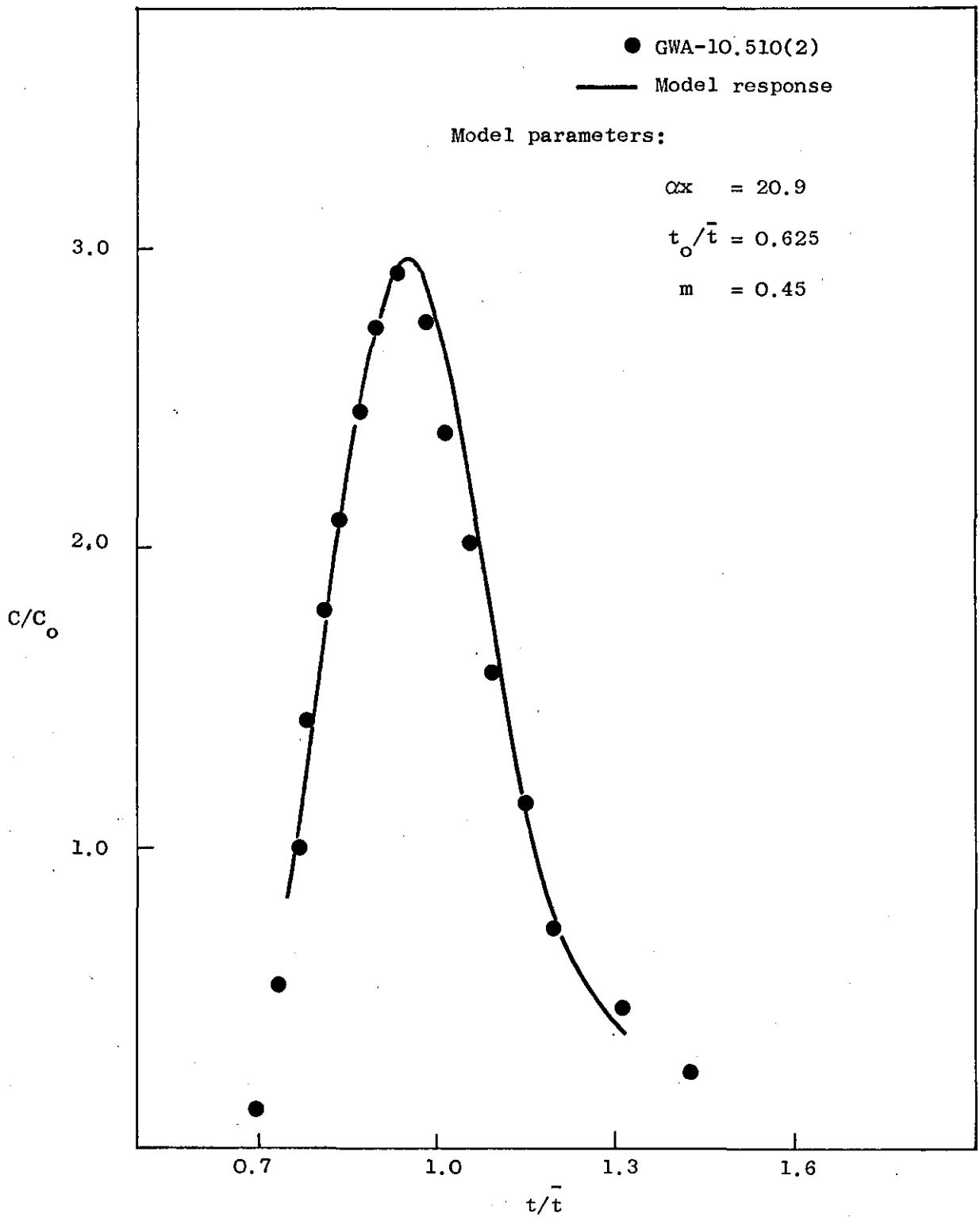

Figure: 9.24. Comparison of the experimental response and the gamma distributed time delay mode solution.

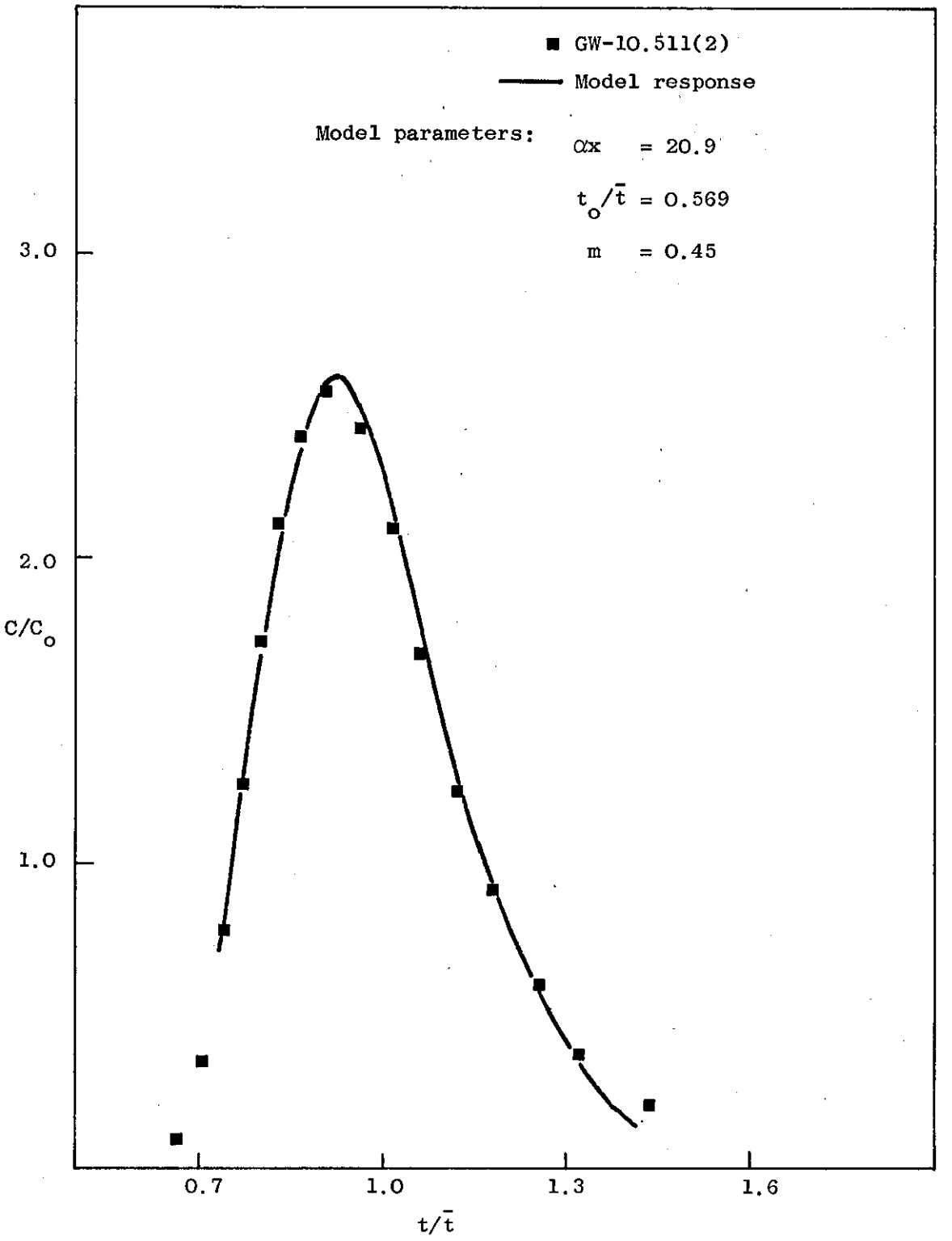

Figure: 9.25. Comparison of the experimental response and the gamma distributed time delay model solution.

The overall model response consists of all:

$$\text{the material that did not stop} = e^{-\alpha x}\ \delta(t - t_o) \qquad (9.3)$$

$$\text{the material that stopped once} = (m/t_D)^m \frac{(t^*)^{m-1}}{\Gamma(m)} \frac{(\alpha x)}{1!} e^{-(\alpha x + mt^*/t_D)} \qquad (9.4)$$

$$\text{the material that stopped twice} = (m/t_D)^{2m} \frac{(t^*)^{2m-1}}{\Gamma(2m)} \frac{(\alpha x)^2}{2!} e^{-(\alpha x + mt^*/t_D)} \qquad (9.5$$

$$\vdots$$

$$\text{the material that stopped n times} = (m/t_D)^{mn} \frac{(t^*)^{mn-1}}{\Gamma(nm)} \frac{(\alpha x)^n}{n!} e^{-(\alpha x + mt^*/t_D)} .$$

$$\ldots\ldots\ldots (9.6)$$

For values of $mn < 1$, plots of individual contribution would appear as shown in Figure: 9.26 in exaggerated form:

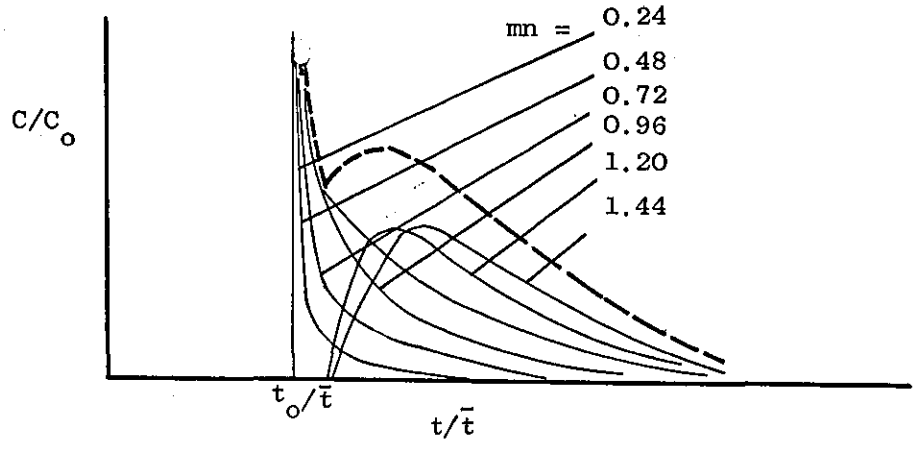

Figure: 9.26

The sum of these individual contributions is the final response. It is clear that at the beginning of the response curve, model response may look as represented by the broken line.

To alleviate this flaw, data points were picked further along the response curves. The evaluated model parameters are listed

in Table: 4D to 6D for all the runs. Again the value of the parameter αx, remains virtually constant for every packed length and a particular liquid.

The parameter m does not appear to change by a large amount under varying operating conditions. The sensitivity of the model response to this parameter, m, has been tested by determining the gamma distribution curves for the values of m of 0.4, 0.5, 0.6 which are the two extremes and one intermediate value. Plots are shown in Figures: 9.27 moreover Figure:9.28shows the plots of the model responses of the three respective values of m for fixed values of the parameter, αx, and the dead time, $t_o/\bar{t}$. The initial rise and the most part of the decaying response is not affected over this range of values of m , however the peak height is somewhat increased.

It can be assumed that the value of m, is, for all practical purposes, constant over the range of studied conditions; an average of 0.49 has been calculated.

Table:9.2 summarises the results of each parameter.

Table: 9.2 Parametric values of gamma distributed delays

Type of fluid	Viscosity of fluid μ cp	α	Standard deviation
Water	1.0	1.39	0.06
Glycerine-solution	4.5	1.98	0.20
Glycerine-solution	7.5		

It is interesting to note that the value of α is not affected by the change of viscosity from 4.5 cp to 7.5 cp, the dependency on viscosity apparently ending somewhere between 1 and 4.5 cp.

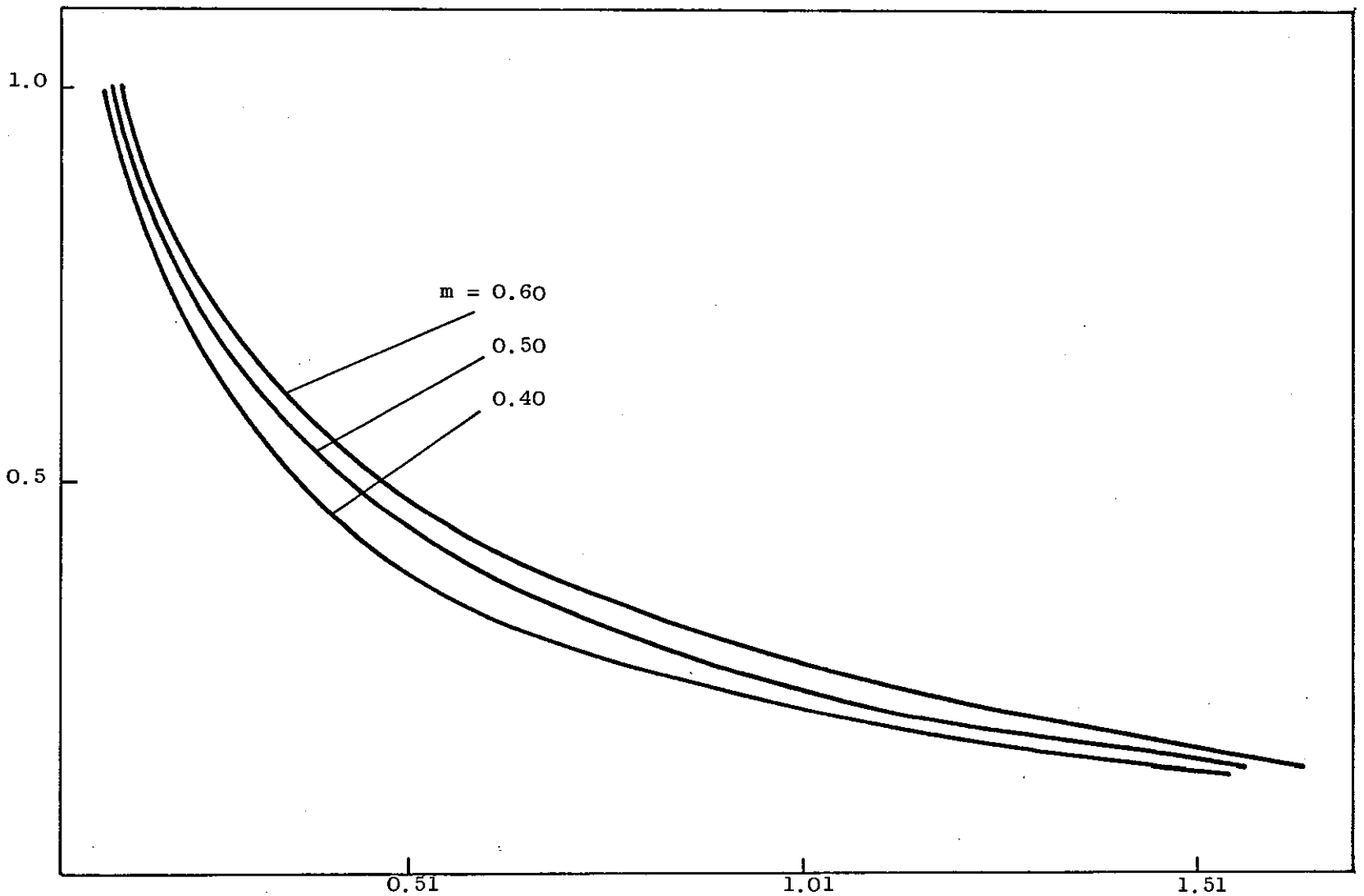

Figure: 9.27. The gamma distribution curves for three different values of m.

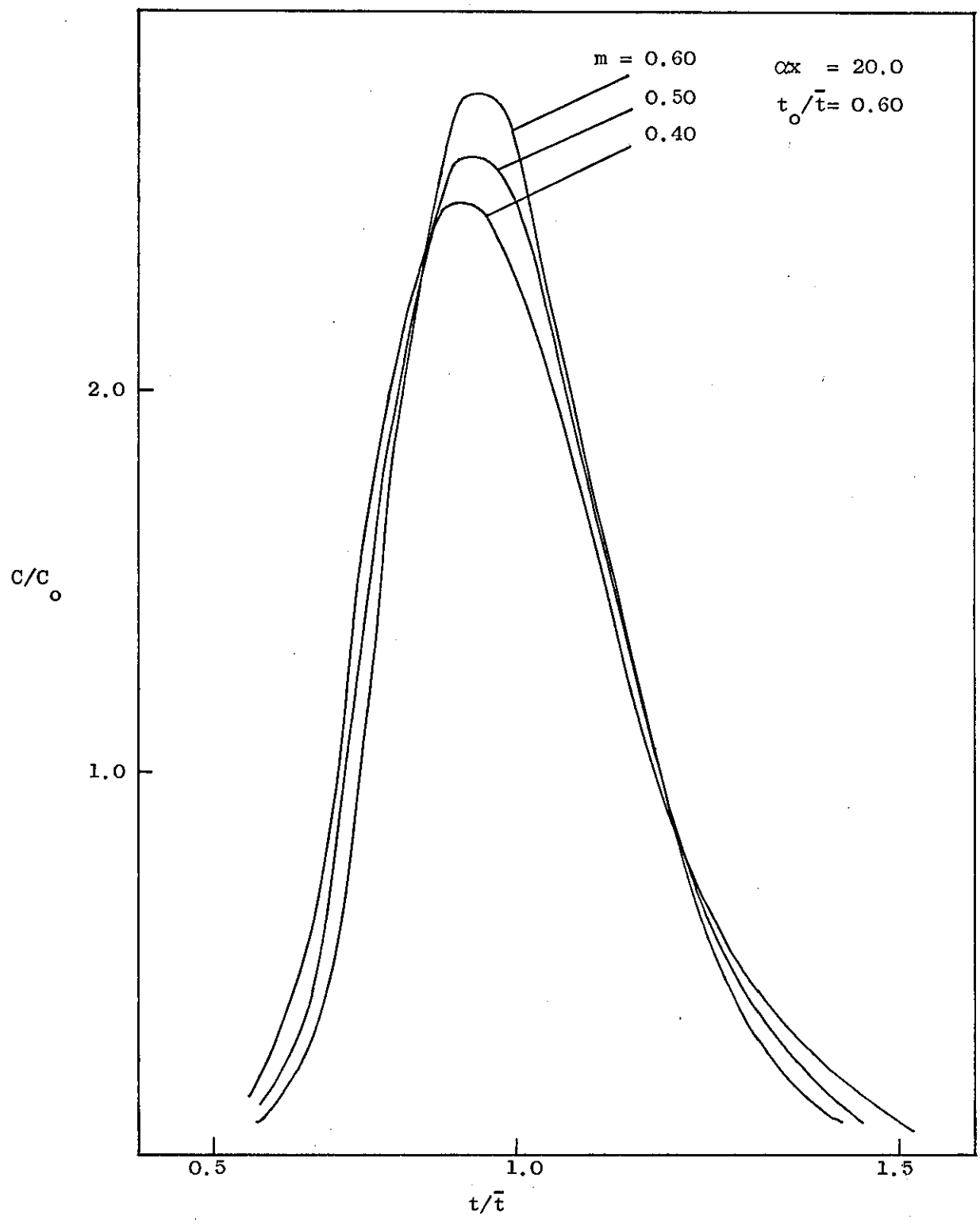

Figure: 9.28. The gamma distributed time delay model solutions for different values of m.

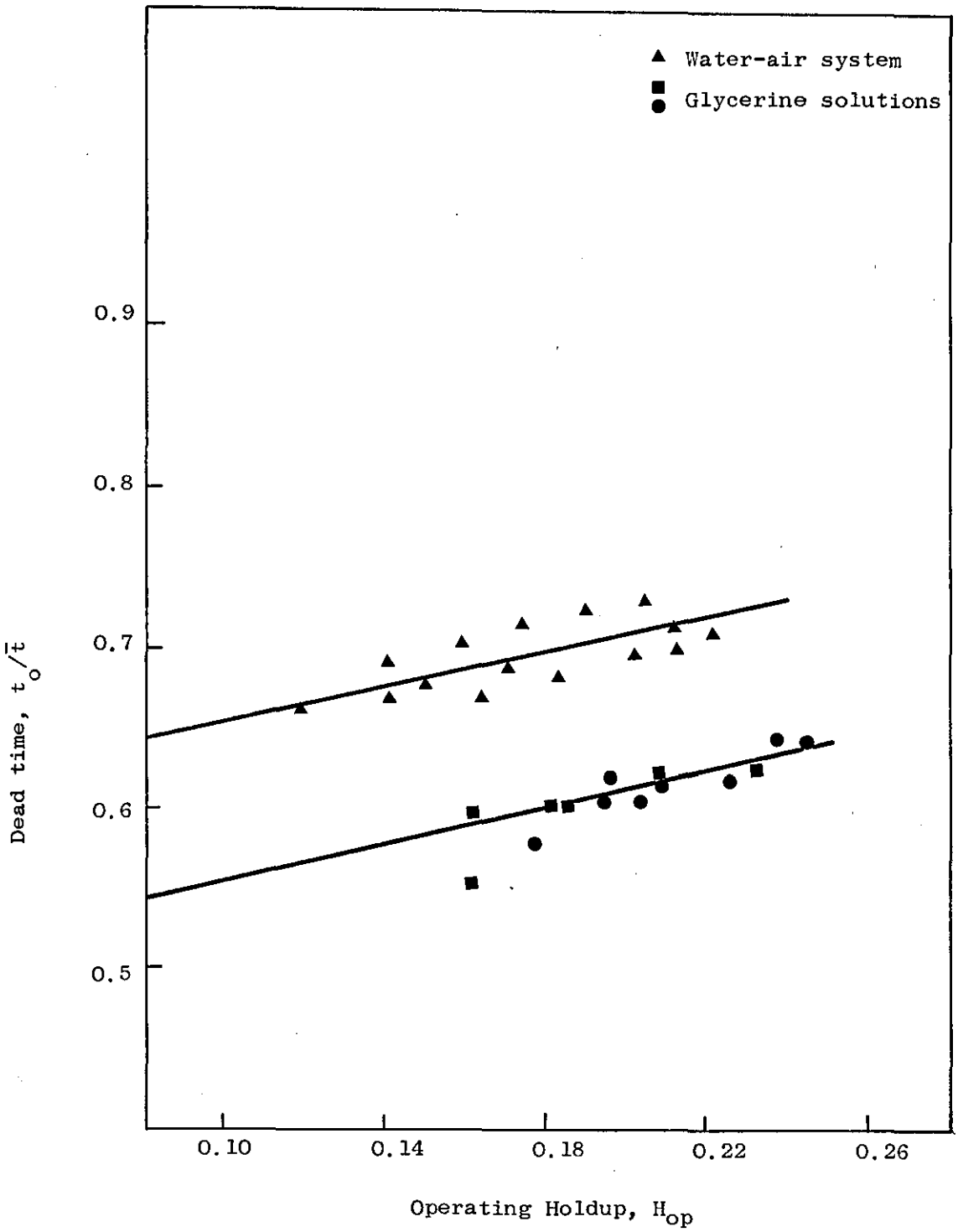

Figure: 9.29. Correlation of the gamma distributed time delay model parameters.

Again the dead time, $t_o/\bar{t}$, increases with increasing liquid flow rates, and the corresponding correlations for the gamma distributed delay time model were also obtained, see Figure 9.29 for the respective plots.

The correlations are as follows:

For water-air system:

$$t_o/\bar{t} = 0.595 + 0.6 \; H_{op} \tag{9.7}$$

For glycerine-solutions:

$$t_o/\bar{t} = 0.495 + 0.6 \; H_{op} \tag{9.8}$$

Figures: 9.30, 9.31 and 9.32, 9.33 show the comparison of the two curve fits, one corresponding to the set of parameters obtained by the optimisation technique and the other by the use of the above correlations, again it is seen that quite good predictions can be made for all the system responses.

9.3. Hopping Model

The upper and lower limits of the model parameters are again estimated as described for the gamma-distributed delay time model in section 9.2.

The hopping model includes direct axial displacement of material in its formulation, which the last model could not incorporate. The original form of the time delay model considered the spreading mechanism via the main plug-flow region to be only due to the retention of the material in the stagnant pockets for an interval of time. The hopping model postulates this assumption but superimposes the hopping effect of the fluid elements which are moved forward during this

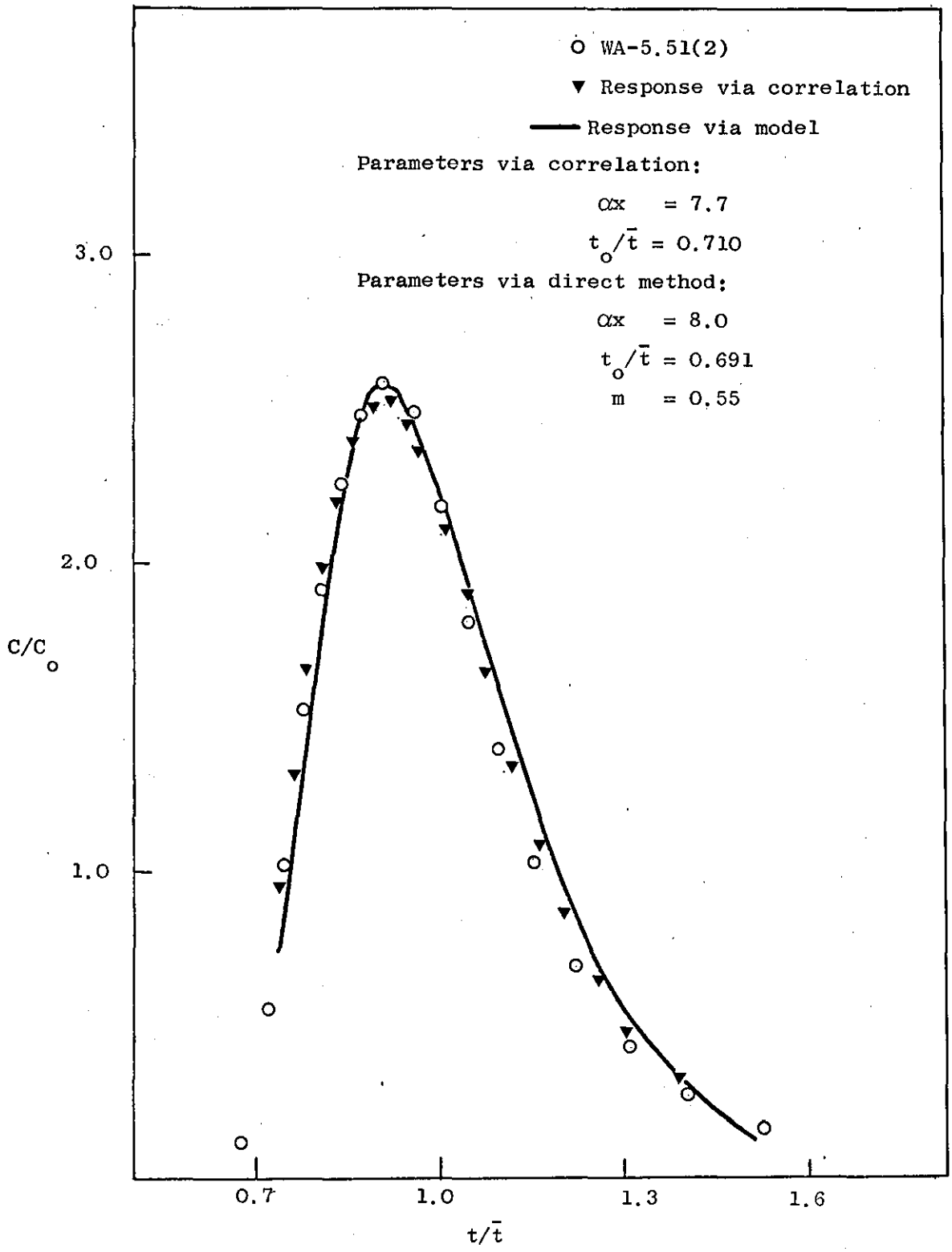

Figure: 9.30. Comparison of the experimental, the correlated and the gamma distributed time delay model responses.

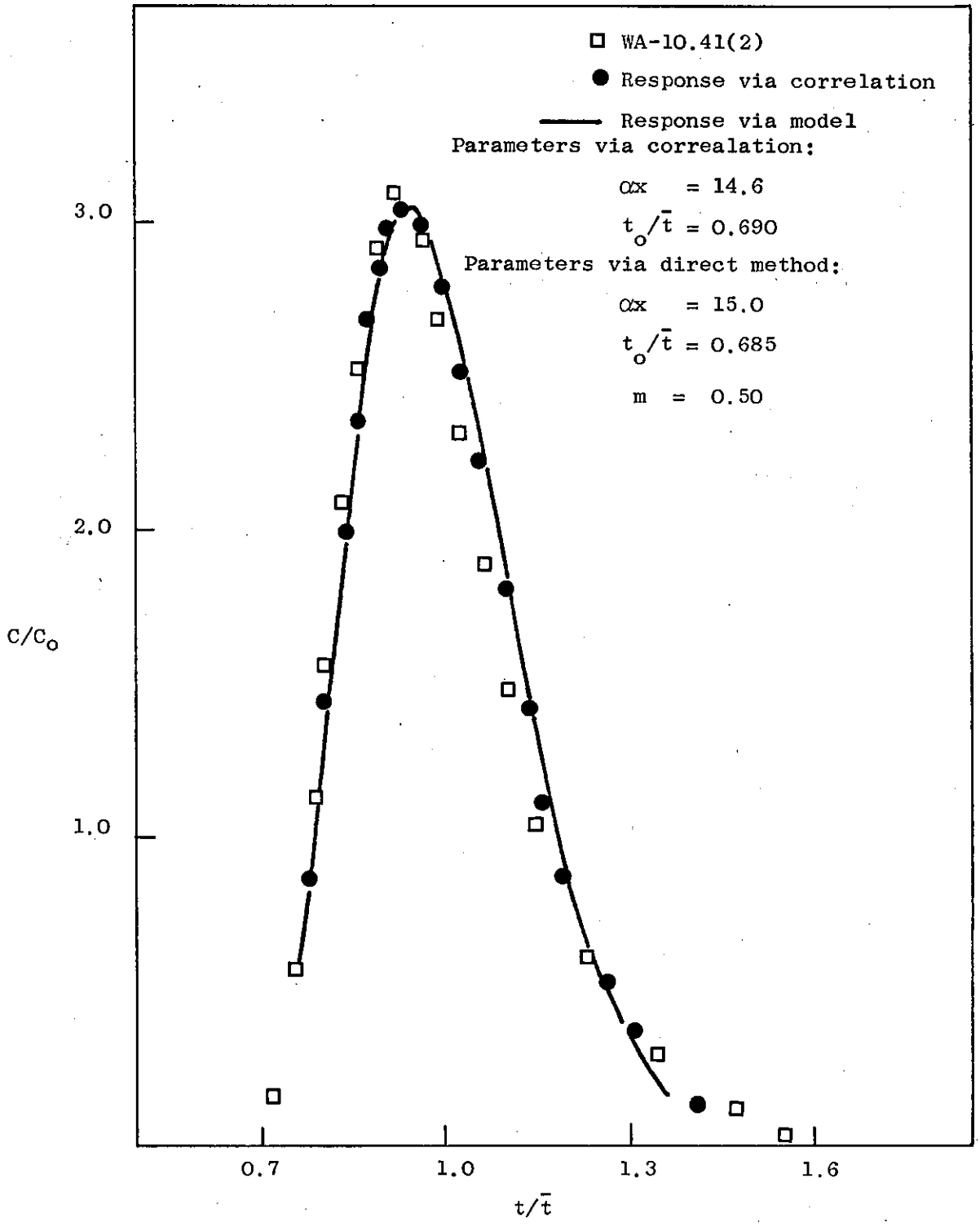

Figure: 9.31. Comparison of the experimental, the correlated and the gamma distributed time delay model responses.

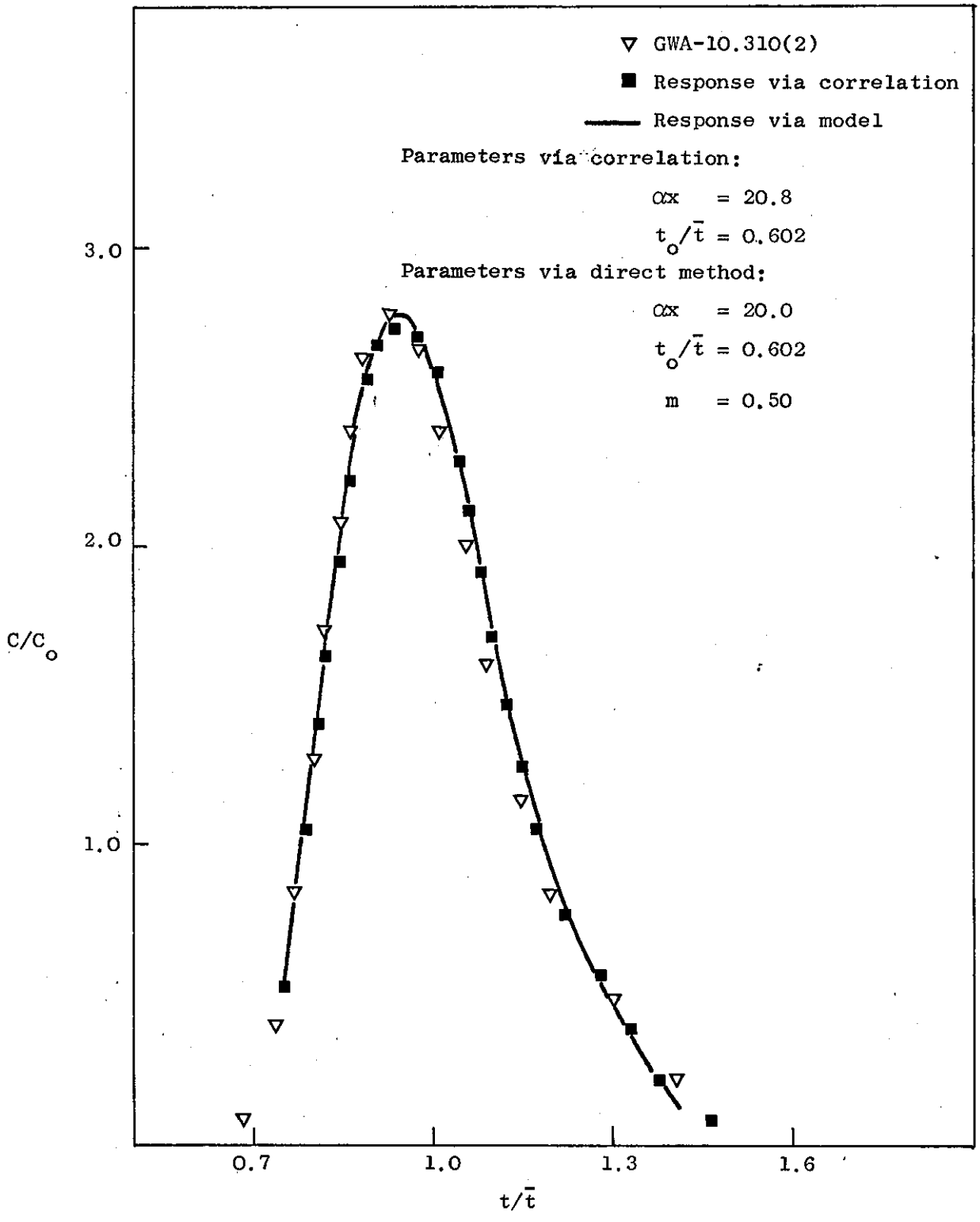

Figure; 9.32. Comparison of the experimental, the correlated and the gamma distributed time delay model responses.

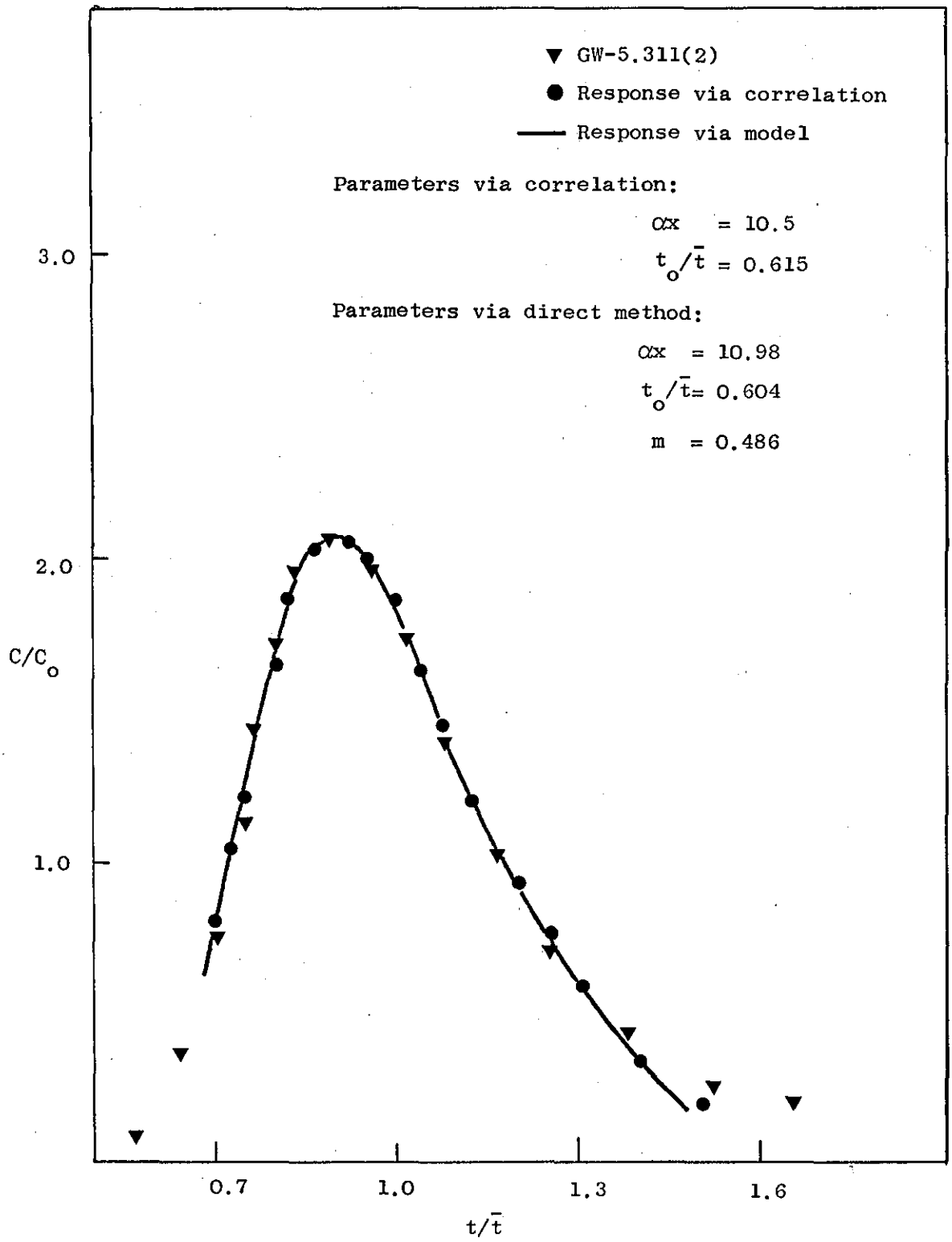

Figure 9.33. Comparison of the experimental, the correlated and the gamma distributed time delay model responses.

retention transition phase and then rejoin the main stream further along, hence resulting in the speeding and delaying of the emergence of the material. The overall effect of this mechanism is to improve the initial sharp rise of the response curve normally encountered in practice without introducing the impulse effects of the gamma-distributed delay time model.

A comprehensive set of tables of the evaluated hopping model parameters are included in Appendix: D , Tables: 7, 8 and 9 . The results show the parameter, α, to increase with the increasing liquid flow rates for the shorter length column viz. $5\frac{1}{2}$ ft. column. For $10\frac{1}{2}$ ft. and $15\frac{1}{2}$ ft. column lengths α remains reasonably constant over the range of operating conditions studied. However, the magnitude of the parameter h, namely the hopping distance, during the water-air runs, increases with the increasing liquid flow rates for all packed lengths, but remains constant for a particular length at high liquid viscosities, decreasing in value for longer columns.

Figures: 9.34 through 9.48 show how the hopping model responses compare with the experimentally determined responses of the systems studied. The hopping model adequately defines the systems, fitting well to the initial part, the peak and subsequent decaying portion of the curve.

An attempt was also made to correlate the hopping model parameters with the operating variables. Although the relationships were established between a number of variables, see Figures:9.49,9.50 but not any generally applicable correlation could be arrived at as in the case of other time delay models. For each column length and the type of fluid, liquid flow rates were found to be proportional to the hopping distance and the dead time. The hopping distance also varied proportionally with the dead time for each packed length and the type of fluid.

Nevertheless the overall picture suggested by the comparison of results with the hopping model is as follows:

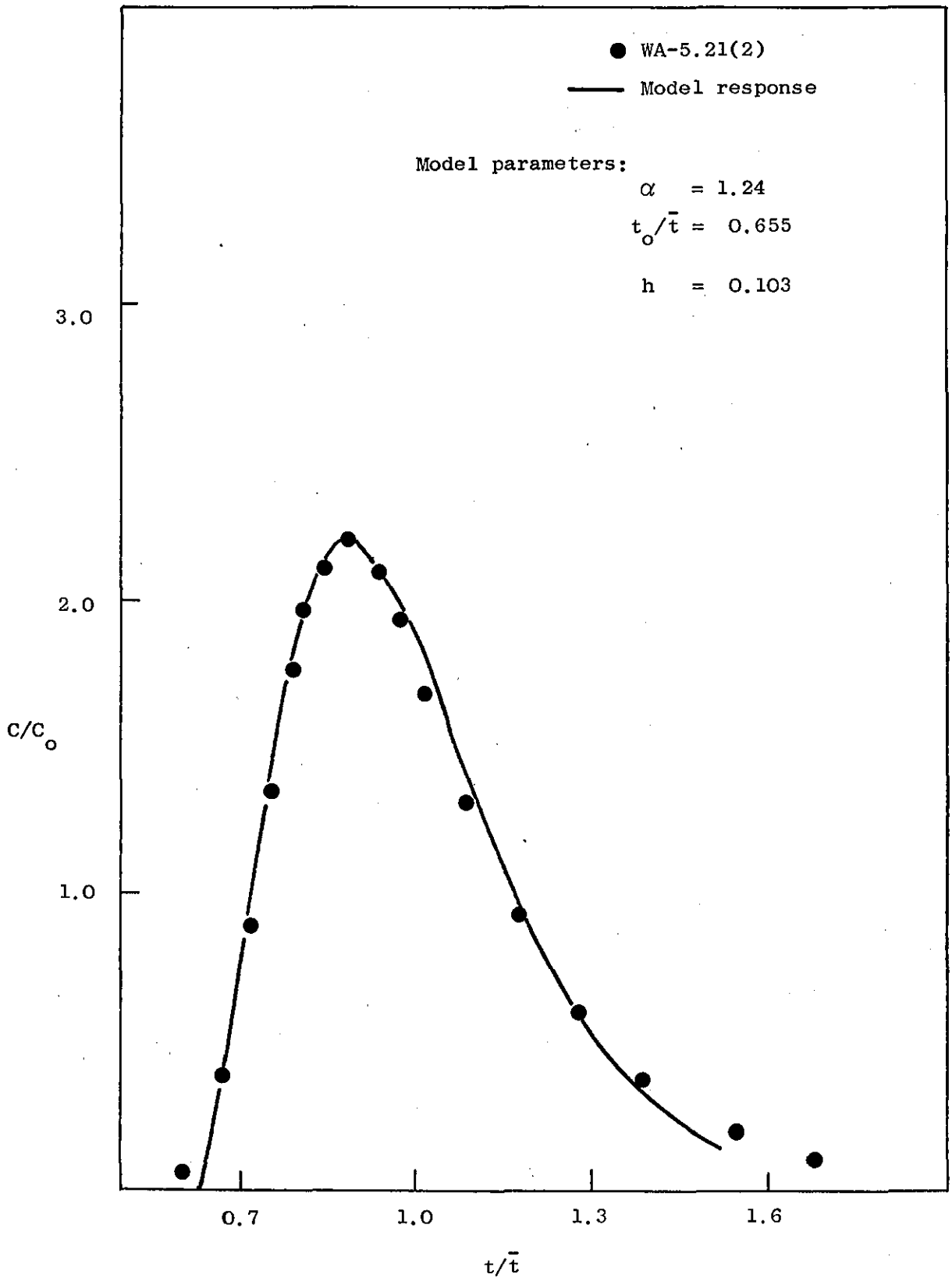

Figure: 9.34. Comparison of the experimental response and the hopping model solution.

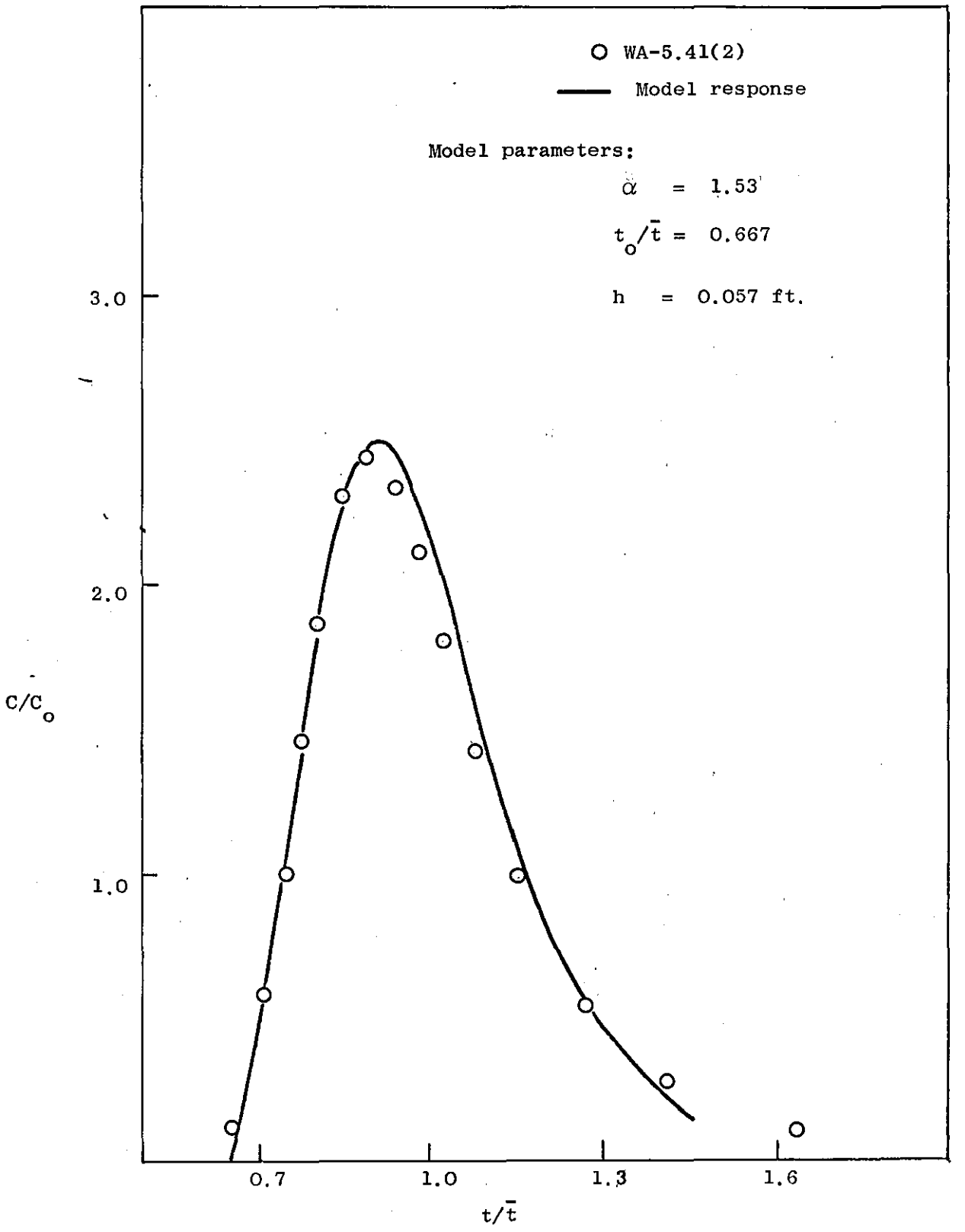

Figure: 9.35. Comparison of the experimental response and the hopping model solution.

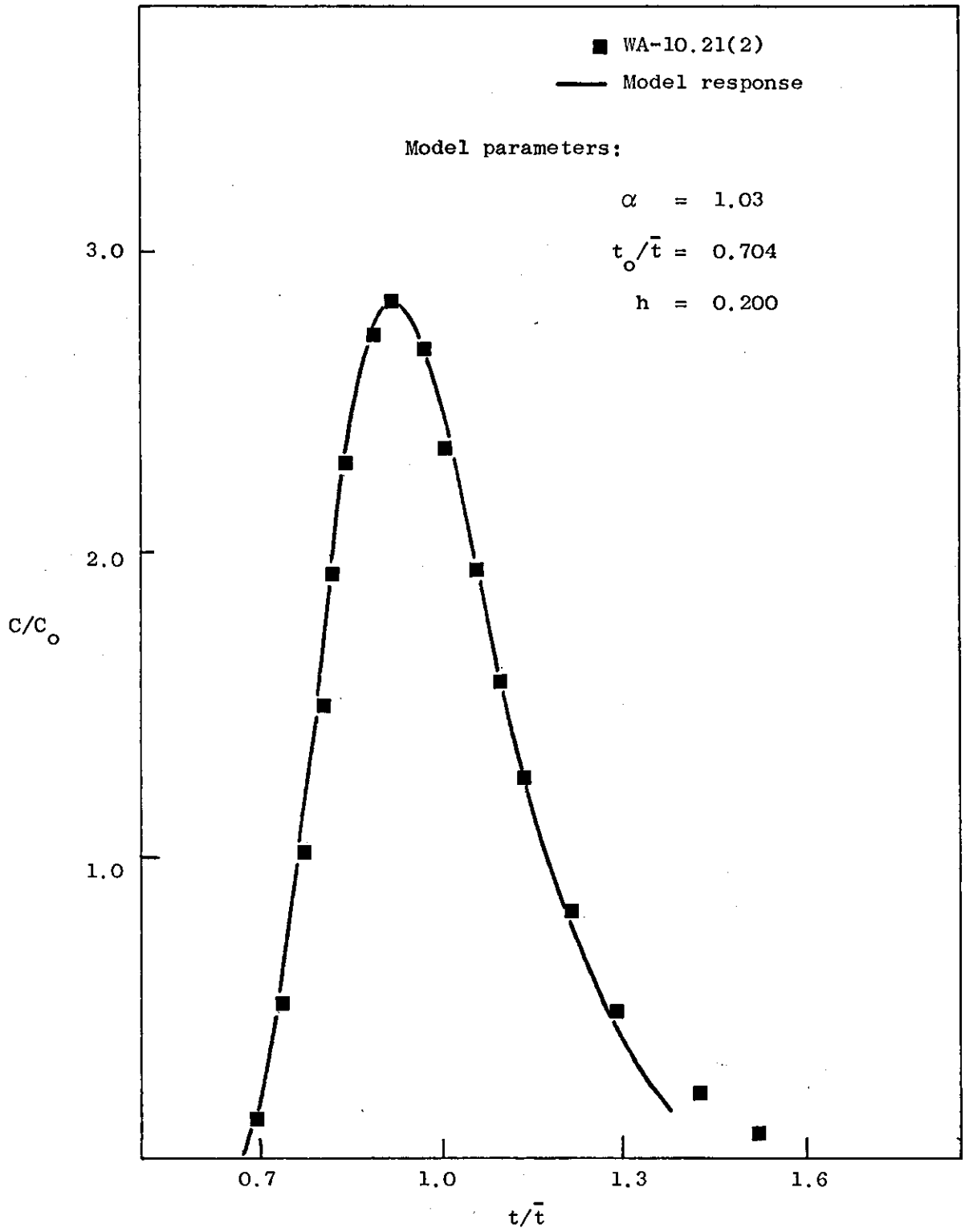

Figure: 9.36. Comparison of the experimental response and the hopping model solution.

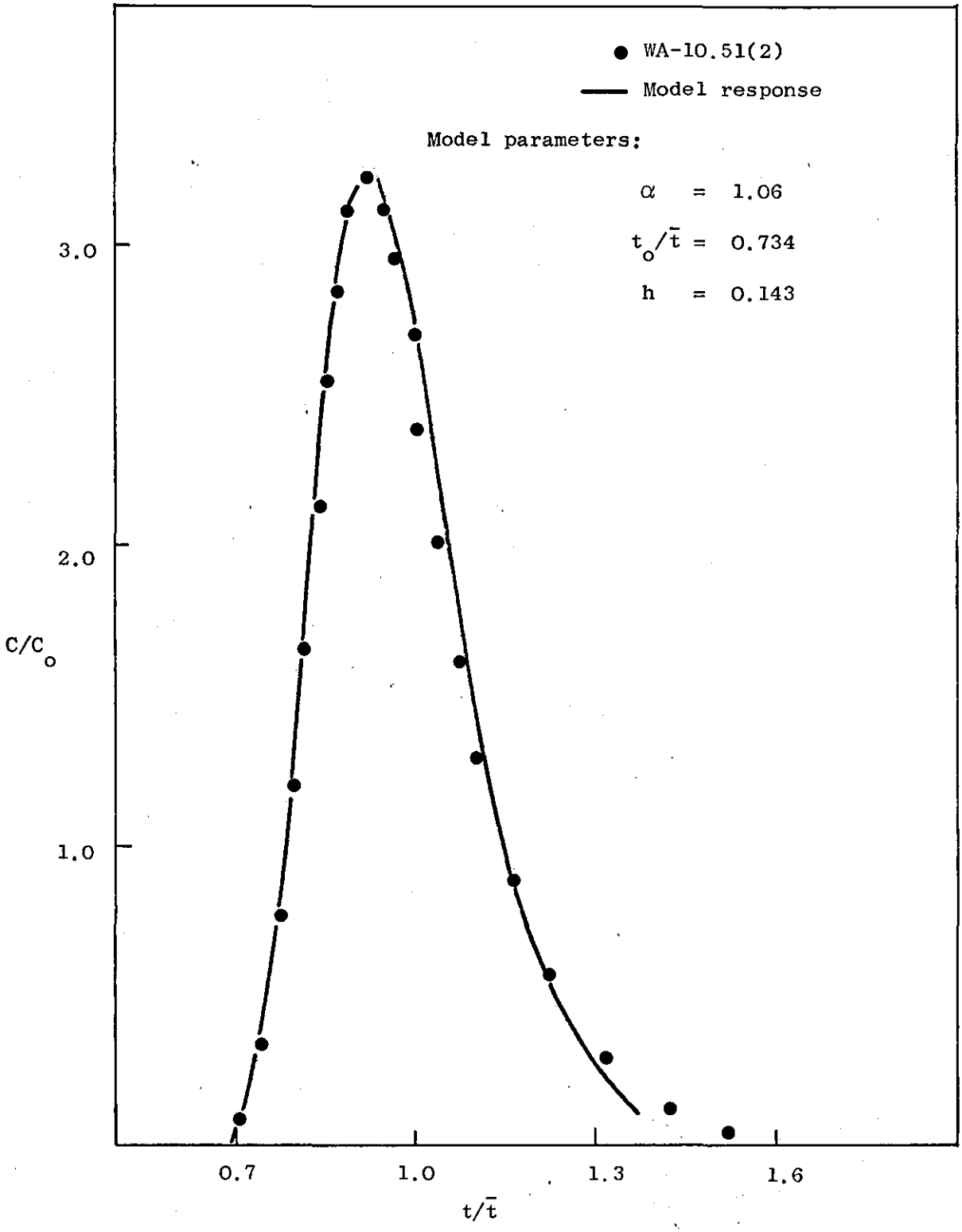

Figure: 9.37. Comparison of the experimental response and the hopping model solution.

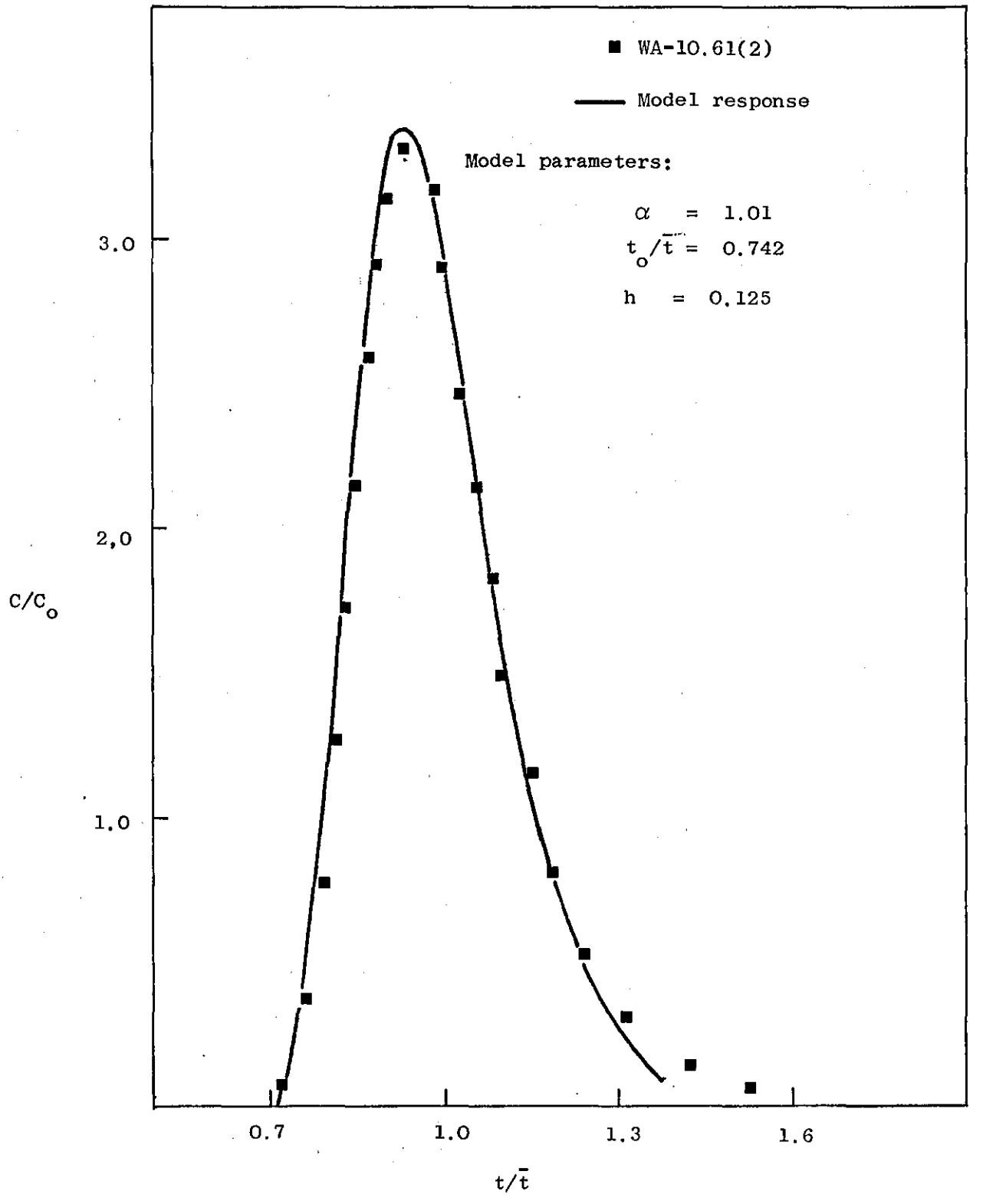

Figure: 9.38. Comparison of the experimental response and the hopping model solution.

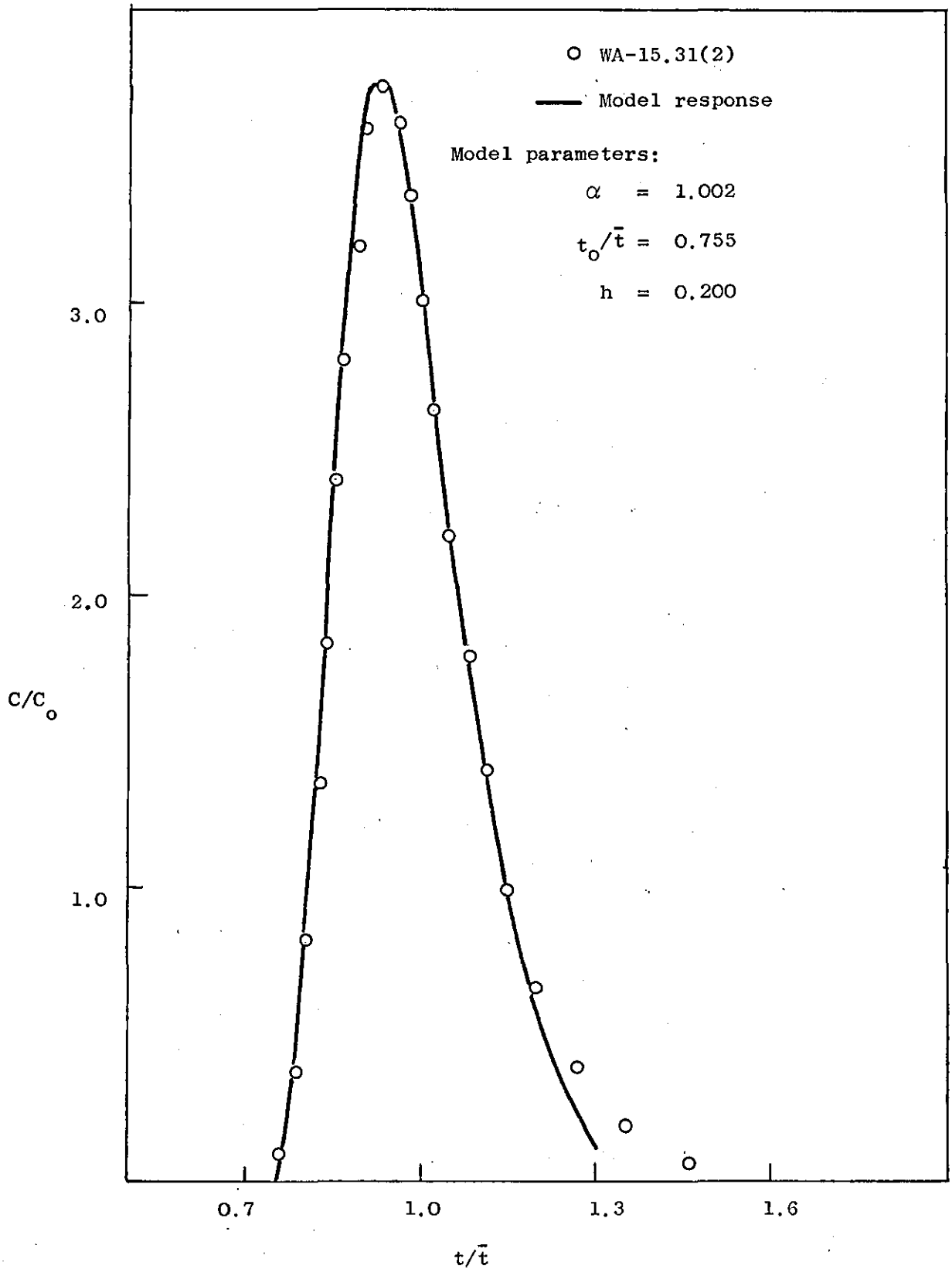

Figure: 9.39. Comparison of the experimental response and the hopping model solution.

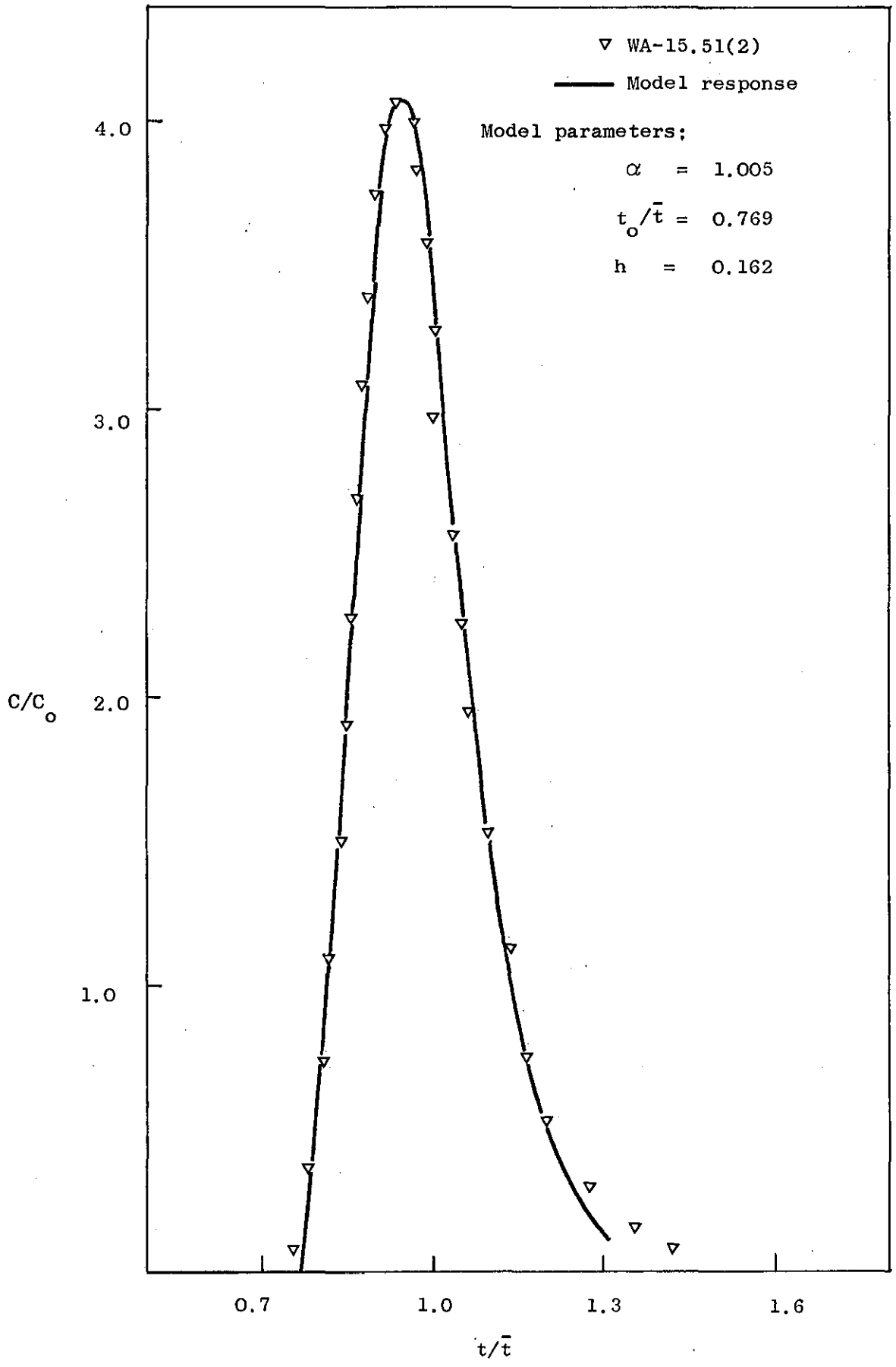

Figure: 9.40. Comparison of the experimental response and the hopping model solution.

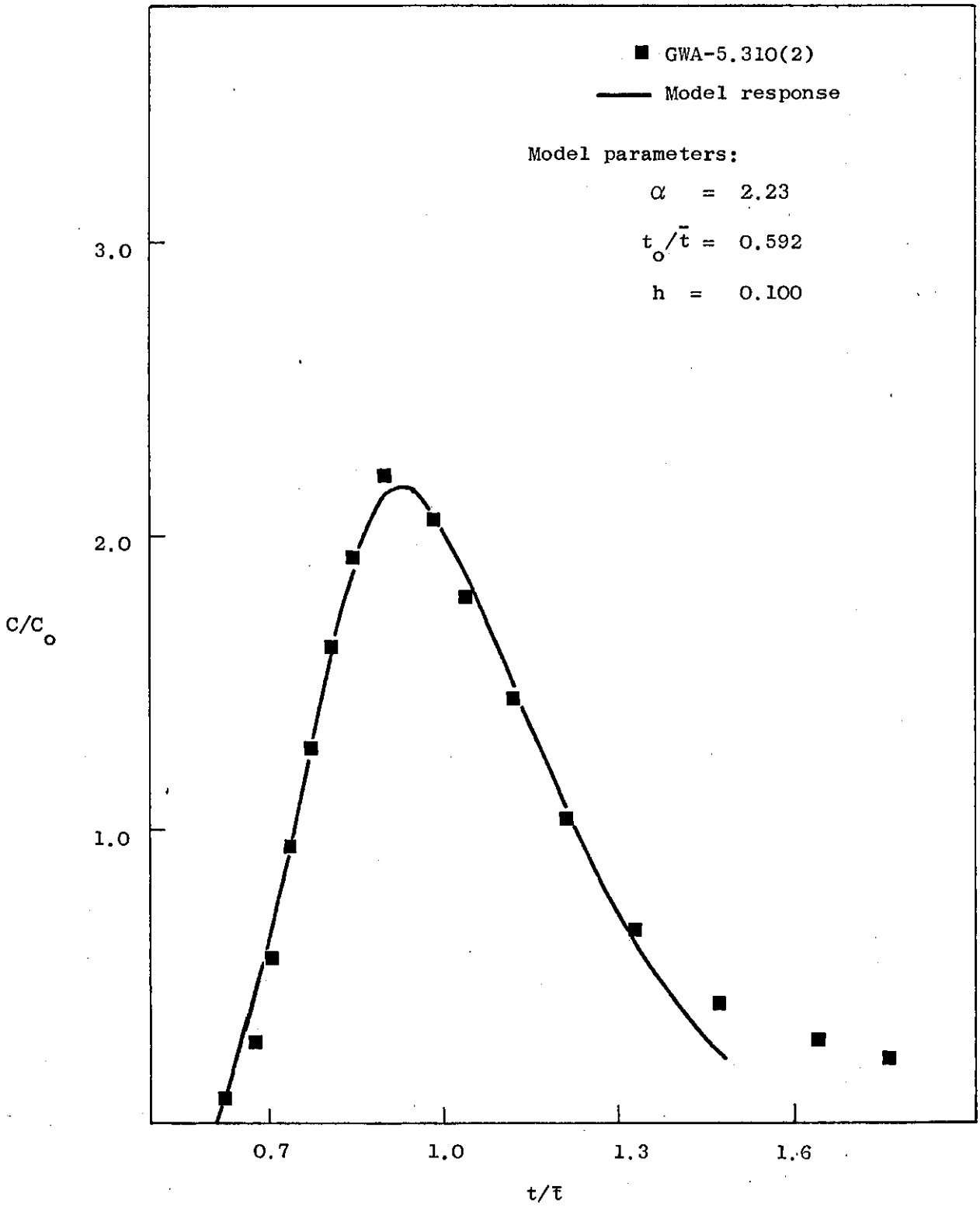

Figure: 9.41. Comparison of the experimental response and the hopping model solution.

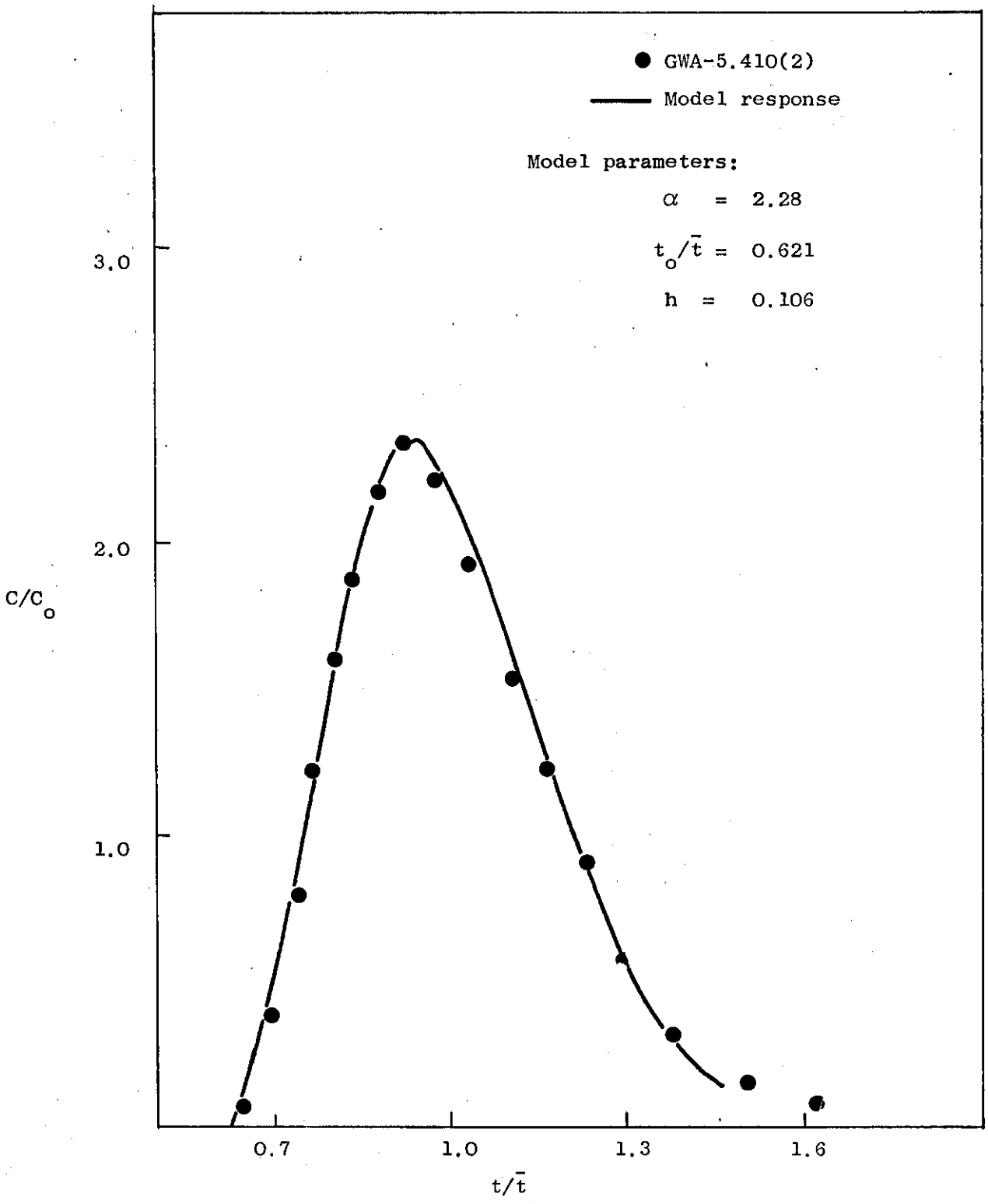

Figure: 9.42. Comparison of the experimental response and the hopping model solution.

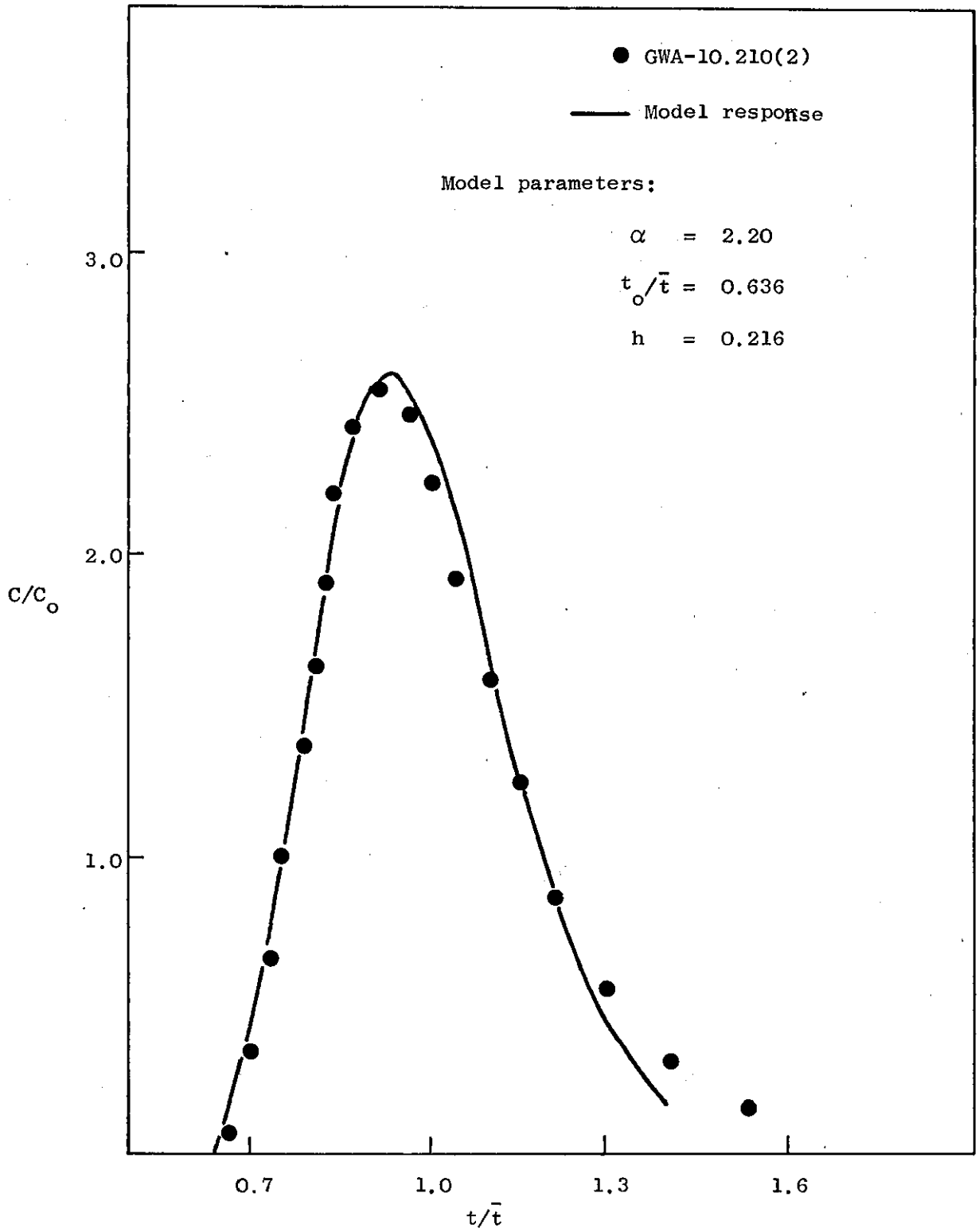

Figure: 9.43. Comparison of the experimental response and the hopping model solution.

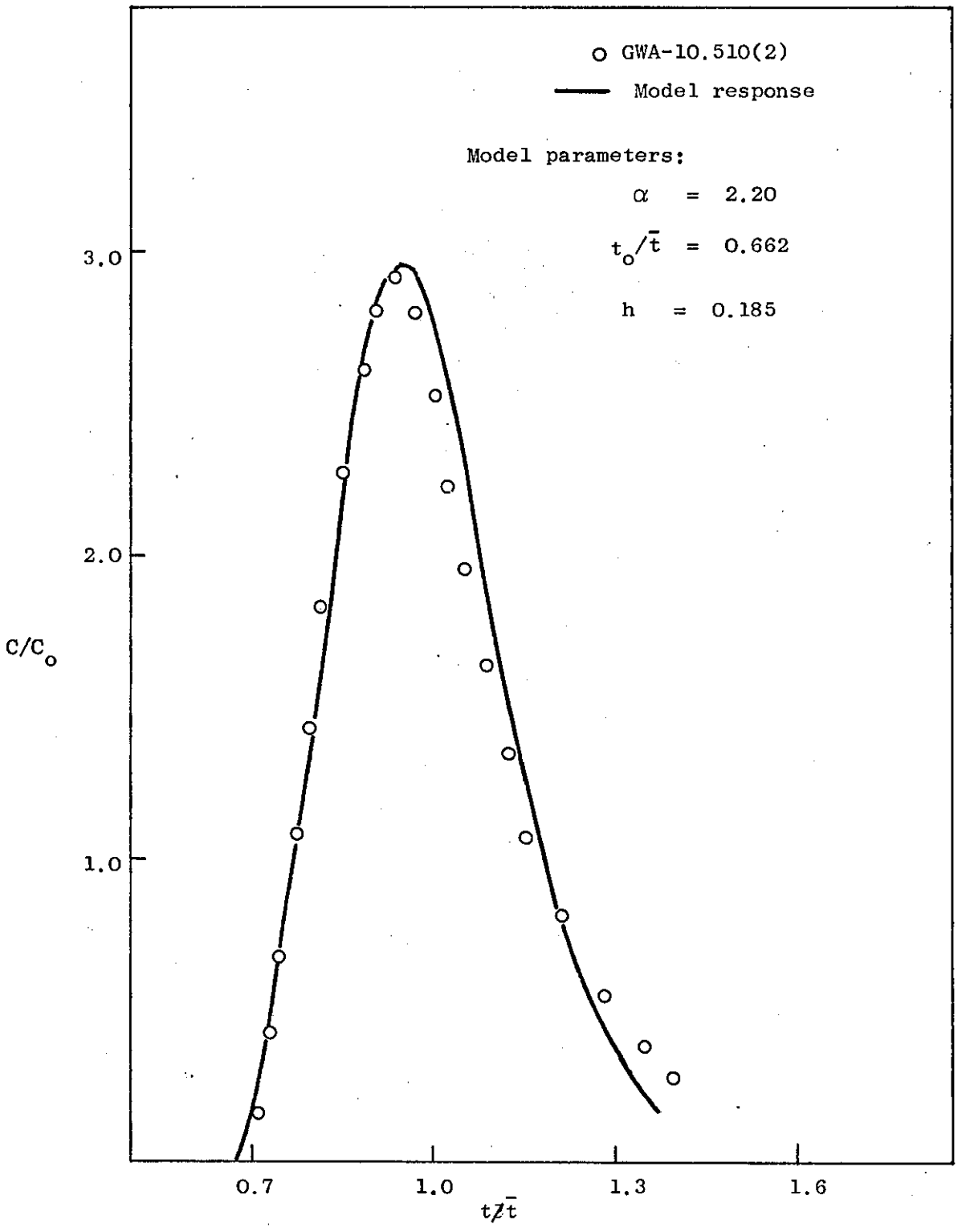

Figure: 9.44. Comparison of the experimental response and the hopping model solution.

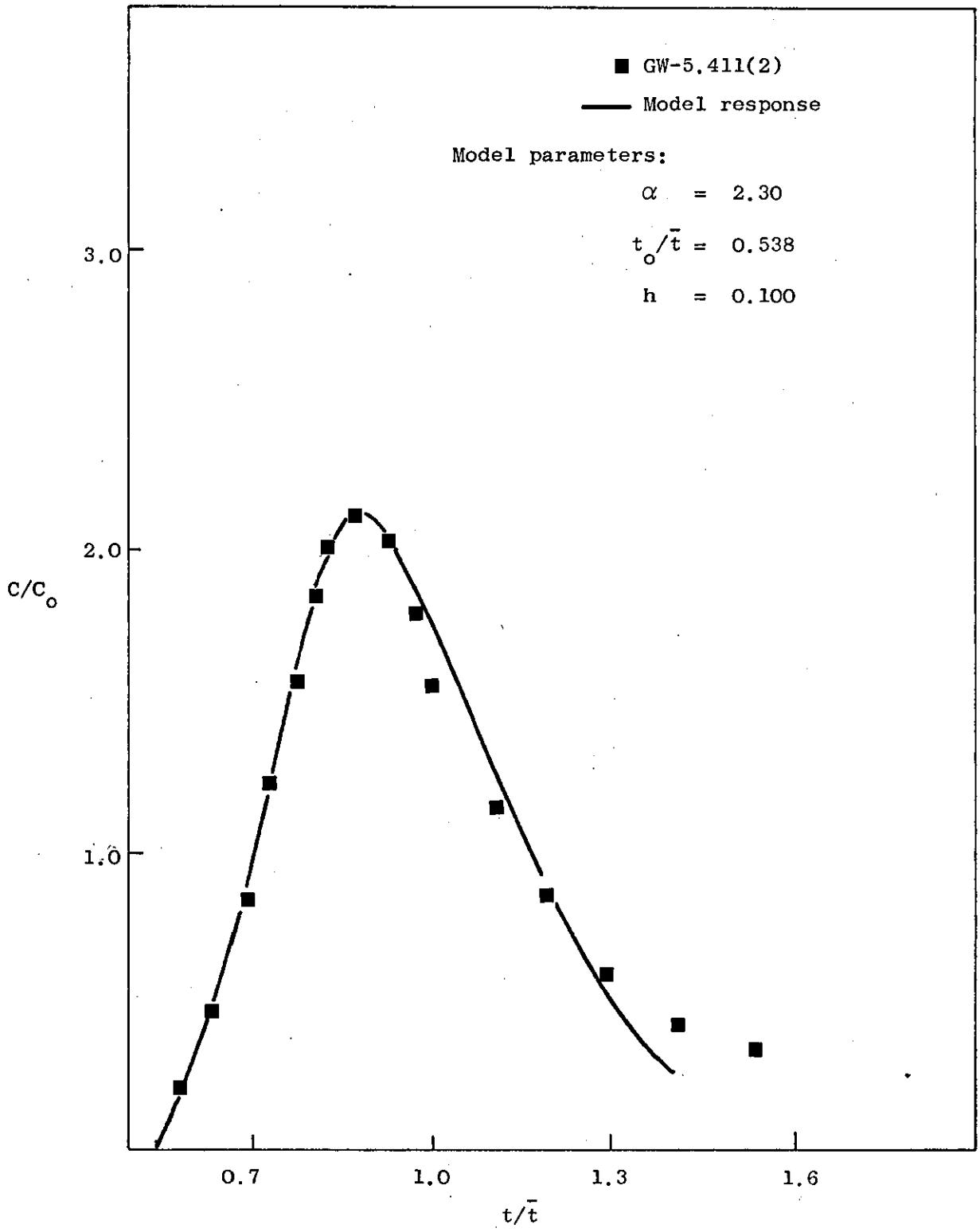

Figure: 9.45. Comparison of the experimental response and the hopping model solution.

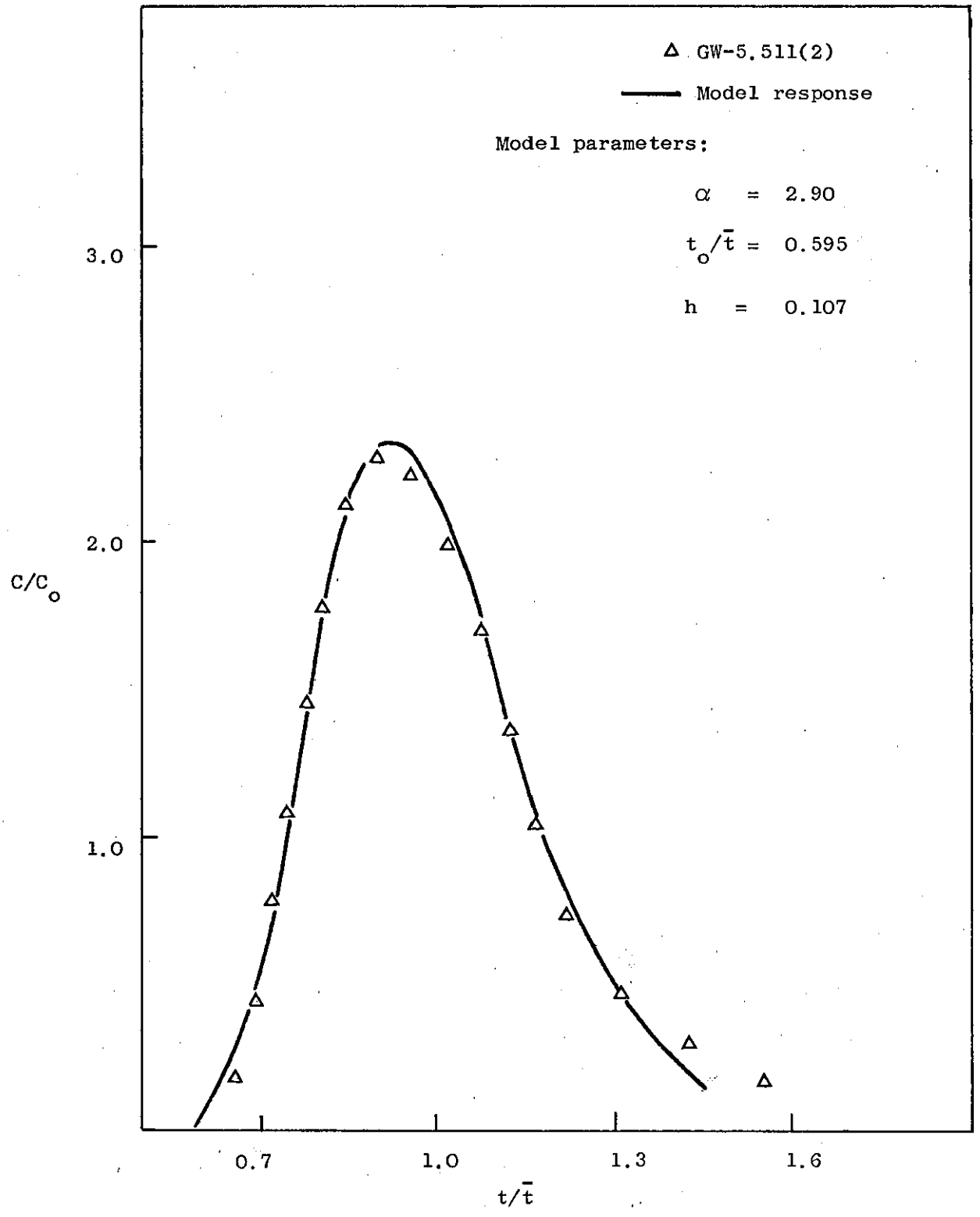

Figure: 9.46. Comparison of the experimental response and the hopping model solution.

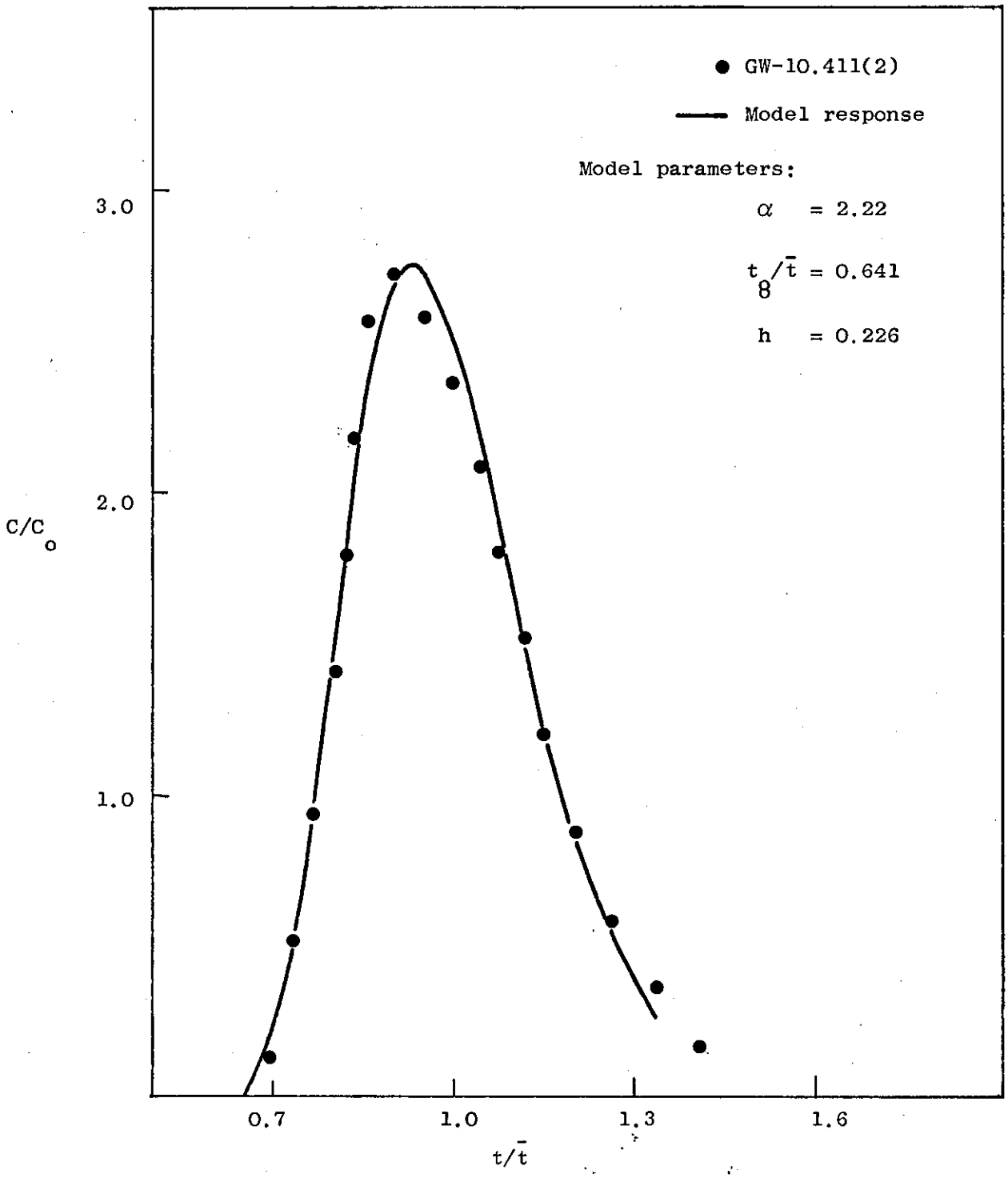

Figure: 9.47. Comparison of the experimental response and the hopping model solution.

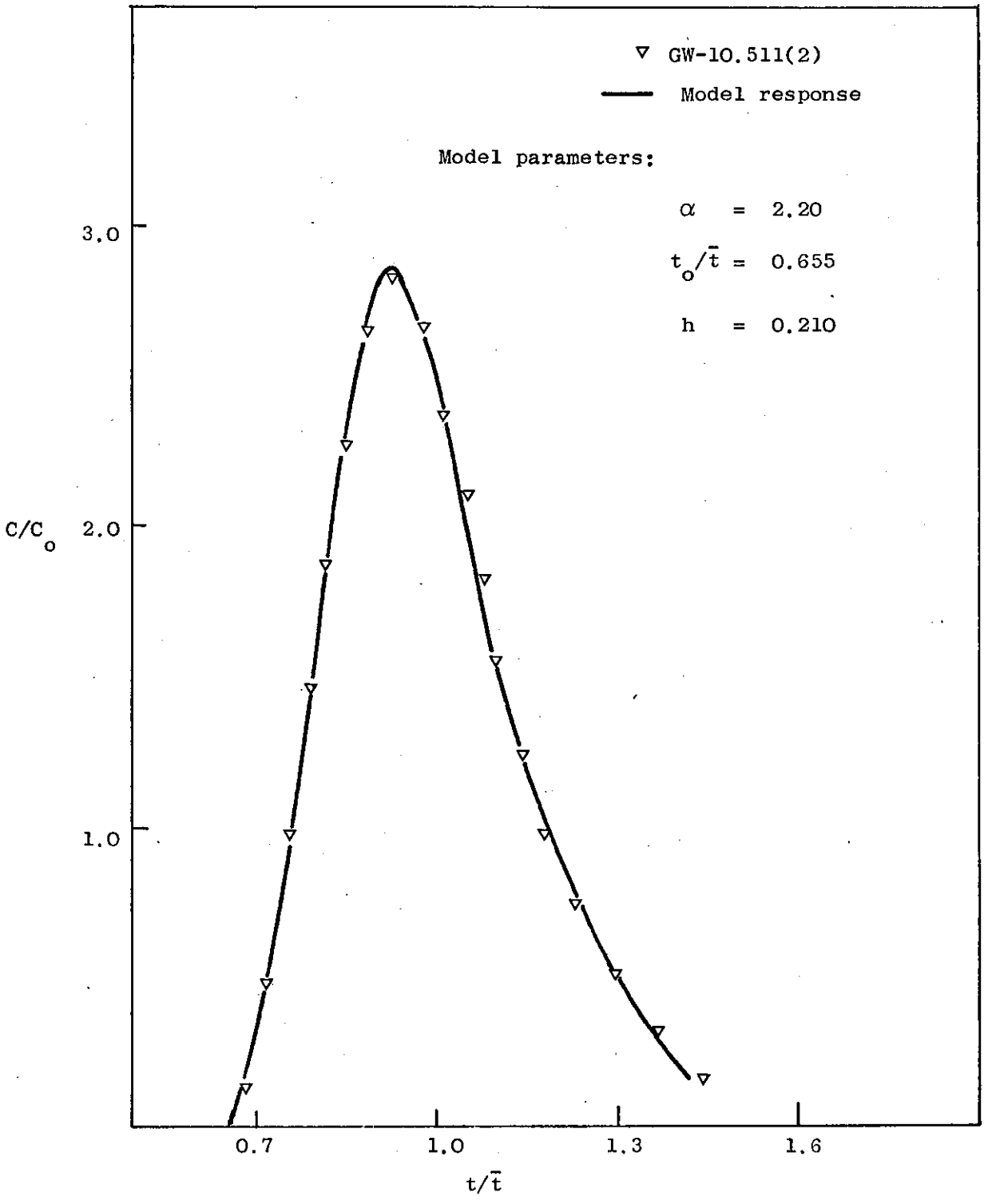

Figure: 9.48. Comparison of the experimental response and the hopping model solution.

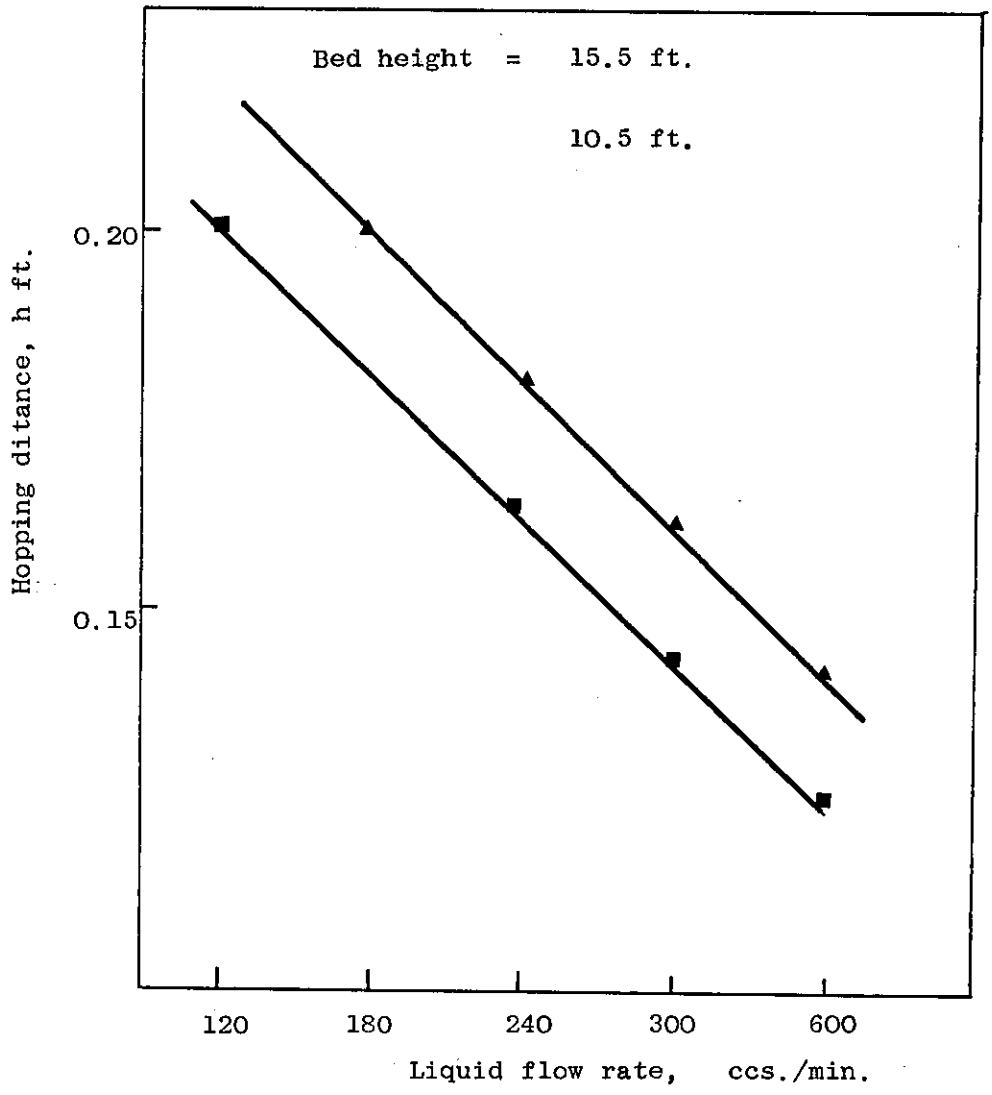

Figure: 9.49. Correlation of the hopping model parameters.

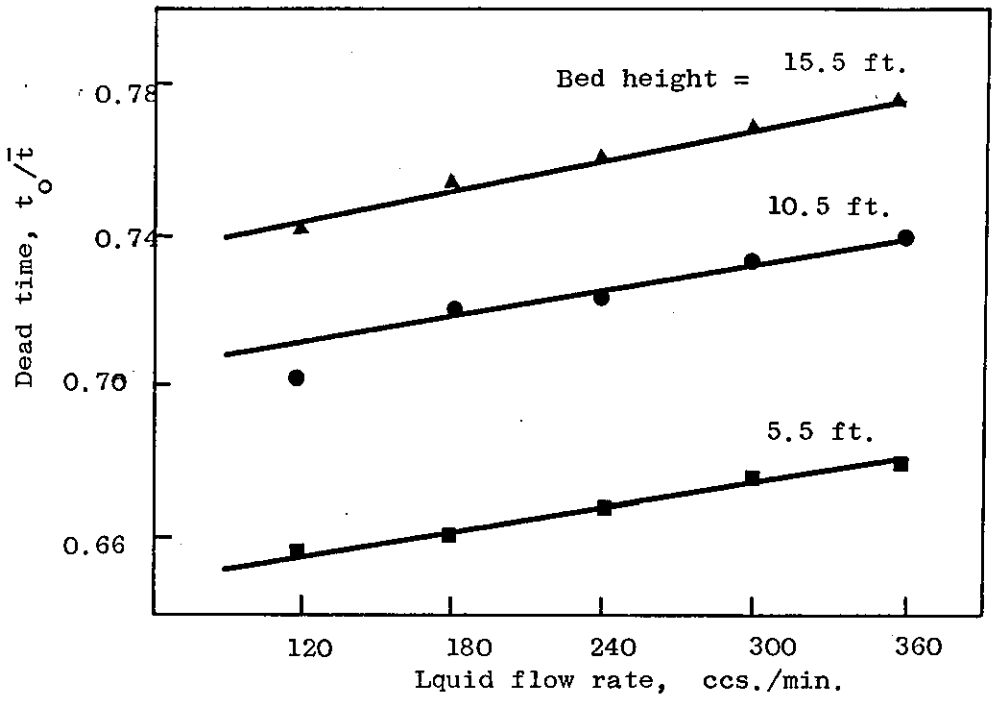

Figure: 9.50. Correlation of the hopping model parameters.

a) In the shorter length column a large proportion of the liquid flowed next to the wall of the column, resulting in an increase of the lateral liquid flow per unit length as the liquid flow rates increased. However, in longer length columns, the liquid at the wall has the chance of returning to the packing thus averaging out the lateral flow to a constant value.

b) The frequency of mixing of the departed fluid elements with the main stream increases with an increase of liquid flow rate, shortening the hopping distance. The results show that as the Reynolds number, N_{Re}, increases from 1.49 to 4.5 the hopping distance,h, decreases from a value of 0.25 to 0.125.ft. Over the same working liquid flow rates the viscous solutions produced a constant hopping distance for a fixed bed length: giving an average value of 0.1 ft. for $5\frac{1}{2}$ ft. column and 0.2 ft. for $10\frac{1}{2}$ ft. column. This indicates that the viscous forces out weigh the gravitational forces only appearing when the fluid elements have trvelled a long distant.

9.5. Conclusions

The response of the time delay models and the hopping model have been compared with the experimentally obtained responses. It has been found that the exponentially distributed delay time model fits well the initial part of the curve, however the peak position and the decaying portion of the curve is displaced to the right of the experimental response, indicating the model response to be more symmetrical.

The gamma distributed delay time model reproduces most parts of the response curve but fails to fit the initial rise of the curve due to the inherent nature of the model around that portion.

The parameters of the both above models have been correlated

and simple relationships put forward. These expressions provide an assesment of the model parameters from the operating conditions.

The hopping model also accounts for the asymmetry of the response curves, its response fitting quite well all the parts except for the "tail" end of the curve. The model parameters could not be correlated as is in the previous cases and the direct method of comparison remained the only method for parameter evaluation.

It is concluded that the time delay model with the gamma distributed delays is the best representative of the considered models as it compares well with the experimental responses and its parameters are easily correlated with the system variables.

Nomenclature

x	distance
C	tracer concentration
C_o	initial tracer concentration
C/C_o	normalised concentration
m	gamma distribution parameter
t	time
t_o	dead time
$\bar{t}$	mean residence time
$t/\bar{t}$	normalised time
$t_o/\bar{t}$	normalised dead time
α	number of stops per unit length

10. DISCUSSION

10. Discussion

The proposed models are now compared, qualitatively with other published formulations to which they bear similarity.

Quantitative comparisons of the above results with the dispersion model are given in section 10.2.

Sections 10.3 and 10.4 summarise respectively the conclusions and suggestions for further work.

10.1 Comparison with Other Models

In this section we examine how the time delay approach is related to previous models of similar intent. The principal distinguishing features of the time-delay model are that it is one-dimensional spatially, uncomplicated by boundary conditions, and based on a mechanism that is non-specific in terms of physical properties. The object in formulating a model with these characteristics is to enable a wide variety of processes to be treated in the same way by suitably choosing the parameters. The ultimate aim is to make a priori predictions of the parameters in particular cases.

The diffusion model of Levenspiel and Smith (62) has as its underlying mechanism shuffling of flow elements backwards and forwards relative to the main stream. Negative flow-element velocities are not precluded. In contrast the time delay approach assigns a constant velocity or zero velocity to a particle at any instant. The effect is that although a flow element is moving either slower or faster than the average velocity the conceptional difficulties of the diffusion model, do not arise. These problems are of identification: it is not possible to establish the magnitude of the flux from the concentration, because an instrument sensing concentration cannot distinguish the direction in

which flow elements are travelling. Even if both the concentration and its gradient are measured, the resulting net flux estimate includes the effects of flow elements moving in both directions. The result is that boundary conditions cause grave difficulty and the impulse response and the residence time distributions are not the same. Except, that is, in the special case where the diffusion mechanism does not operate across the boundary, the so-called closed-closed case. Mathematically the particular time delay derivations presented above are less complex than the solutions of moving diffusion equations. A further advantage is that a second parameter is introduced in a natural way which enables the skewness of the residence time distributions to be adjusted for a fixed variance. Klinkenberge's method of adding variances (29) can be used to introduce a second parameter into the one-dimensional diffusion model to achieve a similar result. A dead time is combined with diffusive mixing so that to obtain the same value of the relative variance a higher dispersion number, and consequently more skewness, is required. Physically the interpretation is that the diffusive mixing process operates for a time equal to the elapsed time less the dead time. An alternative procedure is to consider that the mixing process only operates for a proportion of the elapsed time. This idea may be incorporated into the mathematics merely multiplying time in the diffusion equation by a constant, but boundary condition problems remain. Which method to adopt should be dictated by the process considered. The time delay approach is more natural for trickle flow.

The earliest work on column dynamics was the investigation of heat transfer between a flowing medium and the packing. The classical model cosiders plug flow of the fluid and heat exchange between the solid and fluid at a rate proportional to the difference of their temperatures, each

of which is uniform at a particular axial position. The solution of this problem was due to Anzelius (106) and now appears in most texts on heat transfer. This model becomes a fluid mixing model on replacing enthalpy by concentration, and considering the two phases to be identical. The model so obtained is identical with the time delay model with exponentially distributed delays, the reason being that, as they are characterised only by their concentrations, the 'phases' are tacitly assumed to be locally well mixed - precisely the assumptions of the exponential time delay model. Giddings 'coupling' theory (107) of chromatography leads to the same Bessel function solution and is close in spirit to the time delay approach.

A third model that is worthy of mention is the Deans cell model (82). This is a modification of the well-known tanks-in-series model in which the effects of 'stagnant' regions are taken into account by attaching to each cell a second well-mixed cell through which fluid recycles. It is of particular interest in the present context because it can be reduced to either the Gaussian or Bessel function form by suitably choosing the limiting process. If the number of stages is increased while keeping the volume and the flows constant the stages become progressively more like well-stirred tanks and the response curve more Gaussian and finally plug flow. Alternatively the number of stages may be increased keeping the volume and the interstage flows constant and reducing the recycle flows proportionately to the inverse of the number of stages. When this is done the time constant for the delays in the 'stagnant' regions is constant and in the limit the exponential time delay (or Anzeluis) model results.

10.2 The Proposed Models

The comparison of the experimental and the model responses in Chapter 9 clearly indicate a reasonably good quantitative predicting ability of the proposed models. To observe the superiority of the proposed

models on the merit of their simplicity over other models, the one-dimensional dispersion model has been considered. The solutions of the dispersion model having the same peak response and the corresponding solutions of the delay-time model with the exponentially distributed delay times are plotted through a number of experimental response curves, see Figures: 10.2 through 10.6 - the dispersion number was obtained with the aid of Figure: 10.1. The latter model, although the least representative of the other proposed versions, still represents a considerable improvement in describing the responses.

For the two delay-time distributions and the hopping models considered, the constancy of α over the widely varying conditions in all these cases seems particularly striking and emphasises the suitability of the model.

The model, although semi-empirical in application, results from a reasonable interpretation of flow behaviour in packed bed systems. The mixing mechanism can be variously ascribed to lateral bulk flow - as would appear to predominate in the physical system here considered, lateral diffusion and even to physical adsorption at the solid/solid interface. The form of the model remains identical, the total effect of these different mechanisms being lumped together in the parameter αx and the distribution of delay times.

If the postulated random stopping process really exists the effect of the distribution of delay times could be considerable as indicated by Figure:10.7. The average number of stops, equal to αx, for both cases illustrated is 10 but the curves are significantly different. However, if it is not required that αx be the same for both cases, very similar responses can be obtained by suitably adjusting this parameter; the variants of the model are thus difficult, if not impossible, to

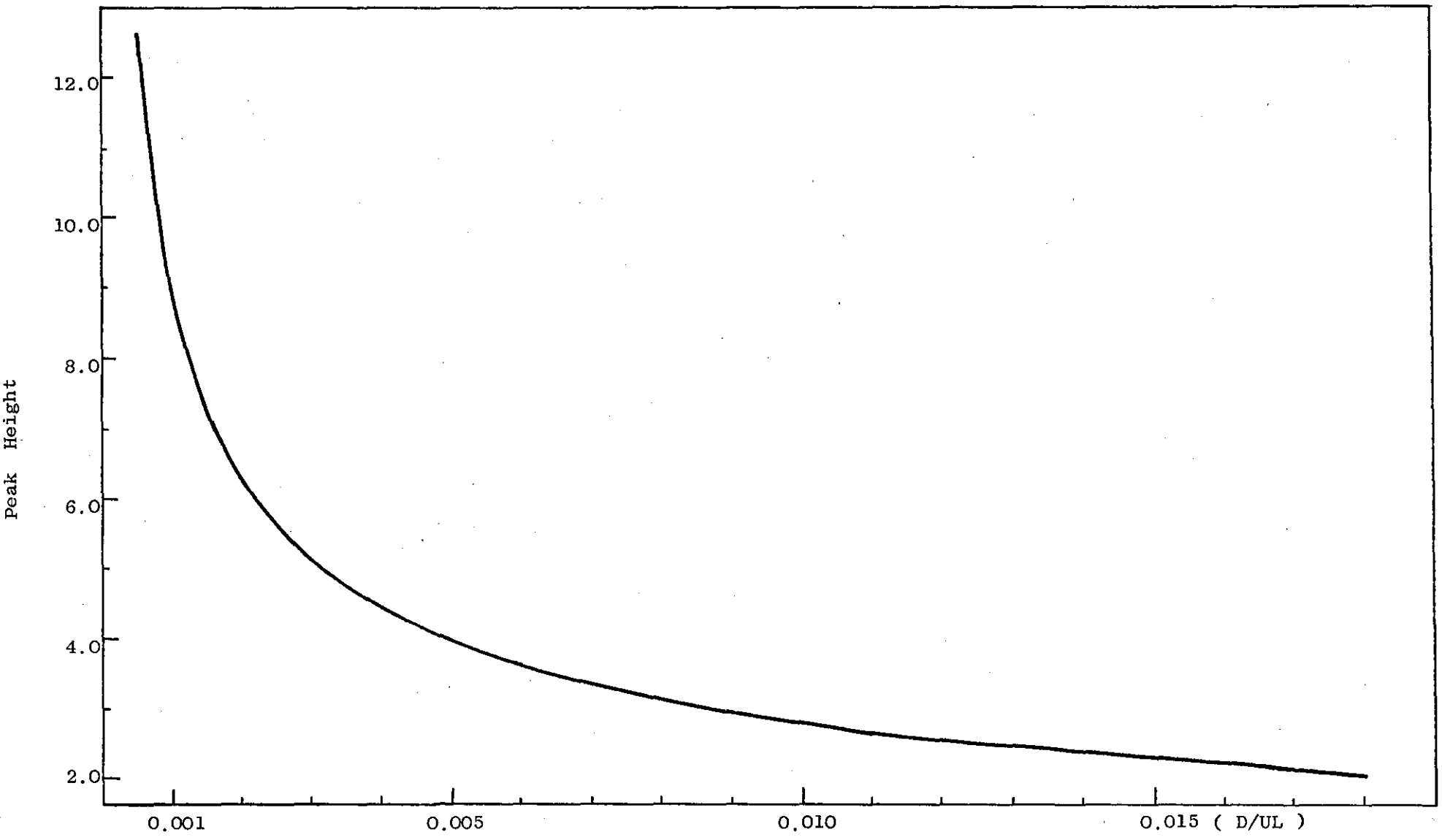

Figure: 10.1. Determination of Peclet number from the peak height.

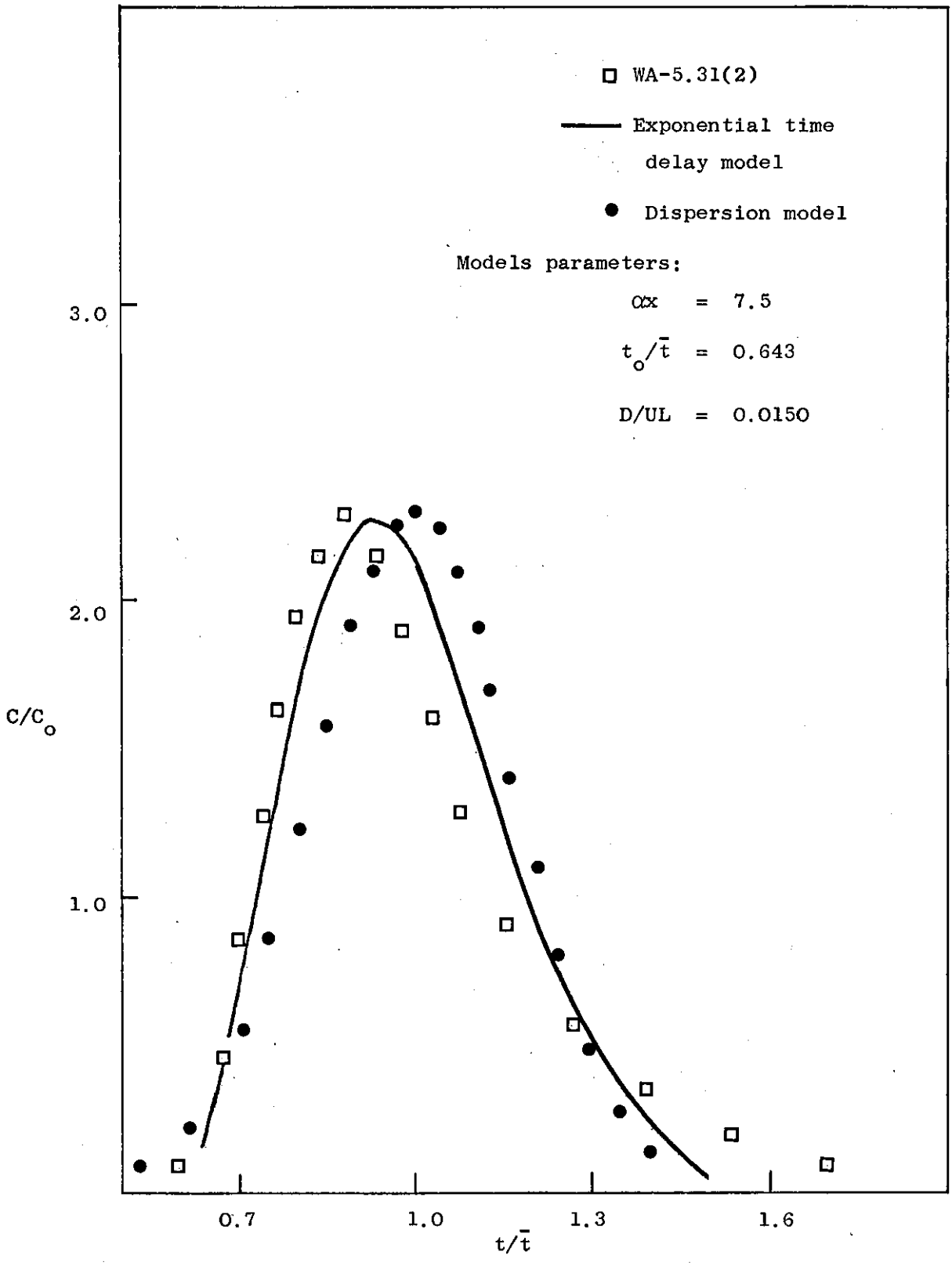

Figure: 10.2. Comparison of the experimental, the exponential time delay model and the dispersion model responses.

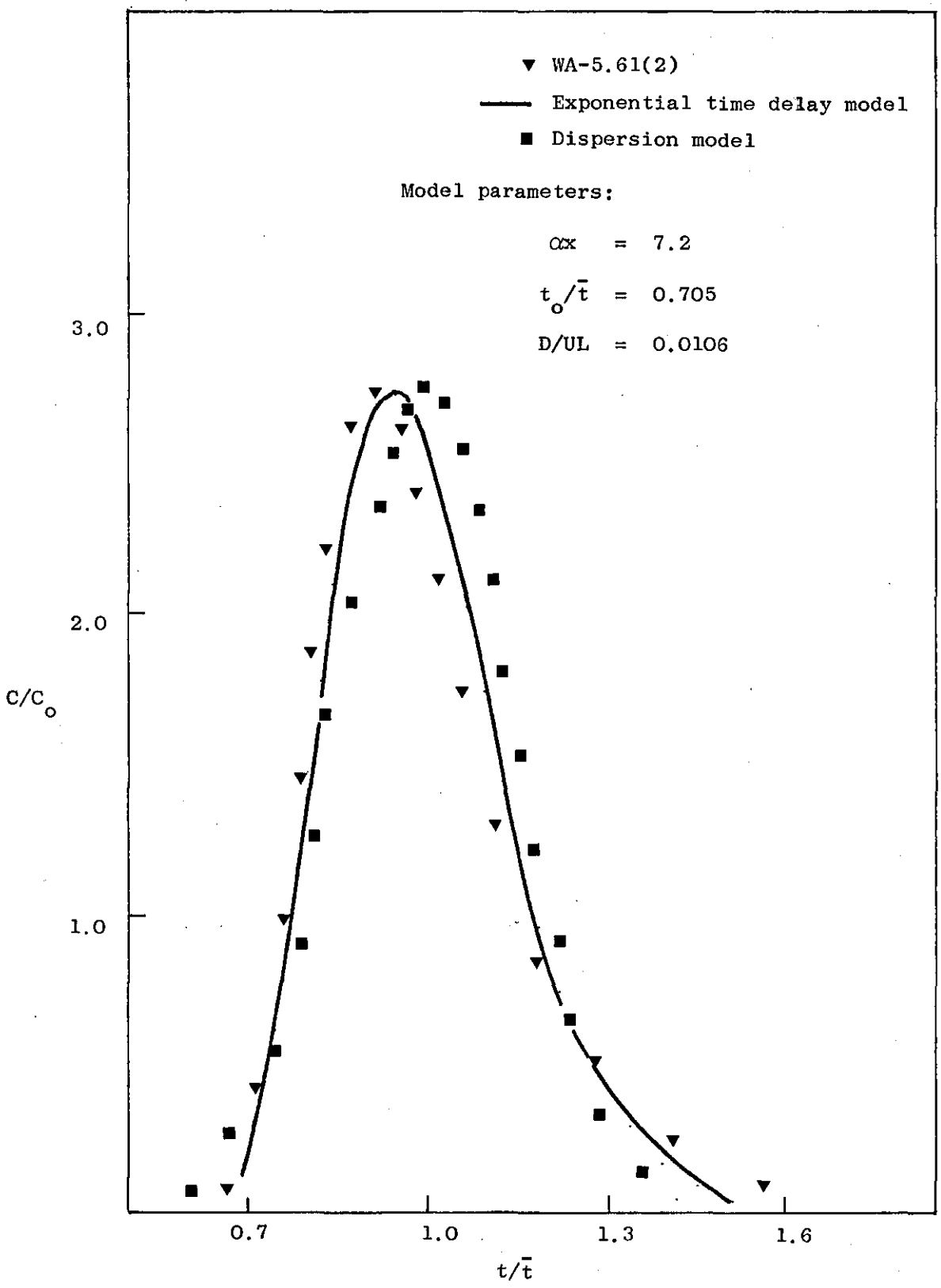

Figure: 10.3. Comparison of the experimental, the exponential time delay model and the dispersion model responses.

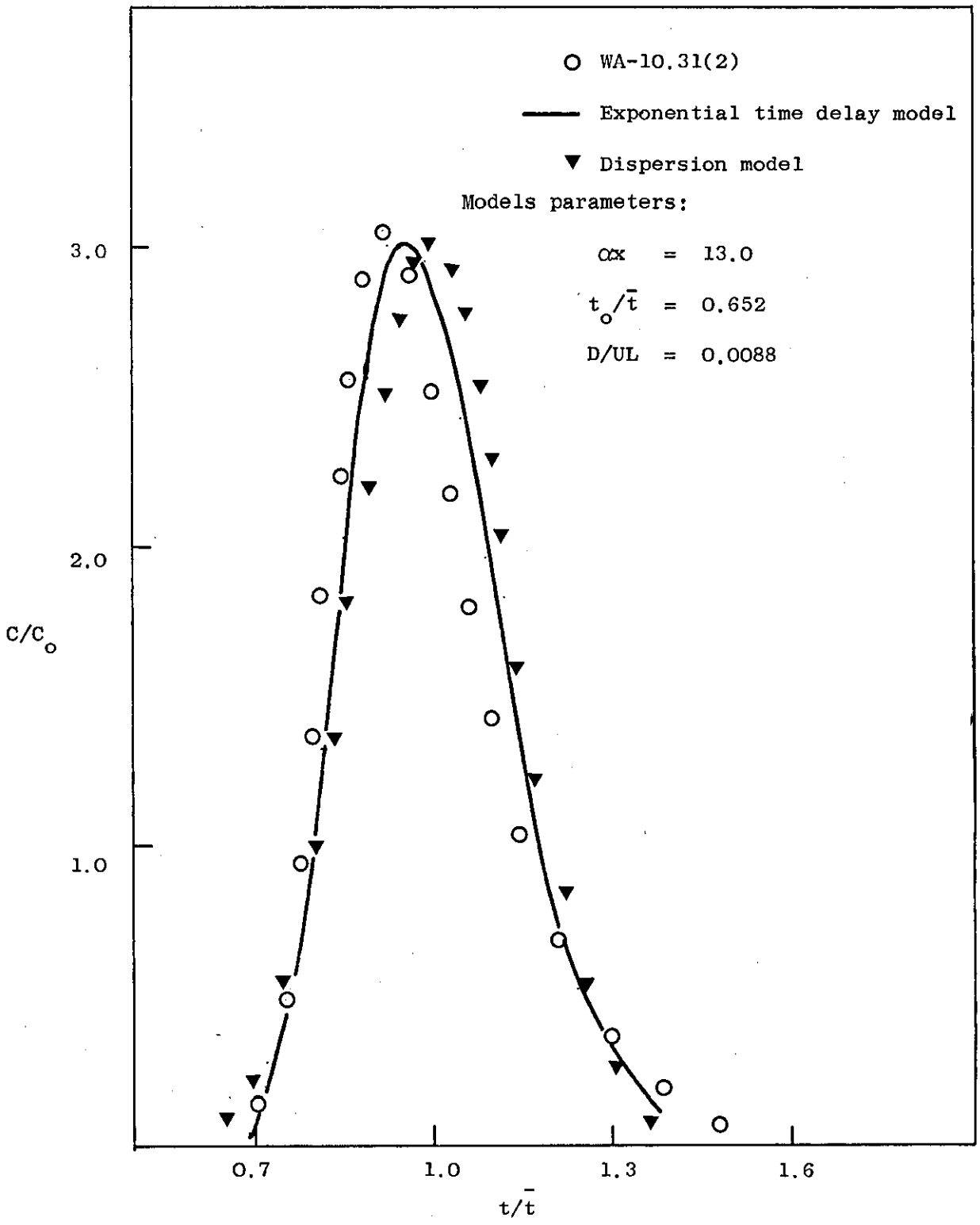

Figure: 10.4. Comparison of the experimental, the exponential time delay model and the dispersion model responses.

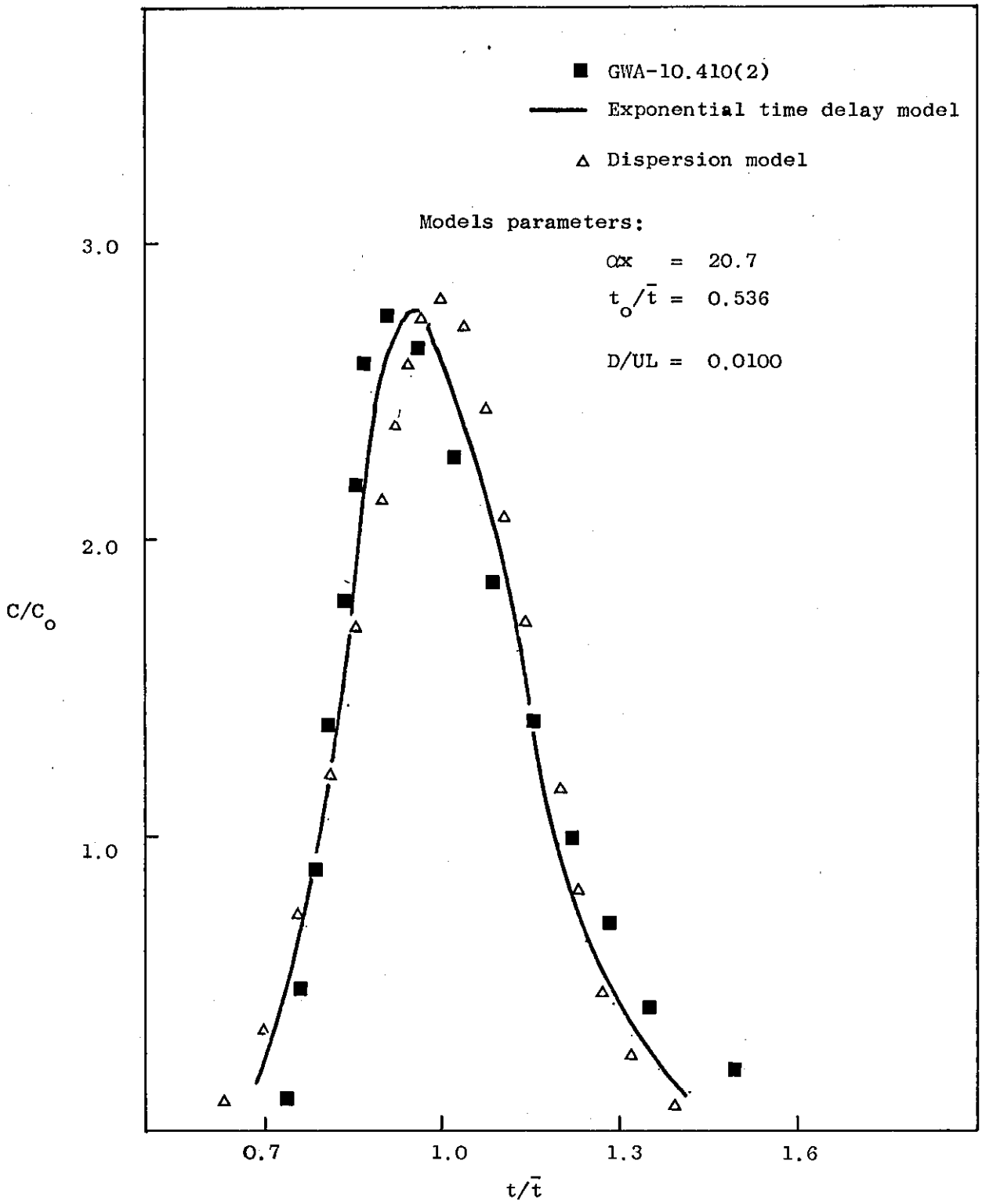

Figure: 10.5. Comparison of the experimental, the exponential time delay model and the dispersion model responses.

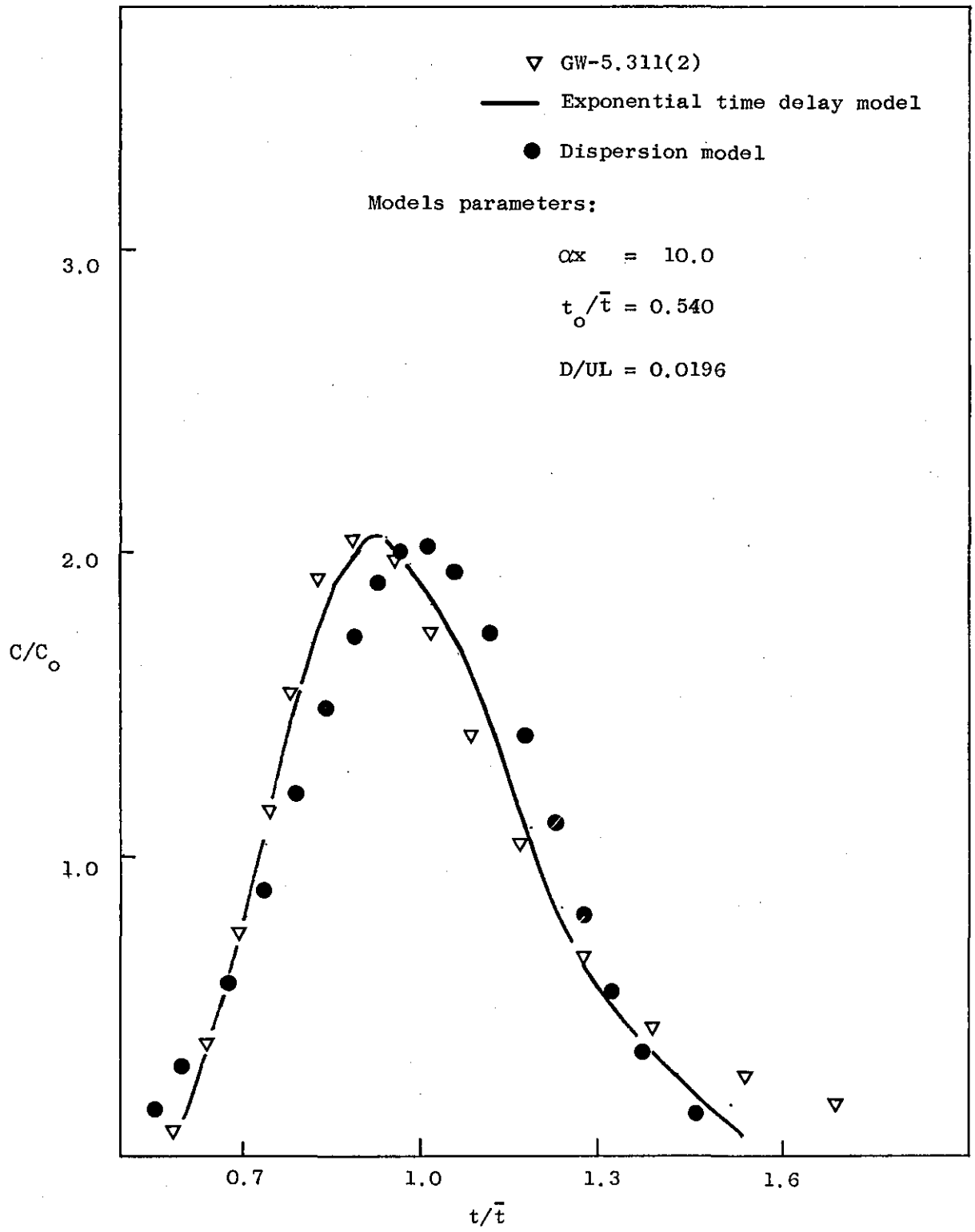

Figure: 10.6. Comparison of the experimental, the exponential time delay model and the dispersion model responses.

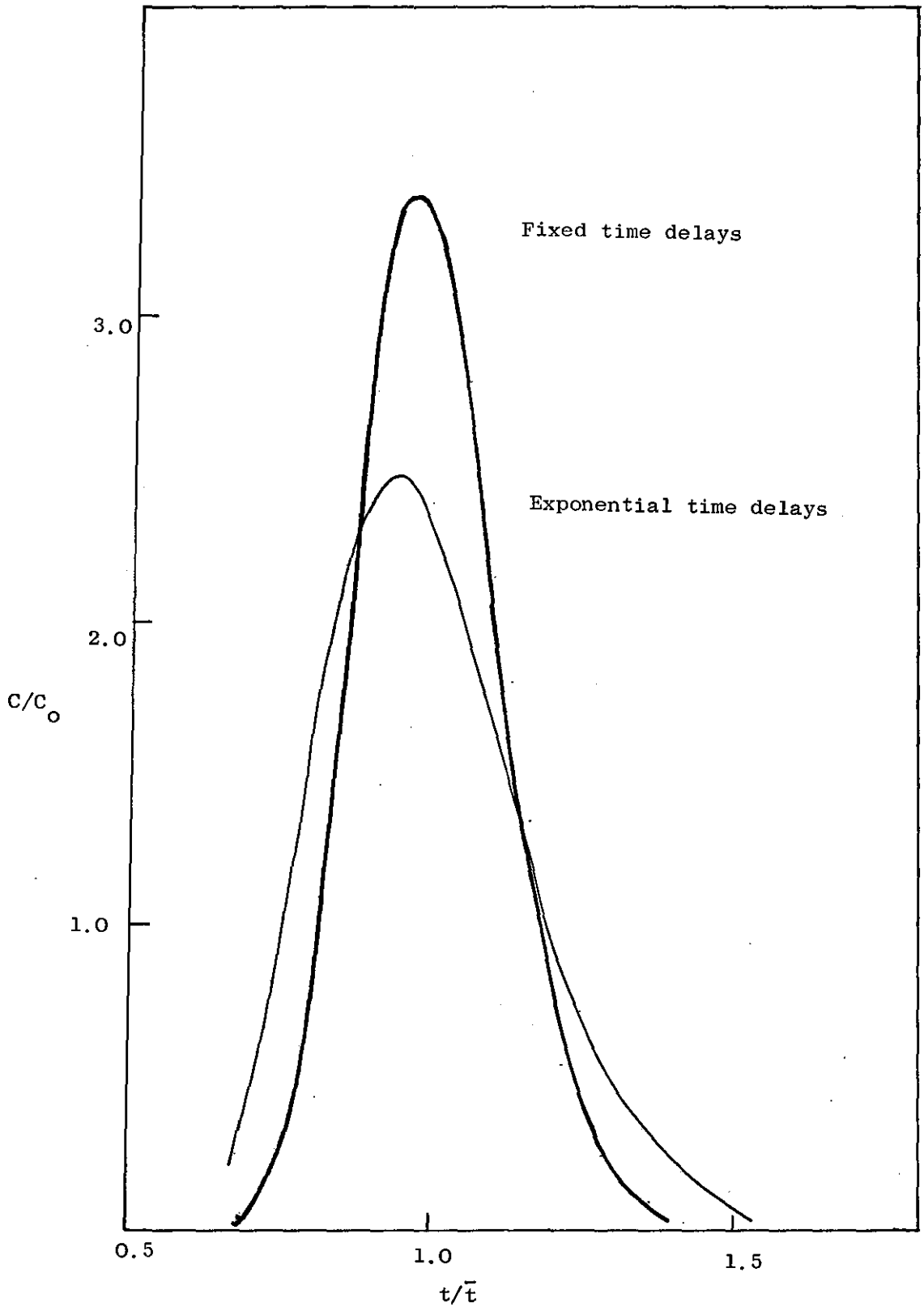

Figure: 10.7. Time delay model: normalised response.

$\alpha x = 10$; $t_o/\bar{t} = 0.62$

identify solely on the basis of residence time distributions; this is analogous to the situation encountered in surface renewal processes where, as here, the mechanism can be usefully applied regardless of the distribution of life times of surface elements (108).

The gamma distribution delay times version of the model represents distributions which are more skewed than the responses of other models, but this flexibility has been achieved at the expense of an extra parameter.

The parameter m provides a measure of the randomness of the delay process. The delay process is completely random for m equal to unity - equalising the chance of all the dealyed elements to move on from the transitional delayed state in the next time increment. When value of m is greater than unity, the randomness of the delay process decreases, favouring longer delays. In the limit as $m \rightarrow \infty$ the spreading due to the delay times reduces approaching zero, hence approaching plug flow. The randomness of the delay process is also reduced for m less than unity, but in this case short delays are favoured and responses become more skewed.

The inability of the time delay models to predict the initial part of the response curve was pointed out in Chapter 4. This is due to the fact that the model attributes axial mixing solely to the delay process so that no material can emerge from the bed earlier than that which travels undelayed in the main stream. Except for this inadequacy at the initial part of the response, the model fits the experimental curves very well and the parameters are well correlated with the operating holdup measurements.

The inclusion of the direct axial displacement of the delayed material in the formulation of the hopping model enables the initial portion of the experimental response to be well fitted: material can by-pass some of the main flow region, thus leading to more gradual rise in the initial response.

In Chapter 5 moments of the model responses were obtained, whilst in principle it is an easy matter to determine the model parameters by the method of matching moments, it is preferable to use either the parameter-matching method, described for the two-parameter model or the optimisation routine employed for the three-parameter models. The moment-matching method places undue weight on the tail of the response curves.

Although the models have been used purely for describing experimental response curves, it may be often possible to make predictions concerning the axial mixing on the transport processes; this requires some knowledge of the location of the most probable delay zones in relation to the transport interface: elements delayed close to this interface are likely to be of primary significance while for systems where the delays occur in isolation from the transfer surface, the steady state behaviour may be virtually unaffected by the delay process. There is some evidence to suggest that this latter situation occurs in packed distillation columns. Kropholler et al (109) measured liquid side distributions and tried to incorporate their effect, by means of a dispersion term, in the equations for a packed batch distillation column. It was found, however, that the dispersion model poorly represented their results; and as subsequent steady state experiments showed the mass transfer to be well represented by a plug flow model, the authors chose to ignore the axial mixing effect on the column dynamics. The time delay model resolves this apparent anomaly: adding a mass transfer term to Equation (4.1) represents the liquid side situation; it will be seen that in the steady state (L.H.S. = 0) the axial mixing does not affect the mass transfer although the effect on the dynamics could be considerable. This applies not only to the simple impulse distribution of Equation (4.1) but any distribution of delay times.

10.3 Conclusions

A plausible abstraction of flow behaviour in a packed bed column leads to a simple probabilistic model for describing the residence time distributions.

Although applied exclusively to liquid side distributions in a counter-current gas/liquid packed bed system, the model lends itself to a variety of physical situations.

All the models were found to fit the responses under widely varying conditions of operation. The degree of "goodness-of-fit" of any model depended on its complexity; ranging from reasonable fits for the two parameter model to extremely good fits for the hopping model. Except for the initial sharp rise of the experimental response curve, the gamma - distributed delay time form of the time-delay model provided the best predictions especially when the decaying ' tail' end of the responses are compared.

A general transfer fuction of the model was also presented and the effect of varying the model parameter studied via the system moments, obtained from this transfer fuction.

The experimental and data processing techniques employed proved satisfactory and the liquid holdup data conformed within the prescribed deviation to several previously established correlations.

The flexibility and mathematical simplicity of the models studied make them an attractive alternatives to the one-dimensional dispersion model which does not account for the skewed distribution that occurs in practice and which on elaboration leads to unwiedly analysis. Many other multiparameter models are available but their mathematical complexity limits their usage.

The effect of increasing the packed height was to reduce the dispersion while an increase of liquid viscosity promoted dispersion. An

increase in liquid flow rate also produced less dispersion and the gas flow rates had no observable effects on the liquid side residence time distributions.

The experiments to investigate the role of molecular diffusion on the overall residence time distribution of the system did not reveal any noticable effect.

10.4. Suggestions for Further Work

The development of the time delay models and their subsequent application to a real system i.e. the trickle flow in packed bed, has revealed the potentialities of these models. It appears that systems with high lateral flow can be adequately described by the time delay model with one of the delay time distribution, such as scraped surface thin-film equipment or flow through filter cakes. The latter case has been investigated by solving the basic hydrodynamic equations which lead to elaborate solutions. The present approach of developing time delay models is useful, for the basic concepts involved are simple and realistic and the mathematical analysis is not tedious. Once the model parameters are correlatable with various system geometry, the fluid properties and other operating variables, these correlations can be employed to predict the system performance without experimentation. However, to prove the existance of the postulated mechanisms, more subtle experiments such as the carrying out of reactions with non-linear kinetics are required.

Nomenclature

x	distance
D/UL	dispersion number
t	time
$\bar{t}$	mean residence time
t_o	dead time
$t/\bar{t}$	normalised time
$t_o/\bar{t}$	normalised dead time

APPENDICES

APPENDIX ..... A

Table: 1. WATER-AIR SYSTEM

5½ feet Packed Height

Run No.	W-5.21	WA-5.22	W-5.31	WA-5.32	W-5.41	WA-5.42	W-5.51	WA-5.52	W-5.61	WA-5.62
Liquid flow rate ccs/min.	120	120	180	180	240	240	300	300	360	360
Gas flow rate l/min.	0	1	0	1	0	1	0	1	0	1

10½ feet Packed Height

Run No.	W-10.21	WA-10.22	W-10.31	WA-10.32	W-10.41	WA-10.42	W-10.51	WA-10.52	W-10.61	WA-10.62
Liquid flow rate ccs/min.	120	120	180	180	240	240	300	300	360	360
Gas flow rate l/min.	0	1	0	1	0	1	0	1	0	1

15½ feet Packed Height

Run No.	W-15.21	WA-15.22	W-15.31	WA-15.32	W-15.41	WA-15.42	W-15.51	WA-15.52	W-15.61	WA-15.62
Liquid flow rate ccs/min.	120	120	180	180	240	240	300	300	360	360
Gas flow rate l/min.	0	1	0	1	0	1	0	1	0	1

Table: 2. GLYCERINE-WATER-AIR SYSTEM

Solution Viscosity = 4.5 cp.

$5\frac{1}{2}$ feet Packed Height

Run No.	GW-5.210	GWA-5.220	GW-5.310	GWA-5.320	GW-5.410	GWA-5.420
Liquid flow rate ccs/min.	120	120	180	180	240	240
Gas flow rate l/min.	0	0.5	0	0.4	0	0.3

$10\frac{1}{2}$ feet Packed Height

Run No.	GW-10.210	GWA-10.220	GW-10.310	GWA-10.320	GW-10.410	GWA-10.420	GW-10.510	GWA-10.520	GW-10.610
Liquid flow rate ccs/min.	120	120	180	180	240	240	300	300	360
Gas flow rate l/min.	0	0.2	0	0.2	0	0.2	0	0.2	0

Table: 2. GLYCERINE-WATER-AIR SYSTEM

Solution Viscosity = 7.5 cp.

$5\frac{1}{2}$ feet Packed Height

Run No.	GW-5.211	GW-5.221	GW-5.311	GW-5.321	GW-5.411	GW-5.421	GW-5.511	GW-5.521
Liquid flow rate ccs/min.	120	120	180	180	240	240	300	300

$10\frac{1}{2}$ feet Packed Height

Run No.	GW-10.211	GW-10.221	GW-10.311	GW-10.321	GW-10.411	GW-10.421	GW-10.511	GW-10.521
Liquid flow rate ccs/min.	120	120	180	180	240	240	300	300

Table: 3. DOUBLE - TRACER EXPERIMENTS

Tracers used : i) Potassium Chloride
ii) Nigrosine Dye

$10\frac{1}{2}$ feet Packed Height

Run No.	DTW-10.21-COND.	DTW-10.22-PHOT.	DTW-10.41-COND.	DTW-10.42-PHOT.	DTW-10.51-COND.	DTW-10.52-PHOT.
Liquid flow rate ccs/min.	120	120	240	240	300	300
Photo-cell detector.		*		*		*
Conductivity cell detector.	*		*		*	

APPENDIX ..... B

NORMALISED EXPERIMENTAL RESPONSE

COLUMN SPECIFICATIONS

Diameter	:	$1\frac{1}{2}$ inch
Packed Height	:	$5\frac{1}{2}$ feet
Type of Packing Used	:	Ceramic Rschig Rings
Size of Packing	:	$\frac{1}{8} \times \frac{1}{8}$ inch

WATER - AIR RUNS.

Run No.	$t/\bar{t}$	C/C_o	Run No.	$t/\bar{t}$	C/C_o
	0.592	0.031		0.568	0.019
	0.611	0.056		0.606	0.111
	0.631	0.165		0.645	0.319
	0.650	0.308		0.683	0.650
	0.669	0.465		0.721	1.079
	0.689	0.657		0.750	1.526
	0.708	0.860		0.798	1.875
	0.727	1.090		0.836	2.074
	0.747	1.348		0.855	2.124
	0.766	1.574		0.874	2.141
	0.785	1.772		0.894	2.124
	0.805	1.940		0.932	2.016
	0.824	2.036		0.970	1.856
	0.843	2.126		1.008	1.674
	0.862	2.180		1.047	1.457
	0.881	2.180		1.085	1.273
	0.901	2.180		1.123	1.101
W-5.21	0.920	2.126	WA-5.22	1.162	0.933
	0.940	2.066		1.200	0.784
	0.959	1.969		1.238	0.673
	0.978	1.881		1.276	0.568
	1.036	1.567		1.315	0.481
	1.075	1.354		1.353	0.408
	1.113	1.142		1.391	0.353
	1.152	0.987		1.430	0.303
	1.191	0.829		1.468	0.262
	1.229	0.706		1.506	0.231
	1.268	0.584		1.525	0.212
	1.307	0.495		1.564	0.183
	1.326	0.448		1.602	0.162
	1.364	0.377		1.640	0.143
	1.403	0.325		1.700	0.110
	1.442	0.279		1.800	0.090
	1.480	0.239			
	1.654	0.103			
	1.800	0.050			

Run No.	$t/\bar{t}$	C/C_o	Run No.	$t/\bar{t}$	C/C_o
	0.612	0.031		0.620	0.077
	0.662	0.295		0.669	0.331
	0.711	0.796		0.717	0.798
	0.761	1.448		0.765	1.437
	0.786	1.723		0.814	1.927
	0.811	2.005		0.862	2.235
	0.835	2.186		0.886	2.290
	0.860	2.268		0.910	2.290
	0.885	2.303		0.935	2.236
	0.909	2.275		0.959	2.122
	0.934	2.213		0.983	2.000
	0.959	2.085		1.007	1.855
W-5.31	0.984	1.953	WA-5.32	1.030	1.723
	1.034	1.666		1.056	1.578
	1.083	1.330		1.080	1.415
	1.133	1.084		1.104	1.270
	1.183	0.866		1.152	1.038
	1.232	0.676		1.201	0.839
	1.282	0.532		1.249	0.658
	1.331	0.427		1.297	0.544
	1.381	0.334		1.346	0.435
	1.431	0.270		1.394	0.345
	1.480	0.218		1.442	0.277
	1.530	0.180		1.491	0.172
	1.580	0.142		1.539	0.160
	1.630	0.124		1.587	0.140
	1.700	0.090		1.650	0.120
	1.800	0.050		1.700	0.080
				1.800	0.040

Run No.	$t/\bar{t}$	C/C_o	Run No.	$t/\bar{t}$	C/C_o
	0.651	0.052		0.644	0.040
	0.709	0.468		0.673	0.250
	0.737	0.935		0.701	0.450
	0.766	1.200		0.729	0.801
	0.795	1.663		0.758	1.201
	0.823	1.975		0.815	1.922
	0.852	2.235		0.843	2.252
	0.881	2.456		0.871	2.442
	0.910	2.456		0.900	2.482
	0.938	2.456		0.928	2.452
	0.967	2.352		0.957	2.282
	0.996	2.131		0.985	2.132
W-5.41	1.025	1.975	WA-5.42	1.014	1.972
	1.053	1.728		1.042	1.722
	1.082	1.559		1.070	1.561
	1.111	1.351		1.099	1.371
	1.139	1.143		1.127	1.211
	1.197	0.884		1.184	0.961
	1.254	0.689		1.241	0.681
	1.312	0.468		1.298	0.520
	1.369	0.325		1.355	0.370
	1.427	0.221		1.411	0.280
	1.455	0.208		1.440	0.250
	1.513	0.117		1.500	0.200
	1.570	0.104		1.554	0.120
	1.628	0.065		1.610	0.090
	1.685	0.013		1.640	0.040

Run No.	$t/\bar{t}$	C/Co	Run No.	$t/\bar{t}$	C/Co
	0.675	0.077		0.645	0.058
	0.711	0.360		0.679	0.255
	0.747	0.842		0.714	0.619
	0.784	1.403		0.748	1.100
	0.820	1.948		0.783	1.652
	0.856	2.347		0.818	2.120
	0.892	2.605		0.852	2.425
	0.928	2.605		0.887	2.552
	0.964	2.475		0.921	2.484
	1.000	2.245		0.956	2.316
	1.034	1.970		0.990	2.064
	1.073	1.656		1.025	1.805
W-5.51	1.109	1.403	WA-5.52	1.059	1.510
	1.145	1.160		1.094	1.299
	1.181	0.944		1.128	1.079
	1.217	0.748		1.163	0.907
	1.254	0.624		1.197	0.751
	1.290	0.497		1.232	0.619
	1.326	0.383		1.267	0.515
	1.362	0.330		1.301	0.457
	1.398	0.260		1.336	0.387
	1.434	0.214		1.370	0.311
	1.471	0.174		1.405	0.280
	1.507	0.122		1.439	0.236
	1.543	0.099		1.474	0.211
	1.579	0.077		1.508	0.180
	1.600	0.050		1.600	0.070

Run No.	$t/\bar{t}$	C/C_o	Run No.	$t/\bar{t}$	C/C_o
	0.668	0.051		0.647	0.034
	0.686	0.123		0.666	0.097
	0.705	0.278		0.684	0.204
	0.724	0.500		0.721	0.548
	0.743	0.756		0.758	1.105
	0.761	1.038		0.777	1.440
	0.780	1.358		0.795	1.736
	0.798	1.730		0.814	2.001
	0.817	1.985		0.833	2.252
	0.836	2.246		0.851	2.434
	0.854	2.457		0.870	2.588
	0.873	2.650		0.888	2.638
	0.892	2.730		0.907	2.664
	0.910	2.742		0.925	2.607
	0.929	2.684		0.944	2.563
	0.947	2.639		0.962	2.434
W-5.61	0.966	2.502	WA-5.62	0.981	2.292
	0.985	2.368		1.000	2.133
	1.003	2.202		1.037	1.812
	1.022	2.027		1.074	1.497
	1.041	1.856		1.111	1.222
	1.059	1.719		1.148	0.987
	1.078	1.511		1.185	0.805
	1.115	1.260		1.222	0.649
	1.152	0.989		1.259	0.518
	1.190	0.804		1.297	0.431
	1.227	0.651		1.334	0.342
	1.264	0.538		1.371	0.290
	1.301	0.416		1.408	0.425
	1.357	0.305		1.445	0.204
	1.395	0.232		1.482	0.167
	1.432	0.195		1.538	0.140
	1.470	0.159		1.575	0.113
	1.525	0.132		1.612	0.092
	1.600	0.060		1.700	0.030

COLUMN SPECIFICATIONS

Diameter	:	$1\frac{1}{2}$ inch
Packed Height	:	$10\frac{1}{2}$ feet
Type of Packing used	:	Ceramic Raschig Rings
Size of Packing	:	$\frac{1}{8} \times \frac{1}{8}$ inch

WATER - AIR RUNS

Run No.	$t/\bar{t}$	C/C_o	Run No.	$t/\bar{t}$	C/C_o
	0.667	0.041		0.685	0.044
	0.693	0.136		0.712	0.220
	0.720	0.355		0.738	0.484
	0.746	0.696		0.765	0.857
	0.772	1.133		0.791	1.275
	0.799	1.557		0.804	1.560
	0.825	2.007		0.818	1.824
	0.851	2.390		0.831	2.066
	0.878	2.633		0.844	2.262
	0.904	2.772		0.857	2.417
	0.930	2.758		0.871	2.593
	0.956	2.649		0.884	2.769
	0.983	2.499		0.897	2.857
W-10.21	1.009	2.281	WA-10.32	0.910	2.857
	1.035	2.007		0.963	2.791
	1.062	1.775		0.990	2.593
	1.088	1.557		1.016	2.351
	1.114	1.338		1.043	2.088
	1.140	1.133		1.069	1.824
	1.167	0.970		1.096	1.560
	1.193	0.806		1.122	1.363
	1.219	0.683		1.149	1.121
	1.246	0.587		1.175	0.923
	1.272	0.519		1.202	0.835
	1.298	0.423		1.228	0.681
	1.324	0.355		1.255	0.593
	1.351	0.314		1.281	0.505
	1.377	0.246		1.307	0.418
	1.403	0.205		1.334	0.330
	1.460	0.150		1.360	0.308
	1.509	0.096		1.387	0.220
				1.466	0.132
				1.506	0.066

Run No.	$t/\bar{t}$	C/Co	Run No,	$t/\bar{t}$	C/C_o
	0.682	0.059		0.698	0.032
	0.722	0.295		0.734	0.287
	0.763	0.768		0.769	0.797
	0.803	1.556		0.804	1.451
	0.823	1.930		0.821	1.818
	0.843	2.324		0.839	2.153
	0.864	2.639		0.857	2.456
	0.884	2.875		0.874	2.663
	0.904	3.033		0.892	2.838
	0.924	3.052		0.909	2.932
	0.944	2.954		0.944	2.982
	0.965	2.796		0.962	2.902
	0.985	2.658		0.980	2.790
	1.005	2.422		0.997	2.599
	1.025	2.166		1.032	2.216
	1.045	1.950		1.067	1.834
W-10.31	1.066	1.772	WA-10.32	1.103	1.514
	1.086	1.556		1.138	1.180
	1.126	1.162		1.173	0.989
	1.146	1.004		1.226	0.686
	1.167	0.906		1.261	0.494
	1.187	0.748		1.296	0.415
	1.227	0.610		1.331	0.351
	1.268	0.433		1.366	0.233
	1.308	0.374		1.436	0.175
	1.348	0.295		1.489	0.112
	1.389	0.197		1.542	0.048
	1.429	0.118		1.600	0.032
	1.590	0.059			

Run No.	$t/\bar{t}$	C/C_o	Run No.	$t/\bar{t}$	C/C_o
	0.702	0.041		0.705	0.060
	0.738	0.371		0.720	0.226
	0.773	0.885		0.755	0.550
	0.809	1.523		0,770	0.770
	0.826	1.873		0.785	1.050
	0.844	2.202		0.800	1.400
	0.862	2.511		0.810	1.650
	0.879	2.696		0.826	1.874
	0.897	2.861		0.846	2.212
	0.915	3.005		0.851	2.410
	0.932	3.005		0.870	2.740
	0.950	2.923		0.898	2.930
	0.968	2.840		0.910	3.000
W-10.41	0.985	2.696	WA-10.42	0.935	3.000
	1.003	2.532		0.970	2.860
	1.021	2.346		0.985	2.700
	1.038	2.202		1.020	2.340
	1.074	1.770		1.065	1.950
	1.109	1.441		1.090	1.620
	1.144	1.194		1.125	1.270
	1.180	0.947		1.160	1.030
	1.215	0.700		1.190	0.780
	1.250	0.535		1.250	0.530
	1.286	0.473		1.300	0.370
	1.321	0.371		1.355	0.225
	1.356	0.226		1.480	0.120
	1.392	0.200		1.510	0.000
	1.462	0.141			
	1.533	0.041			

Run No.	$t/\bar{t}$	C/C_o	Run No.	$t/\bar{t}$	C/C_O
	0.687	0.048		0.869	0.040
	0.710	0.144		0.712	0.137
	0.734	0.264		0.735	0.337
	0.757	0.552		0.758	0.636
	0.780	1.008		0.781	1.035
	0.792	1.225		0.815	1.783
	0.804	1.417		0.838	2.282
	0.815	1.681		0.861	2.681
	0.827	1.993		0.884	2.968
	0.838	2.186		0.907	3.130
	0.850	2.474		0.919	3.130
	0.862	2.642		0.930	3.130
	0.874	2.858		0.941	3.080
W-10.51	0.885	3.026	WA-10.52	0.953	3.018
	0.897	3.146		0.965	2.918
	0.908	3.146		0.988	2.681
	0.920	3.218		1.011	2.419
	0.932	3.218		1.034	2.120
	0.946	3.122		1.057	1.821
	0.967	2.930		1.080	1.571
	o.990	2.667		1.114	1.235
	1.013	2.337		1.149	0.985
	1.036	2.089		1.183	0.773
	1.095	1.489		1.218	0.586
	1.153	0.936		1.241	0.524
	1.200	0.648		1.287	0.374
	1.305	0.336		1.390	0.187
	1.409	0.144		1.505	0.070
	1.503	0.072			

Run No.	$t/\bar{t}$	C/C_o	Run No.	$t/\bar{t}$	C/C_o
	0.720	0.084		0.725	0.094
	0.732	0.105		0.754	0.281
	0.740	0.168		0.774	0.566
	0.748	0.252		0.802	1.054
	0.756	0.357		0.834	1.804
	0.764	0.441		0.862	2.460
	0.788	0.840		0.866	2.554
	0.828	1.701		0.878	2.835
	0.840	2.016		0.890	2.999
	0.848	2.184		0.902	3.116
	0.856	2.373		0.914	3.187
	0.864	2.520		0.922	3.304
	0.872	2.689		0.930	3.300
	0.880	2.857		0.950	3.280
	0.888	2.941		0.970	3.160
	0.892	3.045		0.990	2.990
	0.896	3.021		1.003	2.810
	0.904	3.130		1.080	1.781
W-10.61	0.908	3.214	WA-10.62	1.127	1.336
	0.916	3.214		1.171	0.961
	0.924	3.298		1.199	0.773
	0.936	3.277		1.231	0.562
	0.960	3.193		1.280	0.398
	0.976	3.109		1.316	0.280
	0.984	3.024		1.380	0.168
	1.000	2.857		1.500	0.075
	1.020	2.542			
	1.060	2.016			
	1.100	1.533			
	1.152	1.092			
	1.180	0.840			
	1.200	0.756			
	1.240	0.525			
	1.280	0.441			
	1.320	0.336			
	1.380	0.168			
	1.449	0.105			
	1.500	0.080			

COLUMN SPECIFICATIONS

Diameter	:	$1\frac{1}{2}$ inch
Packed Height	:	$15\frac{1}{2}$ feet
Type of Packing Used	:	Ceramic Raschig Rings
Size of Packing	:	$\frac{1}{8} \times \frac{1}{8}$ inch

WATER - AIR RUNS

Run No.	$t/\bar{t}$	C/C_o	Run No.	$t/\bar{t}$	C/C_o
	0.724	0.041		0.721	0.063
	0.740	0.148		0.738	0.190
	0.756	0.321		0.756	0.388
	0.771	0.562		0.774	0.706
	0.787	0.875		0.792	1.071
	0.803	1.206		0.810	1.521
	0.819	1.685		0.827	1.972
	0.834	2.107		0.845	2.425
	0.842	2.242		0.863	2.796
	0.858	2.667		0.881	3.066
	0.874	2.988		0.898	3.282
	0.890	3.217		0.917	3.312
	0.905	3.352		0.925	3.370
	0.921	3.413		0.934	3.310
	0.937	3.382		0.943	3.282
	0.952	3.261		0.961	3.094
	0.968	3.115		0.979	2.915
W-15.21	0.976	3.002	WA-15.22	0.997	2.681
	0.992	2.784		1.015	2.449
	1.008	2.579		1.032	2.186
	1.024	2.347		1.050	1.961
	1.039	2.140		1.077	1.634
	1.063	1.828		1.113	1.255
	1.087	1.538		1.139	1.046
	1.102	1.368		1.166	0.857
	1.126	1.162		1.184	0.751
	1.189	0.754		1.211	0.633
	1.252	0.487		1.264	0.449
	1.307	0.335		1.309	0.340
	1.347	0.277		1.344	0.274
	1.402	0.189		1.407	0.190
	1.457	0.134		1.451	0.151
	1.504	0.101		1.496	0.113
	1.552	0.074		1.549	0.082
	1.607	0.054		1.603	0.057

Run No.	$t/\bar{t}$	C/C_o	Run No.	$t/\bar{t}$	C/C_o
	0.755	0.056		0.748	0.029
	0.776	0.320		0.769	0.222
	0.797	0.713		0.790	0.567
	0.819	1.234		0.812	0.978
	0.840	1.900		0.833	1.568
	0.851	2.253		0.843	1.927
	0.861	2.547		0.854	2.282
	0.872	2.855		0.864	2.616
	0.883	3.161		0.875	2.938
	0.893	3.391		0.886	3.197
	0.904	3.537		0.986	3.468
	0.925	3.724		0.907	3.662
	0.936	3.743		0.917	3.720
	0.947	3.705		0.928	3.800
	0.957	3.630		0.938	3.800
W-15,31	0.918	3.391	WA-15.32	0.959	3.700
	1.010	2.905		0.970	3.573
	1.042	2.360		0.991	3.247
	1.106	1.538		1.012	2.891
	1.160	0.943		1.044	2.311
	1.245	0.467		1.076	1.783
	1.287	0.331		1.107	1.336
	1.330	0.231		1.150	0.978
	1.373	0.165		1.192	0.683
	1.426	0.099		1.255	0.422
	1.479	0.046		1.308	0.292
	1.554	0.035		1.350	0.232
	1.607	0.013		1.403	0.164
				1.445	0.115
				1.551	0.039

Run No.	$t/\bar{t}$	C/C_o	Run No.	$t/\bar{t}$	C/C_o
	0.765	0.059		0.765	0.060
	0.791	0.321		0.791	0.322
	0.818	0.930		0.817	0.930
	0.844	1.969		0.844	1.968
	0.857	2.566		0.857	2.565
	0.871	3.070		0.870	3.068
	0.884	3.472		0.884	3.469
	0.897	3.833		0.897	3.831
	0.910	4.027		0.910	4.025
	0.924	4.030		0.923	4.098
	0.950	3.885		0.950	3.883
	0.963	3.714		0.976	3.485
	0.990	3.273		1.002	3.012
W-15.41	1.030	2.503	WA-15.42	1.029	2.504
	1.069	1.802		1.069	1.802
	1.109	1.288		1.108	1.288
	1.148	0.913		1.148	0.914
	1.188	0.685		1.187	0.680
	1.228	0.506		1.227	0.507
	1.281	0.321		1.267	0.357
	1.333	0.231		1.293	0.294
	1.373	0.177		1.333	0.232
	1.426	0.124		1.386	0.165
	1.479	0.094		1.438	0.112
	1.545	0.065		1.505	0.079
	1.598	0.045		1.557	0.060
	1.651	0.033		1.597	0.047
	1.677	0.026		1.650	0.034
	1.717	0.019		1.703	0.020
	1.743	0.013		1.757	0.008

Run No.	$t/\bar{t}$	C/C_o	Run No.	$t/\bar{t}$	C/C_o
	0.754	0.019		0.754	0.018
	0.784	0.256		0.785	0.255
	0.814	0.815		0.815	0.815
	0.845	1.766		0.845	1.766
	0.875	2.905		0.860	2.300
	0.890	3.357		0.875	2.900
	0.905	3.705		0.890	3.358
	0.920	3.947		0.906	3.707
	0.935	4.056		0.921	3.949
	0.951	4.040		0.936	4.058
	0.966	3.911		0.951	4.040
	0.966	3.433		0.966	3.914
	1.026	2.801		0.996	3.435
	1.056	2.223		1.042	2.506
	1.102	1.430		1.087	1.653
W-15.51	1.147	0.948	WA-15.52	1.132	1.085
	1.208	0.564		1.163	0.808
	1.253	0.381		1.193	0.632
	1.298	0.268		1.253	0.381
	1.344	0.195		1.314	0.243
	1.389	0.141		1.374	0.158
	1.419	0.112		1.450	0.099
	1.450	0.099		1.495	0.064
	1.495	0.065		1.556	0.041
	1.525	0.053		1.601	0.029
	1.571	0.042		1.647	0.023
	1.616	0.030		1.692	0.012
	1.661	0.019		1.753	0.006
	1.752	0.007			

Run No.	$t/\bar{t}$	C/C_o	Run No.	$t/\bar{t}$	C/C_o
	0.781	0.067		0.782	0.056
	0.815	0.557		0.816	0.535
	0.849	1.582		0.850	1.544
	0.866	2.243		0.867	2.196
	0.883	2.926		0.884	2.902
	0.900	3.541		0.901	3.505
	0.917	3.998		0.918	3.966
	0.934	4.270		0.935	4.230
	0.951	4.270		0.952	4.270
	0.968	4.230		0.968	3.946
	0.985	3.979		1.038	2.852
	1.037	2.832		1.072	2.120
	1.088	1.760		1.106	1.516
W-15.61	1.122	1.231	WA-15.62	1.123	1.260
	1.156	0.901		1.157	0.925
	1.207	0.557		1.174	0.776
	1.241	0.423		1.208	0.571
	1.275	0.312		1.225	0.476
	1.309	0.233		1.259	0.348
	1.360	0.144		1.310	0.212
	1.411	0.096		1.345	0.156
	1.445	0.067		1.379	0.098
	1.479	0.048		1.430	0.056
	1.513	0.029		1.498	0.023
	1.548	0.020		1.515	0.012
	1.599	0.010		1.566	0.001
	1.633	0.001			

COLUMN SPECIFICATIONS

Diameter	:	$1\frac{1}{2}$ inch
Packed Height	:	$5\frac{1}{2}$ feet
Type od Packing Used	:	Ceramic Raschig Rings
Size of Packing	:	$\frac{1}{8} \times \frac{1}{8}$ inch

GLYCERINE - WATER - AIR RUNS.

VISCOSITY = 4.5cp.

Run No.	$t/\bar{t}$	C/C_o	Run No.	$t/\bar{t}$	C/C_o
	0.520	0.085		0.525	0.090
	0.550	0.180		0.565	0.265
	0.575	0.343		0.600	0.400
	0.610	0.420		0.646	0.540
	0.650	0.680		0.672	0.728
	0.685	0.720		0.686	0.915
	0.701	1.030		0.712	1.103
	0.729	1.163		0.725	1.197
	0.771	1.429		0.752	1.385
	0.826	1.850		0.792	1.667
	0.909	1.961		0.818	1.854
	1.034	1.562		0.858	1.948
	1.075	1.429		0.885	1.948
	1.103	1.163		0.911	1.940
GW-5.21	1.158	1.030	GWA-5.22	0.951	1.854
μ=4.5cp	1.186	0.897	μ=4.5cp	0.991	1.667
	1.227	0.764		1.044	1.348
	1.269	0.631		1.084	1.291
	1.366	0.498		1.097	1.197
	1.400	0.366		1.137	1.009
	1.600	0.233		1.176	0.915
	1.800	0.001		1.190	0.822
				1.230	0.728
				1.256	0.633
				1.376	0.446
				1.495	0.352
				1.681	0.164
				1.801	0.002

Run No.	$t/\bar{t}$	C/C_o	Run No.	$t/\bar{t}$	C/C_o
	0.660	0.155		0.700	0.150
	0.668	0.462		0.710	0.800
	0.705	0.797		0.748	1.097
	0.761	1.301		0.785	1.389
	0.836	1.804		0.842	1.974
	0.911	2.140		0.899	2.266
	0.986	1.972		0.974	1.974
	1.042	1.804		1.106	1.681
	1.098	1.468		1.162	1.389
GW-5.31	1.173	1.133	GWA-5.32	1.200	1.097
μ =4.5 cp	1.229	0.965	μ =4.5 cp	1.294	0.804
	1.266	0.797		1.379	0.629
	1.380	0.461		1.435	0.462
	1.470	0.380		1.452	0.420
	1.540	0.340		1.502	0.350
	1.600	0.300		1.590	0.300
	1.700	0.240		1.675	0.272
	1.800	0.120		1.700	0.240
				1.800	0.200

Run No.	$t/\bar{t}$	C/C_o	Run No.	$t/\bar{t}$	C/C_o
	0.650	0.060			
	0.700	0.460		0.691	0.349
	0.754	0.989		0.714	0.549
	0.769	1.253		0.730	0.749
	0.801	1.510		0.738	0.948
	0.856	2.044		0.762	1.148
	0.890	2.300		0.785	1.348
	0.911	2.540		0.793	1.547
	0.943	2.308		0.809	1.747
	0.989	2.140		0.840	1.943
	1.045	1.925		0.872	2.146
GW-5.41	1.070	1.730	GWA-5.42	0.887	2.345
μ =4.5 cp	1.145	1.350	μ=4.5 cp	0.903	2.520
	1.190	1.128		0.927	2.346
	1.250	0.720		0.982	2.146
	1.320	0.390		1.055	1.800
	1.355	0.300		1.115	1.505
	1.405	0.270		1.200	1.100
	1.450	0.200		1.282	0.460
	1.515	0.155		1.310	0.460
	1.600	0.105		1.352	O 315
				1.440	0.200
				1.492	0.180
				1.530	0.120
				1.580	0.100

COLUMN SPECIFICATIONS

Diameter	:	$1\frac{1}{2}$ inch
Packed Height	:	$5\frac{1}{2}$ feet
Type of Packing Used	:	Ceramic Raschig Rings
Size of Packing	:	$\frac{1}{8} \times \frac{1}{8}$ inch

GLYCERINE - WATER SOLUTION RUNS.

VISCOSITY, = 7.5cp

Run No.	$t/\bar{t}$	C/Co	Run No.	$t/\bar{t}$	C/C_o
	0.566	0.089		0.571	0.141
	0.600	0.177		0.618	0.282
	0.612	0.265		0.641	0.423
	0.624	0.354		0.653	0.565
	0.647	0.531		0.665	0.706
	0.659	0.619		0.688	0.847
	0.682	0.885		0.711	1.129
	0.705	1.062		0.735	1.411
	0.717	1.239		0.758	1.552
	0.752	1.504		0.782	1.693
	0.763	1.593		0.805	1.835
	0.798	1.858		0.829	1.975
	0.821	1.946		0.840	1.975
	0.868	1.960		0.900	1.900
	0.902	1.946		0.934	1.835
	0.937	1.858		0.969	1.693
GW-5.21	0.972	1.769	GW-5.22	0.993	1.552
μ =7.5 cp	1.019	1.504	μ=7.5 cp	1.016	1.411
	1.042	1.327		1.051	1.270
	1.112	1.061		1.122	0.988
	1.135	0.973		1.204	0.706
	1.158	0.885		1.309	0.430
	1.205	0.708		1.415	0.282
	1.240	0.619		1.614	0.141
	1.274	0.531			
	1.333	0.442			
	1.400	0.354			
	1.472	0.265			
	1.750	0.088			

Run No.	$t/\bar{t}$	C/C_o	Run No.	$t/\bar{t}$	C/C_o
	0.600	0.140		0.630	0.240
	0.630	0.320		0.662	0.405
	0.665	0.500		0.690	0.600
	0.729	0.744		0.710	0.805
	0.783	1.116		0.740	1.205
	0.837	1.859		0.770	1.620
	0.890	2.040		0.815	1.825
	0.903	2.030		0.840	2.000
	0.980	1.910		0.875	2.030
	1.015	1.720		0.955	1.960
	1.060	1.495		1.010	1.820
GW-5.31	1.100	1.325	GW-5.32	1.035	1.620
μ=7.5 cp	1.245	0.680	μ=7.5 cp	1.105	1.210
	1.305	0.562		1.150	1.050
	1.415	0.353		1.230	0.760
	1.515	0.240		1.300	0.600
	1.550	0.260		1.390	0.425
	1.615	0.200		1.460	0.315
	1.840	0.140		1.590	0.225
				1.640	0.200
				1.780	0.160

Run No.	$t/\bar{t}$	C/C_o	Run No.	$t/\bar{t}$	C/C_o
	0.631	0.355		0.600	0.305
	0.671	0.533		0.610	0.383
	0.691	0.710		0.669	0.575
	0.711	1.065		0.690	0.766
	0.751	1.420		0.731	1.149
	0.791	1.775		0.752	1.341
	0.850	1.953		0.834	1.916
	0.910	2.130		0.875	2.110
	0.930	2.130		0.895	2.110
	0.949	1.953		0.936	1.916
	0.989	1.775		0.977	1.724
	1.049	1.420		1.039	1.533
GW-5.41	1.089	1.243	GW-5.42	1.080	1.341
μ =7.5 cp	1.149	1.065	μ=7.5 cp	1.141	1.149
	1.189	0.888		1.162	0.958
	1.249	0.710		1.223	0.766
	1.309	0.533		1.346	0.575
	1.345	0.533		1.428	0.383
	1.400	0.400		1.525	0.290
	1.500	0.360		1.809	0.220
	1.600	0.320			

Run No.	$t/\bar{t}$	C/C_o	Run No.	$t/\bar{t}$	C/C_o
	0.658	0.184		0.680	0.333
	0.705	0.552		0.715	0.666
	0.729	0.736		0.739	0.998
	0.753	1.104		0.763	1.331
	0.777	1.471		0.812	1.664
	0.801	1.655		0.836	1.996
	0.824	1.839		0.859	2.200
	0.848	2.200		0.884	2.300
	0.872	2.250		0.908	2.300
	0.896	2.300		0.980	2.200
	0.910	2.300		1.030	1.994
	0.979	2.200		1.077	1.664
	1.086	1.655		1.125	1.331
GW-5.51	1.109	1.471	GW-5.52	1.173	0.998
μ =7.5 cp	1.133	1.287	μ=7.5 cp	1.221	0.666
	1.157	1.104		1.342	0.333
	1.181	0.920		1.415	0.320
	1.205	0.736		1.500	0.200
	1.276	0.552		1.600	0.141
	1.371	0.368			
	1.466	0.184			
	1.510	0.160			
	1.600	0.140			

COLUMN SPECIFICATIONS

Diameter	:	$1\frac{1}{2}$ inch
Packed Height	:	$10\frac{1}{2}$ feet
Type of Packing Used	:	Ceramic Raschig Rings
Size of Packing	:	$\frac{1}{8}$ X $\frac{1}{8}$ inch

GLYCERINE - WATER - AIR SOLUTION RUNS

VISCOSITY, μ = 4.5cp

Run No.	$t/\bar{t}$	C/C_o	Run No.	$t/\bar{t}$	C/C_o
	0.660	0.060		0.642	0.142
	0.672	0.161		0.657	0.189
	0.687	0.282		0.679	0.330
	0.717	0.484		0.693	0.377
	0.732	0.767		0.708	0.519
	0.747	0.807		0.730	0.755
	0.769	1.130		0.745	0.944
	0.792	1.412		0.752	1.132
	0.814	1.775		0.767	1.274
	0.822	1.896		0.774	1.321
	0.837	2.098		0.796	1.699
	0.852	2.219		0.818	1.840
	0.867	2.380		0.840	2.076
	0.882	2.420		0.855	2.217
	0.897	2.580		0.884	2.450
GW-10.21	0.934	2.541	GWA-10.22	0.913	2.599
μ =4.5 cp	0.979	2.420	μ=4.5 cp	0.928	2.406
	1.002	2.259		0.986	2.217
	1.025	2.050		1.030	1.840
	1.047	1.936		1.060	1.463
	1.077	1.614		1.111	1.274
	1.107	1.452		1.147	1.132
	1.137	1.251		1.184	0.896
	1.189	0.968		1.235	0.708
	1.227	0.767		1.301	0.519
	1.257	0.605		1.353	0.330
	1.301	0.484		1.469	0.189
	1.406	0.322		1.505	0.130
	1.504	0.161			
	1.571	0.120			

Run No.	$t/\bar{t}$	C/C_o	Run No.	$t/\bar{t}$	C/Co
	0.696	0.289		0.700	0.150
	0.737	0.385		0.744	0.507
	0.768	0.771		0.764	0.797
	0.788	1.060		0.774	0.869
	0.819	1.542		0.784	1.158
	0.840	1.927		0.805	1.376
	0.881	2.601		0.815	1.665
	0.912	2.698		0.835	1.955
	0.994	2.601		0.845	2.245
	1.045	2.216		0.875	2.534
	1.107	1.445		0.916	2.700
	1.179	1.156		0.931	2.705
GW-10.31	1.210	0.771	GWA-10.32	0.996	2.607
μ =4.5 cp	1.271	0.674	μ =4.5 cp	1.037	2.245
	1.323	0.507		1.087	1.738
	1.340	0.290		1.118	1.448
	1.441	0.210		1.158	1.159
	1.500	0.182		1.239	0.579
	1.605	0.150		1.289	0.507
	1.713	0.100		1.360	0.289
	1.823	0.090		1.451	0.271
				1.502	0.201
				1.583	0.180

Run No.	$t/\bar{t}$	C/C_o	Run No.	$t/\bar{t}$	C/C_o
	0.741	0.311		0.740	0.300
	0.765	0.725		0.751	0.623
	0.777	1.139		0.775	0.935
	0.802	1.242		0.799	1.480
	0.814	1.656		0.835	1.870
	0.826	2.070		0.871	2.493
	0.851	2.381		0.919	2.805
	0.875	2.483		0.928	2.805
	0.899	2.800		0.991	2.493
	0.924	2.795		1.016	2.410
	1.046	2.381		1.087	1.792
	1.070	2.070		1.123	1.247
	1.107	1.553		1.171	1.168
	1.156	1.242		1.207	0.856
	1.217	0.828		1.243	0.623
GW-10.41 μ =4.5cp	1.241	0.725	GWA-10.42 μ =4.5cp	1.302	0.545
	1.260	0.414		1.339	0.312
	1.315	0.311		1.400	0.234
	1.370	0.300		1.430	0.210
	1.415	0.250		1.480	0.180
	1.501	0.175		1.532	0.141
	1.540	0.140			

Run No.	$t/\bar{t}$	C/C_o	Run No.	$t/\bar{t}$	C/C_o
	0.689	0.130		0.705	0.240
	0.717	0.246		0.724	0.394
	0.731	0.575		0.751	0.690
	0.745	0.657		0.779	1.083
	0.759	0.986		0.792	1.477
	0.773	1.314		0.806	1.576
	0.800	1.643		0.834	1.871
	0.814	1.889		0.888	2.364
	0.842	2.218		0.902	2.758
	0.883	1.547		0.925	2.807
	0.911	2.630		0.957	2.659
	0.925	2.900		1.040	2.364
GW-10.51	0.939	2.632	GWA-10.52	1.067	1.970
μ =4.5 cp	1.008	2.300	μ =4.5 cp	1.095	1.871
	1.050	1.889		1.136	1.576
	1.105	1.561		1.191	1.083
	1.133	1.314		1.246	0.690
	1.175	0.986		1.383	0.394
	1.216	0.904		1.432	0.212
	1.244	0.657		1.499	0.181
	1.286	0.570		1.530	0.130
	1.327	0.329		1.600	0.110
	1.400	0.246		1.650	0.080
	1.505	0.150			
	1.600	0.150			
	1.600	0.090			

Run No.	$t/\bar{t}$	C/C_o
	0.741	0.429
	0.763	0.751
	0.773	0.859
	0.784	1.181
	0.827	1.717
	0.848	2.146
	0.880	2.468
	0.901	2.576
	0.912	2.898
	0.940	3.005
	0.965	2.890
	1.008	2.578
GW-10.61	1.051	2.146
μ = 4.5cp	1.083	2.039
	1.125	1.610
	1.189	1.181
	1.211	0.856
	1.307	0.429
	1.403	0.322
	1.502	0.200
	1.613	0.100
	1.700	0.080

COLUMN SPECIFICATIONS

Diameter	:	$1\frac{1}{2}$ inch
Packed Height	:	$10\frac{1}{2}$ feet
Type of Packing Used	:	Ceramic Raschig Rings
Size of Packing	:	$\frac{1}{8} \times \frac{1}{8}$ inch

GLYCERINE - WATER SOLUTION RUNS.

VISCOSITY, μ = 7.5cp

Run No.	$t/\bar{t}$	C/C_o	Run No.	$t/\bar{t}$	C/C_o
	0.672	0.083		0.691	0.169
	0.692	0.222		0.704	0.394
	0.705	0.443		0.716	0.451
	0.732	0.665		0.729	0.676
	0.759	0.969		0.742	0.845
	0.773	1.191		0.755	1.127
	0.793	1.551		0.781	1.521
	0.806	1.772		0.806	1.747
	0.826	1.994		0.838	2.197
	0.847	2.215		0.877	2.423
	0.853	2.298		0.896	2.500
	0.874	2.437		0.928	2.423
GW-10.21	0.894	2.520	GW-10.22	0.999	2.254
μ =7.5cp	0 901	2.550	μ =7.5cp	1.018	1.972
	0.914	2.540		1.044	1.803
	0.968	2.437		1.095	1.524
	0.995	2.298		1.165	0.902
	1.008	2.187		1.185	0.845
	1.022	2.077		1.249	0.676
	1.049	1.883		1.304	0.394
	1.136	1.218		1.364	0.225
	1.163	1.080		1.456	0.169
	1.204	0.886		1.502	0.111
	1.224	0.775		1.600	0.080
	1.251	0.637			
	1.332	0.442			
	1.359	0.332			
	1.440	0.194			
	1.547	0.111			
	1.574	0.083			

Run No.	$t/\bar{t}$	C/C_o	Run No.	$t/\bar{t}$	C/C_o
	0.693	0.141		0.723	0.280
	0.702	0.188		0.741	0.490
	0.721	0.376		0.769	0.840
	0.748	0.753		0.815	1.610
	0.767	0.941		0.861	2.170
	0.776	1.129		0.888	2.450
	0.794	1.458		0.898	2.520
	0.812	1.646		0.925	2.610
	0.831	1.882		0.944	2.620
	0.849	2.070		0.980	2.520
	0.858	2.211		1.017	2.450
	0.895	2.446		1.063	2.170
GW-10.31	0.913	2.634	GW-10.32	1.081	1.960
μ =7.5 cp	0.932	2.634	μ =7.5cp	1.146	1.330
	0.996	2.587		1.219	0.770
	1.051	2.023		1.265	0.490
	1.078	1.882		1.366	0.280
	1.124	1.505		1.486	0.210
	1.169	1.082		1.521	0.160
	1.206	0.941		1.635	0.110
	1.279	0.517		1.700	0.100
	1.326	0.376			
	1.417	0.188			
	1.548	0.141			
	1.600	0.100			

Run No.	$t/\bar{t}$	C/C_o	Run No.	$t/\bar{t}$	C/C_o
	0.715	0.191		0.721	0.156
	0.737	0.447		0.755	0.468
	0.748	0.702		0.778	0.858
	0.770	0.957		0.801	1.403
	0.792	1.404		0.812	1.481
	0.813	1.723		0.835	2.027
	0.846	2.233		0.857	2.105
	0.889	2.488		0.903	2.729
	0.901	2.750		0.925	2.729
	0.955	2.480		1.027	2.651
	1.009	2.233		1.084	2.105
GW-10.41	1.075	1.978	GW-10.42	1.118	1.715
μ=7.5cp	1.108	1.723	μ =7.5cp	1.175	1.170
	1.140	1.404		1.220	0.858
	1.184	1.148		1.265	0.546
	1.249	0.638		1.333	0.468
	1.282	0.447		1.357	0.233
	1.369	0.383		1.424	0.156
	1.489	0.128		1.600	0.110
	1.552	0.110			
	1.632	0.100			

Run No.	$t/\bar{t}$	C/C_o	Run No.	$t/\bar{t}$	C/C_o
	0.685	0.120		0.708	0.256
	0.711	0.299		0.734	0.683
	0.749	0.837		0.772	1.024
	0.774	1.016		0.798	1.365
	0.813	1.794		0.823	1.706
	0.851	2.212		0.861	1.962
	0.877	2.451		0.887	2.389
	0.902	2.690		0.912	2.730
	0.928	2.850		0.925	2.805
	0.966	2.690		0.963	2.645
	0.992	2.511		1.028	2.389
	1.030	2.271		1.065	2.048
GW-10.51	1.055	1.973	GW-10.52	1.103	1.621
μ =7.5cp	1.068	1.734	μ =7.5cp	1.141	1.280
	1.094	1.554		1.192	1.024
	1.119	1.256		1.243	0.683
	1.170	1.016		1.307	0.597
	1.209	0.837		1.358	0.341
	1.247	0.598		1.421	0.256
	1.278	0.538		1.521	0.180
	1.362	0.299			
	1.451	0.120			
	1.500	0.100			

COLUMN SPECIFICATIONS

Diameter	:	$1\frac{1}{2}$ inch
Packed Height	:	$10\frac{1}{2}$ feet
Type of Packing Used	:	Ceramic Raschig Rings
Size of Packing	:	$\frac{1}{8} \times \frac{1}{8}$ inch

DOUBLE - TRACER RUNS.

Run No.	$t/\bar{t}$	C/C_o	Run No.	$t/\bar{t}$	C/C_o
	0.680	0.060		0.690	0.080
	0.706	0.131		0.707	0.167
	0.733	0.394		0.727	0.389
	0.747	0.591		0.741	0.500
	0.767	0.919		0.755	0.667
	0.780	1.182		0.775	1.056
	0.801	1.510		0.795	1.446
	0.821	1.904		0.815	1.835
	0.841	2.298		0.829	2.057
	0.861	2.495		0.856	2.502
DTW -10.21	0.875	2.695	DTW-10.22	0.870	2.669
COND	0.881	2.756	PHOT	0.883	2.780
	0.909	2.820		0.903	2.820
	0.940	2,720		0.910	2.820
	0.972	2.560		0.958	2.700
	1.003	2.429		0.978	2.613
	1.023	2.232		0.998	2.391
	1.071	1.773		1.039	2.002
	1.098	1.510		1.052	1.890
	1.152	1.051		1.066	1.779
	1.179	0.919		1.140	1.112
	1.213	0.722		1.181	0.890
	1.233	0.591		1.208	0.723
	1.287	0.460		1.255	0.556
	1.314	0.394		1.296	0.445
	1.456	0.197		1.357	0.333
	1.577	0.080		1.540	0.110

Run No.	$t/\bar{t}$	C/C_o	Run No.	$t/\bar{t}$	C/C_o
	0.707	0.089		0.693	0.083
	0.733	0.268		0.711	0.125
	0.750	0.447		0.736	0.334
	0.768	0.670		0.771	0.792
	0.794	1.161		0.805	1.543
	0.811	1.563		0.831	1.918
	0.837	2.144		0.857	2.627
	0.854	2.501		0.874	2.877
	0.880	2.903		0.882	2.961
	0.898	3.082		0.891	3.003
	0.907	3.120		0.908	3.086
	0.915	3.120		0.917	3.126
DTW-10.41	0.949	3.080	DTW-10.42	0.943	3.003
COND	0.976	2.859	PHOT	0.977	2.752
	0.993	2.680		1.003	2.460
	1.011	2.457		1.037	2.043
	1.037	2.189		1.063	1.751
	1.054	1.965		1.089	1.502
	1.080	1.653		1.132	1.126
	1.149	1.027		1.158	0.959
	1.175	0.893		1.278	0.417
	1.236	0.581		1.347	0.292
	1.271	0.447		1.425	0.208
	1.384	0.223		1.468	0.167
	1.444	0.179		1.537	0.125
	1.505	0.134		1.600	0.083
	1.600	0.089			

APPENDIX C

LIQUID HOLDUP CORRELATION DATA

Run No.	$(H_T)_{exp.}$	$(H_{op.})_{exp.}$	$(N_{Re})_L$	X	Y	Z
W-5.21 WA-5.22	0.146	0.119	1.490	0.0687	0.0075	1.940
W-5.31 WA-5.32	0.196	0.163	2.230	0.0903	0.0101	2.520
W-5.41 WA-5.42	0.209	0.182	2.970	0.1100	0.0125	2.780
W-5.51 WA-5.52	0.228	0.201	3.710	0.1280	0.0148	2.950
W-5.61 WA-5.62	0.240	0.213	4.460	0.1450	0.0170	3.180
W-10.21 WA-10.22	0.165	0.140	1.490	0.0687	0.0075	2.200
W-10.31 WA-10.32	0.175	0.150	2.230	0.0903	0.0101	2.320
W-10.41 WA-10.42	0.196	0.171	2.970	0.1100	0.0125	3.130
W-10.51 WA-10.52	0.236	0.211	3.710	0.1280	0.0148	3.240
W-10.61 WA-10.62	0.245	0.220	4.460	0.1450	0.0170	3.240
W-15.21 WA-15.22	0.165	0.140	1.490	0.0687	0.0075	2.180
W-15.31 WA-15.32	0.183	0.158	2.230	0.0903	0.0101	2.430
W-15.41 WA-15.42	0.198	0.173	2.970	0.1100	0.0125	2.630
W-15.51 WA-15.52	0.214	0.189	3.710	0.1250	0.0148	2.840
W-15.61 WA-15.62	0.229	0.204	4.460	0.1450	0.0170	3.030
GW-5.210 GWA-5.220	0.248	0.190	0.370	0.0917	0.0106	1.450
GW-5.310 GWA-5.320	0.251	0.193	0.550	0.1210	0.0143	1.470
GW-5.410 GWA-5.420	0.266	0.208	0.730	0.1470	0.0177	1.550

Run No.	(H_T)exp.	$(H_{op.})$exp.	$(N_{Re})_L$	X	Y	Z
GW-10.210 GWA-10.220	0.219	0.161	0.370	0.0917	0.0106	1.280
GW-10.310 GWA-10.320	0.241	0.183	0.550	0.1210	0.0143	1.410
GW-10.410 GWA-10.420	0.266	0.208	0.730	0.1470	0.0177	1.550
GW-10.510 GWA-10.520	0.299	0.241	0.920	0.1700	0.0211	1.740
GW-5.211 GW-5.221	0.262	0.172	0.230	0.0960	0.0121	1.150
GW-5.311 GW-5.321	0.293	0.203	0.340	0.1230	0.0163	1.280
GW-5.411 GW-5.421	0.314	0.224	0.450	0.1530	0.0201	1.380
GW-5.511 GW-5.521	0.327	0.237	0.560	0.1780	0.0236	1.430
GW-10.211 GW-10.221	0.251	0.161	0.230	0.0960	0.0121	1.100
GW-10.311 GW-10.321	0.269	0.179	0.340	0.1230	0.0163	1.180
GW-10.411 GW-10.421	0.302	0.211	0.450	0.1530	0.0201	1.320
GW-10.511 GW-10.521	0.323	0.233	0.560	0.1780	0.0236	1.410

X = dimensionless groups in OTAKE and OKADA (21) correlation:

Y = dimensionless groups in MOHUNTA and LADDAH'S (24) correlation:

and

Z = dimensionless groups in GELBE'S (26) correlation:

APPENDIX ..... D

TIME DELAY MODEL

Exponentially distributed time delays.

Table: 1 , $5\frac{1}{2}$ feet Packed Height

Run No.	Mean Time t mins.	Dispersion No. D3UL	Apparent Dead_Time t_o'/t	True Dead_Time t_o/t	αx	α
W-5.21 WA-5.22	2.333	0.0174	0.662	0.630	7.2	1.31
W-5.31 WA-5.32	2.017	0.0150	0.670	0.643	7.5	1.36
W-5.41 WA-5.42	1.670	0.0132	0.700	0.680	7.3	1.32
W-5.51 WA-5.52	1.420	0.0124	0.710	0.693	7.2	1.31
W-5.61 WA-5.62	1.275	0.0106	0.720	0.705	7.2	1.31
GW-5.211 GWA-5.221	4.170	0.0245	0.522	0.480	11.0	2.00
GW-5.311 GWA-5.321	3.000	0.0196	0.568	0.540	10.0	1.82
GW-5.411 GWA-5.421	2.470	0.0184	0.580	0.554	10.5	1.92
GW-5.511 GWA-5.521	2.100	0.0166	0.604	0.580	10.2	1.90
GW-5.210 GWA-5.220	3.940	0.0200	0.515	0.475	11.5	2.10
GW-5.310 GWA-5.320	3.000	0.0170	0.600	0.580	10.0	1.82
GW-5.410 GWA-5.420	2.120	0.0150	0.612	0.578	11.0	2.00

Table: 2 , 10½ feet Packed Height

Run No.	Mean Time $\bar{t}$ mins.	Dispersion No. D/UL	Apparent Dead Time $t_o'/\bar{t}$	True Dead Time $t_o/\bar{t}$	αx	α
W-10.21 WA-10.22	5.07	0.0098	0.670	0.624	13.0	1.24
W-10.31 WA-10.32	3.55	0.0088	0.690	0.652	13.0	1.24
W-10.41 WA-10.42	2.97	0.0082	0.700	0.660	13.2	1.26
W-10.51 WA-10.52	2.87	0.0078	0.715	0.672	13.0	1.24
W-10.61 WA-10.62	2.48	0.0074	0.725	0.685	13.3	1.27
GW-10.210 GW-10.220	6.67	0.0124	0.612	0.480	20.8	1.98
GW-10.310 GW-10.320	5.00	0.0108	0.640	0.520	21.0	2.00
GW-10.410 GW-10.420	4.00	0.0100	0.652	0.536	20.7	1.99
GW-10.510 GW-10.520	3.60	0.0094	0.664	0.556	20.8	1.98
GW-10.610 GW-10.620	3.10	0.0088	0.672	0.568	20.8	1.98
GW-10.211 GW-10.221	7.60	0.0126	0.616	0.488	20.7	1.97
GW-10.311 GW-10.321	5.50	0.0120	0.628	0.500	21.0	2.00
GW-10.411 GW-10.421	4.50	0.0108	0.640	0.520	20.5	1.94
GW-10.511 GW-10.521	3.90	0.0088	0.652	0.540	20.7	1.97

Table: 3 , 15½ feet Packed Height

Run No.	Mean Time $\bar{t}$ mins.	Dispersion No. D/UL	Apparent Dead Time $t'_o / \bar{t}$	True Dead Time $t_o / \bar{t}$	αx	α
W-15.21 WA-15.22	7.40	0.0068	0.715	0.636	20.5	1.32
W-15.31 WA-15.32	5.48	0.0056	0.735	0.650	20.5	1.32
W-15.41 WA-15.42	4.46	0.0050	0.748	0.668	21.0	1.35
W-15.51 WA-15.52	3.85	0.0046	0.757	0.679	21.0	1.35
W-15.61 WA-15.62	3.42	0.0041	0.774	0.708	20.0	1.30

TIME DELAY MODEL

Gamma distributed time delays.

Table: 4 , $5\frac{1}{2}$ feet Packed Height

Run No.	αx	m	Dead Time $t_o / \bar{t}$	Normalised Mean Time.
W-5.21 WA-5.22	7.50	0.530	0.660	0.995
W-5.31 WA-5.32	7.50	0.520	0.665	0.995
W-5.41 WA-5.42	8.00	0.550	0.678	0.995
W-5.51 WA-5.52	8.00	0.550	0.691	0.995
W-5.61 WA-5.62	8.00	0.550	0.716	0.995
GW-5.210 GWA-5.220	11.10	0.600	0.550	0.985
GW-5.310 GWA-5.320	11.96	0.574	0.605	1.004
GW-5.410 GWA-5.420	11.93	0.578	0.614	1.003
GW-5.211 GWA-5.221	11.25	0.450	0.569	0.982
GW-5.311 GWA-5.321	10.98	0.486	0.604	1.008
GW-5.411 GWA-5.421	10.00	0.420	0.622	0.994
GW-5.511 GWA-5.521	10.15	0.500	0.650	0.999

Table: 5 , 10½ feet Packed Height

Run No.	αx	m	Dead Time $t_o / \bar{t}$	Normalised Mean Time.
W-10.21 WA-10.22	15.00	0.500	0.665	0.995
W-10.31 WA-10.32	15.00	0.500	0.675	0.992
W-10.41 WA-10.42	15.00	0.500	0.685	0.992
W-10.51 WA-10.52	13.0	0.500	0.695	0.980
W-10.61 WA-10.62	15.00	0.500	0.705	0.990
GW-10.210 GW-10.220	20.00	0.521	0.550	0.990
GW-10.310 GW-10.320	20,00	0.500	0.602	0.992
GW-10.410 GW-10.420	20.95	0.450	0.625	0.985
GW-10.211 GW-10.221	20.97	0.450	0.569	0.985
GW-10.311 GW-10.321	20.01	0.490	0.602	1.002
GW-10.511 GW-10.521	20.10	0.460	0.622	0.990

Table: 6 , 15½ feet Packed Height

Run No.	αx	m	Dead Time $t_o / \bar{t}$	Normalised Mean Time.
W-15.21 WA-15.22	21.00	0.350	0.690	0.980
W-15.31 WA-15.32	21.50	0.400	0.705	0.982
W-15.41 WA-15.42	21.00	0.400	0.718	0.980
W-15.51 WA-15.52	21.00	0.400	0.728	0.980
W-15.61 WA-15.62	22.00	0.400	0.739	0.987

HOPPING MODEL

Table: 7 , $5\frac{1}{2}$ feet Packed Height

Run No.	α	Hopping Distance h	$t_o / \bar{t}$	Normalised Mean Time.
W-5.21 WA-5.22	1.24	0.103	0.655	0.980
W-5.31 WA-5.32	1.44	0.075	0.660	0.985
W-5.41 WA-5.42	1.53	0.057	0.667	0.987
W-5.51 WA-5.52	1.67	0.050	0.675	0.987
W-5.61 WA-5.62	2.30	0.090	0.680	0.985
GW-5.210 GWA-5.220	2.35	0.110	0.480	0.981
GW-5.310 GWA-5.320	2.23	0.100	0.592	1.000
GW-5.410 GWA-5.420	2.28	0.106	0.621	1.000
GW-5.211 GWA-5.221	2.30	0.100	0.520	0.980
GW-5.411 GWA-5.421	2.30	0.100	0.538	0.980
GW-5.511 GWA-5.521	2.90	0.107	0.565	0.985

Table: 8 , 10½ feet Packed Height

Run No.	α	Hopping Distance h	$t_o / \bar{t}$	Normalised Mean Time.
W-10.21 WA-10.22	1.03	0.200	0.704	0.980
W-10.31 WA-10.32	1.05	0.179	0.718	0.980
W-10.41 WA-10.42	1.05	0.161	0.726	0.980
W-10.51 WA-10.52	1.06	0.143	0.734	0.980
W-10.61 WA-10.62	1.01	0.125	0.744	0.980
GW-10.210 GW-10.220	2.20	0.250	0.636	0.985
GW-10.310 GW-10.320	2.20	0.216	0.646	0.986
GW-10.510 GW-10.520	2.20	0.185	0.662	0.988
GW-10.211 GW-10.221	2.30	0.250	0.600	0.982
GW-10.311 GW-10.321	2.30	0.213	0.625	0.991
GW-10.411 GW-10.421	2.22	0.226	0.641	0.982
GW-10.511 GW-10.521	2.20	0.210	0.655	0.982

Table: 9 , 15½ feet Packed Height

Run No.	α	Hopping Distance h	$t_o / \bar{t}$	Normalised Mean Time.
W- 15.21 WA-15.22	1.003	0.230	0.742	0.980
W-15.31 WA-15.32	1.002	0.200	0.755	0.980
W-15.41 WA-15.42	1.004	0.180	0.763	0.980
W-15.51 WA-15.52	1.005	0.162	0.769	0.981
W-15.61 WA-15.62	1.005	0.141	0.777	0.982

APPENDIX ..... E

Programme for the Normalised Response Curves and the Truncation Point

During an impulse response experiment, the output of the photo or conductivity cell detector was logged at a suitably chosen time interval on punched paper tape. The print out was typically as given below:

Photo cell detector: the logged data,

+ 0620 + 0620 + 0620 + 0600 + 0540 + 0500 + 0400

etc.

Conductivity cell detector: the logged data,

- 0010 - 0010 - 0010 - 0050 - 0070 - 0100 - 0180

etc.

The second data tape contained the following:

liquid flow rate F

logging time interval t

calibration curve intercept

calibration curve slope

The computation is straight forward. Before proceeding to the actual calculation the truncation of the response curve is required in order to save computational time and to avoid introducing any errors due to the tail end of the response.

An ideal truncation point is reached when the response returns to the base line, however, this point varies from one curve to the next. Thus a suitable truncation criterion should fit all the experimental responses.

A computational procedure was devised to find the peak position of the response curve; it was found that on doubling the number of readings reached at this point, the response had invariably returned to the base line.

The readings are then converted into concentrations units and stored; the area between the successive pairs of points is computed using the trapezoidal rule; the moments of these areas about the origin are also computed and cumulative record is kept of these moments and areas until the truncation point is reached. The first moment i.e. the mean time and the system total holdup is then calculated and printed out. The stored concentrations are then converted to normalised concentrations using the previously calculated area and the corresponding normalised time the calculated mean time of the system - and both normalised quantities printed out after every three time intervals.

COMPUTER PROGRAMME FOR THE NORMALISED RESPONSE.

```
          N
MNR-NORMALIZED RESPONSE

JV1
N1=0
N2=0
V1=-700
V2=0
N6=0
N3=21
V4=0

STOP
V12=TAPE1

ST*OP
V21=TAPE*

*1) VN3=-1XVN3
N3=N3+1
→5, VN3>610

→6
5) VN3=610
→6
6) VN3=-VN3
N2=N2+1
→2, VN3>V1
→3
2) N2=N2+N1
N1=0
V1=VN3+V4
N4=N2X2
→1
3) N1=N1+1
→4, N2>N4
→1
4) VN3=-1XVN3
N5=N4-1*

V22=0
V1=0
V2=0
V3=140.54
V4=21.94
V8=.75
N1=22
7) N1=N1+1
N6=N6+1
V5=LOGVN1
V5=V5XV4
V5=V3-V5
→8, 0>V5
→9
8) V5=0
9) VN1=V5
V6=VN1+V(-1+N1)
```

```
V7=0.25XV6
V1=V1+V7
V9=V7XV8
V2=V2+V9
V8=V8+0.5
⍎→7, ⍝6≠⍝5
V10=V2/V1
V11=V1/V10
V13=V10XV12

TEXT
HOLDUP

MEAN  TIME

PRINTV0, 3042

PRINTV13, 3062

TEXT
N-TIME      N-CONC.

V14=3
⍝1=20
10) ⍝1=⍝1+7
V15=V14/V10
V16=V⍝1/V11
PRINTV15, 3064
PRINTV16, 4044
V14=V14+3.5
→10, ⍝6≥⍝1
(→0)
```

APPENDIX ..... F

COMPUTER PROGRAMMES FOR:

1. Fixed delay times: time delay model
2. Exponentially distributed delay times: time delay model
3. Gamma distributed delay times: time delay model
4. Hopping model
5. Rosenbrock's optimisation method

```
N
TIME DELAY MODEL - FIXED TIME DELAYS

JV1
Π1=11
STOP
V1=TAPE2
V3=.9999
V4=1
V5=EXPMV1
V6=V5
V7=V5
VΠ1=V5
1) Π1=Π1+1
V7=V1XV7
V7=V7/V4
VΠ1=V7
V6=V6+V7
→2, V6≥V3
V4=V4+1
→1

2) V8=0
V9=0
V3=1-V2
V3=V3/V1
V3=V3/2
V5=V2+V3
V10=2XV3
Π2=12
3) V4=V(-1+Π2)+VΠ2
V4=V4XV3
V8=V8+V4
V4=V4XV5
V9=V9+V4
V5=V5+V10
Π2=Π2+1
→3, Π2≠Π1
V4=V9/V8
V5=V8/V4
Π3=11
V6=V2
4) V7=V6/V4
V8=VΠ3/V5
PRINTV7, 3043
PRINTV8, 4043
Π3=Π3+1
V6=V6+V10
→4, Π3≠Π2
(→0)
```

```
N
TIME-DELAY  MODEL--  EXPONENTIAL  DELAYS

JV1
STOP
9)V1=TAPE

TEXT
ALPHA-X  TO

PRINTV1, 3083
V0=.9999
V2=1
V3=EXPMV1
V4=V3
V5=V3
1)V5=V1XV5
XPV5=V5/V2
V4=V4+V5
→2,V4>V0
V2=V2+1
→1

2)V4=TAPE2
PRINTV4, 4042
V0=TAPE
V9=1-V4
V9=V9/V1
V10=V1/V9
V6=0

TEXT
NORM-TIME  NORM-CONC

3)V7=1
V11=1
V8=0
4)V11=V11XV10
V12=V7XV7
V11=V11/V12
V12=V11XV7
V13=V7-1
→6,V6=0
V14=LOGV6
V14=V14XV13
V15=V6/V9
7)V14=V14-V15
V14=EXPV14
V12=V12XV14
V8=V8+V12
V7=V7+1
→4,V2>V7
V8=V8XV3
V15=V6+V4
PRINTV15,3044
PRINTV8,4123
V6=V6+V5
```

```
→3,V0>V6
→9
6)V14=0
→7

(→0)
```

```
*FORTRAN G118,M. N. RATHOR GAMMA DISTRIBUTED TIME DELAYS
      NO TRACE
      MASTER CURVE FIT
      DIMENSION X(9),G(18),H(18),A(90),D(9),E(9),W(1000)
      COMMON T,DELTAT,NW,A1,A2,A3,A4,A5,A6,A7,A8,NNN
      A1=-.57719165
      A2=.98820589
      A3=-.89705694
      A4=.91820686
      A5=-.75670408
      A6=.48219939
      A7=-.19352782
      A8=.035868343
      READ(1,210)NNN
210   FORMAT(I4)
      READ(1,20)T,DELTAT
      READ(1,21)N,KMAX,NW,M
      READ(1,20)(X(I),I=1,N),(G(I),I=1,N),(H(I),I=1,N)
20    FORMAT(900F0.0)
      READ(1,20)(W(I),I=1,NW)
21    FORMAT(4I4)
      IPRINT=0
      BJ=-1.
      NG=2*M
      NA=N*(N+1)
      CALL PXS6D(N,M,KMAX,IPRINT,BJ,F,X,G,H,W,NW,NA,NG,A,D,E)
      STOP
      END
```

```
      SUBROUTINE CALXGH(N,M,IT,F,X,G,H,W)
      DIMENSION X(9),G(18),H(18),W(1000)
      COMMON T,DELTAT,NW,A1,A2,A3,A4,A5,A6,A7,A8,NNN
      WRITE(2,70)X(1),X(2),X(3),X(4)
70    FORMAT(4G14.4)
      XH=T
      IF(X(1))71,71,72
72    CONTINUE
      IF(X(2))71,71,73
73    CONTINUE
      IF(X(3))71,71,74
74    CONTINUE
      IF(X(3).GE.1.)GO TO 71
      Y=.999*EXP(X(1))
      B1=(X(1)*X(2)/(X(4)-X(3)))
      Z1=1.
      PN=1.
      K=NW+1
      DO 5 I=1,10000
      AJ=I
      Z1=Z1*X(1)/AJ
      PN=PN+Z1
      V=X(2)*AJ
      CALL GAMMA(Y1,V)
      W(K)=ALOG(Z1)+V*ALOG(B1)-ALOG(Y1)-X(1)
      IF((PN-Y).GT.0.)GO TO 12
      K=K+1
5     N1=I+1
12    F=0.
      Y1=0.
```

```
      DO 100 I=1,NW
      K=NW+1
      C1=B1*(T-X(3))
      SUM=0.
      IF(X(3)-T)76,78,78
76    CONTINUE
      DO 11 J=1,N1
      AJ=J
      B=W(K)-C1
      V=X(2)*AJ-1.
      C2=B+V*ALOG(T-X(3))
      S=EXP(C2)
      K=K+1
      SUM=SUM+S
11    CONTINUE
      WRITE(2,70)T,W(I),SUM
      Z=SUM
      GO TO 79
78    Z=0.
79    CONTINUE
      Y=(Z-W(I))**2
      Y1=Y1+Y
      IF(ABS(I-NNN).LE.1)Y=1000.*Y
      F=F+Y
      T=T+DELTAT
100   CONTINUE
      GO TO 75
71    F=100.
      T=T+DELTAT
 75   T=XH
```

```
      WRITE(2,70)F,v1
      RETURN
      END
      SUBROUTINE GAMMA(Y1,P)
      COMMON T,DELTAT,NW,A1,A2,A3,A4,A5,A6,A7,A8,NNN
      X4=1.
      I=INT(P)
      IF(I-1)1,3,4
4     Y=P
      DO 5 J=1,I
      Y=Y-1.
      IF(Y.LT.1.)GO TO 7
5     X4=X4*Y
      GO TO 7
3     Y=P-1.
      GO TO 7
1     Y=P
      X4=1./P
7     Y1=1.+Y*(A1+Y*(A2+Y*(A3+Y*(A4+Y*(A5+Y*(A6+Y*(A7+A8*Y)))))))
      Y1=Y1*X4
      RETURN
      END
```

```
*FORTRAN G148,M. N. RATHOR HOPPING MODEL MULTIFIT
      NO TRACE
      MASTER CURVEFIT
      DIMENSION X(9),G(18),H(18),A(90),D(9),E(9),W(1000)
      COMMON T,DELTAT,NW,HT,NNN
      READ(1,210)NNN
210   FORMAT(I4)
      READ(1,20)T,DELTAT,HT
      READ(1,21)N,KMAX,NW,M
      READ(1,20)(X(I),I=1,N),(G(I),I=1,N),(H(I),I=1,N)
20    FORMAT(900F0.0)
21    FORMAT(4I4)
      READ(1,20)(W(I),I=1,NW)
      IPRINT=0
      BJ=-1.
      NG=2*M
      NA=N*(N+1)
101   FORMAT(4G14.4)
      WRITE(2,101)G(1),G(2),G(3),G(4)
      WRITE(2,101)H(1),H(2),H(3),H(4)
      CALL PXS6D(N,M,KMAX,IPRINT,BJ,F,X,G,H,W,NW,NA,NG,A,D,E)
      STOP
      END
```

```
      SUBROUTINE CALXGH(N,M,IT,F,X,G,H,W)
      DIMENSION X(9),G(18),H(18),W(1000)
      COMMON T,DELTAT,NW,HT,NNN
70    FORMAT(4G14.4)
      Z10=0.
      WRITE(2,70)X(1),X(2),X(3),X(4)
      XH=T
      IF(X(1).LE.0..OR.X(2).LE.0..OR.X(3).LE.0.)GO TO 71
      IF(X(2).LE..0001)GO TO 71
      FNMAX=HT/X(2)
      NMAX=FNMAX
      Z1=1.
      Z2=0.
      PN=0.
      K=NW+1
      PNN=0.
      DO 5 I=1,NMAX
      AI=I
      Z2=Z2+ALOG(AI)
      Z1=X(1)*(HT-AI*X(2))
      IF(Z1.LE.1.0E-10)Z1=1.0E-10
      Z1=AI*ALOG(Z1)-Z1-Z2
      Z1=EXP(Z1)
      PN=PN+Z1
      W(K)=Z1
      K=K+1
5     PNN=PNN+Z1*AI
      PNN=PNN/PN
      TAU=(X(4)-X(3)*(1.-X(2)*PNN/HT))/PNN
      K=NW+1
```

```
      NSTART=-1
      FNMAX=.002/FNMAX
      NEW=K
      Z1=1.
      AI=1.
      DO 12 I=1,NMAX
      Z1=Z1/(TAU*AI)
      W(NEW)=W(K)/PN
      IF(W(NEW)-FNMAX)6,6,8
6     IF(NSTART-0)7,7,9
8     W(NEW)=W(NEW)*Z1
      NEW=NEW+1
      IF(NSTART.LE.0)NSTART=I
7     AI=I
12    K=K+1
      GO TO 1
9     NMAX=I-1
      Y1=0.
1     F=0.
      Z3=X(3)*X(2)/HT
      DO 100 I=1,NW
      K=NW+1
      Z2= T-X(3)
15    SUM=0.
      DO 11 J=NSTART,NMAX
      AJ=J
       TT=Z2+Z3*AJ
      IF(TT)50,50,52
50    S=0.
      GO TO 51
```

```
52      Z1=(AJ-1.)*ALOG(TT)-TT/TAU
        S=W(K)*EXP(Z1)
51      SUM=SUM+S
11      K=K+1
        Y=(SUM-W(I))**2
        Y1=Y1+Y
        WRITE(2,70)T,W(I),SUM
        IF(ABS(I-NNN).LE.1)Y=1000.*Y
        F=F+Y
100     T=T+DELTAT
        GO TO 75
71      F=100.
75      T=XH
        WRITE(2,70)F,Y1
        RETURN
        END
```

```
      SUBROUTINE PXS6D(N,M,KMAX,IPRINT,BJ,F,X,G,H,W,NW,NA,NG,A,D,E)
      DIMENSION B(2),U(2),A(NA),D(N),E(N),G(NG),H(NG),X(M),W(NW)
      CALL PXS6C1(N,L,IT,ICOUNT,NA,B,A,E)
  201 CALL CALXGH(N,M,IT,F,X,G,H,W)
      CALL PXS6C3(N,M,L,IT,ICOUNT,INDIC,KMAX,NA,NG,BJ,F,U,A,D,E,G,H,X)
      GO TO (202,204,201),INDIC
  202 CALL PXS6C2(N,L,NA,B,A,D)
  204 CALL PXS6C4(N,M,L,IT,ICOUNT,IPRINT,INDIC,KMAX,NA,BJ,B,U,A,D,E,X)
      GO TO (201,203),INDIC
  203 RETURN
      END
```

```
      SUBROUTINE PXS6C1(N,L,IT,ICOUNT,NA,B,A,E)
      DIMENSION B(2),A(NA),E(N)
      EXPF(X) =EXP(X)
      LOGF(X) = ALOG(X)
      SINF(X) = SIN(X)
      COSF(X) = COS(X)
      ATANF(X) =ATAN(X)
      SQRTF(X) = SQRT(X)
      ABSF(X) =ABS(X)
      B(1)=0.
      B(2)=0.
      ICOUNT=0
      DO 1L=1,N
      A(L)=0.1
      E(L)=0.
      K=L
      DO 1 KR=1,N
      K=K+N
      A(K)=0.
      IF(L-KR)1,3,1
    3 A(K)=1.
    1 CONTINUE
      L=N
      IT=1
      WRITE(2,2)
    2 FORMAT(5X,50HPXS6C,MAXIMUM OR MINIMUM OF A CONSTRAINED FUNCTION)
      RETURN
      END
```

```
      SUBROUTINE PXS6C2(N,L,NA,B,A,D)
      DIMENSION B(2),A(NA),D(N)
      SQRTF(X)=SQRT(X)
    4 L=N-1
      JO=1
  106 K=N*JO+N
      A(K)=D(N)*A(K)
      KR=L
  104 K=N*JO+KR
   41 A(K)=D(KR)*A(K)+A(K+1)
      KR=KR-1
      IF(KR)103,103,104
  103 JO=JO+1
      IF(N-JO)105,106,106
  105 DO 29 L=1,2
      B(L)=0.
      K=L
      DO 31 JT=1,N
      K=K+N
   31 B(L)=A(K)*A(K)+B(L)
   29 B(L)=SQRTF(B(L))
      B(2)=B(2)/B(1)
      JO=1
    5 L=1
    6 IF(L-JO)43,7,43
   43 BO=0.
      K=JO
      DO 44 KR=1,N
      K=K+N
      JS=K-L
```

```
44 BO=A(K)*A(JS)+BO
   K=JO
   DO 45 KR=1,N
   K=K+N
   JS=K-L
45 A(K)=-A(JS)*BO+A(K)
   L=L+1
   GO TO 6
 7 BO=0.
   K=L
   DO 46 JT=1,N
   K=K+N
46 BO=A(K)*A(K)+BO
   BO=SQRTF(BO)
   K=JO
   AD=1./BO
   DO 47 JT=1,N
   K=K+N
47 A(K)=AD*A(K)
   JO=JO+1
   IF(N-JO)8,5,5
 8 RETURN
   END
```

```
      SUBROUTINE PXS6C3(N,M,L,IT,ICOUNT,INDIC,KMAX,NA,NG,BJ,F,U,A,D,E,G,
     1H,X)
      DIMENSION U(2),A(NA),D(N),E(N),G(NG),H(NG),X(M)
      ABSF(X) =ABS(X)
      U(IT)=F*BJ
      IS=1
  102 IF(G(IS)-X(IS))61,22,22
   61 IF(X(IS)-H(IS))62,22,22
   62 IF(U(1)-U(IT))63,63,16
   63 KR=M+IS
      GO=0.9999*G(IS)+0.0001*H(IS)
      HO=G(IS)+H(IS)-GO
      IF(GO-X(IS))64,64,24
   64 IF(X(IS)-HO)65,65,26
   65 G(KR)=U(1)
      H(KR)=U(1)
   98 IS=IS+1
      IF(IS-M)102,102,21
   21 IF(IT-2)166,14,166
  166 IT=2
   66 INDIC=2
      GO TO 101
   22 IF (IT-2)23,16,23
   23 WRITE(2,99)
   99 FORMAT(42HINITIAL VALUES OF X NOT WITHIN CONSTRAINTS)
      GO TO 66
   24 IF (IT-1)68,23,68
   68 GO=(GO-X(IS))/(GO-G(IS))
      HO=U(IT)-G(KR)
   25 BO=(-2.*GO+4.)*GO-3.
```

```
      U(IT)=BO*GO*HO+U(IT)
      GO TO 98
   26 IF(IT-1)67,23,67
   67 GO=(X(IS)-HO)/(H(IS)-HO)
      HO=U(IT)-H(KR)
      GO TO 25
   14 IF(U(1)-U(2))54,54,16
   54 GO=ABSF(E(L))
      IF(GO-1.)55,55,15
   55 E(L)=1.5
   15 D(L)=D(L)+A(L)
      U(1)=U(2)
      A(L)=3.*A(L)
      GO TO 17
   16 KR=L
      DO 56 IS=1,N
      KR=KR+N
   56 X(IS)=-A(KR)*A(L)+X(IS)
      A(L)=-0.5*A(L)
      IF (E(L))17,57,57
   57 E(L)=-E(L)
   17 IF(ICOUNT-N*KMAX)58,58,66
   58 DO 59 IS=1,N
      IF (E(IS)+1.)59,59,18
   59 CONTINUE
      INDIC=1
      GO TO 101
   18 IF (L-N)60,12,60
   60 L=L+1
      GO TO 13
```

```
 12 L=1
 13 K=L
    DO 76 KR=1,N
    K=K+N
 76 X(KR)=A(L)*A(K)+X(KR)
    ICOUNT=ICOUNT+1
    IT=2
    INDIC=3
101 RETURN
    END
```

```
      SUBROUTINE PXS6C4(N,M,L,IT,ICOUNT,IPRINT,INDIC,KMAX,NA,BJ,B,U,A,D,
     1E,X)
      DIMENSION B(2),U(2),A(NA),D(N),E(N),X(M)
      BO=BJ*U(1)
      IF(IPRINT)33,48,33
   48 WRITE(2,102)ICOUNT,BO,B(1),B(2)
      DO 49 L=1,M
   49 WRITE(2,103)X(L)
   33 IF(ICOUNT-N*KMAX)50,50,9
   50 IF(IT-1)11,9,11
    9 INDIC=2
      GO TO 105
  102 FORMAT(I5,2(8X,E12.5),F20.5)
  103 FORMAT(8X,E12.5)
   11 DO 52 L=1,N
      D(L)=0.
   52 E(L)=0.
      L=1
      K=L
      DO 53 KR=1,N
      K=K+N
   53 X(KR)=A(L)*A(K)+X(KR)
      ICOUNT=ICOUNT+1
      IT=2
      INDIC=1
  105 RETURN
      END
```

BIBLIOGRAPHY

Bibliography

1. Klinkenberg, A., Trans. Instn. Chem. Engrs,, 1965, 43, 141.
2. Hunter, F., J. Soc. Chem. Ind., 1893, 12, 227.
3. Tour, R.S., and Lerman, F., Trans. Instn. Chem. Engrs., 1939, 35, 719.
4. Kirschbaum, E., "Distillation and Rectification", translation by M. Wulfinghoff, Chemical Publishing Co., New York, 1948.
5. Weimann, M., Z. Ver. Deut. Ing. Beihefte, No. 6.,1933.
6. Scott, A.H., Trans. Instn. Chem. Engrs., 1935, 13, 211.
7. Baker, T.T., Chilton, H., and Vernon, H.C., Trans. A.I.Ch. Engrs., 1935, 31, 296.
8. Uchida, A.S., and Fujita, S., J. Soc. Chem. Ind., Japan, Supplt., 1934, 37, 274., 1936, 39, 432., 1938, 41, 275.
9. Eckerts, J.S., Chem. Eng. Prog., 1961, 57, 54.
10. Porter, K.E., and Jones, M.C., Trans. Instn. Chem. Engrs., 1963, 41, 240.
11. Cihla, and Schmidt, W., Collection of Czechoslovakian chemical communications, 1957, 22, 896.
12. Jameson, G.J., Trans. Instn. Chem. Engrs., 1966, 44, 198.
13. Jameson, G.J., Trans. Instn. Chem. Engrs., 1967, 45, 174.
14. Paye, J.W., and Dodge, B.E., Ind. Eng. Chem., 1932, 24, 630.
15. Fenske, M.R. et.al., Ind. Eng. Chem., 1934, 26, 1169.
16. Simon, C.W., and Osborn , H.B., Ind. Enf. Chem., 1934, 26, 529.
17. Uchida, S., and Fugita, S.J., Soc. Chem. Ind., Japan, 1936, 39, 886.
18. Furnas, C.C., and Bellinger, F.M., Trans. A.I.Ch. Engrs., 1938, 34, 251.
19. Elgin, J.C. and Weiss, F.B., Ind. Eng. Chem., 1939, 31, 435.
20. Jesser, B.W., and Elgin, J.C., Trans. A.I.C E, 1935, 31, 296.
21. Otake, T., and Okada, K., Chem. Eng.(Japan), 1953, 17, 176.
22. Shulman, H.L. et.al., Am. Instn. Chem. Eng. J., 1955, 1, 247.
23. Otake, T.,
24. Mohunta, D.M., and Laddha, G.S., Chem. Eng. Science, 1965, 20, 1069.
25. Buchanan, J.E., Ind. Eng. Chem.Fundls., 1967, 6, 400.
26. Gelbe, H., Chem. Eng. Science, 1968, 23, 1401.

27. Ref. no. 28

28. Bischoff, K.B., and Levenspiel, O., Chem. Eng. Science, 1962, 17, 245 and 257.
29. Klinkenberg, A., and Sjenitzer, F., Chem. Eng. Science, 1956, 5, 258.
29a. Ref. nos. 5, 15, 18, and 19.
30. Ham, A. and Coe, H.S., Chem. Met. Eng., 1918, 19, 663.
31. Aris, R., Chem. Eng. Science., 1959, 9, 266.
32. Bischoff, B.K., Chem. Eng. Science, 1960, 12, 69.
33. Aris, R. and Amundson, N.R., A.I.Ch.E.Jl., 1957, 3, 380.
34. Carberry, J.J., A.I.Ch.E.Jl., 1958, 4, 13M.
35. Deans, H.A., and Lapidus, L., A.I. Ch. E. Jl., 1960, 6, 656.
36. Kramers, H., and Alberda, G., Chem. Eng. Science, 1953, 2, 173.
37. Levenspiel, O., Chem. Eng. Science, 1962, 17, 575.
38. Trambouze, P.J., Rev. Instn. Franc. Petrole Ann. Combust. Liquides., 1957, 15, 1948.
39. Ranz, W.E., Chem. Eng. Prog., 1952, 48, 247.
40. Beran, M.,J, Chem. Phys., 1957, 27, 270.
41. Schneidegger, A.E., "The Physics of Flow through Porous Media", McMillan, New York, 1960.
42. de Josselin de Yong, G., Trans. Am. Geophys. Union, 1958, 39, 87.
43. Saffman, P.G., J. Fluid Mechanics, 1959, 6, 321.
44. Saffman, P.G., Chem. Eng. Science, 1959, 11, 125.
45. Saffman, P.G., J. Fluid Mechanics, 1960, 7, 194.
46. Evans, R.B.et.al., J. Chem. Phys., 1961, 35, 2076.
47. Prager, S., J. Chem. Phys., 1960, 33, 122.
48. Scheidegger, A.E., Can. J. Phys., 1961, 39, 1573.
49. Prausnitz, J.M., A.I.Ch.E.Jl., 1958, 4, 14M.
50. Baron, T., Chem. Eng. Prog., 1952, 48, 118.
51. Latinen, G.A.,Ph.D., Dissertation, Princeton University, New Jersey, 1957.
52. Hinze, J.O., "Turbulence", McGraw-Hill, New York, 1959.
53. Le Goff, P., and Lespinesse, B., Revue Instn. Fr. Petrole, 1962, 27, 21.
54. Porter, K.E., Trans. Instn. Chem. Engrs., 1968, 46, T69.

55. Einstein, H.A., Dissertation, Eidg. tech. Hochschule, Zurich, Switzerland, 1937.
56. Jacques, G.L., Vermeulen, T., Univ. of Calif., Radiation Laboratory, UCRL-8029.
57. Cairns, E.J., Ph.D. Dissertation, Univ. of Calif., 1959.
58. Cairns, E.J.,and Prausnitz, J.M., Chem. Eng. Science, 1960, 12, 20.
59. Giddings, J.C., and Eyring, H.J., J.Chem. Phys., 1955, 59, 410.
60. Giddings, J.C., J. Chem. Pyhs., 1957, 26, 169.
61. Klinkenberg, A., J. Phys. Chem., 1955, 59, 1184.
62. Levenspiel, O., Smith, W.K., Chem. Eng. Science, 1957, 6, 227.
63. Van der Laan, E.T., Chem.Eng. Science, 1958, 7, 187.
64. Wehner, J.F., and Wilhelm, R.H., Chem. Eng. Science, 1956, 6, 89.
65. Carberry, J.J., and Bretton, R.H., A.I.Ch. E. Jl., 1958, 4, 367.
66. Ebach, E.A., and White, R.R., A.I.Ch.E.Jl., 1958, 4, 161.
67. Sater, E.V., Ph.D. Dissertation, Illinois Institute of Technology, 1963.
68. Ampilogov, I.E., Kharin, A.N., and Kurochkina, I.S., Zh. Fiz. Khim., 1958, 32, 141.
69. Danckwerts, P.V., Chem. Eng. Science., 1953, 2, 1.
70. Von.Rosenberg, D.V., A.I.Ch.E.Jl., 1956, 2, 55.
71. Liles, A.W., and Geankoplis, C.J., A.I.Ch.E.Jl., 1960, 6, 591.
72. Strang, D.A., and Geankoplis, C.J., Ind. Eng. Chem., 1958, 50, 1305.
73. Towle, W.L., and Sherwood, T.K., Ind. Eng. Chem., 1939, 31, 457.
74. Bernard, R.A., and Wilhelm, R.H., Chem. Eng. Prog., 1950, 46, 233.
75. Klinkenberg, A., Krajenbrink, H.J., and Lauwerier, H.A., Ind. Eng. Chem., 1953, 45, 1202.
76. Fahien, R.W., and Smith, J.M., A.I.Ch.E.Jl., 1955, 1, 28.
77. Prausnitz, J.M., Ph.D. Dissertation, Princeton Univ., New Jersey, 1955.
78. Blackwell, R.J., A.I.Ch.E.Soc. Petrol. Eng. Symp., San Francisco, Calif., Dec.6, 1959.
79. Doweiler, V.P. and Fahien, R.W., A.I.Ch. E.Jl., 1959, 5, 134.
80. Plautz, D.A., and Johnstone, H.F., A.I.Ch.E.Jl., 1955, 1, 193.
81. Aris, R., Chem. Eng. Science, 1959, 11, 194.
82. Deans, H.A., Soc. Petrol. Engrs. Jl., 1963, 3, 49.

83. Levich, V.G., Markin, V.S. and Chismadzhev, Yu.A., Chem. Eng. Science, 1967, 22, 1357.

84. Buffham, B.A., and Gibilaro, L.G., Chem. Eng. Science., 1968, 23, 1399.

85. Gottschlich, C.F., A.I.Ch.E.Jl., 1963, 9, 89.

86. Van Deemter, T.J., Zuiderweg, F.J., and Klinkenberg, A., Chem. Eng. Science, 1956, 5, 271.

87. Lapidus, L., and Amundson, N.R., J. Phys. Chem., 1952, 56, 683.

88. Rosen, J., Ind. Eng. Chem., 1954, 46, 1590.

89. Kasten, P.R., Lapidus, L., and Amundson, N.R., J. Phys. Chem., 1952, 56, 683.

90. Deisler, P.F., and Wilhelm, R.H., Ind. Eng. Chem., 1953, 45, 121.

91. McHenry, K.W., and Wilhelm, R.H., A.I.Ch.E.Jl., 1957, 3, 83.

92. Glaser, M.B., and Lichtenstein,I., Ind. Eng. Chem., 1963, 9, 30.

93. Glaser, M.B., and Litt, M.A., A.I.Ch.E.Jl., 1963, 9, 103.

94. Babcock, R.E., Green, D.W., and Perry, R.H., A.I.Ch.E.Jl., 1966, 12, 922.

95. Olbrich, W.E., Agnew, J.B., and Potter, O.E., Trans. Instn. Chem. Engrs., 1966, 44, 207.

96. Higbie, R., Trans. A.I.Ch. Engrs., 1935, 31, 365.

97. Corrigan, T.E., Lander, H.R., Shaefer, R., and Dean, M.J., A.I.Ch.E.Jl., 1967, 13, 1029.

98. Van de Vusse, J.G., Chem. Eng. Science, 1962, 17, 507.

99. Porter, K.E., Trans. Instn. Chem. Engrs., 1968, 46, T69.

100. Paynter, H.M., "On an Analogy between Stochastic Processes and Monotone Dynamic Systems", Regelungstechnik, P-243 (Ed. G. Muller), R. Oldenbourg, 1957.

101. Kendall, M.G., and Stuart, A., "The Advanced Theory of Statistics", Vol.1, Griffin, 1958.

102. Hydronyl Publication, "Tower Packings", P-34, Hydronyl Ltd.

103. Gibilaro, L.G.,Ph.D. Thesis, Loughborough University of Tech., Loughborough, 1967.

104. Nienow, A.W., Unahabhokha, R., and Mullin, J.W., J. App. Chem. , 1968, 18, 154.

105. Couper, A. and Stepto, R.F., Trans. Faraday Soc., 1969, 65, 2486.

106. Anzelius, A., Z. Angew. Math. U. Mech., 1926, 6, 291.

107. Gidding, J.C., "Dynamics of Chromatography", Part I, 1965, (New York: Marcel Dekker Inc.)

108. Astarita, G., "Mass Transfer with Chemical Reaction", 1967, (Amsterdam: Elsevier Publishing Co.).

109. Kropholler, H.W., Spikins, D.J., and Whalley, F., Measurement and Control, 1968, 1, T55.

110. Levenspiel, O., "Chemical Reaction Engineering", Wiley, New York, 1962.